MEDICAL UNIVERSITY OF GDAŃSK

EUROPEAN JOURNAL OF TRANSLATIONAL AND CLINICAL MEDICINE

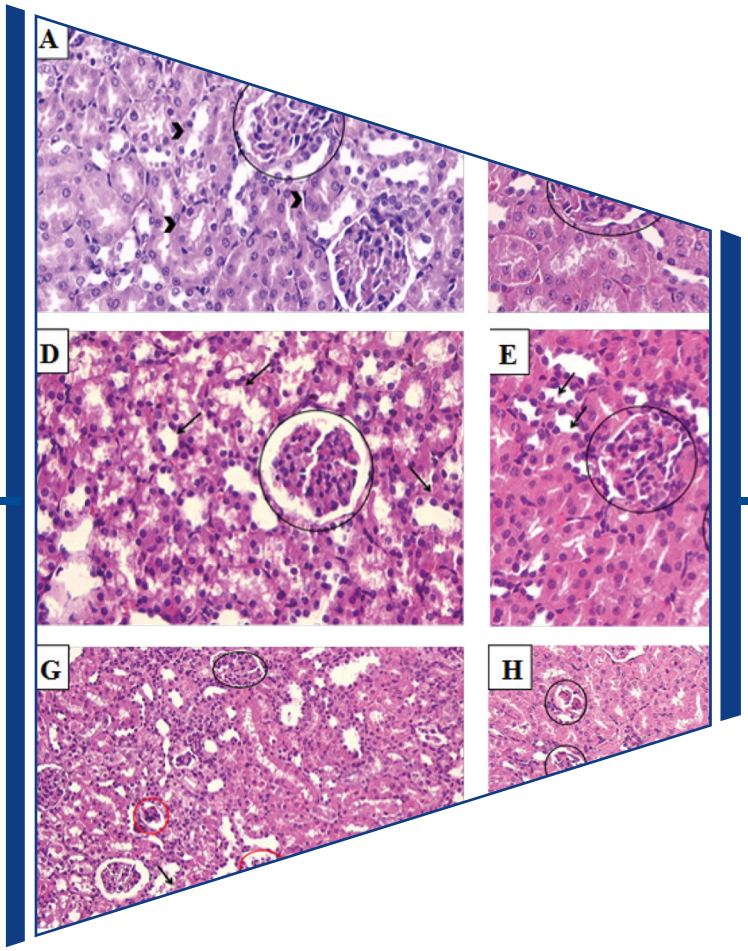

e-ISSN 2657-3156 2025 Vol. 8 No. 1 ejtcm.gumed.edu.pl

Photo on the cover of the issue
by Mahmoud Fadl Bakr et al.
(page 25)

EUROPEAN JOURNAL OF TRANSLATIONAL AND CLINICAL MEDICINE

Editorial Office

Medical University of Gdańsk
European Journal
of Translational Medicine
Dębinki 1 Street,
80-210 Gdańsk, Poland

Phone: +48 58 349 15 37

E-mail: ejtcm@gumed.edu.pl
ejtcm.gumed.edu.pl

Publisher

Medical University of Gdańsk
M. Skłodowskiej-Curie 3 A
80-210 Gdańsk, Poland

Gdańsk 2025
e-ISSN 2657-3156

Online edition is the
original version of the journal.

EUROPEAN JOURNAL OF TRANSLATIONAL
AND CLINICAL MEDICINE 2025;8(1):1-119

CONTENTS

SHORT COMMUNICATION

RESEARCH ARTICLE

REVIEW ARTICLE

TECHNICAL REPORT

EUROPEAN JOURNAL OF TRANSLATIONAL
AND CLINICAL MEDICINE 2025;8(1):5-9

SHORT COMMUNICATION

Preliminary assessment of microcirculation in the ascending aorta in patients with normal and dilated ascending aorta using laser Doppler perfusion monitoring

Mikołaj Krysiak[1], Andrzej Łoś[1], Rafał Pawlaczyk[1], Mateusz Janeczek[1], Marcin Hellmann[2]

[1] Department of Cardiac & Vascular Surgery, Medical University of Gdańsk, Poland
[2] Division of Cardiac Diagnostics, Medical University of Gdańsk, Poland

Abstract

Background: Microcirculation within the ascending aortic wall, supplied by the vasa vasorum, is increasingly recognized as a potential factor in the pathogenesis of aortic aneurysms. However, in vivo assessment remains challenging. This pilot study aimed to evaluate ascending aortic microcirculation intraoperatively using Laser Doppler Perfusion Monitoring (LDPM). **Material and methods:** Twenty-four patients (18 males, 6 females) undergoing elective cardiac surgery were enrolled. LDPM was performed on the exposed ascending aorta prior to surgical manipulation. A probe was sutured to the aortic wall and perfusion was recorded in Perfusion Units (PU). A brief probe compression test was conducted to evaluate perfusion response. **Results:** The mean LDPM value was 281.58 PU (males: 339.94 PU; females: 139.86 PU). In males, LDPM negatively correlated with age ($r = –0.593$, $p = 0.0121$), whereas a moderate but non-significant correlation was noted with BMI ($r = –0.303$, $p = 0.2366$). No significant associations were observed with hypertension, diabetes, smoking, or aortic dilation. A paradoxical increase in PU during probe compression occurred in 54% of patients. **Conclusions:** LDPM provides real-time intraoperative assessment of aortic microcirculation. Age-related decline in perfusion may contribute to aortic wall vulnerability. Further studies with larger cohorts are needed to validate these findings.

Keywords: ascending aorta · dilatation of ascending aorta · laser Doppler perfusion monitoring

Corresponding author:
Mikołaj Krysiak, Department of Cardiac & Vascular Surgery, Medical University of Gdańsk, Poland
e-mail: krysiak.mikolaj@gumed.edu.pl
Available online: ejtcm.gumed.edu.pl

Citation

Krysiak M, Łoś A, Pawlaczyk R, Janeczek M, Hellmann M. Preliminary assessment of microcirculation in the ascending aorta in patients with normal and dilated ascending aorta using laser Doppler perfusion monitoring. Eur J Transl Clin Med. 2025;8(1):5-9.

DOI: 10.31373/ejtcm/205392

Introduction

Microcirculation and its impairment as elements of the pathophysiology of cardiovascular diseases is recently gaining attention in recent research. In the aortic wall the microcirculation is a network of small vessels (vasa vasorum) that supply its tissue with blood flow and nutrients. Impairments in this network are considered an early pathogenic factor in cardiovascular diseases, and may often precede structural changes, e.g. formation of an aneurysm. The microscopic scale of these vessels poses a significant technical challenge in the evaluation of microcirculation. Laser Doppler Perfusion Monitoring (LDPM) provides a non-invasive method to measure tissue perfusion and its dynamic response to stimuli. Recent studies have explored the potential involvement of microcirculatory dysfunction in conditions such as aortic aneurysm, ischemic heart disease and hypertrophic cardiomyopathy.

Prior applications of LDPM in cardiac surgery have primarily focused on myocardial perfusion during off-pump coronary artery bypass grafting (OPCABG) [1-2]. LDPM has been utilized more widely in neurology [3], hypertension [4], nephrology [5], and plastic surgery [6]. However, studies involving LDPM in the assessment of aortic microcirculation remain scarce. Herein, we present preliminary LDPM data obtained intraoperatively from cardiac surgery patients at a single institution. In this pilot study, we aimed to establish a method of direct measurement microcirculation within the wall of the ascending aorta intraoperatively using LDPM. To the best of our knowledge, no reports have been published on the use of LDPM measurements in the ascending aorta, apart from a single press release authored by our team [7].

Materials and methods

We enrolled patients undergoing cardiac surgery in accordance with the European Society of Cardiology (ESC) guidelines, provided that replacement of the ascending aorta with a vascular prosthesis was not planned. The study population consisted of 24 patients (18 males, 6 females). The mean age for males was 63.88 years (median 65.0), and for females 71.14 years (median 70.0) (Figure 1). Six patients had ascending aortic dilation (> 35 mm), 6 had diabetes mellitus (25%), 18 had hypertension (66.6%), 2 had chronic kidney disease (8.3%), 14 were current or former smokers (58.3%) and 10 had a body mass index (BMI) of ≥ 30 (41.67%). All participants provided informed and voluntary consent to participate

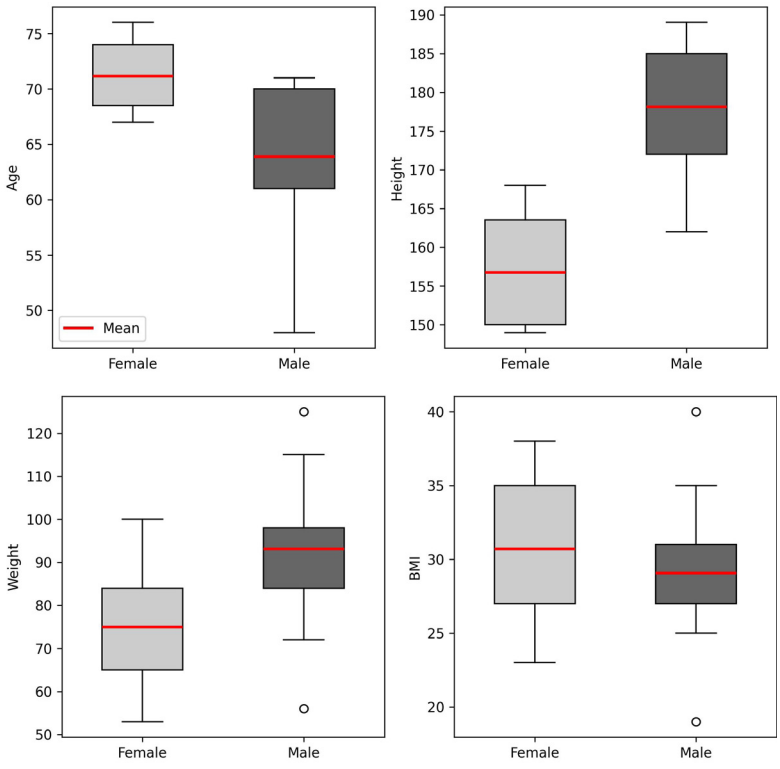

Figure 1. Population parameters: age (years), height (cm), weight (kg), BMI (kg/m²)

in the study. The research protocol was approved by an independent bioethics committee for scientific research.

Surgical procedures were conducted by 1 of the 2 surgeons trained in the use of LDPM. Using laser Doppler technology, LDPM detects perfusion within within a tissue volume of approximately 1 mm^3, penetrating up to 1 mm in depth. Perfusion values are reported in perfusion units (PU), which are not standardized and therefore allow for a relative comparison of measurements obtained with the same manufacturer's equipment only.

All measurements were taken using the Probe 404-1 and Periflux 5000 base unit (PeriMed AB, Järfälla, Sweden). After exposure of the mediastinum and ascending aorta, the probe was sutured to the aortic wall using three single 5-0 stitches (Figure 2). Baseline perfusion was recorded for 1 minute. A compression test was then performed by applying pressure to the probe, and changes in perfusion were visualized graphically. Due to the need to maintain sterility in the surgical field, it was not possible to measure the amount of pressure applied during the probe compression test. However, the measurements were performed by only 2 cardiac surgeons, who aimed to apply a consistent amount of pressure in each test. While the compression test remains subjective, our goal was to minimize the variability resulting from differences between operators as much as possible. This test aimed to determine whether compression reduced the blood flow through the vasa vasorum, supporting the hypothesis that increased wall stress (e.g. in hypertension) may impair aortic wall perfusion, contributing to aneurysm formation [8].

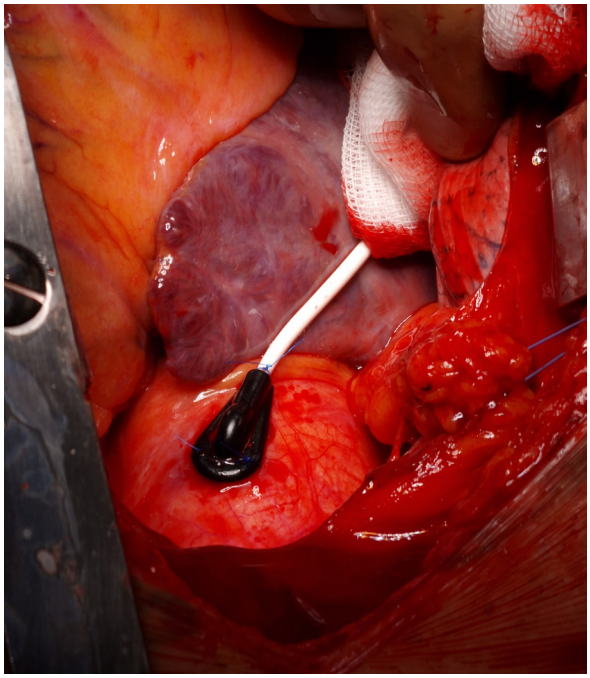

Figure 2. LDPM probe sutured to the ascending aorta

Results

The mean LDPM value in the study cohort was 281.58 PU, with a median of 215.5 PU. In male patients, the mean was 339.94 PU (standard deviation (SD) 241.2), and the median 252.0 PU, whereas in female patients the mean was 139.86 PU (SD 53.0), and median 149 PU (Figure 3). In males, LDPM negatively correlated with age (Spearman's r = –0.593, p = 0.0121) (Figure 4); a moderate but non-significant correlation was noted in females (Spearman's r = 0.429, p = 0.3374). A moderate but non-significant correlation between BMI and LDPM was found in males (Spearman's r = –0.303, p = 0.2366), with no significant correlation in females.

In the group with an enlarged ascending aorta, the mean LDPM value was 312.17 PU (SD 213.71 PU), with a median of 238.5 PU. In the group without aortic enlargement, the mean LDPM was 271.39 PU (SD 231.41 PU), and the median was 185.5 PU. No statistically significant difference was observed between the groups with and without ascending aortic enlargement (Mann-Whitney U test, p = 0.505). No significant

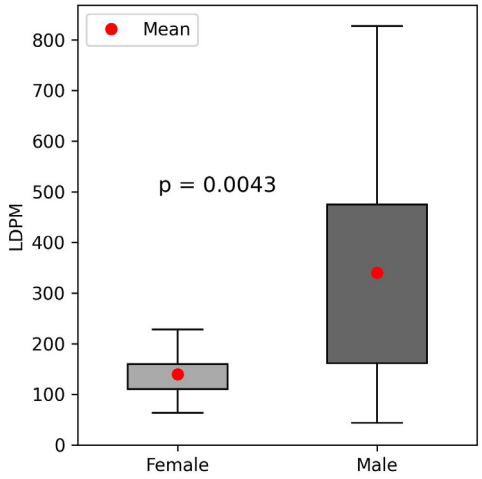

Figure 3. LDPM in the male and female populations

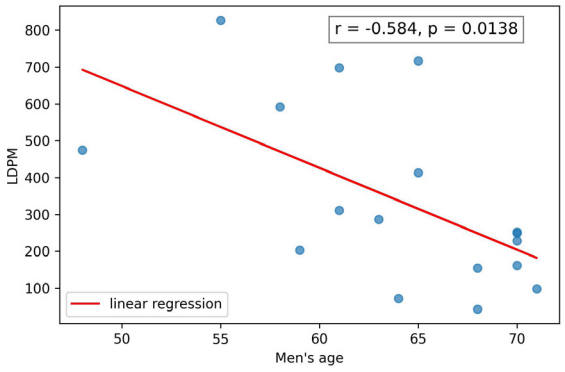

Figure 4. The relationship between LDMP and age in men

correlations were observed between LDPM values and smoking (Pearson's r = 0.199), diabetes mellitus (r = –0.09), or hypertension (r = –0.036). Interestingly, 54% of patients exhibited a paradoxical increase in PU during the compression test; the remaining patients showed the expected decrease in perfusion.

Discussion

Our microcirculatory assessment of the ascending aorta is an early but promising step toward understanding the pathophysiology of aneurysm formation. Cystic medial degeneration, a primary cause of ascending aortic aneurysms, is often associated with hypertension-induced vascular remodeling [9]. Hypertensive arteriopathy may extend to the aortic vasa vasorum, impairing their function. Similarly, poorly controlled diabetes is known to damage microvasculature in organs such as the retina and kidneys, raising the possibility that similar damage occurs in the aortic wall [10]. This pilot study suggests several promising directions for further exploration, including correlating intraoperative LDPM data with the histopathological analysis of aortic adventitia.

One of our aims was to evaluate the impact of hypertension and diabetes on ascending aortic microcirculation. However, our small sample size (n = 24) limited the statistical power and may explain the absence of statistically significant correlations. Depending on the assumed parameters, the sample size required to achieve adequate statistical power ranges from 75 to 128 participants. We anticipate that a study with 100 participants, combined with improved data collection, would enable the detection of statistically significant correlations and the drawing of meaningful conclusions.

Another limitation of LDPM is the laser's penetration depth, which reaches a maximum of approximately 1 mm into the wall of the ascending aorta. As a result, individual differences in the thickness of the aortic wall layers, and the associated variability in tissue vascular density, may lead to discrepancies in measurements between patients. This represents an additional limitation of the LDPM, highlighting the need for further analysis and the development of standardized techniques for measurements. Another unresolved issue involves the heterogeneous response to the compression test, suggesting the need for further validation of this method.

Additionally, the use of a single perfusion probe significantly limited our measurement throughput, as each probe required prolonged sterilization between surgical procedures. In our study the aortic diameter was determined via echocardiography, a modality subject to operator variability [11]. Whereas computed tomography angiography would provide more precise measurements and may be advisable in future studies.

Conclusions

This pilot study demonstrates the feasibility of directly measuring microcirculation in the ascending aortic wall intraoperatively using LDPM. The observed negative correlation with age may reflect the age-related decline in aortic microvascular function. No statistically significant correlations were found between LDPM and aortic dilation, diabetes, hypertension, smoking, or BMI. Further investigations in larger cohorts with an extended parameter analysis are warranted to validate these preliminary findings.

Funding

The project was funded by the state budget, granted by the Ministry of Science and Higher Education as part of the program "Student Research Groups Create Innovations."

Conflict of interest statement

The authors declare no financial relationships with any commercial entity that could have influenced the outcomes or interpretations presented in this manuscript, and report no conflicts of interest.

References

1. Piotrowski J, Anisimowicz L, Hellmann M. Laser Doppler flowmetry to assess myocardial microcirculation. Cardiol J [Internet]. 2020;27(2):197–9. Available from: https://journals.viamedica.pl/cardiology_journal/article/view/66850
2. Hellmann M, Piotrowski J, Anisimowicz L, Cracowski J-L. A mystery of the myocardial microcirculation during coronary artery bypass grafting. Eur J Cardio-Thoracic Surg [Internet]. 2018;54(2):405–405. Available from: https://academic.oup.com/ejcts/article/54/2/405/4917834

3. Wårdell K, Blomstedt P, Richter J, Antonsson J, Eriksson O, Zsigmond P, et al. Intracerebral Microvascular Measurements during Deep Brain Stimulation Implantation using Laser Doppler Perfusion Monitoring. Stereotact Funct Neurosurg [Internet]. 2007;85(6):279–86. Available from: https://karger.com/article/doi/10.1159/000107360
4. Rizzoni D, Nardin M, Coschignano MA, Rossini C, De Ciuceis C, Caletti S, et al. Methods of evaluation of microvascular structure: state of the art. Eur J Transl Clin Med [Internet]. 2018;1(1):7–17. Available from: https://ejtcm.gumed.edu.pl/articles/10
5. Kruger A, Stewart J, Sahityani R, O'Riordan E, Thompson C, Adler S, et al. Laser Doppler flowmetry detection of endothelial dysfunction in end-stage renal disease patients: Correlation with cardiovascular risk. Kidney Int [Internet]. 2006;70(1): 157–64. Available from: https://linkinghub.elsevier.com/retrieve/pii/S0085253815517523
6. Sundheim LK, Sporastøyl AH, Wester T, Salerud G, Kvernebo K. Acute skin trauma induces hyperemia, but superficial papillary nutritive perfusion remains unchanged. Microcirculation [Internet]. 2017;24(7). Available from: https://onlinelibrary.wiley.com/doi/10.1111/micc.12389
7. Łoś A, Walczak I, Bieńkowski M, Kutryb-Zając B, Hellmann M. New insight into the aortic microcirculation in coronary disease: Intraoperative laser Doppler flow measurement and vasa vasorum imaging. Polish Hear J [Internet]. 2024;82(10):1008–9. Available from: https://journals.viamedica.pl/polish_heart_journal/article/view/101739
8. Chumachenko P V, Ivanova AG, Bagheri Ekta M, Omelchenko A V, Sukhorukov VN, Markin AM, et al. Condition 'Vasa Vasorum' in Patients with Thoracic Aortic Aneurysm. J Clin Med [Internet]. 2023;12(10). Available from: http://www.ncbi.nlm.nih.gov/pubmed/37240684
9. Srivastava P, Gupta M, Mandal A. Cystic Medial Degeneration Leading to Aortic Aneurysm and Aortic Regurgitation. Hear India [Internet]. 2014;2(4):107. Available from: https://journals.lww.com/10.4103/2321-449X.146617
10. Alnaser RI, Alassaf FA, Abed MN. Melatonin as a potential treatment option in diabetes complications. Eur J Transl Clin Med [Internet]. 2024;7(2):78–91. Available from: https://ejtcm.gumed.edu.pl/articles/192108
11. Beetz NL, Trippel TD, Philipp K, Maier C, Walter-Rittel T, Shnayien S, et al. Discrepancy of echocardiography and computed tomography in initial assessment and 2-year follow-up for monitoring Marfan syndrome and related disorders. Sci Rep [Internet]. 2022;12(1):15333. Available from: https://www.nature.com/articles/s41598-022-19662-y

EUROPEAN JOURNAL OF TRANSLATIONAL
AND CLINICAL MEDICINE 2025;8(1):10-18

RESEARCH ARTICLE

Breath-holding index – a new approach to an old method

Marta Nowakowska-Kotas[1], Weronika Lisiak[2], Emilia Wiśniewska[3], Sławomir Budrewicz[1], Piotr Wiśniewski[2]

[1] Department of Neurology, Wrocław Medical University, Poland
[2] Faculty of Mathematics and Computer Science, Nicolaus Copernicus University in Toruń, Poland
[3] Faculty of Computer Science, University of Wrocław, Poland

Abstract

Background: Despite technical challenges and uncertainties, transcranial Doppler (TCD) ultrasonography remains a promising tool due to its non-invasive nature, safety, and cost-effectiveness. In this study we aimed to develop an advanced automatic calculation method for the breath-holding index (BHI) to enhance the reliability of cerebrovascular reactivity (CVR) measurements. **Material and methods:** This study involved the automatic calculation of BHI during the breath-holding maneuver, targeting a reduction in variability and an increase in the accuracy of CVR assessment. **Results:** The BHI_to_max method was identified as the most effective, which revealed the least variability. This method calculates the steepest slope of blood flow velocity change during CO_2-induced vasodilation. By focusing on a minimized time interval and adjusting for potential shifts in the start and end points, this approach captures the most dynamic phase of the cerebrovascular response to CO_2. **Conclusions:** We propose an automatic calculation method, which accounts for individual differences in CO_2 sensitivity and CVR. It offers a potentially more precise and personalized assessment of CVR, leading to a more reproducible and individualized measurement.

Keywords: breath-holding index (BHI) • transcranial Doppler ultrasonography (TCD) • CO_2-induced vasodilation automatic calculation

Citation

Nowakowska-Kotas M, Lisiak W, Wiśniewska E, Budrewicz S, Wiśniewski P. Breath-holding index – a new approach to an old method. Eur J Transl Clin Med. 2025;8(1):10-18.

DOI: 10.31373/ejtcm/204417

Corresponding author:
Marta Nowakowska-Kotas, Department of Neurology, Wrocław Medical University, Poland
e-mail: marta.nowakowska-kotas@umw.edu.pl
Available online: ejtcm.gumed.edu.pl

Introduction

The human brain requires stable perfusion of its tissues, which is maintained by regulating cerebral blood flow (CBF). Control of the CBF relies on mechanisms such as the myogenic response and changes in vessel diameter in response to vasoactive stimuli, collectively known as cerebrovascular reactivity (CVR). Measurement of CVR can provide information about the vessels' condition and the brain's ability to maintain required perfusion parameters [1-3]. Routinely employed tests of CVR are based on the change of the blood's carbon dioxide (CO_2) concentration. Hypocapnia, induced by hyperventilation during deep breathing tests, results in decreased mean velocities (Vmean) in the arteries of the brain, while increased CO_2 concentrations lead to maximal flow, as demonstrated by several tests: breath-holding index (BHI), acetazolamide infusion, carbogen inhalation, or closed-circuit breathing [4-7]. It is assumed that in all those tests change in blood flow velocity (BFV) change reflects the changes in CBF. During the breath-holding test, CO_2 concentration in the blood is transiently increased, resulting in a decrease of the resistance of cortical arterioles and increased velocity in main arteries of the brain. Those secondary alternations to a vasodilatory stimulus can be monitored in the middle cerebral artery (MCA) by transcranial Doppler (TCD) ultrasonography [8].

However, several technical problems arise during the breath-holding test, causing the variability of the BHI [8]. Among them, the conflicting correlations between BHI and inspired CO_2 (ranging from weak to moderate), the role of patient's body position and the influence of blood pressure are listed [9-14]. The sex and age differences, obesity, anxiety or difficulties with proper breath-holding, which were reasons for exclusion of some patients are discussed in the literature [12, 15-18]. The repeatability of the BHI test is also concerning, since standard deviation can vary from subject to subject from 0.15 up to 0.61 or the intraclass correlation coefficient for two consecutive measurements in one subject reaching 0.91 for CVR examinations in other study [16, 19].

The above-mentioned technical problems led to the search for a method of processing the data acquired via TCD acquired data in a way that would have the highest repeatability from one examination to the next, so as to reflect the CVR as accurately as possible. One example is the Breath-hold acceleration index, which is based on the linear regression of the most linear portion of the flow velocity change [20]. Different approaches would involve the automatic search for such time-related combination of parameters so the least variances of the results would be observed.

In this study we aimed to improve the accuracy of the BHI test by identifying the most dependable automatic technique for analyzing changes in CBF velocities during the breath-holding procedure.

Material and methods

A cohort of 8 healthy white individuals (4 males and 4 females) 20-56 years of age and devoid of chronic illness (e.g. diabetes, cardiovascular or cerebrovascular diseases), underwent assessment in a seated posture. Exclusion criteria were: < 18 years of age, nicotine consumption 24 hours before before the examination, medication use (including headache-alleviating medications) within 24 hours, consumption of fluids (apart from water) within 2 hours, and inadequate insonation of the MCA through the temporal window. This study was approved by the Bioethics Committee at the Wroclaw Medical University and informed consent was taken from each participant.

TCD

Participants underwent continuous, noninvasive monitoring of the BFV in both of the MCAs successively with the use of Nicolet™ Sonara/tek™ Transcranial Doppler System (Natus Medical Inc., San Carlos, CA, USA) with a fixed 2 MHz probe. The mean flow velocity (MFV) at certain time points of the test was considered. A baseline measurement of the MFV in the MCA was taken while the participant breathed normally for 4 minutes. Participants were explicitly directed not to start their breath-holding with a Valsalva maneuver. Instead, they were asked to simply cease breathing after inhaleing and then hold their breath for up to 30 seconds or until they felt the need to breathe inhale again. A total of 35 recordings were collected, which were used for further calculations of BHI in 150 variants for each recording.

Data processing

BFV data were recorded and then exported for further analysis in Excel (Microsoft, Redmond, WA, USA). A customized program was written in the Python language (Python Software Fundation, Wilmington, Delaware, USA) to help with processing of the obtained velocity data at a sampling rate of 0.625 samples per second (1.6 Hz). During the experiment the beginning

and the end of the breath-hold maneuver were marked in the data set, so the data for further calculations were acquired simultaneously with the data used for the traditional BHI calculations.

Data analysis

The alternative methods of calculating BHI were implemented in the program and compared to the original method 'standard_BHI_value', which is the standard method for calculating the average percentage increase in arterial BFV compared to its original value. The initial value was determined manually by the diagnostician as the moment the test began. The value of the standard approach was determined by the following formula:

$$\mathrm{BHI} = \frac{(V|m,max - V_{m,b})}{\frac{V_{m,b}}{\Delta t}}$$, where:

- Vm, max – mean flow velocity at the end of the breath hold
- Vm, b – mean flow velocity at the baseline
- Δt – the duration of examination.

The calculations of the alternative methods were as follows:

- 'max_BHI_value'
  This approach analyzes the graph of BFV over time. The test start time can be adjusted slightly by the diagnostician and the time interval with the steepest slope is selected.
- 'BHI_to_max'
  The 'BHI_at_maximal_mean_val' is an inverse method to determine the maximum gradient of the graph's slope. It first finds the highest mean BFV within the allowed time window, then pairs it with the lowest value in the permitted range. The interval with the steepest slope is chosen.
- 'BHI_from_min'
  The 'maximal_BHI_from_minimal_mean_val' method selects the steepest slope starting from the lowest initial BFV within the allowed time range and ending at the test's specified endpoint.

For each method, the pre-set parameters were defined, including the minimum duration of the analyzed test, how many seconds ahead of the start (in case the participant reacted earlier than the voice command), and how many seconds after the standard beginning and end of the test the algorithm should search for the highest BHI (Figure 1). The sets of these results were subsequently collected for each patient and averaged. Later, the variance was used as a measure of the fit of the results. The variance was normalized according to the average results of a given patient as in the formula below:

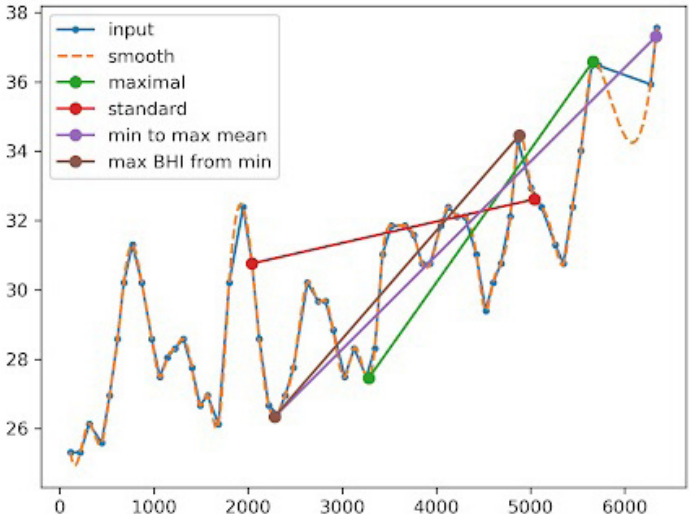

Figure 1. Representative raw traces of the mean flow velocity (MFV) during the resting state and during the breath-holding test
The red line marks the start and end of the procedure). The visualization in different colors of proposed alternative methods of calculating BHI (detailed description in the text). Input – raw data. The smooth dashed line represents cubic interpolation.

$$normalized\ variance_k = \frac{val_k}{avd_k} - 1$$, where:

- val_k is the value of the measurement from each method relative to the patient's measurements, for k being the key, represented as a list ['standard_BHI', 'max_BHI', 'BHI_to_max', 'BHI_from_min']
- $avd_k = \frac{1}{n_k} \sum_{i=1}^{n_k} val_k^i$

  within a patient for each analysed set of 4 relevant parameters (minimum_time, advance, delay, extension), where:
  - minimum_time – the earliest possible start of the exmination, determined by the diagnostician,
  - advance – the time before minimum_time when the program can start calculations,
- delay – the time between the actual end of the examination and its recorded endpoint,

- extension – the maximum time after the examination's end within which calculations can expand (Figure 2-5).

The five sets with the lowest normalized variance and lowest squared normalized variance are presented in graphs (Table 1).

Statistical analysis

The normality assumption of the data collected, resulting from their previous normalization, was confirmed using the Shapiro-Wilk statistical test. Levene's test and Cohen's Kappa were used to assess whether differences in variances across groups were

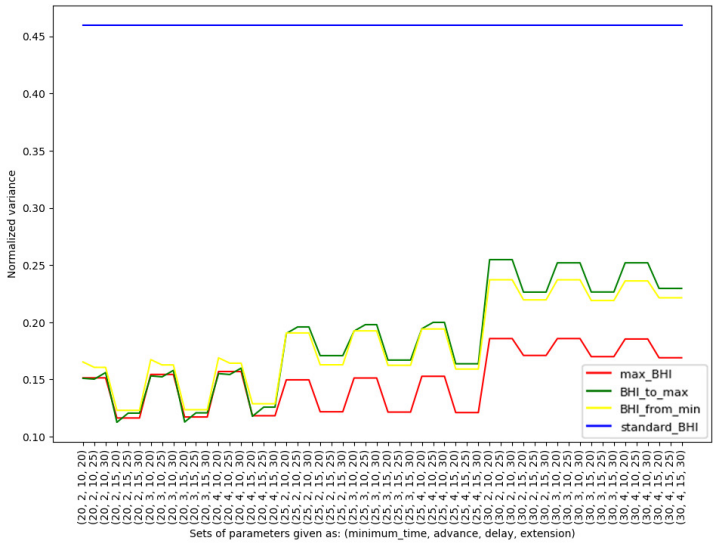

Figure 2. Normalized variance for each individual participant within specific methods (max_BHI, BHI_to_max, BHI_from_min, standard_BHI) against the parameters
The color of the graph corresponds to the methods described in the text.

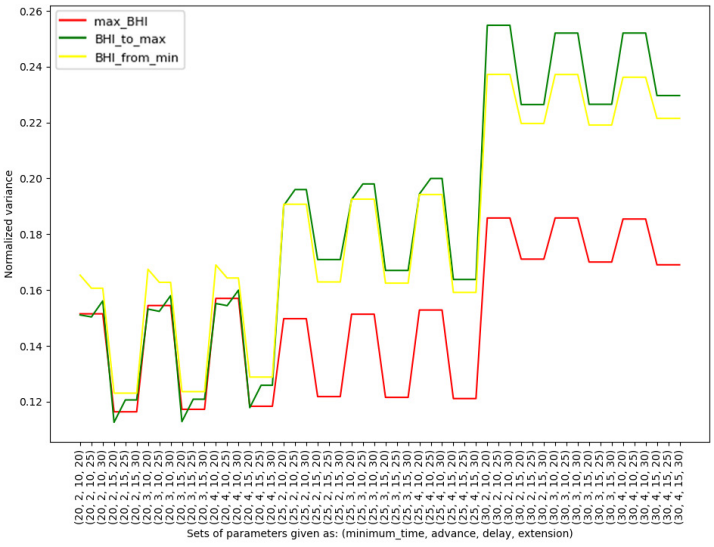

Figure 3. Normalized variance for each individual participant within specific methods (max_BHI, BHI_to_max, BHI_from_min) against the parameters
The color of the graph corresponds to the methods described in the text.

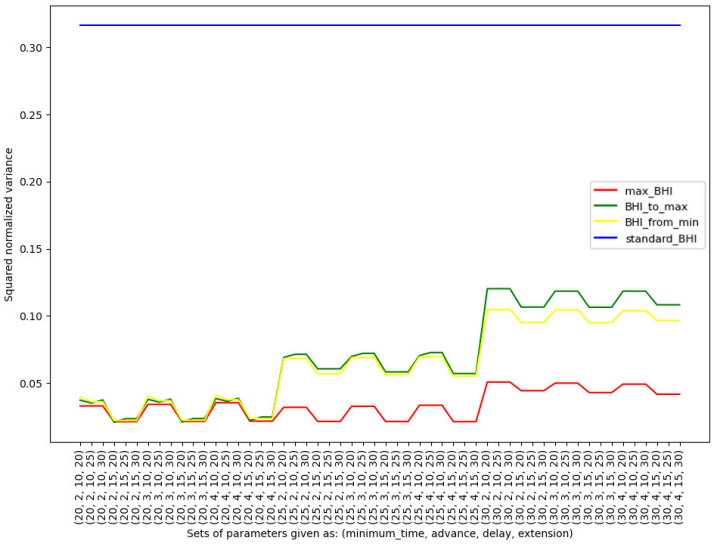

Figure 4. Squared normalized variance due to an individual participant together with specific methods (max_BHI, BHI_to_max, BHI_from_min, standard_BHI) and used parameters

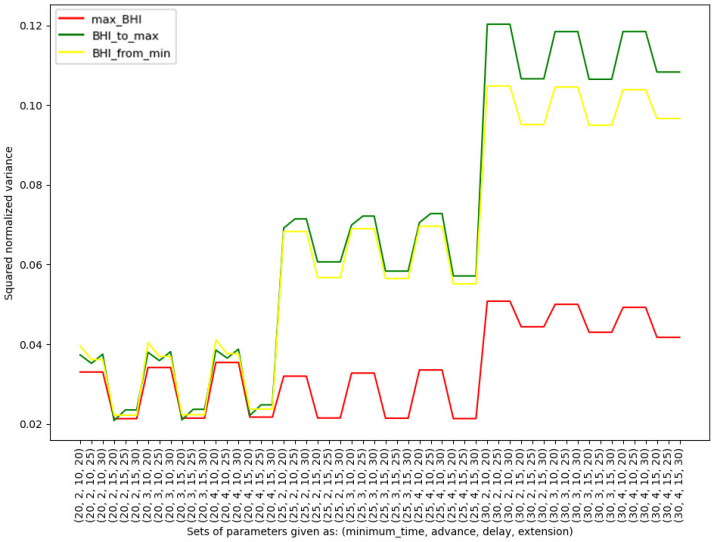

Figure 5. Squared normalized variance due to an individual participant together with specific methods (max_BHI, BHI_to_max, BHI_from_min) and used parameters
The 'standard_BHI' method was not included.

statistically significant and to measure the consistency between two diagnostic methods. For all the statistical tests the level of significance was set to be $\alpha = 0.05$ and compared to the p-values for each test.

Results

The best-performing sets of parameters for determining BHI were: Minimum_time = 20, Advance = 2, Delay = 15, Extension = 20, and Minimum_time = 20, Advance = 3, Delay = 15, Extension = 20. Values for each BHI calculation method for those parameters are shown in Figure 6 and Figure 7.The results of the normalized variances for the standard_BHI were identical for each set of parameters, therefore in the rest of this article the term 'standard_BHI' refers to the standard method for the following parameters: Minimum_time = 20, Advance = 2, Delay = 15 and Extension = 20. Despite normalization of data, the SD of the standard_BHI remained extremely high, which can be seen in performance overview of all analyzed methods showing mean and standard deviations (SD) (Table 2).

Levene's test revealed a statistically significant difference between the variances, demonstrating that each of the alternative methods is more effective for calculating BHI than the standard method for each of the five best-performing sets of parameters and methods (Table 3). This also confirmed the conclusions based on the results of Table 1: the lower the p-value of Levene's test, the better the alternative method performs in calculating the BHI. Subsequently, Cohen's coefficients were calculated between the standard method and the alternative methods, which show the poor fit of each alternative method for calculating BHI relative to the standard method (Table 3).

Discussion

In this study, we introduced 3 innovative approaches to data analysis, improving the standard method of measuring the BHI index using a breath-hold manoeuvre. These methods have demonstrated statistically significant smaller participant-specific normalized variance values compared to the standard BHI (Table 1). The most robust model, BHI_to_max, focuses on identifying the greatest

Table 1. Five sets of parameters and the names of their methods for which the normalized variance is the smallest

No.	Method	Normalized variance value	Squared normalized variance value	Minimum_time [s]	Advance [s]	Delay [s]	Extension [s]
1	'BHI_to_max'	0.1126	0.0209	20	2	15	20
2	'BHI_to_max'	0.1128	0.0210	20	3	15	20
3	'max_BHI'	0.1163	0.0213	20	2	15	20
4	'max_BHI'	0.1163	0.0213	20	2	15	25
5	'max_BHI'	0.1163	0.0213	20	2	15	30

Table 2. Methods of calculating BHI together with their mean values and standard deviations

No.	Method	Mean	Standard deviation
1	'standard'	1.0	0.5717
2	'BHI_to_max'	1.0	0.1463
3	'BHI_to_max'	1.0	0.1468
4	'max_BHI'	1.0	0.1480
5	'max_BHI'	1.0	0.1480
6	'max_BHI'	1.0	0.1480

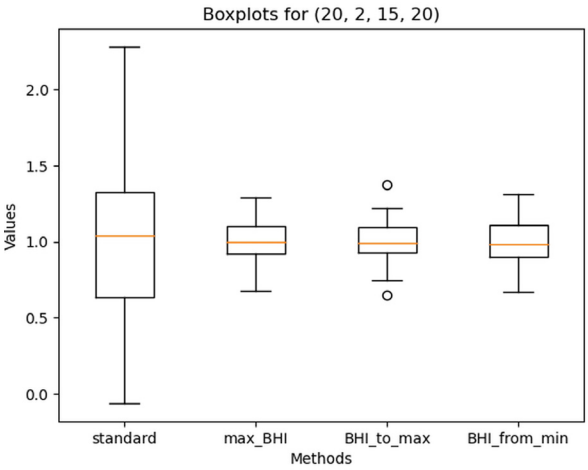

Figure 6. Boxplot of Breath holding index (BHI) calculated with different methods for the following parameters: Minimum_time = 20, Advance = 2, Delay = 15, Extension = 20
Standard – standard method, max_BHI – calculated according to the maximal BHI value approach, BHI_to_max calculated according to the 'BHI_at_maximal_mean_val' method and BHI_from_min calculated according to maximal_BHI_from_minimal_mean_val' approach. Dots – outlier values

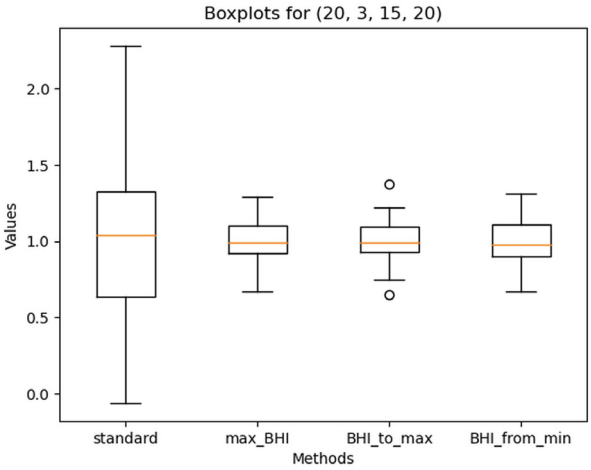

Figure 7. Boxplot of Breath holding index (BHI) calculated with different methods for the following parameters: Minimum_time = 20, Advance = 3, Delay = 15, Extension = 20
Standard – standard method, max_BHI – calculated according to the maximal BHI value approach, BHI_to_max calculated according to the 'BHI_at_maximal_mean_val' method and BHI_from_min calculated according to maximal_BHI_from_minimal_mean_val' approach. Dots – outlier values

Table 3. Comparison of five sets of parameters with lowest variance in comparison to standard method of BHI calculation using Levene's test and values of Cohen's kappa coefficient

No.	Method	Levene's test statistics	P-value	Cohen's kappa
1.	BHI_to_max (1st variant)	36.4210	8.0584E-08	0.20136
2.	BHI_to_max (2nd variant)	36.3364	8.2868E-08	0.20140
3.	max_BHI (1st variant)	35.7424	1.0092E-07	0.20150
4.	max_BHI (2nd variant)	35.7424	1.0092E-07	0.20150
5.	max_BHI (3rd variant)	35.7424	1.0092E-07	0.20150

slope angle for the calculations, with parameters presets: minimum_time = 20, Advance = 2, Delay = 15 and Extension = 20. This model is calculated based on a minimal time interval of 20 sec (out of 30 s standard ones), while also considering the possible shift of the starting point in time of 2 sec, delay of the ending point of maximum 15 sec and the maximum extension of the exam up to 20 seconds counting from the end of the breath-holding test.

The method we present, which essentially captures the steepest slope, can reveal the most dynamic phase of the cerebrovascular response to CO_2, offering a more precise and individualized assessment of CVR. This is a significant advancement, considering the individual variability in the threshold for CO_2-induced changes in CBF [19]. By identifying the steepest portion of the response curve with this method, we may provide a more measure of reproducible measure of CVR, similar to the approach of Alwatban et al., but with the added benefit of automatic optimization of starting or ending points [20]. This approach aligns with the observed variability among individuals and potentially offers a more refined tool for assessing CVR in each individual.

The model tested the effect of prolongation of trial duration (using the parameter Extension) and found that reproducibility of the acquired parameters was negatively affected with prolongation of the minimum analyzed time period above 20 seconds – all models had a higher variance between individual trials performed by the same proband. However, this can be linked to the set initially test length being 30 s. On the other hand, the reduction in the required time, allowed the measurement to be optimized in those participants who, even perhaps unintentionally, shortened or lengthened the test period in a way that was unnoticeable to the investigator. Reducing the required time should not affect the biological value of the test, since it is postulated that the breath-hold length is not strongly correlated with changes in partial pressure of CO_2 [21-22].

There is a lack of agreement on the protocols and methods for analyzing CVR. Some studies measured the peak MFV immediately, but not precisely describing how long, after the end of the period of breath-holding, while others assessed the peak during the breath-hold itself [8, 20-21]. Our approach circumvents these uncertainties by automatically considering a number of potential velocities in some extent from the above-mentioned points (switching the onset and/or ending of the test using such parameters as "Advance" and "Delay"), so as to select them in the most favorable way for the proband.

The introduction of the relatively simple but stable method, with would also be easy for the potential patient to tolerate is the main advantage of the presented automation of the calculation of the signal obtained during breath holding test. The automatic accurate identification of the steepest slope and adjustment for shifts simplifies the procedure, facilitating its adoption in clinical settings.

This study, while innovative in its approach to measuring CVR using an automatic calculation of the BHI, also has several limitations. The small sample size and design based on specific criteria and adjustments for starting and ending point shifts in just 8 participants are the most critical limitations. However, it should be emphasized that despite the small number of samples, it was possible to demonstrate lower variability in the results with repeated sampling than with the standardized approach to the BHI index. The participants were within a narrow age range and of the same ethnicity, the parameters may not be universally applicable across different populations, making it challenging to generalize the findings without extensive validation in diverse cohorts. Despite the automation of calculations, the accuracy of the method still relies on the patient's ability to perform the breath-holding maneuver consistently. However, shortening the analysed time seems to have strongly stabilized the repeatability of the sample, as it was shown as the significant lowering of the variability in results in comparison to standard BHI measure. We used an analogue capnograph to monitor the correctness of the test execution, however numerical data were not collected, accounting for the limitation. In this study we propose a new approach but it lacks comprehensive comparison and validation against existing CVR measurement techniques other than BHI. By focusing on optimizing the calculation method for the most dynamic phase of the cerebrovascular response, there is a risk of overfitting the model to specific patterns of response. This could lead to less robust performance when the method is applied to individuals with atypical cerebrovascular responses to CO_2-induced vasodilation. Finally, our study was performed on healthy volunteers, therefore its clinical value is limited and further studies that include patients with cerebrovascular conditions are needed to validate this methodology.

Conclusions

The proposed method of data analysis represents a step forward in the non-invasive assessment of cerebrovascular reactivity. It could improving the accuracy and reliability of CVR measurements. Additional research is required to address the method's limitations, validate its effectiveness across a broader range of patient populations with various cerebrovascular conditions and facilitate its integration into routine clinical practice.

Conflicts of interest

None.

Funding

Wroclaw Medical University (SUBZ.C220.24.053.2025) and the HeartBit 4.0 project.

References

1. Al-Khazraji BK, Shoemaker LN, Gati JS, Szekeres T, Shoemaker JK. Reactivity of larger intracranial arteries using 7 T MRI in young adults. J Cereb Blood Flow Metab [Internet]. 2019;39(7):1204–14. Available from: https://journals.sagepub.com/doi/10.1177/0271678X18762880
2. Hoiland RL, Ainslie PN. CrossTalk proposal: The middle cerebral artery diameter does change during alterations in arterial blood gases and blood pressure. J Physiol [Internet]. 2016;594(15):4073–5. Available from: https://physoc.onlinelibrary.wiley.com/doi/10.1113/JP271981
3. Brothers RM, Zhang R. CrossTalk opposing view: The middle cerebral artery diameter does not change during alterations in arterial blood gases and blood pressure. J Physiol [Internet]. 2016;594(15):4077–9. Available from: http://www.ncbi.nlm.nih.gov/pubmed/27010011
4. Terborg C, Gora F, Weiller C, Röther J. Reduced Vasomotor Reactivity in Cerebral Microangiopathy. Stroke [Internet]. 2000;31(4):924–9. Available from: https://doi.org/10.1161/01.STR.31.4.924
5. Pretnar-Oblak J, Sabovic M, Zaletel M. Associations between Systemic and Cerebral Endothelial Impairment Determined by Cerebrovascular Reactivity to Arginine. Endothelium [Internet]. 2007;14(2):73–80. Available from: http://www.tandfonline.com/doi/full/10.1080/10623320701346692
6. Karlsson WK, Sørensen CG, Kruuse C. l-arginine and l-NMMA for assessing cerebral endothelial dysfunction in ischaemic cerebrovascular disease: A systematic review. Clin Exp Pharmacol Physiol [Internet]. 2017;44(1):13–20. Available from: https://onlinelibrary.wiley.com/doi/10.1111/1440-1681.12679
7. Regenhardt RW, Nolan NM, Das AS, Mahajan R, Monk AD, LaRose SL, et al. Transcranial Doppler cerebrovascular reactivity: Thresholds for clinical significance in cerebrovascular disease. J Neuroimaging [Internet]. 2024;34(3):348–55. Available from: https://onlinelibrary.wiley.com/doi/10.1111/jon.13197
8. Markus HS, Harrison MJ. Estimation of cerebrovascular reactivity using transcranial Doppler, including the use of breath-holding as the vasodilatory stimulus. Stroke [Internet]. 1992;23(5):668–73. Available from: https://www.ahajournals.org/doi/10.1161/01.STR.23.5.668
9. Palazzo P, Maggio P, Passarelli F, Altavilla R, Altamura C, Pasqualetti P, et al. Lack of Correlation Between Cerebral Vasomotor Reactivity and Flow-Mediated Dilation in Subjects Without Vascular Disease. Ultrasound Med Biol [Internet]. 2013;39(1):10–5. Available from: https://linkinghub.elsevier.com/retrieve/pii/S0301562912005236
10. Haussen DC, Katsnelson M, Rodriguez A, Campo N, Campo-Bustillo I, Romano JG, et al. Moderate correlation between breath-holding and CO 2 inhalation/hyperventilation methods for transcranial doppler evaluation of cerebral vasoreactivity. J Clin Ultrasound [Internet]. 2012;40(9):554–8. Available from: https://onlinelibrary.wiley.com/doi/10.1002/jcu.21944
11. Tymko MM, Skow RJ, MacKay CM, Day TA. Steady-state tilt has no effect on cerebrovascular CO2 reactivity in anterior and posterior cerebral circulations. Exp Physiol. 2015;100(7):839–51.
12. Favre ME, Lim V, Falvo MJ, Serrador JM. Cerebrovascular reactivity and cerebral autoregulation are improved in the supine posture compared to upright in healthy men and women. PLoS One. 2020;15(3):1–20.
13. Webb AJS, Paolucci M, Mazzucco S, Li L, Rothwell PM. Confounding of Cerebral Blood Flow Velocity by Blood Pressure During Breath Holding or Hyperventilation in Transient Ischemic Attack or Stroke. Stroke [Internet]. 2020;51(2):468–74. Available from: https://www.ahajournals.org/doi/10.1161/STROKEAHA.119.027829
14. van Beek AH, Claassen JA, Rikkert MGO, Jansen RW. Cerebral Autoregulation: An Overview of Current Concepts and Methodology with Special Focus on the Elderly. J Cereb Blood Flow Metab [Internet]. 2008;28(6):1071–85. Available from: https://journals.sagepub.com/doi/10.1038/jcbfm.2008.13
15. Deegan BM, Sorond FA, Galica A, Lipsitz LA, O'Laighin G, Serrador JM. Elderly Women Regulate Brain Blood Flow Better Than Men Do. Stroke [Internet]. 2011;42(7):1988–93. Available from: https://www.ahajournals.org/doi/10.1161/STROKEAHA.110.605618
16. Kozera GM, Dubaniewicz M, Zdrojewski T, Madej-Dmochowska A, Mielczarek M, Wojczal J, et al. Cerebral Vasomotor Reactivity and Extent of White Matter Lesions in Middle-Aged Men With Arterial Hypertension: A Pilot Study. Am J Hypertens [Internet]. 2010;23(11):1198–203. Available from: https://academic.oup.com/ajh/article-lookup/doi/10.1038/ajh.2010.152

17. Settakis G, Páll D, Molnár C, Bereczki D, Csiba L, Fülesdi B. Cerebrovascular reactivity in hypertensive and healthy adolescents: TCD with vasodilatory challenge. J Neuroimaging. 2003;13(2):106–12. Available from: https://doi.org/10.1111/j.1552-6569.2003.tb00166.x
18. Jung K, Lee S, Lee T. A Breath-Holding Index Applied to the Internal Carotid Artery Siphon in Transcranial Doppler Studies. J Neuroimaging [Internet]. 2020;30(6):862–6. Available from: https://onlinelibrary.wiley.com/doi/10.1111/jon.12752
19. Porter A, Burger M, Alwatban M, Hage B, Bashford GR. Analysis of Breath-Holding Index as an Assessment of Cerebrovascular Reactivity [Internet]. 2016. Available from: https://digitalcommons.unl.edu/ucarere-search/89/
20. Alwatban M, Truemper EJ, Al-rethaia A, Murman DL, Bashford GR. The Breath-Hold Acceleration Index: A New Method to Evaluate Cerebrovascular Reactivity using Transcranial Doppler. J Neuroimaging [Internet]. 2018;28(4):429–35. Available from: https://onlinelibrary.wiley.com/doi/10.1111/jon.12508
21. Settakis G, Lengyel A, Molnár C, Bereczki D, Csiba L, Fülesdi B. Transcranial Doppler study of the cerebral hemodynamic changes during breath-holding and hyperventilation tests. J Neuroimaging [Internet]. 2002;12(3):252–8. Available from: http://www.ncbi.nlm.nih.gov/pubmed/12116744

EUROPEAN JOURNAL OF TRANSLATIONAL
AND CLINICAL MEDICINE 2025;8(1):19-31

RESEARCH ARTICLE

Role of zinc and vitamin D in modulating diabetic nephropathy in experimental models

Mahmoud Fadl Bakr[1], Mahmoud A. Elrehany[2], Othman A. Othman[1]

[1] Biochemistry Division, Chemistry Department, Faculty of Science, Minia University, El-Minia, Egypt
[2] Biochemistry Department, Faculty of Medicine, Minia University, El-Minia, Egypt

Abstract

Background: Diabetes mellitus (DM) manifests itself in consistently high blood glucose concentrations as a result of insufficient insulin secretion, action, or both. This can result in long-term complications, including diabetic nephropathy (DN). The aim of this study was to examine the impact of a four-week administration of zinc sulfate (Zn) and vitamin D (Vit D) in controlling glycemia and preventing renal damage in an experimental model of DM. **Material and methods**: A total of 55 rats, each weighing between 100 and 150 grams, were grouped into 11 groups: diabetic control rats, healthy control rats, and diabetic rats that had received Zn, Vit D and metformin as reference medication before and after alloxan injection. **Results:** DM induced by alloxan led to notable rises in blood urea nitrogen, creatinine and uric acid concentrations. Moreover, it caused damage to kidney tissues, with severe morphological damage in the renal tissues of diabetic rats. Elevated levels of kidney function markers and other biochemical parameters were decreased by administering zinc and Vit D, but Zn produced the greatest reduction. Additionally, histopathological examination of the excised kidneys revealed increased protection following supplementation. **Conclusions:** The findings of this study suggest that Zn and Vit D are effective in managing DM and protecting against DN.

Keywords: diabetes mellitus · zinc · vitamin D · nephropathy · caspase-3

Citation

Bakr MF, Elrehany MA, Othman OA. Role of zinc and vitamin D in modulating diabetic nephropathy in experimental models. Eur J Transl Clin Med. 2025;8(1):19-31.

DOI: 10.31373/ejtcm/204524

Corresponding author:
Mahmoud Fadl Bakr, Biochemistry Division, Chemistry Department, Faculty of Science, Minia University, 61519, El-Minia, Egypt
e-mail: mahmoud.fadl@mu.edu.eg
Available online: ejtcm.gumed.edu.pl

Introduction

Diabetes mellitus (DM) is a complicated, multi-causal and chronic condition manifested by increased levels of blood sugar (hyperglycemia). It is characterized by a total or partial decrease of insulin synthesis or secretion by β-cells of the pancreas, in addition to its inability to produce normal physiological effects [1].

By specifically inhibiting glucokinase, the β-cells' sensor of glucose, insulin release induced by glucose is selectively inhibited by alloxan. Additionally, alloxan causes reactive oxygen species (ROS) to generate, which leads selective necrosis of β-cells and the development of IDDM. The preferential cellular uptake and alloxan accumulation by β-cells is the common denominator between these two pathways. This is explained by the unique chemical properties of alloxan [2].

Hyperglycemia induces oxidative and nitrosative stress in various cell types, leading to the generation of reactive species like superoxide, nitric oxide, and peroxynitrite. These ROS contribute to apoptotic cell death, which is associated with diabetes mellitus complications such as nephropathy, neuropathy, and cardiovascular disease. Key proteins involved in this process include caspases and BCL-2 family members [3].

Diabetic nephropathy (DN) is a microvascular complication of diabetes that ultimately results in end-stage renal disease [4]. Because DN is a common cause of chronic kidney disease (CKD), dialysis patients with DM have a greater death rate than patients without the disease [5]. Thus, effective antioxidants might be effective in the treatment of disorders associated with DM [6].

DN is caused by the interplay of metabolic and hemodynamic variables [7]. Increased intraglomerular and systemic pressure, as well as the activation of vasoactive hormone pathways, such as the renin-angiotensin system (RAS) and endothelin, are hemodynamic factors that lead to the development of DN [8-9]. In the diabetic kidney, glucose-dependent pathways are also triggered, leading to increased oxidative stress, the production of renal polyol [10], and the buildup of advanced glycation end products (AGEs) [11]. When these mechanisms work together, they eventually result in increased extracellular matrix accumulation and renal albumin permeability, which leads to proteinuria, glomerulosclerosis, and tubulointerstitial fibrosis.

Zinc sulfate (Zn) is a necessary trace element that maintains many of the body's cellular processes. Zn plays a vital role in facilitating the transport of glucose into cells, as well as in improving glucose storage, insulin crystallization and signaling, which is necessary for glucose metabolism. When Zn supplementation was administered to rats with DN, proteinuria, fibrosis, and renal oxidative stress were all reduced, protecting kidney structure and function [12-15].

Vitamin D (Vit D) is one of the fat-soluble vitamins [16]. There is a long history of the use of various Vit D derivatives in the management of renal disorders and some research studies have indicated that Vit D compounds may reduce the death rate in CKD [17]. Furthermore, Vit D helps maintain low resting levels of free radicals and ROS, normalizes Ca2+ signaling, reduces the expression of pro-inflammatory cytokines, and increases the production of anti-inflammatory cytokines [18].

Numerous studies have shown that oxidative stress (excess free radicals) contributes to the development of DM, reduces insulin function, and increases the risk of DM complications, therefore antioxidants have already demonstrated promise in the management of T1D and T2D [19]. The aim of this study was to examine the impact of a 4-week administration of Zn and Vit D in controlling glucose levels and preventing renal damage.

Material and methods

Animals

Adult male albino rats, weighing 100 to 150 g, were obtained from the National Research Center in Giza (Egypt) and kept in the animal house of the Faculty of Pharmacy in Deraya University (El-Minia, Egypt). A 12-hour cycle of light and dark and constant environmental factors (humidity 50% ± 10%, temperature 23 °C ± 3 °C) were provided. During the experiment, the rats were allowed free access to water and a standard chow diet, unless otherwise stated. For two weeks before the experimental procedures, the animals were kept in separate aerated cages to acclimate to the new environment and ensure they were disease-free.

Experimental design

The current study was performed in accordance with the international guidelines regarding animal experiments [20]. A total of 55 adult male albino rats were divided randomly into eleven groups (n = 5 for each) as follows:

- Group 1: healthy controls receiving normal saline only.
- Group 2: diabetic controls receiving a solution of alloxan monohydrate.
- Group 3: healthy controls treated with Zn only.
- Group 4: healthy controls treated with Vit D only.
- Group 5: healthy controls treated with metformin only.
- Group 6: diabetic post-treated with Zn.
- Group 7: diabetic post-treated with Vit D.
- Group 8: diabetic post-treated with metformin.
- Group 9: diabetic pre-treated with Zn.

- Group 10: diabetic pre-treated with Vit D.
- Group 11: diabetic pre-treated with metformin.

Chemicals and drugs

Alloxan monohydrate, metformin (Glucophage 500 mg/tablet), Zinc sulfate (Octozinc 110 mg/capsule) and vitamin D (Vi drop 2800 unit/ml) were obtained from Loba Chemie Pvt Ltd (India), Mina Pharm (Egypt), October Pharma S.A.E and Medical Union Pharmaceuticals (Egypt), respectively. The administered drugs were freshly prepared daily for 28 days except for alloxan, which was freshly prepared once before and after the experiment. Metformin (120 mg/kg BW), Zn (100 mg/kg BW) and Vit D solution (10 IU/kg BW) were administered orally using an oral gavage feeding needle, whereas the alloxan solution was injected intraperitoneally with an insulin syringe, while the rat was held securely to avoid harming it [21-23].

Induction of diabetes

Since alloxan is less stable when dissolved and its half-life is short (1.5 minutes at pH 7.4 and 37 °C), the rats (apart from the control groups) underwent overnight fasting and were given a single dose (150 mg/kg BW) of freshly prepared alloxan immediately after dissolving in 0.9% saline solution [24]. Then, in order to overcome the alloxan-induced hypoglycemia (due to the large pancreatic insulin release following beta cell damage), the rats were given free access to a glucose solution (5%) for 24 hours [21, 25]. A glucometer (PreciChek Autocode, AC-302, Germany) and compatible test strips of blood glucose were used to measure the rats' fasting glycemia after 3 days in order to confirm that DM had been successfully induced. Blood was collected from the tail vein. In this study, only rats with fasting blood glucose levels exceeding 250 mg/dl were selected as diabetics [26].

Blood sample collection and dissection

Four weeks following treatment, the rats were decapitated after fasting overnight. Their blood was then collected in sterile centrifuge tubes, allowed to coagulate for 30 min at room temperature, and then centrifuged at 4000 rpm for 10 min (Z 200 A, Hermle LaborTechnik GmbH, Germany). The obtained serum (supernatant) was then stored at –80° C immediately after separation for biochemical analysis. Finally, each rat's abdomen was dissected, the right kidney was rapidly excised, weighed, and subsequently stored in formaline solution for histopathological examinations.

Biochemical analysis

- Glucose and Kidney function markers

Glucose, creatinine, blood urea nitrogen (BUN) and uric acid were assessed using colorimetric assay kits (purchased from Spectrum Diagnostics in Cairo, Egypt) by a semi-automated chemistry analyzer (SK3002B, Sinothinker Technology Co. Limited, Shenzen, China).

- Glucose

In the presence of glucose oxidase, glucose is measured following enzymatic oxidation. Under the catalytic action of peroxidase (PAP), the generated hydrogen peroxide combines with phenol and 4-aminoantipyrine to generate a red violet quinoneimine dye that serves as an indicator.

- Creatinine

Creatinine reacts with picric acid in alkaline solution to form a colored complex.

- Blood urea nitrogen

Urea hydrolyzes in water to release carbon dioxide and ammonia. In an alkaline pH, free ammonia forms a colored complex that is proportionate to the specimen's urea concentration when an indicator is present.

- Uric Acid

Uric acid is oxidized to allantoin by uricase with the production of hydrogen peroxide. The peroxide reacts with 4-amino-antipyrine and (DCHB) in the presence of peroxidase to yield a quinoneimine dye.

Apoptotic markers

β-cell lymphoma 2 (BCL-2) and caspase 3 (CASP-3) ELISA kits were purchased from Elabscience, Texas, USA. These markers were determined using an ELISA System (ChroMate SF 4300 Microplate Reader, Awareness Technology, Palm City, FL, USA). Both ELISA kits use the Sandwich-ELISA method. The microplate is pre-coated with an antibody specific to BCL-2 or CASP-3, and samples or standards were added to the wells. A biotinylated detection antibody and Avidin-HRP conjugate were then added, followed by incubation. After washing away unbound components, a substrate solution was added, resulting in a color change in the wells containing BCL-2 or CASP-3. The optical density (OD) at 450 nm was measured, which is proportional to the BCL-2 or CASP-3 concentration.

Histopathological examination

The right kidney from each experimental rat was washed with 0.9% saline solution and instantly fixed in a solution of formalin (10%) prepared in saline for 3 days. Then the organ was washed, dehydrated in increasing ethanol grades from 70% to absolute, cleared in xylene, impregnated and embedded in paraffin wax. Serial sections (5 μm thick) were obtained

using a microtome and stained with hematoxylin and eosin (H&E) for histopathological examination using a light microscope equipped with a digital camera (Olympus, Japan) [27].

Statistical Analysis

The Statistical Package for Social Sciences (SPSS) software (version 26.0, IBM, Armonk, NY, United States) was used to perform the statistical analyses. The mean of the results ± standard deviation (SD) was presented. Differences of $p < 0.05$, $p < 0.01$ or $p < 0.001$ were accepted as significant, moderately significant or highly significant, respectively. Insignificant is denoted by the symbol (#), significant by the symbol (*), moderately significant by the symbol (**), and highly significant by the symbol (***).

Results

Effects of zinc, vitamin D and metformin administration on blood glucose levels

The effects of the oral administration of Zn and Vit D on fasting blood glucose are presented in Table 1. The experimentally induced DM caused a highly significant ($p > 0.001$) increase in the level of fasting glucose in the diabetic control group (2) compared to the control levels of healthy groups. However, post and pre-treatment with Zn and Vit D caused a highly significant ($p > 0.001$) reduction in the fasting glucose levels of the alloxan-diabetic rats of groups (6, 7, 9 and 10) compared with the diabetic control group (2), as shown in Figure 1A. However, the rats in the post-treated groups (6 and 9) showed a higher reduction of glycemia than the pre-treated groups (7 and 10).

Effects of zinc, vitamin D and metformin administration on selected kidney function markers

The experimental rats' serum kidney function marker concentrations were measured and summarized in Table 1. In alloxan-diabetic rats of group (2), the concentrations of serum creatinine, blood urea nitrogen (BUN) and uric acid underwent a highly significant ($p > 0.001$) increase compared to the healthy control groups (Figure 1 B-D). On the other hand, post-treatment of the diabetic rats with Zn and Vit D caused a highly significant ($p > 0.001$) reduction in the concentrations of these markers in the serum of groups (6 and 7) compared to the mean values of the diabetic control group (2), except for uric acid levels in rats of group (7), which underwent a moderately significant ($p > 0.01$) reduction. However, pre-treatment with Zn and Vit D resulted in a highly significant ($p > 0.01$) reduction in the BUN level of groups (9 and 10), a significant ($p > 0.05$) reduction in the creatinine and uric acid levels of

Table 1. Mean glycemia before & after the experiment and mean of selected kidney function markers concentrations in experimental rats after administration of alloxan and test drugs

Group	Pancreatic function		Kidney function		
	Initial FBS (mg/dl)	Final FBS (mg/dl)	Creatinine (mg/dl)	BUN (mg/dl)	Uric Acid (mg/dl)
1	104.98 ± 2.45	106 ± 0.73	0.89 ± 0.07	10.98 ± 2.06	3.29 ± 0.24
2	267 ± 1.55	307*** ± 1.67	1.7*** ± 0.09	60.44*** ± 3.15	4.1*** ± 0.16
3	112.1 ± 2.45	110.02 ± 1.89	0.9 ± 0.11	11.1 ± 0.54	3.31 ± 0.11
4	106 ± 1.89	106 ± 1.76	0.85 ± 0.05	10.91 ± 1.77	3.3 ± 0.18
5	101.04 ± 2.19	95 ± 2.35	0.97 ± 0.04	11.49 ± 0.66	3.36 ± 0.23
6	258 ± 2.28	189*** ± 1.99	1.29*** ± 0.07	41.58*** ± 0.88	3.54*** ± 0.09
7	264 ± 1.30	215.03*** ± 2.10	1,46*** ± 0.03	49.4*** ± 2.10	3.61** ± 0.07
8	254 ± 1.40	115 ± 1.79	1.07 ± 0.09	16.8 ± 1.18	3.43 ± 0.12
9	109 ± 1.27	205*** ± 1.70	1.53* ± 0.08	46.01*** ± 1.14	3.68* ± 0.13
10	102 ± 1.41	237.01*** ± 1.30	1.57# ± 0.04	51.2*** ± 0.76	3.76# ± 0.07
11	106 ± 1.45	244 ± 2.00	1.62 ± 0.04	52.03 ± 1.58	3.8 ± 0.12

All values are expressed as mean ± standard deviation of 5 rats from each group.
BUN – blood urea nitrogen, FBS – fasting blood sugar

group (9) and an insignificant ($p > 0.05$) reduction in the creatinine and uric acid levels of group (10).

Effects of zinc, vitamin D and metformin administration on apoptotic markers

As shown in Table 2 & Figure 1E-F, the 2 apoptotic markers we investigated were affected by the alloxan injection. The diabetic control group (2) showed a highly significant ($p < 0.001$) increase in levels of CASP-3 and decrease in levels of BCL-2 compared to the healthy control groups (1, 3, 4 and 5). However, post and pre-treatment with Zn and Vit D insignificantly ($p < 0.05$) increased the levels of BCL-2, significantly ($p < 0.05$) decreased the levels of CASP-3 in groups (6, 9 and 10) and insignificantly ($p > 0.05$) decreased the CASP-3 levels in group (7). Thus, the administration of Zn and Vit D reversed the levels of apoptotic makers compared to the diabetic control group (2).

Effects of zinc, vitamin D and metformin administration on renal tissues

Our study also showed that alloxan-induced DM in the rats of group (2) caused damage to the renal structures while the healthy control groups (1, 3, 4 and 5) showed no significant pathological changes. Histological sections of the kidney excised from the diabetic group (2) showed congested glomerular capillary tuft, congested blood vessels and interstitial haemorrhage with signs of renal tubular injury (Figure 2B). In contrast, sections of healthy groups' kidneys (1, 3, 4 and 5) showed normal glomeruli and normal renal tubules (Figure 2A, Figure 2C-E). However, sections obtained from post and pre-treated diabetic rats of groups (6, 7, 9 and 10) with Zn and Vit D showed reduced glomeruli congestion and necrosis, normal tubules, dilated Bowman's space, and some had signs of renal tubular injury (Figure 2F-G, 2I-K), compared to the diabetic control group (2).

Discussion

DN is caused by renal tissue destruction resulting from toxic levels of elevated blood sugar. Patients with DM experience impaired kidney function due to hemodynamic alterations in renal tissue caused by hyperglycemia and glycosylated proteins, linked to increased oxidative stress [28]. In our study, injection of alloxan in Group 2 induced hyperglycemia and significantly elevated serum glucose levels compared to the healthy control (Group 1), supporting previous findings that chronic hyperglycemia leads to pathological renal changes such as tubulointerstitial alterations and thickening of the tubular basement membrane, which is further characterized by

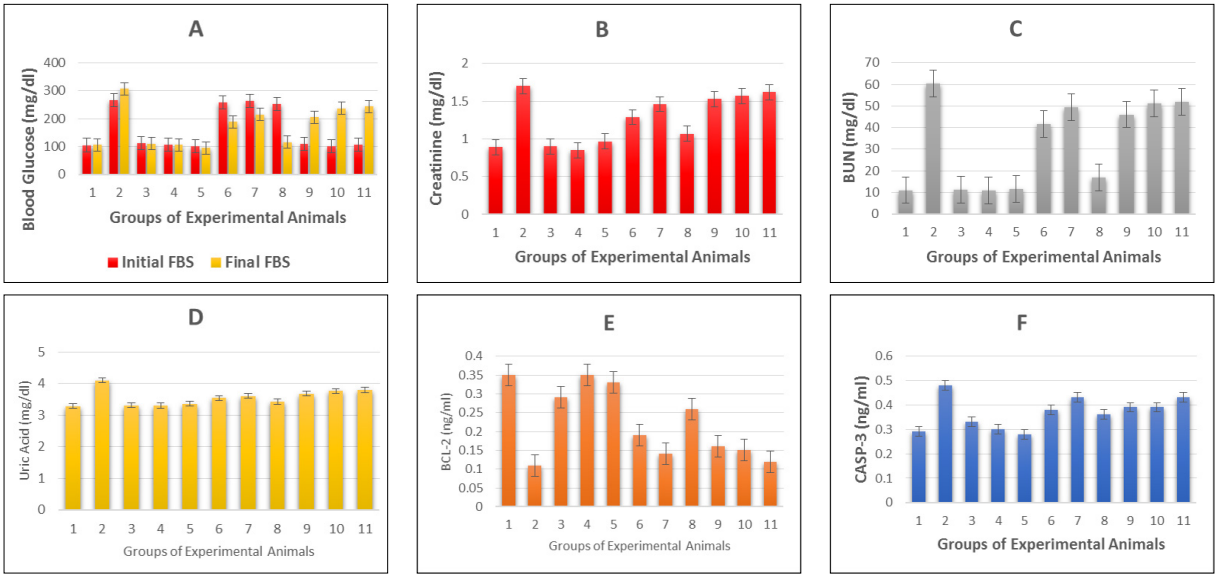

Figure 1. Illustrates effect of metformin, zinc and vitamin D administration either before alloxan injection (prophylactic) or after injection (therapeutic) on:
1A. the initial fasting blood sugar (3 days after alloxan injection) and final fasting blood sugar (28 days after test drugs administration) of alloxan-induced diabetic rats
1B. creatinine levels of alloxan-induced diabetic rats
1C. blood urea nitrogen (BUN) levels of alloxan-induced diabetic rats
1D. uric acid levels of alloxan-induced diabetic rats
1E. β-cell lymphoma 2 (BCL-2) levels of alloxan-induced diabetic rats
1F. caspase 3 levels of alloxan-induced diabetic rats

Table 2. Mean of some apoptotic markers concentrations in experimental rats after administration of alloxan and test drugs

Group	Apoptosis markers	
	BCL-2 (ng/ml)	CASP-3 (ng/ml)
1	0.35 ± 0.06	0.29 ± 0.05
2	0.11*** ± 0.03	0.48*** ± 0.04
3	0.29 ± 0.06	0.33 ± 0.04
4	0.35 ± 0.06	0.3 ± 0.03
5	0.33 ± 0.03	0.28 ± 0.02
6	0.19# ± 0.03	0.38* ± 0.02
7	0.14# ± 0.05	0.43# ± 0.05
8	0.26 ± 0.04	0.36 ± 0.04
9	0.16# ± 0.02	0.39* ± 0.11
10	0.15# ± 0.03	0.39* ± 0.04
11	0.12 ± 0.02	0.43 ± 0.03

All values are expressed as mean ± standard deviation of 5 rats from each group.
BCL-2 – β-cell lymphoma 2, CASP-3 – caspase 3

the accumulation of matrix protein, tubular and glomerular hypertrophy, and renal hypertrophy [29].

Numerous complications of DM, including DN, are linked to oxidative stress triggered by hyperglycemia [30]. Chronic hyperglycemia in renal tissues leads to oxidative stress and release of ROS, which activate the nuclear transcription factor (NF-κB), thereby promoting kidney inflammation [31]. In agreement with these mechanisms, our diabetic control group (Group 2) exhibited significant increases in markers of renal damage, such as creatinine, blood urea nitrogen (BUN), uric acid, and CASP-3, while BCL-2 was reduced, indicating enhanced apoptosis due to oxidative damage. These findings align with the established role of ROS and oxidative stress in promoting renal fibrosis and end-stage renal disease (ESRD) through extracellular matrix (ECM) accumulation and glomerulosclerosis which is associated with deteriorating renal function [32-33].

Sustained hyperglycemia contributes to nephropathy through multiple cellular mechanisms, such as PKC pathway activation, the generation of cytokines, enhanced polyol pathways, the increased formation of AGEs, increased oxidative stress, and the hexosamine pathway [34]. In our study, the deleterious renal effects observed in Group 2 further confirm the damaging impact of these pathways, as shown by significant biochemical and apoptotic alterations. Furthermore, DM-related hyperglycemia damages mitochondria and raises reactive free radicals, which in turn damages DNA and triggers the apoptosis process. Additionally, hyperglycemia raises lipid peroxidation, glutathione (GSH) oxidation, and oxidative stress. Lastly, hyperglycemia causes diabetic nephrons to experience oxidative stress, which stimulates a number of biochemical mechanisms that result in the death of renal cells, elevated albuminuria, and kidney failure that were likely contributors to the observed elevation of apoptotic markers such as CASP-3 [35].

Among diabetic patients, DN remains a leading cause of renal failure [36]. Chronic low-grade inflammation and activation of the innate immune system play critical roles in DN progression [37]. Our findings, showing elevated CASP-3 and reduced BCL-2 in diabetic controls, are consistent with reports that TNF-α and other pro-inflammatory cytokines promote renal injury by inducing apoptosis and necrotic cell death [38-40].

DN has a complicated etiology involves direct effects of extracellular glucose on renal cells, activating growth factors and cytokines like monocyte chemoattractant protein (MCP)-1, transforming growth factor-b (TGF-b), and angiotensin II (Ang II), which further mediate development of DN [41-43]. The role of the renin-angiotensin system (RAS) in DN is well established, with intrarenal Ang II levels contributing significantly to glomerulosclerosis and fibrosis. So, It is thought that intrarenal RAS plays a primary injurious role in causing kidney

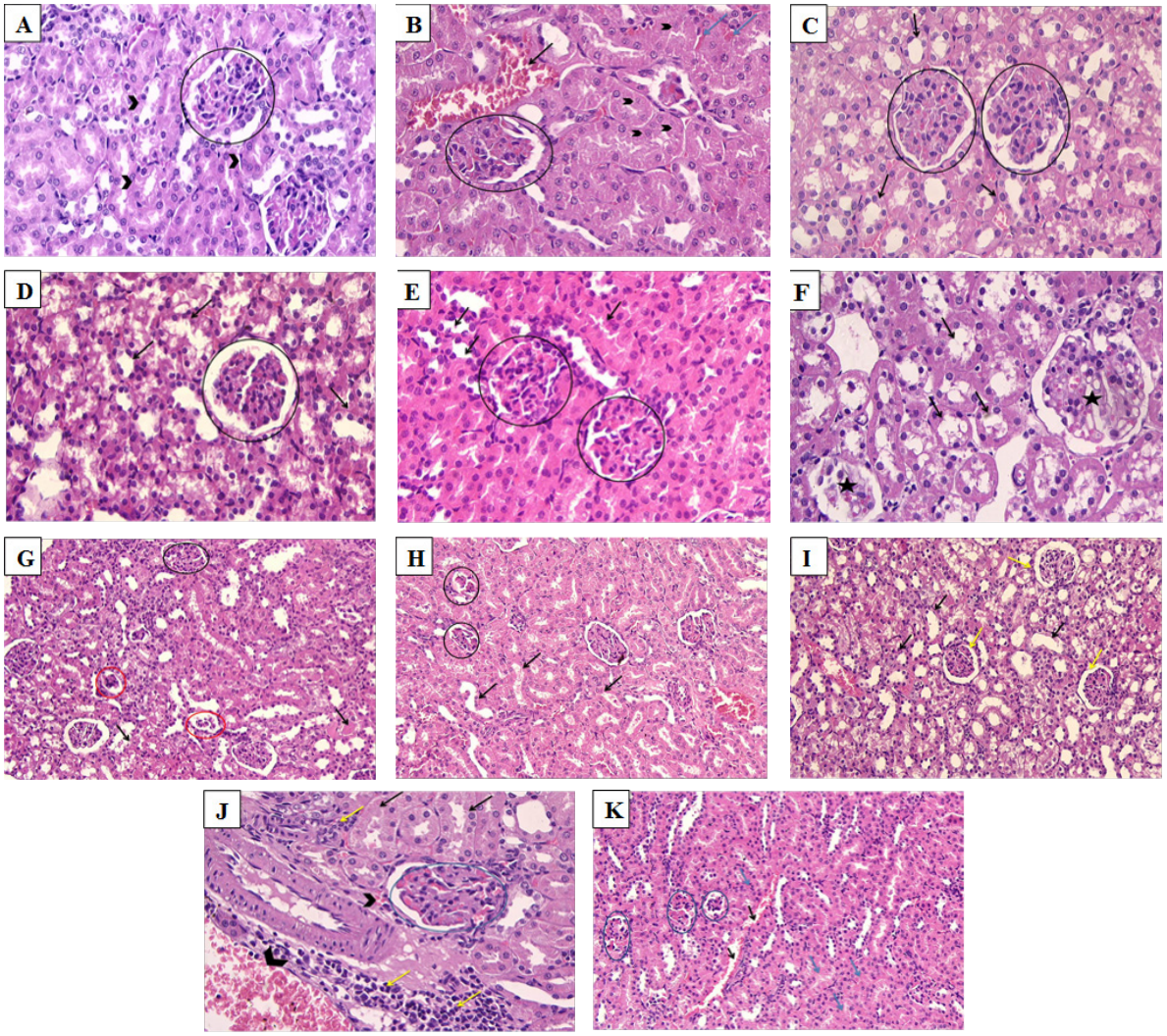

Figure 2A. Photomicrographs of rat renal tissues of healthy control group showing normal glomeruli (black circles) and normal renal tubules (black arrow head) × 400
Figure 2B. Photomicrographs of rat renal tissues of diabetic control group showing congested glomerular capillary tuft (black circle), congested blood vessels (black arrow), interstitial haemorrhage (blue arrows) with signs of renal tubular injury and necrosis (arrow head) × 400
Figure 2C. Photomicrographs of rat renal tissues of healthy control group treated with zinc sulfate only showing normal glomeruli (circle) and normal renal tubules (arrows) × 400
Figure 2D. Photomicrographs of rat renal tissues of healthy control group treated with vitamin D only showing normal glomeruli (circle) and normal renal tubules (black arrows) × 400
Figure 2E. Photomicrographs of rat renal tissues of healthy control group treated with metformin only showing normal looking glomeruli (circles) and tubules (arrows) × 400
Figure 2F. Photomicrographs of rat renal tissues of diabetic group post-treated with zinc sulfate showing normal glomeruli (star) and normal tubules (arrows) × 400
Figure 2G. Photomicrographs of rat renal tissues of diabetic group post-treated with vitamin D showing some glomeruli are normal (black circle) while others are necrotic or sclerotic (red circles) with dilated Bowman's space, some tubules show signs of renal tubular injury (black arrow) × 200
Figure 2H. Photomicrographs of rat renal tissues of diabetic group post-treated with metformin showing some atrophic glomeruli (black circle), mild cloudy swelling of renal tubular epithelium (black arrow) × 200
Figure 2I. Photomicrographs of rat renal tissues of diabetic group pre-treated with zinc sulfate showing normal glomeruli (yellow arrows) and renal tubules (black arrows) × 200
Figure 2J. Photomicrographs of rat renal tissues of diabetic group pre-treated with vitamin D showing congested glomerular tuft (blue circle), signs of renal tubular injury and cloudy swelling (black arrows), interstitial haemorrhage (arrow head) and chronic inflammatory cellular infiltrate (yellow arrows) × 400
Figure 2K. Photomicrographs of rat renal tissues of diabetic group pre-treated with metformin showing congested or atrophic renal glomeruli (blue circles), interstitial haemorrhage (black arrows), moderate cloud swelling of renal tubular epithelium (blue arrows) × 200

damage [44-45]. Our study supports these concepts indirectly by demonstrating that unregulated diabetes induced by alloxan led to substantial renal damage, which could be associated with the known effects of elevated Ang II on promoting inflammation, cell proliferation, and fibrosis [41, 46].

Given the critical role of oxidative stress and inflammation in DN, attention has been directed towards potential nephroprotective agents, such as zinc (Zn). Zn is a vital cofactor for over 300 enzymes and plays a crucial role in antioxidant defense [47]. Zn deficiency has been linked to increased susceptibility to infections and elevated ROS generation [48], which aligns with the observed exacerbation of oxidative damage in the diabetic group of our study.

Necessity of Zn for superoxide dismutase activation, a potent antioxidant enzyme [49], underlines its antioxidant role. Low serum Zn concentrations have been associated with higher incidences of DM, glucose tolerance and cardiovascular diseases [50]. The administration of Zn in our study, both as treatment (Group 6) and prophylaxis (Group 9), significantly improved glycemic control and reduced markers of renal dysfunction compared to the diabetic group. These results are consistent with previous findings that restoring Zn status mitigates oxidative stress and prevents complications related to DM [51].

Zn facilitates glucose transporter 4 (GLUT4) translocation and insulin receptor β-subunit phosphorylation [52-53], both crucial for glucose metabolism. Furthermore, Zn ions are vital for insulin hexamer formation, while insulin combines with two Zn ions to form a hexameric structure, which is required for insulin to mature inside pancreatic β-cell secretory granules and release insulin [54-55]. Certain Zn carrier proteins that are essential for insulin release are expressed by pancreatic β-cells [56-58]. One such important protein is ZnT8, which is necessary for the general metabolism of glucose as well as the crystallization, processing, storage and secretion of insulin [59-62]. Moreover, the Zn transporter protein ZnT7 is in charge of delivering Zn to the pancreatic β-cells' Golgi apparatus, which is a necessary step for the correct synthesis of insulin [63-64]. Our observation that Zn supplementation improved glycemic parameters and renal function supports the established role of Zn in enhancing insulin secretion and action.

Supplementing with Zn decreased the rate of renal damage in comparison to the control groups by activating metallothionein, a cysteine-rich protein that interacts with Zn and iron to reduce ROS and, in turn, the oxidation process [65-67]. Another key mechanism by which Zn can protect the kidneys from chronic hyperglycemia-induced damage is through apoptotic regulation. Zn supplementation in our study reduced serum CASP-3 and elevated BCL-2 levels compared to the diabetic group, indicating its anti-apoptotic properties. Previous studies have demonstrated that Zn reduces apoptosis by the inhibition of CASP-3 and promoting BCL-2 expression [68].

Similar protective effects were observed with vitamin D (Vit D) administration. Vit D, acting primarily through its receptor in renal tissues, has been reported to exert nephroprotective effects in diabetic models [69]. In our study, both treatment (Group 7) and prophylaxis (Group 10) with Vit D improved serum glucose levels and renal function markers, consistent with studies linking optimal Vit D levels to better glucose homeostasis and insulin sensitivity [70-71].

Vit D's nephroprotective mechanisms include enhancing glucose metabolism, inhibiting the renin-angiotensin system, blocking oxidative stress pathways, and reducing the production of inflammatory mediators like TNF-α and IL-6 [72-73]. Our observation of reduced renal injury with Vit D treatment supports previous findings that Vit D modulates RAS activity and protects against DN by regulating BCL-2 and CASP-3 expression [74].

The nephroprotective properties of Vit D may be attributed to several mechanisms, including suppressing the RAS and inhibiting inflammatory cytokines and profibrotic growth factors. First, TGF-β and CTGF, which are crucial mediators for the formation of sclerosis in DN, may be targeted by 1,25(OH)2D3 [45, 75-76]. Second, the nephroprotective effects of Vit D may also be linked to its control of the RAS, specifically renin [77]. DM causes an increase in the intrarenal RAS activity, which is crucial for the onset of diabetic nephropathy [78-79]. Ang II causes mesangial and tubular cells to produce more ECM proteins and express TGF-β [80]. Additionally, Ang II causes glomerular damage and increases glomerular permeability, which results in proteinuria. It has been noted that diabetic nephropathy can be improved by inhibiting renin or Ang II activity [81-82].

Thus, both Zn and Vit D demonstrated significant protective effects against alloxan-induced diabetic nephropathy by reducing oxidative stress, improving glycemic control, modulating apoptotic pathways, and preserving renal function, as reflected by the improvement of biochemical markers and apoptotic regulators compared to untreated diabetic rats.

Conclusion

Zn is an important microelement that plays a role in vital processes that control body homeostasis. Supplementing with Zn appears to have a positive impact on DN risk factors as well as slowing the development of the disease. The potential of supplemental Zn in reducing renal damage in DN was investigated in this study. External administration of Zn repaired the pathological changes in the renal tissues of rats with DM. By reversing proinflammatory and profibrotic markers implicated in the pathophysiology of DN, Vit D therapy has been

shown to protect the kidneys from damage. This can happen through the expression of the Vit D receptor and by preventing the compensatory activation of renin-angiotensin II. Therefore, supplementation with both Zn and Vit D needs to be regarded as key targets in the prevention and treatment of DM.

Acknowledgements

We extend our gratitude to Dr. Dina Moustafa Thabit (Lecturer of Pathology, Faculty of Medicine, Minia University) for her valuable contributions in conducting the histological examinations in this study.

Funding

There is no source of funding for this study.

Conflicts of interest

The authors declare that there is no conflict of interest.

Ethical approval

This study and the handling of rats were carried out as stated by the guidelines of the Committee of Research Ethics of the Faculty of Pharmacy, Minia University, Egypt (MPEC-230202), and following the principles outlined in the Guide for the Care and Use of Lab Animals [20]. Every attempt was made to reduce animal suffering and use as few animals as possible.

References

1. Ke C, Narayan KV, Chan JC, Jha P, Shah BR. Pathophysiology, phenotypes and management of type 2 diabetes mellitus in Indian and Chinese populations. Nat Rev Endocrinol. 2022;18(7):413-432. Available from: https://www.nature.com/articles/s41574-022-00669-4
2. Lenzen S. The mechanisms of alloxan-and streptozotocin-induced diabetes. Diabetologia 2008;51(2):216-226. Available from: https://link.springer.com/article/10.1007/S00125-007-0886-7
3. Allen DA, Yaqoob MM, Harwood SM. Mechanisms of high glucose-induced apoptosis and its relationship to diabetic complications. J Nutr Biochem. 2005;16(12):705-713. Available from: https://doi.org/10.1016/j.jnutbio.2005.06.007
4. Gomes IB, Porto ML, Santos MCL, Campagnaro BP, Pereira TM, Meyrelles SS, Vasquez EC. Renoprotective, anti-oxidative and anti-apoptotic effects of oral low-dose quercetin in the C57BL/6J model of diabetic nephropathy. Lipids Health Dis. 2014;13:1-10. Available from: https://link.springer.com/article/10.1186/1476-511x-13-184
5. Zhang G, Zhou L, Xu Z, Pronyuk K, Chen X, Wang H. Diabetic nephropathy: causative and protective factors. Glob J Med Res. 2015;15(2):17-26. Available from: https://medicalresearchjournal.org/index.php/GJMR/article/view/901/3-Diabetic-Nephropathy_html
6. Alam MM, Meerza D, Naseem I. Protective effect of quercetin on hyperglycemia, oxidative stress and DNA damage in alloxan induced type 2 diabetic mice. Life sci. 2014;109(1):8-14. Available from: https://doi.org/10.1016/j.lfs.2014.06.005
7. Cooper ME. Interaction of metabolic and haemodynamic factors in mediating experimental diabetic nephropathy. Diabetologia 2001;44(11):1957-72. Available from: https://doi.org/10.1007/s001250100000
8. Zatz R, Dunn BR, Meyer TW, Anderson S, Rennke HG, Brenner BM. Prevention of diabetic glomerulopathy by pharmacological amelioration of glomerular capillary hypertension. J Clin Invest. 1986;77(6):1925-30. Available from: https://doi.org/10.1172/jci112521
9. Hargrove GM, Dufresne J, Whiteside C, Muruve DA, Wong NC. Diabetes mellitus increases endothelin-1 gene transcription in rat kidney. Kidney Int. 2000;58(4):1534-45. Available from: https://doi.org/10.1046/j.1523-1755.2000.00315.x
10. Dunlop M. Aldose reductase and the role of the polyol pathway in diabetic nephropathy. Kidney Int Suppl. 2000;77:S3-12. Available from: https://doi.org/10.1046/j.1523-1755.2000.07702.x
11. Soulis-Liparota T, Cooper M, Papazoglou D, Clarke B, Jerums G. Retardation by aminoguanidine of development of albuminuria, mesangial expansion, and tissue fluorescence in streptozocin-induced diabetic rat. Diabetes 1991;40(10):1328-34. Available from: https://doi.org/10.2337/diab.40.10.1328
12. Ahmad R, Shaju R, Atfi A, Razzaque MS. Zinc and Diabetes: A Connection between Micronutrient and Metabolism. Cells 2024;13(16):1359. Available from: https://doi.org/10.3390/cells13161359

13. Piao M, Liu Y, Yu T, Lu Y. Dietary zinc reduces endoplasmic reticulum stress and autophagy to protect against diabetic renal damage in streptozotocin-induced diabetic rats. Int J Diabetes Dev Ctries. 2019;39:340-345. Available from: https://link.springer.com/article/10.1007/s13410-018-0681-7
14. Tang Y, Yang Q, Lu J, Zhang X, Suen D, Tan Y, Cai L. Zinc supplementation partially prevents renal pathological changes in diabetic rats. J Nutr Biochem. 2010;21(3):237-246. Available from: https://doi.org/10.1016/j.jnutbio.2008.12.010
15. Zhang X, Liang D, Lian X, Chi ZH, Wang X, Zhao Y, Ping Z. Effect of zinc deficiency on mouse renal interstitial fibrosis in diabetic nephropathy. Mol Med Rep. 2016;14(6):5245-5252. Available from: https://www.spandidos-publications.com/10.3892/mmr.2016.5870?text=fulltext
16. Fidan F, Alkan BM, Tosun A. Çağın pandemisi: D vitamini eksikliği ve yetersizliği. Turk J Osteoporos. 2014;20(2):71-74. Available from: https://turkosteoporozdergisi.org/articles/doi/tod.94830
17. Teng M, Wolf M, Ofsthun MN, Lazarus JM, Hernán MA, Camargo Jr CA, Thadhani R. Activated injectable vitamin D and hemodialysis survival: a historical cohort study. J Am Soc Nephrol. 2005;16(4):1115-1125. Available from: https://journals.lww.com/jasn/abstract/2005/04000/activated_injectable_vitamin_d_and_hemodialysis.39.aspx
18. Vasdeki D, Tsamos G, Dimakakos E, Patriarcheas V, Koufakis T, Kotsa K, Cholewka A, Stanek A. Vitamin D Supplementation: Shedding Light on the Role of the Sunshine Vitamin in the Prevention and Management of Type 2 Diabetes and Its Complications. Nutrients 2024;16(21):3651. Available from: https://doi.org/10.3390/nu16213651
19. Ali A, Kumar M, Srivastava N, Khan MM, Khan MA. Free radicals and diabetes mellitus. Int J Pharm Sci Med. 2023; 8;1-19. Available from: http://dx.doi.org/10.47760/ijpsm.2023.v08i03.001
20. National Research Council (US) Committee for the Update of the Guide for the Care and Use of Laboratory Animals. Guide for the Care and Use of Laboratory Animals. 8th ed. Washington (DC): National Academies Press (US); 2011. Available from: https://doi.org/10.17226/12910
21. Hamadjida A, Tchiengang FT, Metechie LC, Otto GN, Eteme ON, Mingoas JK. Hypoglycemic and hypolipidemic effects of hydroethanolic stem bark extract of Boswellia dalzielii in alloxan-induced diabetic rats. World J Pharm Pharmaceut Sci. 2023;12:1910-1929. Available from: http://dx.doi.org/10.20959/wjpps20237-25388
22. Bolkent S, Yanardag R, Bolkent S, Mutlu O, Yildirim S, Kangawa K, Suzuki H. The effect of zinc supplementation on ghrelin--immunoreactive cells and lipid parameters in gastrointestinal tissue of streptozotocin-induced female diabetic rats. Mol Cell Biochem. 2006;286:77-85. Available from: https://link.springer.com/article/10.1007/s11010-005-9095-1
23. Pittas AG, Dawson-Hughes B, Li T, Van Dam RM, Willett WC, Manson JE, Hu FB. Vitamin D and calcium intake in relation to type 2 diabetes in women. Diabetes Care 2006;29(3):650-656. Available from: https://doi.org/10.2337/diacare.29.03.06.dc05-1961
24. Ighodaro OM, Adeosun AM, Akinloye OA. Alloxan-induced diabetes, a common model for evaluating the glycemic-control potential of therapeutic compounds and plants extracts in experimental studies. Medicina 2017;53(6):365-374. Available from: https://doi.org/10.1016/j.medici.2018.02.001
25. Dhandapani S, Subramanian VR, Rajagopal S, Namasivayam N. Hypolipidemic effect of Cuminum cyminum L. on alloxan--induced diabetic rats. Pharmacol Res. 2002;46(3):251-255. Available from: https://doi.org/10.1016/S1043-6618(02)00131-7
26. Hamadjida A, Metechie LC, Tchiengang FDT, Otto GLN, Eteme ON, Njintang NY, Mingoas JPK. Antidiabetic potential of Hibiscus sabdariffa extract in alloxan-induced diabetic rats. GSC Biol Pharm Sci. 2023;23(1):193-203. Available from: https://doi.org/10.30574/gscbps.2023.23.1.0158
27. Levison DA. Book Reviews: Theory and practice of histological techniques. 4th Edition. J Pathol. 1997;183:243-244.
28. Madhan Kumar SJ, Malarvani T, Sathiyanarayamurthy S. Nephroprotective effects of Cynodon dactylon aqueous extract in STZ induced diabetic male rats – histological study. Int J Pharmacogn Phytochem Res. 2016;8:1812-1817. Available from: https://impactfactor.org/PDF/IJPPR/8/IJPPR,Vol8,Issue11,Article10.pdf
29. Gupta P, Sharma P, Shanno K, Jain V, Pareek A, Agarwal P, Sharma V. Nephroprotective role of alcoholic extract of Pterocarpus marsupium heartwood against experimentally induced diabetic nephropathy. J Pharm Pharmacogn Res. 2016;4(5):174-186. Available from: http://www.redalyc.org/articulo.oa?id=496053937002
30. Yaribeygi H, Atkin SL, Sahebkar A. A review of the molecular mechanisms of hyperglycemia-induced free radical generation leading to oxidative stress. J Cell Physiol. 2019;234(2):1300-1312. Available from: https://doi.org/10.1002/jcp.27164
31. Das K, Ghosh M. Structured DAG oil ameliorates renal injury in streptozotocin-induced diabetic rats through inhibition of NF-κB and activation of Nrf2 pathway. Food Chem Toxicol. 2017;100:225-238. Available from: https://doi.org/10.1016/j.fct.2016.12.033
32. Meng XM, Nikolic-Paterson DJ, Lan HY. Inflammatory processes in renal fibrosis. Nat Rev Nephrol. 2014;10(9):493-503. Available from: https://www.nature.com/articles/nrneph.2014.114

33. Zanchi C, Macconi D, Trionfini P, Tomasoni S, Rottoli D, Locatelli M, Rudnicki M, Vandesompele J, Mestdagh P, Remuzzi G, Benigni A, Zoja C. MicroRNA-184 is a downstream effector of albuminuria driving renal fibrosis in rats with diabetic nephropathy, Diabetologia 2017;60:1114-1125. Available from: https://link.springer.com/article/10.1007/s00125-017-4248-9
34. Ashrafi M, Nazifi S, Namazi F, Kazemipour N, Karimi B, Goudarzi T, Talebanzadeh S. Renal protective effect of saffron aqueous extract in streptozotocin induced diabetic rats. Int J Med Sci Public Health 2017;6:151-161. Available from: https://www.ijmrhs.com/medical-research/renal-protective-effect-of-saffron-aqueous-extract-in-streptozotocin-induced-diabetic-rats.pdf
35. Jamshidi HR, Zeinabady Z, Zamani E, Shokrzadeh M. Attenuation of diabetic nephropathy by carvacrol through anti-oxidative effects in alloxan-induced diabetic rats. Res J Pharmacogn. 2018;5(2):57-64. Available from: https://doi.org/10.22127/rjp.2018.58508
36. Maeder M, Klein M, Fehr T, Rickli H. Contrast nephropathy: review focusing on prevention. J Am Coll Cardiol. 2004;44(9):1763-1771. Available from: https://doi.org/10.1016/j.jacc.2004.06.075
37. Pickup JC, Crook MA. Is type II diabetes mellitus a disease of the innate immune system? Diabetologia 1998;41:1241-1248. Available from: https://link.springer.com/article/10.1007/s001250051058
38. Sun L, Kanwar YS. Relevance of TNF-α in the context of other inflammatory cytokines in the progression of diabetic nephropathy. Kidney Int. 2015;88(4):662-665. Available from: https://doi.org/10.1038/ki.2015.250
39. Bertani T, Abbate M, Zoja C, Corna D, Perico N, Ghezzi P, Remuzzi G. Tumor necrosis factor induces glomerular damage in the rabbit. Am J Pathol. 1989;134(2):419. Available from: https://pubmed.ncbi.nlm.nih.gov/2916653/
40. Boyle JJ, Weissberg PL, Bennett MR. Human macrophage-induced vascular smooth muscle cell apoptosis requires NO enhancement of Fas/Fas-L interactions. Arterioscler Thromb Vasc Biol. 2002; 22(10):1624-1630. Available from: https://doi.org/10.1161/01.ATV.0000033517.48444.1A
41. Carey RM, Siragy HM. The intrarenal renin–angiotensin system and diabetic nephropathy. Trends Endocrinol Metab. 2003;14(6):274-281. Available from: https://www.cell.com/ajhg/abstract/S1043-2760(03)00111-5#
42. Ziyadeh FN. Mediators of diabetic renal disease: the case for TGF-β as the major mediator. J Am Soc Nephrol. 2004;15(1_suppl):S55-S57. Available from: https://doi.org/10.1097/01.asn.0000093460.24823.5b
43. Banba N, Nakamura T, Matsumura M, Kuroda H, Hattori Y, Kasai K. Possible relationship of monocyte chemoattractant protein-1 with diabetic nephropathy. Kidney Int. 2000;58(2):684-690. Available from: https://doi.org/10.1046/j.1523-1755.2000.00214.x
44. Price DA, Porter LE, Gordon M, Fisher ND, De' Oliveira JMF, Laffel LM, Hollenberg NK. The paradox of the low-renin state in diabetic nephropathy. J Am Soc Nephrol. 1999;10(11):2382-2391. Available from: https://doi.org/10.1681/asn.v10112382
45. Nishiyama A, Seth DM, Navar LG. Renal interstitial fluid concentrations of angiotensins I and II in anesthetized rats. Hypertension 2002;39(1):129-134. Available from: https://doi.org/10.1161/hy0102.100536
46. Gilbert RE, Krum H, Wilkinson-Berka J, Kelly DJ. The renin–angiotensin system and the long-term complications of diabetes: pathophysiological and therapeutic considerations. Diabet Med. 2003;20(8):607-621. Available from: https://doi.org/10.1046/j.1464-5491.2003.00979.x
47. King JC, Shames DM, Woodhouse LR. Zinc homeostasis in humans. J Nutr. 2000;130(5):1360S-1366S. Available from: https://doi.org/10.1093/jn/130.5.1360S
48. Prasad AS. Clinical manifestations of zinc deficiency. Annu Rev Nutr. 1985;5:341-363. Available from: https://doi.org/10.1146/annurev.nu.05.070185.002013
49. Prasad AS, Bao B. Molecular mechanisms of zinc as a pro-antioxidant mediator: clinical therapeutic implications. Antioxidants. 2019;8(6):164. Available from: https://doi.org/10.3390/antiox8060164
50. Parham M, Amini M, Aminorroaya A, Heidarian E. Effect of zinc supplementation on microalbuminuria in patients with type 2 diabetes: a double blind, randomized, placebo-controlled, cross-over trial. Rev Diabet Stud. 2008;5(2):102-9. Available from: https://doi.org/10.1900/rds.2008.5.102
51. Matzke GR, Aronoff GR, Atkinson AJ Jr, Bennett WM, Decker BS, Eckardt KU, Golper T, Grabe DW, Kasiske B, Keller F, Kielstein JT, Mehta R, Mueller BA, Pasko DA, Schaefer F, Sica DA, Inker LA, Umans JG, Murray P. Drug dosing consideration in patients with acute and chronic kidney disease-a clinical update from Kidney Disease: Improving Global Outcomes (KDIGO). Kidney Int. 2011;80(11):1122-37. Available from: https://doi.org/10.1038/ki.2011.322
52. Kelishadi R, Hashemipour M, Adeli K, Tavakoli N, Movahedian-Attar A, Shapouri J, Poursafa P, Rouzbahani A. Effect of zinc supplementation on markers of insulin resistance, oxidative stress, and inflammation among prepubescent children with metabolic syndrome. Metab Syndr Relat Disord. 2010;8(6):505-10. Available from: https://doi.org/10.1089/met.2010.0020
53. Vardatsikos G, Pandey NR, Srivastava AK. Insulino-mimetic and anti-diabetic effects of zinc. J Inorg Biochem. 2013;120:8-17. Available from: https://doi.org/10.1016/j.jinorgbio.2012.11.006

54. Chimienti F. Zinc, pancreatic islet cell function and diabetes: new insights into an old story. Nutr Res Rev. 2013;26(1):1-11. Available from: https://doi.org/10.1017/s0954422412000212
55. Li YV. Zinc and insulin in pancreatic beta-cells. Endocrine 2014;45(2):178-89. Available from: https://doi.org/10.1007/s12020-013-0032-x
56. Myers SA. Zinc transporters and zinc signaling: new insights into their role in type 2 diabetes. Int J Endocrinol. 2015;2015: 167503. Available from: https://doi.org/10.1155/2015/167503
57. Kambe T, Hashimoto A, Fujimoto S. Current understanding of ZIP and ZnT zinc transporters in human health and diseases. Cell Mol Life Sci. 2014;71(17):3281-95. Available from: https://doi.org/10.1007/s00018-014-1617-0
58. Cai Y, Kirschke CP, Huang L. SLC30A family expression in the pancreatic islets of humans and mice: cellular localization in the β-cells. J Mol Histol. 2018;49(2):133-145. Available from: https://doi.org/10.1007/s10735-017-9753-0
59. Wijesekara N, Dai FF, Hardy AB, Giglou PR, Bhattacharjee A, Koshkin V, Chimienti F, Gaisano HY, Rutter GA, Wheeler MB. Beta cell-specific Znt8 deletion in mice causes marked defects in insulin processing, crystallisation and secretion. Diabetologia 2010;53(8):1656-68. Available from: https://doi.org/10.1007/s00125-010-1733-9
60. Davidson HW, Wenzlau JM, O'Brien RM. Zinc transporter 8 (ZnT8) and β cell function. Trends Endocrinol Metab. 2014;25(8):415-24. Available from: https://doi.org/10.1016/j.tem.2014.03.008
61. Foster M, Chu A, Petocz P, Samman S. Zinc transporter gene expression and glycemic control in post-menopausal women with Type 2 diabetes mellitus. J Trace Elem Med Biol. 2014;28(4):448-52. Available from: https://doi.org/10.1016/j.jtemb.2014.07.012
62. Lefebvre B, Vandewalle B, Balavoine AS, Queniat G, Moerman E, Vantyghem MC, Le Bacquer O, Gmyr V, Pawlowski V, Kerr-Conte J, Pattou F. Regulation and functional effects of ZNT8 in human pancreatic islets. J Endocrinol. 2012;214(2):225-32. Available from: https://doi.org/10.1530/joe-12-0071
63. Cruz KJC, de Oliveira ARS, Morais JBS, Severo JS, Mendes PMV, de Sousa Melo SR, de Sousa GS, Marreiro DDN. Zinc and Insulin Resistance: Biochemical and Molecular Aspects. Biol Trace Elem Res. 2018;186(2):407-412. Available from: https://doi.org/10.1007/s12011-018-1308-z
64. Huang L, Yan M, Kirschke CP. Over-expression of ZnT7 increases insulin synthesis and secretion in pancreatic beta-cells by promoting insulin gene transcription. Exp Cell Res. 2010;316(16):2630-43. Available from: https://doi.org/10.1016/j.yexcr.2010.06.017
65. Özcelik D, Nazıroglu M, Tunçdemir M, Çelik Ö, Öztürk M, Flores-Arce MF. Zinc supplementation attenuates metallothionein and oxidative stress changes in kidney of streptozotocin-induced diabetic rats. Biol Trace Elem Res. 2012;150:342-349. Available from: https://link.springer.com/article/10.1007/s12011-012-9508-4
66. Zhou Z, Sun X, Kang YJ. Metallothionein protection against alcoholic liver injury through inhibition of oxidative stress. Exp Biol Med. 2002;227(3):214-222. Available from: https://doi.org/10.1177/153537020222700310
67. Cai L. Metallothionein as an adaptive protein prevents diabetes and its toxicity. Nonlinearity Biol Toxicol Med. 2004;2(2):15401420490464367. Available from: https://doi.org/10.1080/15401420490464367
68. Zhang X, Zhao Y, Chu Q, Wang ZY, Li H, Chi ZH. Zinc modulates high glucose-induced apoptosis by suppressing oxidative stress in renal tubular epithelial cells. Biol Trace Elem Res. 2014;158:259-267. Available from: https://doi.org/10.1007/s12011-014-9922-x
69. Derakhshanian H, Shab-Bidar S, Speakman JR, Nadimi H, Djafarian K. Vitamin D and diabetic nephropathy: a systematic review and meta-analysis. Nutrition 2015;31(10):1189-1194. Available from: https://doi.org/10.1016/j.nut.2015.04.009
70. Flores M. A role of vitamin D in low-intensity chronic inflammation and insulin resistance in type 2 diabetes mellitus? Nutr Res Rev. 2005;18(2):175-82. Available from: https://doi.org/10.1079/nrr2005104
71. Karnchanasorn R, Ou HY, Chiu KC. Plasma 25-hydroxyvitamin D levels are favorably associated with β-cell function. Pancreas 2012;41(6):863-8. Available from: https://doi.org/10.1097/mpa.0b013e31823c947c
72. Nakai K, Fujii H, Kono K, Goto S, Kitazawa R, Kitazawa S, Nishi S. Vitamin D activates the Nrf2-Keap1 antioxidant pathway and ameliorates nephropathy in diabetic rats. Am J Hypertens. 2014;27(4):586-595. Available from: https://doi.org/10.1093/ajh/hpt160
73. Chen N, Wan Z, Han SF, Li BY, Zhang ZL, Qin LQ. Effect of vitamin D supplementation on the level of circulating high-sensitivity C-reactive protein: a meta-analysis of randomized controlled trials. Nutrients 2014;6(6):2206-2216. Available from: https://doi.org/10.3390/nu6062206
74. Wang Y, Deb DK, Zhang Z, Sun T, Liu W, Yoon D, Li YC. Vitamin D receptor signaling in podocytes protects against diabetic nephropathy. J Am Soc Nephrol. 2012;23(12):1977-1986. Available from: https://doi.org/10.1681/asn.2012040383

75. Gupta S, Clarkson MR, Duggan J, Brady HR. Connective tissue growth factor: potential role in glomerulosclerosis and tubulointerstitial fibrosis. Kidney Int. 2000;58(4):1389-99. Available from: https://doi.org/10.1046/j.1523-1755.2000.00301.x
76. Goldschmeding R, Aten J, Ito Y, Blom I, Rabelink T, Weening JJ. Connective tissue growth factor: just another factor in renal fibrosis? Nephrol Dial Transplant. 2000;15(3):296-9. Available from: https://doi.org/10.1093/ndt/15.3.296
77. Li YC, Kong J, Wei M, Chen ZF, Liu SQ, Cao LP. 1,25-Dihydroxyvitamin D(3) is a negative endocrine regulator of the renin-angiotensin system. J Clin Invest. 2002;110(2):229-38. Available from: https://doi.org/10.1172/jci15219
78. Carey RM, Siragy HM. The intrarenal renin-angiotensin system and diabetic nephropathy. Trends Endocrinol Metab. 2003;14(6):274-81. Available from: https://doi.org/10.1016/s1043-2760(03)00111-5
79. Anderson S, Jung FF, Ingelfinger JR. Renal renin-angiotensin system in diabetes: functional, immunohistochemical, and molecular biological correlations. Am J Physiol. 1993;265(4 Pt 2):F477-86. Available from: https://doi.org/10.1152/ajprenal.1993.265.4.f477
80. Kagami S, Border WA, Miller DE, Noble NA. Angiotensin II stimulates extracellular matrix protein synthesis through induction of transforming growth factor-beta expression in rat glomerular mesangial cells. J Clin Invest. 1994;93(6):2431-7. Available from: https://doi.org/10.1172/jci117251
81. Andersen S, Tarnow L, Rossing P, Hansen BV, Parving HH. Renoprotective effects of angiotensin II receptor blockade in type 1 diabetic patients with diabetic nephropathy. Kidney Int. 2000;57(2):601-6. Available from: https://doi.org/10.1046/j.1523-1755.2000.00880.x
82. Ichihara A, Hayashi M, Kaneshiro Y, Suzuki F, Nakagawa T, Tada Y, Koura Y, Nishiyama A, Okada H, Uddin MN, Nabi AH, Ishida Y, Inagami T, Saruta T. Inhibition of diabetic nephropathy by a decoy peptide corresponding to the “handle” region for nonproteolytic activation of prorenin. J Clin Invest. 2004;114(8):1128-35. Available from: https://doi.org/10.1172/jci21398

EUROPEAN JOURNAL OF TRANSLATIONAL
AND CLINICAL MEDICINE 2025;8(1):32-44

RESEARCH ARTICLE

Effects of HRV biofeedback training on recovery, stress management, reaction time and concentration in competitive rowing – preliminary study

Zuzanna Myszka[1], Maria Wolff[2], Piotr Basta[3], Dariusz Kozłowski[4]

[1] Centrum Medyczne Zdrowy Profil, Gdańsk, Poland
[2] Rehasport Clinic, Gdańsk, Poland
[3] Departament of Biological Sciences, Poznań University of Physical Education, Faculty of Physical Culture in Gorzów Wielkopolski, Poland
[4] Institute of Health Sciences, Pomeranian University in Słupsk, Poland

Abstract

Background: Our aim was to determine the effect of HRV biofeedback (HRVB) training on psychophysiological factors, e.g. reaction time, stress management and concentration during the starting period in competitive rowing. **Material and methods:** 12 senior national team rowers aged 20-40 (both men and women) were assigned to an experimental (n = 6) and a control (n = 6) group. The experimental group performed HRVB training for 4 weeks, for 20 minutes, twice a day. The control group did not perform any respiratory training. Parameters such as reaction time, resting breathing rate, concentration, subjective stress and heart rate variability were evaluated during the pre-test, post-test and post-post test phases. **Results:** We noted an improvement in reaction time in the experimental group after HRVB training (pre-test 63.8 sec to post-post test 58.8 sec) and no significant statistical differences in the control group, as well as a statistically significant reduction in resting respiratory rate frequency in the experimental group in comparison to the control group in the post-test ($p = 0.0398$). Other analyses did not exceed the threshold for statistical significance. **Conclusions:** Our results suggest that HRVB training may reduce the resting respiratory rate in the experimental group and may improve the reaction time of rowers.

Keywords: concentration • heart rate variability • reaction time • biofeedback • peak performance

Citation

Myszka Z., Wolff M., Basta P., Kozłowski D. Effects of HRV biofeedback training on recovery, stress management, reaction time and concentration in competitive rowing – preliminary study. Eur J Transl Clin Med. 2025;8(1):32-44.

DOI: 10.31373/ejtcm/207342

Corresponding author:
Zuzanna Myszka, Centrum Medyczne Zdrowy Profil, Gdańsk, Poland
email: zuzanna@waves.com.pl, phone: +48 793435793
Available online: ejtcm.gumed.edu.pl

Abbreviations

- HRV – heart rate variability
- HRVB – heart rate variability biofeedback
- BDI-II – Beck Depression Inventory – 2nd Edition
- TUS – Attention and Perceptiveness Tests
- SDNN – standard deviation of RR intervals
- RMSSD – root mean square of successive RR interval differences
- HR – heart rate
- LF – low frequency
- HF – high frequency
- VO_2 max – maximum oxygen uptake
- PZTW – Polish Federation of Rowing Associations

Introduction

Rowing is largely an endurance sport and requires athletes to have highly developed skills to manage their mental and physical resources. The development of peak physical performance continues to evolve as new insights emerge from the field of human physiology. This domain encompasses a broad range of topics from nutrition science (e.g. the effects of caffeine intake on rowing performance), to exercise physiology (e.g. the impact of kettlebell training on muscular strength and endurance of rowers) [1-2]. Furthermore, recent research explores more specific interventions, such as the effects of blood flow restriction on power output during the start phase, heart rate (HR), and systemic acidosis [3].

In contrast, the level of knowledge and its practical application in research and training aimed at enhancing the psychophysiological and mental skills of rowers remains considerably underdeveloped. A review of the available literature revealed no studies investigating the Polish senior elite rowing population with respect to the assessment of mental skills (e.g. focus, reaction time) or stress levels. Existing publications are limited to research on stress responses, primarily examining cortisol fluctuations in relation to varying training intensities, or studies exploring changes in antioxidant defense systems in young rowers following an annual training cycle [4-5].

Moreover, no research was identified concerning the effects of heart rate variability biofeedback (HRVB) training in the context of Polish sport. Considering the fact that competitive rowing demands years of training and sacrifice (often leading to overuse of the body and injuries), simple and effective tools to reduce fatigue levels or to accelerate the recovery seems to be the basis of modern training [6].

One of the analyses of the psychophysiological state, depicting the body's ability to determine stress levels and regulatory capacity, is the analysis of HRV [7]. A high HRV is a sign that the heart is healthy since it has more flexibility to react to stressors (physiological or environmental) [8]. From a practical point of view, it remains to be determined if it can also be used as a predictor of athletic condition and of athletic achievements [9]. Cardiovascular functions (including the HRV rate) are regulated by the autonomic nervous system, which via sympathetic and parasympathetic innervation of the blood vessels, directly modifies vascular wall tension and influences cardiac function [10].

However, humans are able to influence their own HRV by using breathing training. One such method is HRVB training. Biofeedback acutely increased both HRV and baroreflex gain, and chronically increased baroreflex gain and peak expiratory flow even among healthy individuals, in whom these measures ordinarily are thought to be stable [11]. Moreover, breathing at this frequency causes an increase or decrease in heart rate depending on the phase of breathing, maximizing the efficiency of gas exchange and affecting the efficiency of the body. HRVB is used to treat a number of diseases and ailments, such as asthma, pain, depression), hypertension or anxiety [12-16].

A growing number of studies conducted abroad are emerging describing the effects of respiratory training on the performance of athletes in various fields. It has been shown that HRVB training can help train stressed athletes to gain control over their psychophysiological processes, thus helping them achieve maximum performance [17]. In addition, HRVB can produce significant benefits in autonomic markers and anxiety levels in young athletes [18]. Also, it is associated with increased HRV and improved subjective training performance in elite female athletes [19]. Furthermore, HRVB training improved HRV parameters and reduced the number of strokes to complete a virtual 18-hole game of golf (46 strokes in the pre-test, 30 in the post-test) in a group of female golf coaches [20]. Finally, it significantly reduced race time in an experimental group, and reduced skin conductance and increased VO_2 max in male and female long-distance running groups [21]. Although research on HRVB training in sports is limited, it suggests that it is a safe, accessible and effective method that appears to offer tangible performance benefits for both athletes and coaches [22].

Rowing races commence with an auditory signal, and subsequently athletes must react swiftly and maintain synchronized oar movements and sustained focus throughout the race. Therefore, our aim was to address the following research question: "does HRVB training influence psychological factors critical to rowing performance (both at the start of and during the race itself) such as reaction time and athlete concentration?". We also attempted to determine the subjectively perceived stress levels of athletes, along with HRV parameters, and investigate the impact of HRVB breathing training (with resonant frequency individually selected for each athlete) on these factors, as well as its effect on the regulation of the autonomic nervous system (e.g. the resting respiratory rate).

Materials and methods

In 2022, 40 senior athletes from the Polish National Rowing Team, participating in centralized training under the PZTW, were invited to take part in a research project. Twenty athletes provided written informed consent to participate in the study. Following a medical consultation with the Team physician and a psychological assessment for depressive symptoms (21 questions, no time limit) an additional 8 rowers were excluded from the study. Five athletes scored above the threshold sten score of 8 on BDI-II, and 3 were undergoing pharmacological treatment that could potentially affect HRV outcomes.

The inclusion criteria were: the athlete's appointment to the National Senior Team of the PZTW and voluntary consent to participate in the project. The exclusion criteria were: having a chronic disease and taking medications that have a significant effect on HRV and obtaining a high sten score (< 8 sten) in the BDI-II psychological test.

Based on the recruitment procedure, and the inclusion and exclusion criteria, 6 women and 6 men were selected and randomly assigned to 2 equal groups:

1) The experimental group received HRVB training (3 females and 3 males).
2) The control group did not receive any training (3 females and 3 males) (Table 1).

Both groups demonstrated an equivalent elite athletic level within Olympic disciplines. Specifically, 4 athletes in both the experimental and control groups held the International Master Class designation, which denotes having achieved at least a medal at the World and/or European Championships, or having reached the finals or secured a medal at the Olympic Games. Additionally, 2 athletes from each group held the National Master Class designation, having reached the finals of the World and/or European Championships and/or won a medal at the Polish National Championships. The recruitment data and selection process throughout the project is depicted in Figure 1. The execution stage included the following phases: pre-test, experimental procedure, post-test, and post-post test (Table 2). The next stage of quality verification included ECG analysis by a sports cardiologist, a consultation with the team physician of the PZTW regarding any infection acquired during the post-test period, and interviews to assess the presence of dyslexia. At this stage the presence of cardiac arrhythmias (in at least one of the HRV assessment recordings) was confirmed in 4 individuals, a severe infection in two athletes (1 from the experimental group and 1 from the control group) during the post-test period, and confirmation of a dyslexia diagnosis in 2 athletes (1 from the experimental group and 1 from the control group).

Table 1. Demographic data

		height (cm)	**weight** (kg)	**age** (years)
Experimental group	min	173.0	64.0	21.0
	max	198.0	100.0	40.0
	median	186.5	80	29.5
	First quartile (Q1)	174	67.5	21.5
	Third quartile (Q3)	193	90	32.5
Control group		**height** (cm)	**weight** (kg)	**age** (years)
	min	170.0	57.0	20.0
	max	196.0	98.0	33.0
	median	183	79.5	25.5
	First quartile (Q1)	170.5	57	21
	Third quartile (Q3)	183	87.5	28

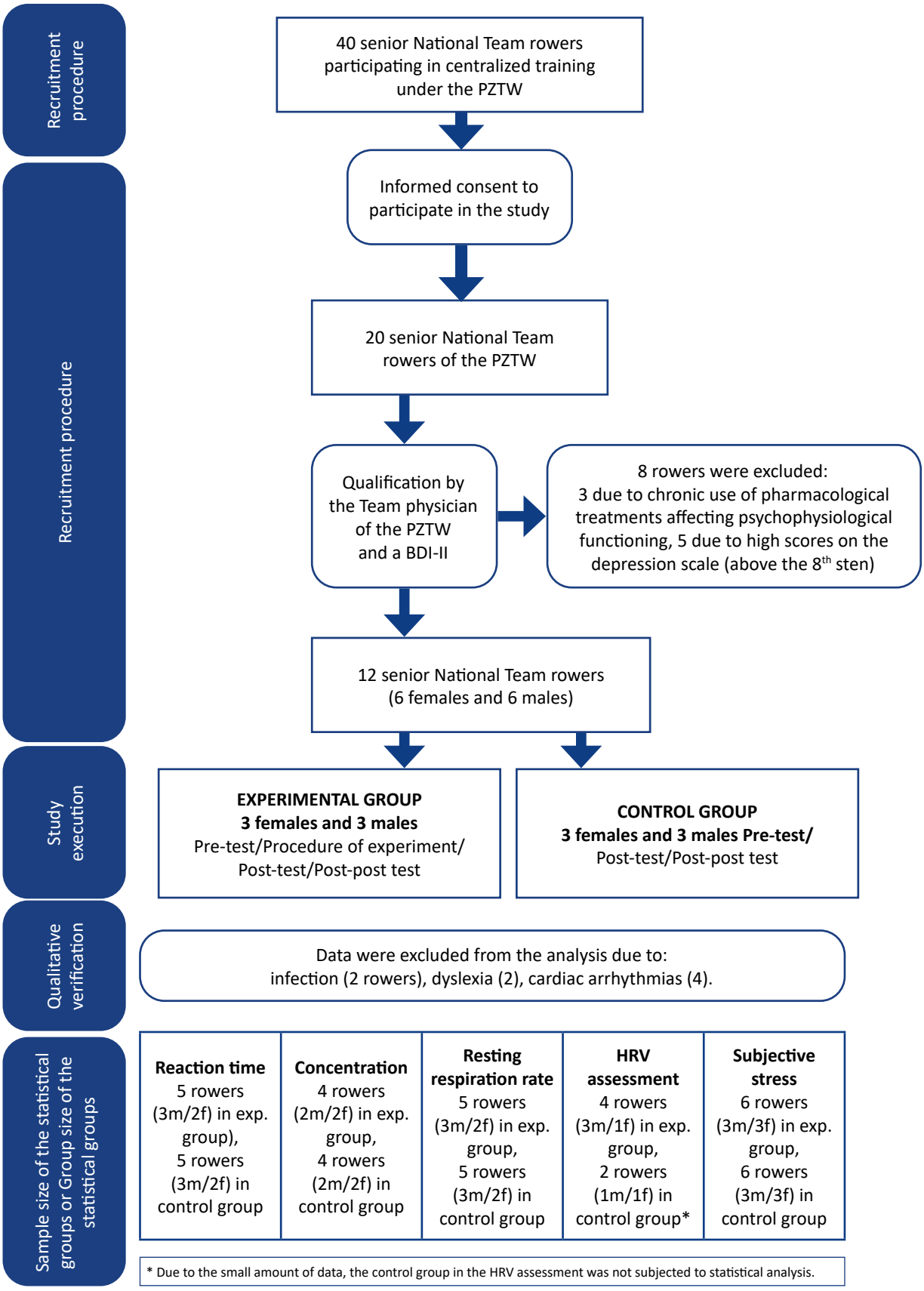

Figure 1. Flowchart of study selection
BDI-II – Beck Depression Inventory 2nd Edition, f – females, m – males, PZTW – Polish Federation of Rowing Associations

Table 2. Execution stage: tasks and measurements

Task and time between measurements	Experimental group	Control group
Pre-test	• subjective sense of stress • concentration • reaction time • HRV assessment • resting respiratory rate	• subjective sense of stress • concentration • reaction time • HRV assessment • resting respiratory rate
4 weeks	HRVB training (2 individual meetings and determination of the resonant frequency)	No tasks
Post-test	• concentration • reaction time • HRV assessment • resting respiratory rate	• concentration • reaction time • HRV assessment resting respiratory rate
4 weeks	No tasks	• No tasks
Post-post test	• subjective sense of stress • concentration • reaction time • HRV assessment • resting respiratory rate	• subjective sense of stress • concentration • reaction time • HRV assessment • resting respiratory rate

The results of athletes with confirmed infection were excluded from the statistical analysis of tests that required an optimal physiological condition (e.g. reaction time, concentration test, resting respiratory rate and HRV assessment). Additionally, the results of the 2 athletes with dyslexia were excluded from the statistical analysis of the concentration test. The subjective stress level measurements were conducted both during the pre-test and the control phase, therefore we included the results from all 12 participants in this analysis. The sample sizes of the subgroups included in the final statistical analyses are presented in Figure 1.

This study was conducted in accordance with established ethical standards, including ensuring the safety of participants. All individuals were informed of the purpose and procedures of the study, provided written informed consent, and were made aware of the benefits of participation as well as their right to withdraw at any stage of the study. These procedures adhered to the principles outlined in the European Convention on Bioethics of the Council of Europe. The research was assigned the consent number of the bioethics committee at the Regional Medical Council in Gdansk No. KB-25/24.

Equipment

The measurements were carried out using the following equipment: ECG electrodes (EK-S 45 PSG, Sorimex, Poland), reaction time apparatus (Rox Pro retention lights, A-Champs Ltd., Hong Kong), a coder for HRV assessment and HRVB training (ProComp Infiniti 5.0, Thought Technology Ltd., Canada), and psychological tests such as the BDI-II and TUS, purchased from the Polish Psychological Association [23-24].

Protocols for concentration and subjective stress tests

Concentration tests were conducted using the TUS test, which consisted of crossing out rows of numbers or letters indicated in the test at the highest possible pace within a 3-minute time limit. The raw scores for the speed-of-work indicator were related to the standard sten for a group of soldiers.

Subjective feelings of stress were assessed using a 5-point Likert scale, where 1 indicated a high level of subjectively perceived stress and 5 indicated a low level. Both measurements were taken both at the pre-test and at the post-post test stage.

Protocol for time reaction

Time reaction was measured in the pre-test, post-test and post-post test. The procedure included 2 measurements; the second trial was the outcome of a task. It consisted of turning off a randomly switched on light as quickly as possible on one of three cubes placed on a table in front of the contestant. The cubes were placed symmetrically at twenty-centimeter intervals.

Protocol for HRV, resting breathing frequency and HRVB training

HRV, resting breathing frequency measurements and HRVB training were conducted in a quiet, darkened room. Each measurement was preceded by a 10-minute rest period, during which the athlete remained in the supine position. Following this period, a 6-minute ECG recording was obtained in the same position using a single-lead ECG, as well as a respiratory sensor positioned at the level of the athlete's navel. The HRVB training protocol consisted of two phases conducted within two days: the determination of the individual resonant frequency according to a modified version of the Lehrer protocol [25] and a self-guided training session performed at the prescribed frequency. HRVB training was conducted in the supine position, during which participants followed a visual cue – a dot moving on the screen, rising during inhalation and falling during exhalation at different respiratory rates for about two minutes (6.5, 6.0, 5.5, 5.0 and 4.5 breaths per minute).

During the HRVB training we utilized a respiratory sensor strap and single-lead ECG electrodes. The system continuously displayed the heart rate alongside a real-time spectral analysis of the interbeat interval, recalculated every second using a 30-60 second rolling window. This setup enabled continuous observation of the phase relationship between respiration and HRV. The resonant frequency was determined based on the convergence of several physiological indicators: optimal phase synchrony between heart rate variability and respiration, the highest peak-to-trough amplitude, the highest low frequency (LF) power, a clear and high-amplitude LF peak in the spectral analysis, and a stable "envelope" of the HR curve. The respiratory rate that exhibited the greatest concentration of these features was identified as the participant's individual resonant frequency, which was then used as the target breathing rate during HRVB training. HRVB training consisted of two 20-minute daily breathing sessions, performed at the individual resonant frequency, supported by mobile breathing applications such as *Prana Breath* or *Breathwork Pacer*. Athletes documented their training duration in a personal training diary. During the month preceding the post-post test, participants in the experimental group were instructed to discontinue HRVB training.

Statistical analysis

All procedures in the project included the following dimensions: the mean time to extinguish the randomly switched-on retention light (measured in seconds), concentration – speed of work (stens), resting respiratory rate (rated on a 1-5 scale, where 1 indicates high stress and 5 low stress), HRV – mean RR (beats per minute, BPM), SDNN (ms), RMSSD (ms), HR max-min (BPM), LF power (ms2), high frequency (HF) power (ms2), LF/HF ratio.

For each parameter, four types of statistical result presentations were performed:

1) A descriptive statistical analysis including value distributions, presented as median (1^{st} and 3^{rd} quartiles) and minimum–maximum values, was conducted for each individual measurement.
2) A statistical analysis between measurements. P-values were calculated for the following comparisons: measurement 1 vs. 2, 2 vs. 3, and 1 vs. 3 – separately for the experimental and control groups.

Additionally, a distribution plot of the values for each parameter was generated for the control and experimental groups across the three measurement points. In each plot, the central square represents the median, the boxes indicate the interquartile range (25^{th} to 75^{th} percentile), and the whiskers extend from the minimum to the maximum values. Statistical significance was defined as follows: *$p \leq 0.05$, **$p \leq 0.01$, ***$p \leq 0.001$, ****$p \leq 0.0001$.

Results

The descriptive statistical analysis conducted for concentration, resting respiratory rate and reaction time indicates a significant reduction in the frequency of resting breathing in athletes performing HRVB training (the average time for all from the experimental group was 807 min over the 4 weeks) compared to athletes not performing training; however, this trend was not maintained when athletes in the study group stopped performing regular HRVB training (Table 3).

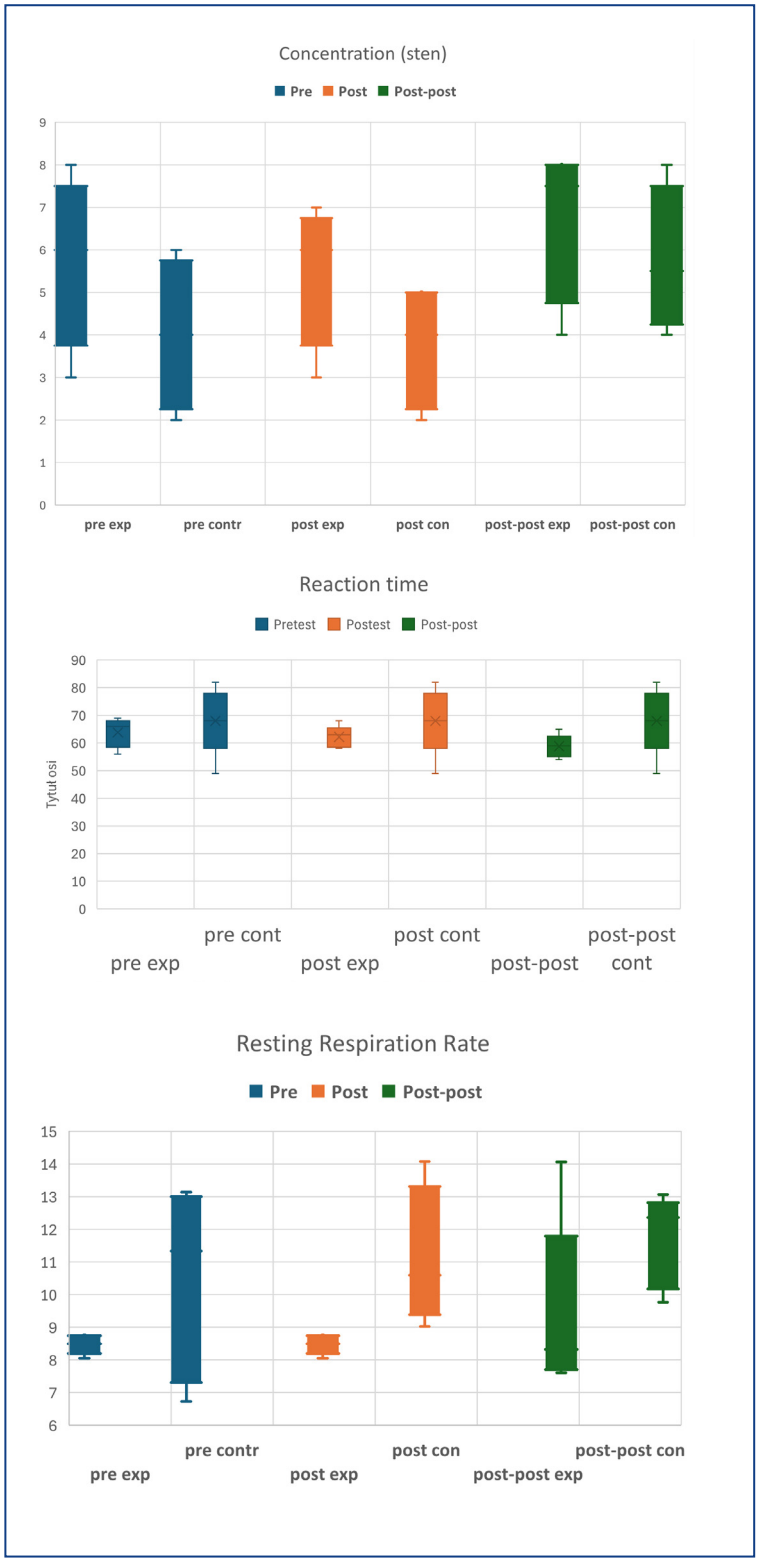

Figure 2. Distribution of test scores in concentration, resting respiration rate, and reaction time across the respective measurement points
Statistically significant results: * $p \leq 0.05$, ** $p \leq 0.01$, *** $p \leq 0.001$, **** $p \leq 0.0001$; pre exp – pre-test experimental group, pre contr – pre-test control group, post exp – post-test experimental group, post contr – post-test control group, post-post exp – post-post test experimental group, post-post contr – post-post test control group

The remaining results indicated that the **concentration** and **reaction time** scores obtained in the respective tests did not differ significantly between the experimental and control groups.

The analysis of the results at each stage indicates that reaction time in the experimental group improved over the course of the study, while in the control group, reaction time showed a slight improvement in the second measurement but significantly worsened in the final measurement. These results suggest that HRVB training can have a significant effect on improving reaction time in the experimental group in the final measurement (Figure 2).

Furthermore, the analysis of concentration parameters, resting respiratory rate and reaction time within each group across measurement points revealed a statistically significant improvement in reaction time in the experimental group between the pre-test and post-post test measurements (Table 4).

In contrast, the same analysis indicated that the control group demonstrated a statistically significant improvement in concentration between the first and third measurements. Additionally, both groups showed substantial improvements in concentration between the second and third measurements. These findings may suggest that HRVB training did not have a significant impact on concentration among the athletes.

However, it is worth noting that the concentration scores in the experimental group were initially higher than those in the control group. Although the experimental group did not show improvement, the trend analysis indicates that it maintained a certain level of stability in performance. In contrast, the results from the control group showed considerable variability, meaning that athletes in this group occasionally achieved extremely high or extremely low scores in individual measurements. Given the

Table 3. Statistical analysis with distribution of values for concentration (speed of work), resting respiration rate and reaction time

	Pre-test	Post-test	Post-post test
Concentration-speed of work (sten)			
Experimental group Median (Q1; Q3) min-max	5.8 (4.5;7.0) 3.0-8.0	5.5 (4.5;7.0) 3.0-7.0	6.8 (5.5;8.0) 4.0-8.0
Control group Median (Q1; Q3) min-max	4.0 (2.5;5.5) 2.0-6.0	3.8 (2.5;5.0) 2.0-5.0	5.8 (4.5;7.0) 4.0-8.0
p-value	0.2754	0.2754	0.4740
Resting respiration rate (breaths/min)			
Experimental group Median (Q1; Q3) min-max	10.9 (10.13;11.88) 8.2-13.9	8.4 (8.34;8.7) 8.0-8.7	9.4 (7.8;9.52) 7.6-14.0
Control group Median (Q1; Q3) min-max	10.4 (7.9;12.87) 6.7-13.1	11.1 (9.73;12.54) 9.0-14.0	11.6 (10.58;12.57) 9.7-13.0
p-value	0.8084	**0.0398**	0.2830
Reaction time (sec)			
Experimental group Median, (Q1; Q3) min-max	66.0 (61.0;67.0) 56.0-69.0	62.2 (59.0;63.0) 58.0-68.0	58.8 (56.0;60.0) 54.0-65.0
Control group Median (Q1; Q3) min-max	61.4 (58.0;64.0) 56.0-68.0	60.8 (57.0;62.0) 54.0-71.0	68.0 (67.0;74.0) 49.0-82.0
p-value	0.5660	0.7398	0.2139

T-test, two-sided, homoscedastic

Table 4. Statistical analysis between measurements for concentration (speed of work), resting respiratory rate and reaction time

Measurement	Concentration-speed of work (sten)		Resting respiratory rate (breath/min)		Reaction time (sec)	
	Experimental group	Control group	Experimental group	Control group	Experimental group	Control group
Post-test vs. Pretest	0.3910	0.3910	0.0742	0.5337	0.3739	0.5529
Post-post test study vs. Pre-test	0.0917	**0.0060**	0.3514	0.3628	**0.0062**	0.2922
Post-test vs. Post-post test	**0.0154**	**0.0163**	0.4256	0.6149	0.1239	0.2717

T-test, two-sided, paired

Table 5. Statistical analysis with distribution of values for heart rate variability in the experimental group

		Pre-test	Post-test	Post-post test
Mean HR (BPM)	min	1201.0	1152.0	1040.0
	max	1284.0	1285.0	1216.0
	median	1231.8	1214.3	1153.8
	Q1;Q3	1207.00;1256.50	1163.00;1265.50	1104.00;1203.50
SDNN (ms)	min	29.7	26.8	32.4
	max	163.0	132.5	164.1
	median	97.8	75.6	94.1
	Q1;Q3	35.85;159.70	42.65;108.55	35.65;152.55
RMSSD (ms)	min	41.7	36.7	42.0
	max	221.6	174.5	180.7
	Median	125.0	92.5	111.8
	Q1;Q3	48.50;201.55	54.10;130.90	43.60;179.90
HR max-min (BPM)	Min	3.0	2.4	3.2
	Max	16.3	12.8	18.4
	Median	9.6	7.8	10.4
	Q1;Q3	3.64;15.53	4.14;11.51	4.30;16.51
LF power (ms2)	Min	77.0	166.0	184.0
	Max	19638.0	4917.0	24555.0
	Median	6182.0	1793.3	7008.8
	Q1;Q3	150.00;2506.50	456.50;3130.00	212.00;13805.50
HF power (ms2)	Min	659.0	473.0	733.0
	Max	21792.0	15042.0	14184.0
	Median	6448.8	4782.8	4743.8
	Q1;Q3	1070.00;11827.50	747.50;8818.00	871.50;8616.00
LF/HF ratio	Min	0.2	0.1	0.2
	Max	10.5	4.8	8.0
	Median	4.5	1.4	2.2
	Q1;Q3	0.20;8.75	0.20;2.60	0.20;4.15

T-test, two-sided, paired. BPM – beats per minute; HF – high frequency; HR – heart rate; LF – low frequency; RMSSD – root mean square of successive RR interval differences; SDNN – standard deviation of RR intervals

Table 6. Statistical analysis between measurements for heart rate variability

Experimental group	Mean RR (BPM)	SDNN (ms)	RMSSD (ms)	HR max-min (bpm)	LF power (ms2)	HF power (ms2)	LF/HF ratio
Post-test vs. Pre-test	0.6194	0.3306	0.2748	0.3556	0.3051	0.8080	0.1835
Post-post test vs. Pre-test	0.1063	0.6111	0.2555	0.1925	0.6032	0.2933	0.2416
Post-test vs. Post-post test	0.1439	0.4488	0.5026	0.2702	0.3594	0.6656	0.4091

P-values obtained via T-test, two-sided, paired. BPM – beats per minute; HF – high frequency; HR – heart rate; LF – low frequency; RMSSD – root mean square of successive RR interval differences; SDNN – standard deviation of RR intervals

small sample size, our results certainly require further investigation. The statistical analysis of changes in the resting respiratory rate did not reveal significant differences between the groups across the measurements.

HRV assessment

The results of the statistical analysis with the distribution of values of HRV (Table 5) and between the measurements for HRV (Table 6) for the study group indicate that there were no statistically significant differences. Due to the small sample size of the analyzed group, no analysis of the distributions of the values of the individual parameters was performed.

Subjective stress

The statistical analysis of the parameter of the level of subjectively perceived stress shows that there were no statistically significant differences in subjective stress between the control and study groups, and both the control and study groups showed no significant statistical differences between the measurements of the two groups (Table 7). However, upon examining the distribution of individual results in both groups, it can be observed that the control group initially demonstrated greater stability, with athletes reporting a similar moderate level of perceived stress. In contrast, in the post-post test, the control group exhibited greater variability in reported stress levels compared to the experimental group (Figure 3).

Table 7. Subjective stress

Subjective stress	Pre-test	Post-post test
Experimental group Median (Q1; Q3) min-max	 3.8 (3.00;4.00) 2.0-5.0	 4.2 (3.50;4.50) 3.0-5.0
Control group Median (Q1; Q3) min-max	 4.0 (4.00;4.00) 4.0-4.0	 3.6 (3.00;4.00) 2.0-5.0
p-value	0.6952	0.2329

T-test, two-sided, homoscedastic. 1 – high stress; 5 – low stress

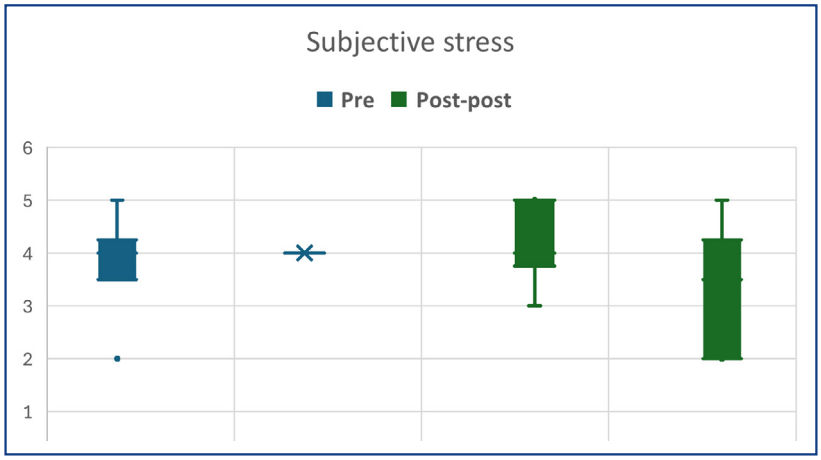

Figure 3. Distribution of scores in the subjective stress test across the respective measure
pre exp – pre-test experimental group, pre contr – pre-test control group, post-post exp – post-post test experimental group, post-post contr – post-post test control group

Discussion

Our findings confirmed that HRVB training may improve the reaction time of rowers, consistent with previous research conducted among basketball players [17]. Improvement in reaction time is particularly relevant in a sport such as rowing, where the start is triggered by an auditory cue (a referee's whistle), and may represent a critical component in professional and effective coaching strategies for athletes at this competitive level.

Additionally, our results indicate that HRVB training led to a significant reduction in resting respiratory rate within the experimental group. However, no statistically significant changes were observed in HRV parameters. Although changes in subjective stress levels did not reach statistical significance, a reduction in perceived stress was noted in the post-post test in the experimental group, whereas an increase was observed in the control group during the same measurement point.

Our findings may cautiously suggest that HRVB training, through its effects on respiratory regulation and pulmonary function, could contribute to autonomic nervous system modulation and stress reduction.

This interpretation aligns with previous findings on the effectiveness of HRVB in managing conditions such as asthma, depression and anxiety in clinical psychology settings, as well as reducing anxiety in athletes [12, 14, 16, 20].

Given the highly demanding nature of elite-level rowing training and the observation that 5 out of 20 participants in this study scored high on the Beck Depression Inventory, it appears warranted to initiate a broader discussion around mental health in competitive sports. Introducing appropriate psychological support tools, including biofeedback-based interventions such as HRVB, may offer valuable assistance to athletes coping with the pressures of elite competition.

Interestingly, the concentration test results did not indicate a significant effect of HRVB training. However, the observed improvement in reaction time, which inherently requires a certain level of concentration, suggests a possible indirect influence. It may be beneficial in future studies to replace the current paper-and-pencil concentration test with a task more closely resembling competitive racing or decision-making under pressure, which may enhance the validity of the findings and increase the likelihood of detecting more consistent effects.

Limitations of the study

As this study represents the first of its kind conducted among Polish Olympic-level rowers, it is challenging for the authors to directly compare the results with those of previous research in this specific context. The pretests were carried out at the beginning of the athletes' competition season and covered the typical course of the season, including participation in the most important competitions (e.g. European Championships or World Championships), ending with the post-post tests. This study, however, has certain limitations, such as the small sample size, the absence of a comprehensive HRV analysis, and a shortened intervention period (4 weeks instead of the 5 weeks recommended in the abbreviated Lehrer protocol). Despite promising results, including a reduction in reaction time by 0.18 seconds and a decrease in the resting respiratory rate, it is important to note that the small sample size, high degree of individualization in training, the psychophysiological variability among athletes suggest that coaches of other athletes should conduct preliminary testing before implementing this method during critical phases of the Olympic preparation period.

Future directions

Researching the effectiveness of using non-invasive and easy-to-apply methods to influence the psychophysical state of athletes is of vital importance in an era of increasingly high performance by athletes around the world. The identification of key psychophysical parameters for a particular sport, and the proper data collection must take place in cooperation with specialists from many fields. Only such research supported by knowledge from various fields of medical, sports or social sciences can bring researchers, coaches and athletes themselves closer to optimizing effective measures that result in winning medals in international competitions

Conclusions

The results of our study suggest that HRVB training may reduce the resting respiratory rate in the experimental group and may improve the reaction time of athletes in accordance with applied methods in rowing.

This study was conducted as part of a research grant awarded by the Ministry of Sport and Tourism, in accordance with the terms specified in contract no. 2022/0768/0017/UDot/61/DSW.

Acknowledgements

The authors would like to thank those involved in this project from the Polish Federation of Rowing Associations, the Rehasport Clinic Sp. z o. o., and coaches Mariusz Goliński, Wojciech Jankowski and Piotr Buliński for their support in carrying out the project.

Conflict of interest

The authors declare that they have no conflict of interest.

Funding

None.

References

1. Grgic J, Diaz-Lara FJ, Del Coso J, Duncan MJ, Tallis J, Pickering C, et al. The Effects of Caffeine Ingestion on Measures of Rowing Performance: A Systematic Review and Meta-Analysis. Nutrients [Internet]. 2020 Feb 8;12(2):434. Available from: https://www.mdpi.com/2072-6643/12/2/434
2. Hwang W-S, Kim H-T. Changes in the Muscle Strength, Muscle Endurance, and Rowing Performance of University Rowing Athletes Following Kettlebell Training and Strength Training. Sport Sci [Internet]. 2024 Dec 31;42(3):27–35. Available from: https://kiss.kstudy.com/Detail/Ar?key=4151011
3. Urbański R, Aschenbrenner P, Żmijewski P, Ewertowska P, Świtała K, Krzysztofik M. Effect of Simultaneous Lower- and Upper-Body Ischemic Preconditioning on Lactate, Heart Rate, and Rowing Performance in Healthy Males and Females. Appl Sci [Internet]. 2024 Apr 23;14(9):3539. Available from: https://www.mdpi.com/2076-3417/14/9/3539
4. Latour E, Arlet J, Latour E, Latour M, Basta P, Skarpańska-Stejnborn A. Stressor-Induced Temporal Cortisol Deficiency as a Primary Trigger for Adaptation to Stress. Int J Environ Res Public Health [Internet]. 2022 May 5;19(9):5633. Available from: https://www.mdpi.com/1660-4601/19/9/5633
5. Piotr B, Anna S-S, Łucja P-S. Influence of Annual Training Cycle on Threshold Power and Reaction of Blood Antioxidative Stress Indices During A Standard Rowing Test. Hum Mov [Internet]. 2008 Jan 1;9(1). Available from: http://www.degruyter.com/view/j/humo.2008.9.issue-1/v10038-008-0008-5/v10038-008-0008-5.xml
6. Kopeć A, Napierała M, Zukow W. Kontuzje i urazy w wioślarstwie = Injuries and trauma in rowing. J Educ Heal Sport [Internet]. 2016;6(4):331–54. Available from: https://apcz.umk.pl/JEHS/article/view/3484
7. Heiss S, Vaschillo B, Vaschillo EG, Timko CA, Hormes JM. Heart rate variability as a biobehavioral marker of diverse psychopathologies: A review and argument for an "ideal range". Neurosci Biobehav Rev [Internet]. 2021 Feb;121:144–55. Available from: https://linkinghub.elsevier.com/retrieve/pii/S0149763420306795
8. Fatisson J, Oswald V, Lalonde F. Influence Diagram of Physiological and Environmental Factors Affecting Heart Rate Variability: An Extended Literature Overview. Heart Int [Internet]. 2016 Jan 25;11(1):heartint.500023. Available from: http://journals.sagepub.com/doi/10.5301/heartint.5000232
9. Aubert AE, Seps B, Beckers F. Heart Rate Variability in Athletes. Sport Med [Internet]. 2003;33(12):889–919. Available from: http://link.springer.com/10.2165/00007256-200333120-00003
10. Staszak O. Odruch z baroreceptorów tętniczych w trakcie testu pochyleniowego u pacjentów z określonymi typami omdleń wazowagalnych. 2015.
11. Lehrer PM, Vaschillo E, Vaschillo B, Lu S-E, Eckberg DL, Edelberg R, et al. Heart Rate Variability Biofeedback Increases Baroreflex Gain and Peak Expiratory Flow. Psychosom Med [Internet]. 2003 Sep;65(5):796–805. Available from: https://journals.lww.com/00006842-200309000-00012
12. Lehrer PM, Vaschillo E, Vaschillo B, Lu S-E, Scardella A, Siddique M, et al. Biofeedback Treatment for Asthma. Chest [Internet]. 2004 Aug;126(2):352–61. Available from: https://linkinghub.elsevier.com/retrieve/pii/S0012369215311430
13. Hallman DM, Olsson EMG, von Schéele B, Melin L, Lyskov E. Effects of Heart Rate Variability Biofeedback in Subjects with Stress-Related Chronic Neck Pain: A Pilot Study. Appl Psychophysiol Biofeedback [Internet]. 2011 Jun 2;36(2):71–80. Available from: http://link.springer.com/10.1007/s10484-011-9147-0
14. Karavidas MK, Lehrer PM, Vaschillo E, Vaschillo B, Marin H, Buyske S, et al. Preliminary Results of an Open Label Study of Heart Rate Variability Biofeedback for the Treatment of Major Depression. Appl Psychophysiol Biofeedback [Internet]. 2007 Mar 26;32(1):19–30. Available from: http://link.springer.com/10.1007/s10484-006-9029-z
15. Lin G, Xiang Q, Fu X, Wang S, Wang S, Chen S, et al. Heart Rate Variability Biofeedback Decreases Blood Pressure in Prehypertensive Subjects by Improving Autonomic Function and Baroreflex. J Altern Complement Med [Internet]. 2012 Feb;18(2):143–52. Available from: http://www.liebertpub.com/doi/10.1089/acm.2010.0607
16. Goessl VC, Curtiss JE, Hofmann SG. The effect of heart rate variability biofeedback training on stress and anxiety: a meta-analysis. Psychol Med [Internet]. 2017 Nov 8;47(15):2578–86. Available from: https://www.cambridge.org/core/product/identifier/S0033291717001003/type/journal_article
17. Paul M, Garg K, Singh Sandhu J. Role of Biofeedback in Optimizing Psychomotor Performance in Sports. Asian J Sports Med [Internet]. 2012 Mar 1;3(1). Available from: https://brieflands.com/articles/asjsm-76716.html

18. Deschodt-Arsac V, Lalanne R, Spiluttini B, Bertin C, Arsac LM. Effects of heart rate variability biofeedback training in athletes exposed to stress of university examinations. Subramanian SK, editor. PLoS One [Internet]. 2018 Jul 26;13(7):e0201388. Available from: https://dx.plos.org/10.1371/journal.pone.0201388
19. Mueller K, Williams PS, Haley L, Heick J. Heart Rate Variability Biofeedback Improves Sports Performance in an Elite Female Athlete. Cardiopulm Phys Ther J [Internet]. 2020 Jul;31(3):123–32. Available from: https://journals.lww.com/10.1097/CPT.0000000000000120
20. Lagos L, Vaschillo E, Vaschillo B, Lehrer P, Bates M, Pandina R. Virtual reality–assisted heart rate variability biofeedback as a strategy to improve golf performance: a case study. Biofeedback [Internet]. 2011;39(1):15––20. Available from: https://meridian.allenpress.com/biofeedback/article-abstract/39/1/15/113152
21. Choudhary R, Trivedi V, Choudhary S. EFFECT OF HEART RATE VARIABILITY BIOFEEDBACK TRAINING ON THE PERFORMANCE OF TRACK ATHLETE. Int J Ther Rehabil Res [Internet]. 2016;5(4):166. Available from: http://www.scopemed.org/fulltextpdf.php?mno=220490
22. Jiménez Morgan S, Molina Mora JA. Effect of Heart Rate Variability Biofeedback on Sport Performance, a Systematic Review. Appl Psychophysiol Biofeedback [Internet]. 2017 Sep 1;42(3):235–45. Available from: http://link.springer.com/10.1007/s10484-017-9364-2
23. Beck A.T., Steer R.A., Brown G.K. Beck Depression Inventory 2nd ed. 2019. Pracownia Testów Psychologicznych Polskiego Towarzystwa Psychologicznego.
24. Ciechanowicz A., Stańczak J. Test Uwagi i Spostrzegawczości. 2006. Pracownia Testów Psychologicznych Polskiego Towarzystwa Psychologicznego.
25. Lehrer P, Vaschillo B, Zucker T, Graves J, Katsamanis M, Aviles M, et al. Protocol for Heart Rate Variability Biofeedback Training. Biofeedback [Internet]. 2013;41(3):98–109. Available from: https://biofeedback.kgl-meridian.com/view/journals/biof/41/3/article-p98.xml

EUROPEAN JOURNAL OF TRANSLATIONAL
AND CLINICAL MEDICINE 2025;8(1):45-58

RESEARCH ARTICLE

Effects of prior antioxidant supplementation on quality of stored erythrocytes: vitamin C + vitamin E and vitamin C + N-acetylcysteine

Masannagari Pallavi[1], Vani Rajashekaraiah[2]

[1] JAIN (Deemed-to-be University), Bangalore, India
[2] Department of Biotechnology and Genetics, JAIN (Deemed-to-be University), Bangalore, India

Abstract

Background: The antioxidant status of donors may impact the quality of stored blood and its components. Therefore, oral antioxidant supplementation prior to blood donation could be a promising approach to improve the efficacy of stored erythrocytes. **Materials and methods:** Wistar rats (3 months old, n = 5/group) were categorized into controls, antioxidant group 1 (vitamin C and vitamin E, VC + VE group), antioxidant group 2 (vitamin C and N-acetylcysteine, VC + NAC group). Experimental rats were supplemented for 30 days. Erythrocytes were stored in additive solution (AS-7) for 42 days and analyzed at two-week intervals. **Results:** Hemoglobin increased on days 28 and 42 in both the antioxidant groups. Superoxide dismutase and catalase activities elevated during initial days and, glutathione peroxidase activity towards the end of storage in the antioxidant groups. Protein carbonyls and malondialdehyde levels decreased in the antioxidant groups. Glutathione levels increased on day 42 in VC + VE. Hemolysis was lower in the VC + VE group until day 28 and was similar in the VC + NAC group. **Conclusion**: VC + VE and VC + NAC supplements protected hemoglobin, blood proteins and lipids from oxidation and elevated antioxidant defenses. Therefore, prior supplementation augments the antioxidant status and quality of stored blood.

Keywords: erythrocytes · vitamin C · vitamin E · N-acetylcysteine · supplementation

Citation

Pallavi M, Rajashekaraiah V. Effects of prior antioxidant supplementation on quality of stored erythrocytes: vitamin C + vitamin E and vitamin C + N-acetylcysteine. Eur J Transl Clin Med. 2025;8(1):45-58.

DOI: 10.31373/ejtcm/202199

Corresponding author:
Vani Rajashekaraiah, Department of Biotechnology and Genetics, JAIN (Deemed-to-be University), Bangalore, India
e-mail: vani.rs@jainuniversity.ac.in
Available online: ejtcm.gumed.edu.pl

Abbreviations

- AS-7 – additive solution-7
- OS – oxidative Stress
- PS – phosphatidyl Serine
- VC – vitamin C
- VE – vitamin E
- NAC – N-acetylcysteine
- MetHb – Methemoglobin
- GSH – reduced glutathione
- GSSG – oxidized glutathione
- ROS – reactive oxygen species
- NADH – nicotinamide adenine dinucleotide
- NADPH – nicotinamide adenine dinucleotide phosphate
- H_2O_2 – hydrogen peroxide

Introduction

Erythrocytes experience physiological and biochemical modifications under blood bank conditions referred to as "storage lesions". Oxidative stress (OS) leads to a decline in antioxidant defenses, oxidation of proteins and lipids, and phosphatidyl serine (PS) externalization [1-3].

Attenuation of oxidative stress could be a promising strategy to diminish storage lesions. Therefore, blood banking research continues to focus on enriching the antioxidant defenses to combat oxidative stress. It has been hypothesized, that enhancing the nutritional status of a donor prior to blood donation could improve the viability and efficacy of stored erythrocytes [4]. Therefore, the primary objective of this study was to explore, whether the antioxidant status of donors influences the quality of stored blood.

There are limited studies on the supplementation of donors with antioxidants. Supplementation of vitamin C and vitamin E resulted in a decrease in plasma malondialdehyde and hemolysis [5]. Nonetheless, the impact of these antioxidant supplements on the OS profile, antioxidant defenses and metabolism of stored erythrocytes has not been explored. The supplementation of β-carotene, vitamin E, vitamin C and selenium decreased the release of hemoglobin and potassium and protected antioxidant enzymes [6].

Animal models offer a platform to mitigate the effects of donor variations, such as age, ethnicity, sex, genetics, and habits (such as smoking), which directly impact the characteristics of stored erythrocytes [7-9].

Therefore, this study aimed to investigate the influence of vitamin C + vitamin E and vitamin C + N-acetylcysteine supplements on the efficacy of banked erythrocytes.

Materials and methods

Ethical committee approval (IAEC/NCP/117/2022) was obtained from the Nargund College of Pharmacy (Bengaluru, India). Animal care and maintenance were in accordance with the ethical committee regulations.

Experimental design

Wistar rats [male, 3 months old, 160-170 g body weight (b.w)] were categorized into three groups (n = 5/group).

A) controls – distilled water (without any antioxidants);

B) antioxidant group 1 (VC + VE group) – vitamin C (400 mg/kg b.w) and vitamin E (50 mg/kg b.w);

C) antioxidant group 2 (VC + NAC group) – vitamin C (400 mg/kg b.w) and N-acetylcysteine (100 mg/kg b.w).

The rats were acclimatized in the animal house for one week and then orally supplemented for 30 days. Erythrocytes were isolated from whole blood and stored for 42 days in AS-7 (additive solution-7) [10]. Hemoglobin, hemolysis, and phosphatidyl serine externalization were measured in erythrocytes. Oxidative stress and antioxidant markers were analyzed in hemolysate at two-week intervals.

Erythrocyte separation

Erythrocytes were isolated by centrifugation at 3500 rpm at 4 ˚C for 20 minutes (min). The erythrocyte pellet was washed and resuspended in isotonic phosphate buffer to a final hematocrit of 50%.

Hemoglobin (Hb)

Hemoglobin content of the erythrocytes was measured by the cyanomethemoglobin method using Hemocor-D Kit and represented in terms of g/dl [11].

Superoxide Dismutase [SOD, EC 1.15.1.1]

Epinephrine was added to the hemolysate diluted in carbonate buffer and measured at 480 nm. SOD activity was expressed as Units/mg protein [12].

Catalase [CAT, EC 1.11.1.6]

Hemolysate was treated with absolute alcohol, 6.6 mM hydrogen peroxide (H_2O_2) and the absorbance was measured at 240 nm. Catalase activity was expressed as Units/mg protein [13].

Glutathione Peroxidase [GPX, EC.1.11.1.9]

Glutathione reductase (0.24 units), and 10 mM glutathione (GSH) were added to hemolysate and preincubated for 10 min at 37 ˚C, followed by the addition of nicotinamide adenine dinucleotide phosphate (NADPH) in 0.1% sodium bicarbonate. The overall reaction was started by adding prewarmed H_2O_2 and the decrease in absorption was monitored at 340 nm for three min. The enzyme activity was expressed as Units/mg protein [14].

Protein Carbonyls (PrC)

An equal volume of 1% trichloroacetic acid (TCA) and the samples were suspended in 10 mM 2,4-dinitrophenyl hydrazine (DNPH). Samples were kept in the dark for 1 hour. An equal volume of 20% TCA was added and left in ice for 10 min, centrifuged at 3000 g, and the pellet was washed with ethanol-ethyl acetate mixture (1:1). The final pellet was dissolved in guanidine HCl, and absorbance was measured at 370 nm [15].

Protein Sulfhydryls (P-SH)

Hemolysate was treated with sodium phosphate buffer containing 0.5 mg/ml of Na_2-EDTA and 2% sodium lauryl sulfate (SDS). 5,5'-dithiobis-2-nitrobenzoic acid (DTNB) was added to the above mixture, vortexed, and absorbance was measured at 412 nm [16].

Malondialdehyde (MDA)

Hemolysate samples were treated with 8.1% SDS, and incubated at room temperature for 10 min. 20% acetic acid was added followed by 0.6% thiobarbituric acid, and the samples were boiled until pink colour developed. Butanol-pyridine was added, and centrifuged for 5 min, and the absorbance was measured at 532 nm [17].

Thiobarbituric acid reactive substances (TBARS)

Hemolysate was treated with 0.9% NaCl and incubated at 37 ˚C for 20 min. 0.8 M HCl containing 12.5% TCA and 1% thiobarbituric acid was boiled for 20 min and cooled. The absorbance was measured at 532 nm [18].

Total Antioxidant Capacity (TAC) Cupric ion-reducing antioxidant capacity – BCS assay [CUPRAC-BCS]

Hemolysate was treated with 0.25mM bathocuproinedisulfonic acid disodium salt (BCS) and the initial absorbance was measured at 490 nm. 0.5 mM Copper sulfate was added and incubated for 3 min, followed by the addition of Na_2EDTA and read at 490 nm [19].

Glutathione (GSH)

Hemolysate was treated with 4% sulfosalicylic acid, and centrifuged at 2500 g for 15 min. The supernatant was treated with 10 mM DTNB and the absorbance was read at 412 nm [20].

Uric acid

Uric acid levels were determined by the Uricase/POD method kit from Aspen Laboratories [21].

Metabolic markers

Glucose

Glucose levels were assessed using the glucose oxidase and peroxidase (GOD-POD) method [22].

Lactate dehydrogenase (LDH)

Hemolysate was treated with the LDH reagent [a mixture of reagent 1 (80 mM Tris, 1.6 mM pyruvate, and 200 mM NaCl) and reagent 2 (0.2 mM NADH) at a ratio of 4:1], and incubated at 37 ˚C. The absorbance was measured at 340 nm [23].

Superoxides

Hemolysate was treated with cytochrome C (160 µM), incubated at 37 ˚C and the absorbance was measured at 550 nm [24].

Nitrites

Hemolysate was added to the coupling reagent, incubated for 10 min and the absorbance was measured at 520 nm [25].

Hemolysis

A 5% suspension of packed erythrocytes were mixed with an equal volume of 8 mM H_2O_2 and incubated at 37 ˚C. Hemolysis was determined by measuring the amount of Hb released into the supernatant at 540 nm [26].

Phosphatidyl Serine (PS) externalization by flow cytometry

The PS exposure on the erythrocyte membrane was analyzed by flow cytometry (CytoFLEX, Beckman Coulter, Inc. USA) according to FITC Annexin V Apoptosis Detection Kit I, BD Biosciences. The data was recorded with an excitation of 488 nm and emission of 530 nm [27], and analyzed by using the CytExpert software. Protein content was determined by Lowry et al. using bovine serum albumin as the standard [28].

Statistical analysis

Results are represented as mean ± standard error (SE) of 5 animals per group. Differences between the controls and antioxidant groups) and within the groups were analyzed by two-way ANOVA. Bonferroni post hoc test was performed. Pearson's correlation coefficient was measured for the relevant markers. The values were considered significant at $p < 0.05$. Statistical analysis was performed using the GraphPad Prism software (version 6, GraphPad Software Inc., Boston, MA, USA).

Results

The significant changes were represented with p-values between the controls and antioxidant groups as well as the sub-groups (storage days).

Hemoglobin (Hb)

Hb levels were significant in all the groups in comparison to day 1. Hb levels increased by 38% ($p < 0.05$) on day 42 in controls with day 1. VC + VE showed increments of 53% ($p < 0.001$) and 61% ($p < 0.0001$) on days 28 and 42 respectively, compared to day 1. Hb levels increased by 37% ($p < 0.05$) and 63% ($p < 0.0001$) on days 28 and 42 respectively, in VC + NAC in comparison to day 1. Hb levels increased by 17% on day 28 in VC + VE and VC + NAC, and 22% on day 42 in VC + NAC compared to controls (Figure 1).

Superoxide dismutase (SOD)

SOD activity was similar throughout the storage period in both control and VC + NAC groups, whereas decreased by 32% ($p < 0.01$) on day 14 in VC + VE compared to day 1. SOD activity increased by 23% on day 1 in VC + VE & VC + NAC compared to controls, and 25% on day 14 in VC + NAC compared to controls & VC + VE (Figure 2A).

Catalase (CAT)

Catalase activity was similar throughout the storage in controls, whereas varied in the antioxidant groups. CAT activity decreased by 35% and 46% on days 14 and 28 respectively, in the VC + VE compared to day 1. CAT activity showed decrements of 56%, 32%, and 45% on days 14, 28, and 42 respectively, in VC + NAC compared to day 1. CAT activity showed increments of 47% and 72 % on day 1 in VC + VE and VC + NAC groups respectively, compared to controls. CAT activity increased by 35% and 47% on day 28 in VC + NAC compared to Control and VC + VE respectively (Figure 2B).

Glutathione peroxidase (GPX)

GPX activity increased in antioxidant groups towards the end of storage period. GPX activity decreased by 27% on day 14 and normalized on day 42 in controls compared to day 1. GPX activity increased by 64% and 105% in VC + VE and 57%

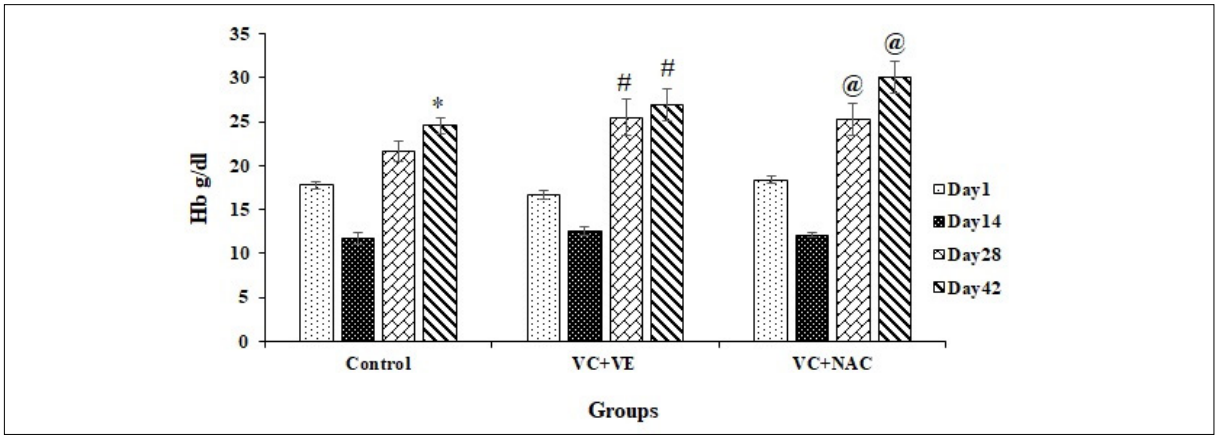

Figure 1. Hemoglobin levels in stored erythrocytes
*represents significant changes during storage in control with respect to day 1
represents significant changes during storage in VC + VE with respect to day 1
@ represents significant changes during storage in VC + NAC with respect to day 1

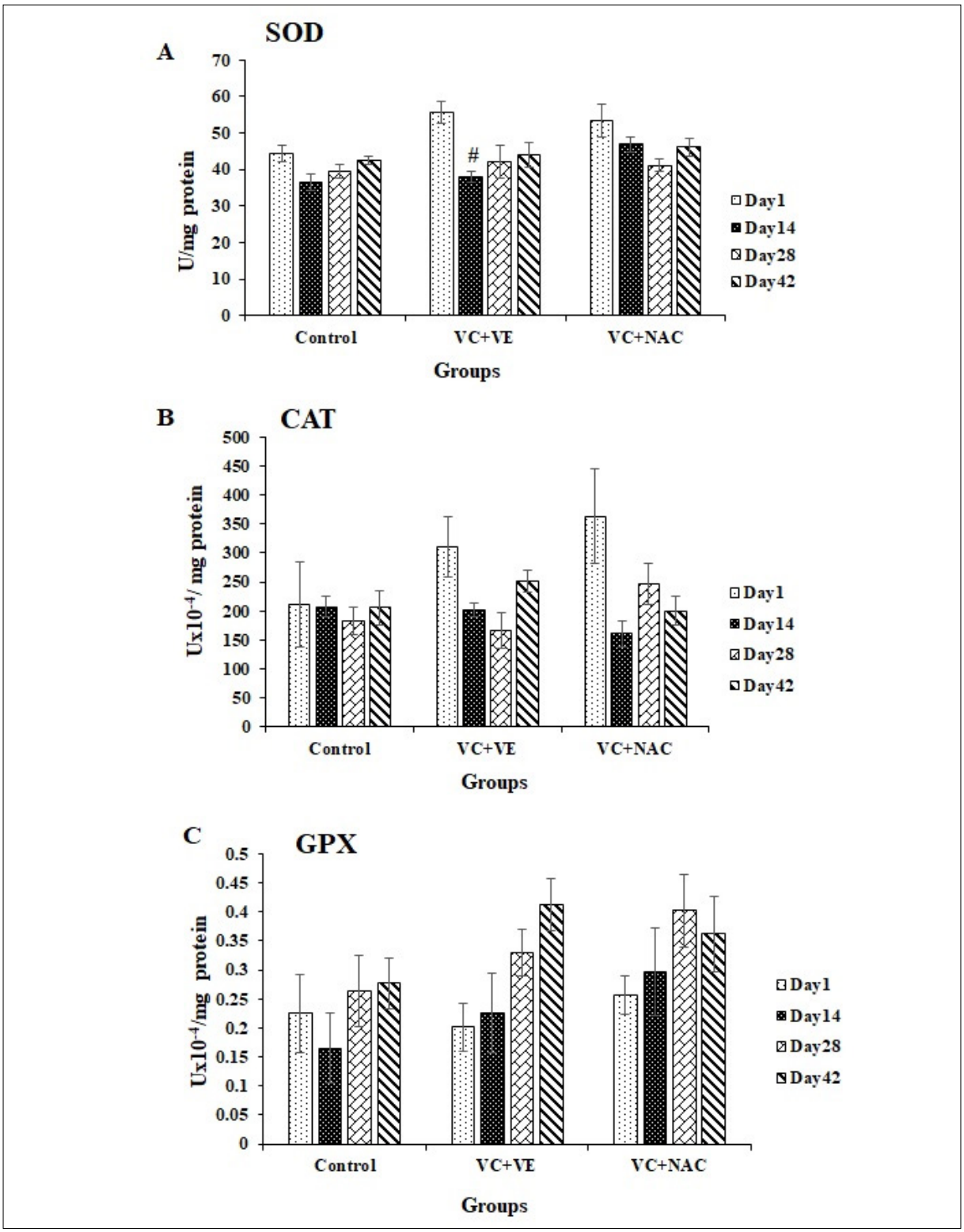

Figure. 2A. Superoxide dismutase activity in stored erythrocytes;
2B. Catalase activity in stored erythrocytes;
2C. Glutathione peroxidase activity in stored erythrocytes.
Values are expressed as mean ± SE from 5 samples. Significance between the groups was analyzed by two-way ANOVA followed by Bonferroni post test, using GraphPad Prism 6 software.
represents significant changes during storage in VC + VE with respect to day 1.

and 41% in VC + NAC on days 28 and 42 respectively, compared to day 1. Increments of 36% & 80% (day 14), 25% & 52% (day 28), and 49% & 31% (day 42) were observed in VC + VE & VC + NAC respectively, compared to controls (Figure 2C).

Protein Carbonyls (PrC)

Carbonyls increased by 21% and 67% on days 28 and 42 respectively, in controls compared to day 1, whereas decreased towards the end of storage in both the antioxidant groups (Table 1).

Protein Sulfhydryls (P-SH)

Sulfhydryls increased by 139%, 85%, and 103% on days 14, 28, and 42 respectively, in controls compared to day 1. Sulfhydryls remained constant throughout storage, whereas lowered by 37% on day 28 and normalized on day 42 in VC + VE with respect to day 1. Sulfhydryls decreased by 25% on days 28 and 42 in VC + NAC in comparison to day 1. Sulfhydryls increased by 1-fold and 2-fold in VC + VE and VC + NAC groups respectively, on day 1 in comparison to controls. VC + NAC showed increments in sulfhydryls on day 1 (26%) and day 28 (55%) when compared to VC + VE (Table 1).

Malondialdehyde (MDA)

Controls showed increments of 32% and 68% on days 28 and 42 respectively, compared to day 1. MDA levels remained constant throughout the storage in VC + VE, whereas decreased by 23% and 30% on days 14 and 42 respectively, in VC + NAC with day 1. VC + NAC showed decrements of 39% and 26% on day 42 compared to controls and VC + VE respectively (Table 1).

Thiobarbituric acid reactive substances (TBARS)

Antioxidant groups had lower levels of TBARS in comparison to Controls. TBARS decreased by 14% on day 28 in VC + VE and VC + NAC respectively, compared to day 1. TBARS were lower by 23% on day 42 in VC + VE compared to Controls (Table 1).

Total Antioxidant Capacity (TAC)

TAC was higher in both the antioxidant groups compared to controls. TAC decreased by 23% on days 28 and 42 respectively, in controls with day 1. Decrements of 20% and 26%

Table 1. Antioxidant effects of melatonin [32]

Storage	Groups	Protein Carbonyls (µM/mg protein)	Protein Sulfhydryls (µM/mg protein)	Malondialdehyde (µM/mg protein)	TBARS (µM/mg protein)
Day 1	Control	2.49 ± 0.76	282. 49 ± 98.74	3.72 ± 0.97	2.85 ± 0.20
	VC+VE	3.46 ± 0.36	691.56 ± 184.92	4.90 ± 1.08	2.62 ± 0.08
	VC+NAC	3.85 ± 0.15	873.63 ± 218.69	5.53 ± 0.169	2.80 ± 0.44
Day 14	Control	2.74 ± 0.31	675.91 ± 235	4.19 ± 0.45	2.38 ± 0.47
	VC+VE	3.78 ± 0.45	701.27 ± 176.13	4.94 ± 0.77	2.15 ± 0.43
	VC+NAC	3.54 ± 0.44	737.18 ± 228.76	4.27 ± 1.20	2.30 ± 0.07
Day 28	Control	3.01 ± 0.49	521.72 ± 173.14	4.91 ± 0.53	2.78 ± 0.49
	VC+VE	3.20 ± 0.49	432.78 ± 53.35	4.67 ± 0.97	2.24 ± 0.12
	VC+NAC	3.33±0.80	668.83 ± 154.87	5.16 ± 0.84	2.43 ± 0.4
Day 42	Control	4.16 ± 0.32	572.13 ± 120.18	6.27 ± 1.18	3.93 ± 1.38
	VC+VE	3.27 ± 0.93	613.50 ± 143.67	5.19 ± 2.10	3.05 ± 0.26
	VC+NAC	3.36 ± 0.41	625.07 ± 113.34	3.85 ± 0.54	3.64 ± 0.40

Values are expressed as mean ± SE from 5 samples. Significance between the groups was analyzed by two-way ANOVA followed by Bonferroni post test, using GraphPad Prism 6 software. TBARS – Thiobarbituric acid reactive substances.

were observed in VC + VE and VC + NAC respectively, on day 42 compared to day 1. TAC showed increments of 20% (day 14) and 34% (day 28) in VC + VE and 43% (day 28) in VC + NAC compared to controls (Figure 3A).

Glutathione (GSH)

The GSH levels were significant towards the end of storage in VC + VE. GSH levels decreased by 17% on day 14 and normalized towards the end of storage in controls. GSH levels increased by 32% ($p < 0.01$) in VC + VE and 18% in VC + NAC on day 42 compared to day 1. VC + VE showed increments of 16% on days 28 and 42 compared to controls. GSH increased by 23% on day 14 in VC + NAC compared to controls and VC + VE respectively (Figure 3B).

Uric acid

Although the variations were similar, uric acid levels were higher in the antioxidant groups throughout the storage (Figure 3C).

Glucose

Glucose levels were similar throughout storage in controls, whereas they varied in the antioxidant groups. Glucose levels varied by 23% on day 14 and 26% on days 28 and 42 in VC + VE with day 1. Glucose levels decreased by 20% on days 14 and 28 in VC + NAC compared to day 1. Glucose levels increased by 20% (day 1) and 37% (day 14) in VC + VE compared to controls. Glucose levels elevated in VC + NAC by 41%, 18%, and 27% on days 1, 28, and 42 respectively, compared to controls and 26% and 46 % on days 28 and 42 compared to VC + VE (Figure 4A).

Lactate dehydrogenase (LDH)

LDH activity decreased by 60% and 77% on day 1 in VC + VE and VC + NAC respectively, compared to controls (Figure 4B).

Superoxides

Superoxide levels were similar in all the groups throughout the storage. Superoxides increased from 0.31 mM/mg protein (day 1) to 0.50 mM/mg protein (days 28 and 42) in controls. Superoxides increased from 0.34 mM/mg protein (day 1) to 0.48 mM/mg protein (day 14) and were stable until day 42 in VC + VE. Superoxides varied from 0.4 mM/mg protein (day 1) to 0.45 mM/mg protein (day 28), and 0.55 mM/mg protein (day 42) in VC + NAC.

Nitrites

Variations were similar in all the groups. Nitrites varied on day 14 (2.89 mM/mg protein) and day 28 (2.69 mM/mg protein) compared to day 1 (2.45 mM/mg protein) in controls. Nitrites increased on day 28 (3.13 mM/mg protein) in comparison to day 1 (2.62 mM/mg protein) and then normalized in VC + VE. Nitrite varied from 2.96 mM/mg protein (day 1) to 2.12 mM/mg protein (day 42) in VC + NAC.

Hemolysis

VC + VE showed a decrease of 43% on days 1, 14 and 28 compared to controls and 74%, 52%, and 25% on days 1, 14 and 28 compared to VC + NAC. VC + NAC showed decrements of 25% and 16% on days 28 and 42 in comparison to controls (Figure 5).

Phosphatidyl Serine (PS) externalization

The variations were observed in the PS exposure with storage. PS exposure increased by 9-fold on day 42 in controls compared to day 1 (0.51%). VC + VE and VC + NAC groups showed increments of 2-fold and 1-fold respectively, on day 42 in comparison to day 1 (VC + VE – 1.27%; VC + NAC – 1.46%).

Discussion

Storage lesions accumulate in erythrocytes when the oxidants overwhelm the antioxidant defenses. Hence, antioxidant augmentation could be a promising approach to maintain the microenvironment equilibrium.

VC + VE group

In this study the Hb levels increased towards the end of storage in the VC + VE group indicates the reverse conversion of methemoglobin (metHb) to Hb by vitamin C and vitamin E. We also noted this in our previous study, where the combination of VC and VE as additives increased Hb levels [29]. Atyabi et al. also reported that the combination of vitamin C and E was effective in reducing sodium nitrite-induced metHb formation [30].

SOD dismutates superoxide into H_2O_2, and catalase scavenges H_2O_2. This was evidenced by an inverse correlation between SOD activity and superoxide levels ($r = –0.9447$) and a positive correlation between SOD and catalase activity in the VC + VE group ($r = 0.8586$). SOD and catalase activities were higher in the VC + VE group on day 1, indicating that supplemented antioxidants upregulated the antioxidant

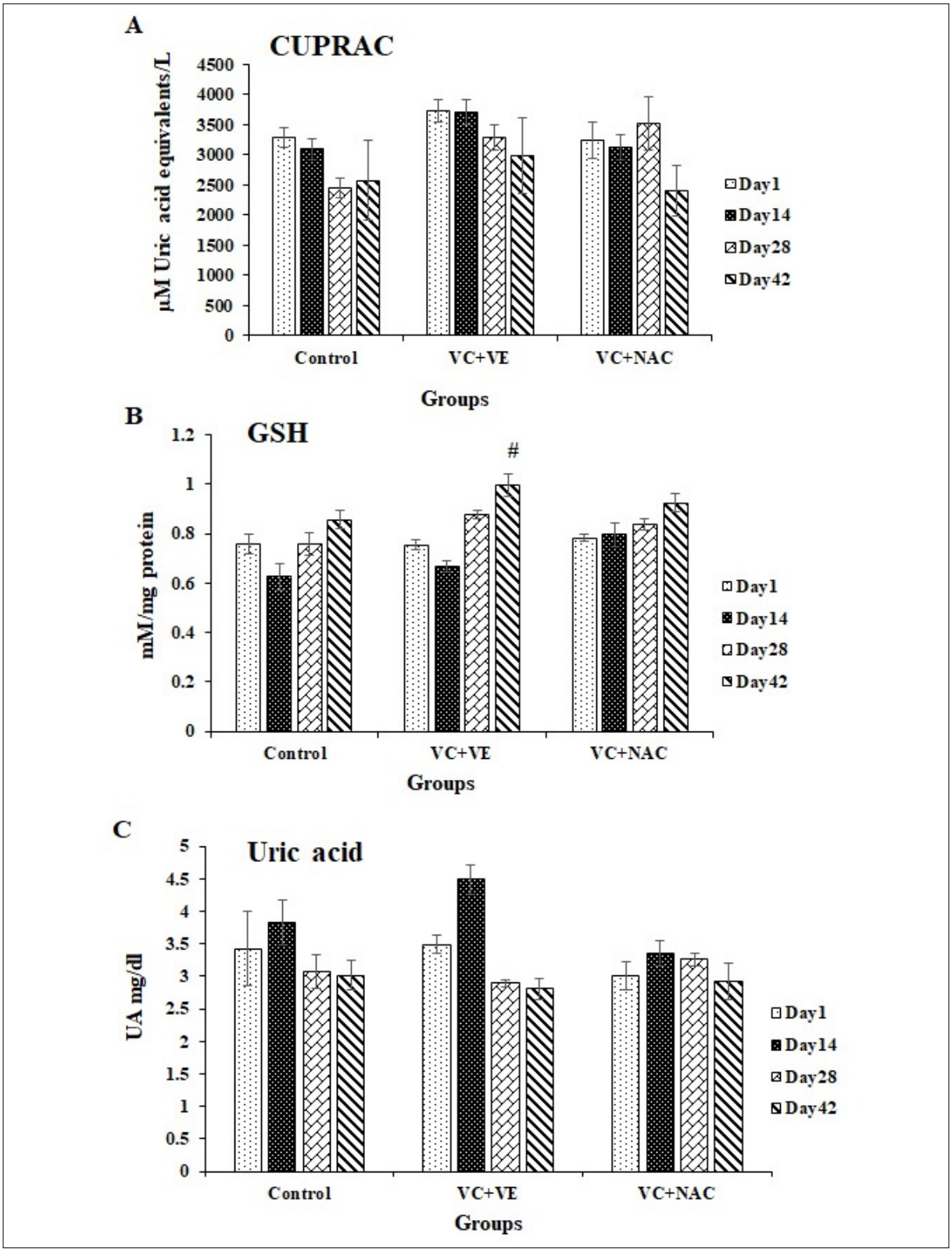

Figure 3A. CUPRAC in stored erythrocytes
3B. Glutathione in stored erythrocytes
3C. Uric acid in stored erythrocytes
Values are expressed as mean ± SE from 5 samples. Significance between the groups was analyzed by Two-way ANOVA followed by Bonferroni post test, using GraphPad Prism 6 software.
represents significant changes during storage in VC + VE with respect to day 1

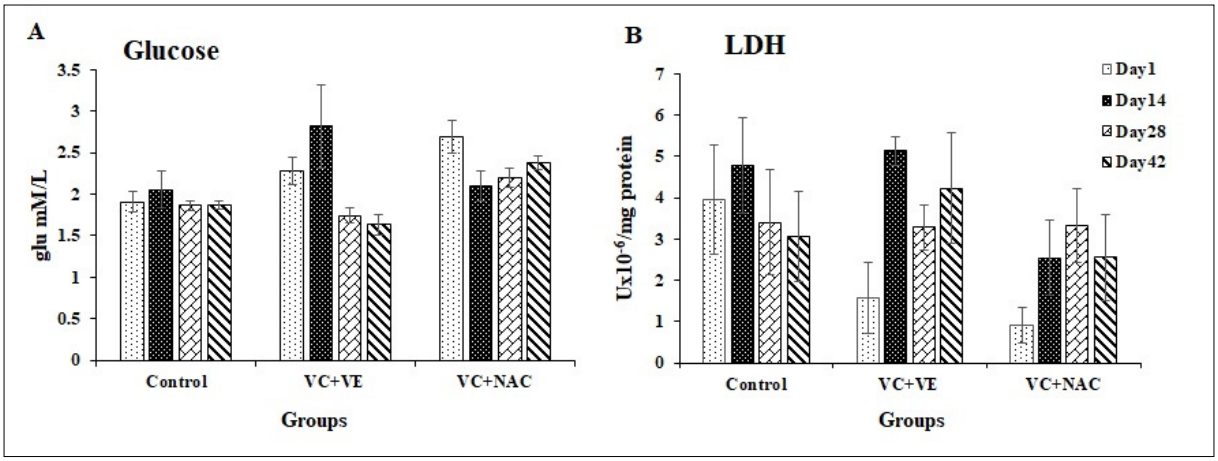

Figure 4A. Glucose in stored erythrocytes
4B. Lactate dehydrogenase in stored erythrocytes
Values are expressed as mean ± SE from 5 samples. Significance between the groups was analyzed by two-way ANOVA followed by Bonferroni post test, using GraphPad Prism 6 software.

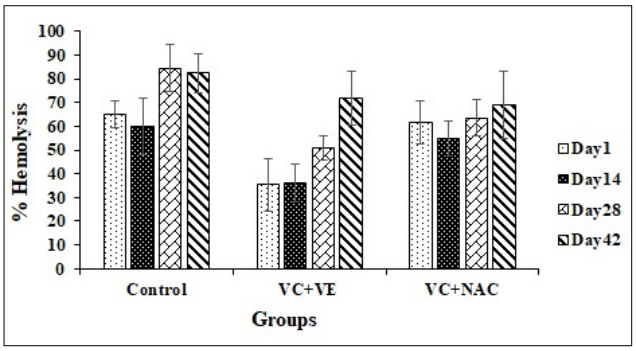

Figure 5. Hemolysis in stored erythrocytes
Values are expressed as mean ± SE from 5 samples. Significance between the groups was analyzed by two-way ANOVA followed by Bonferroni post test, using GraphPad Prism 6 software.

enzymes. Gultekin and Bhogade have also reported that vitamin C and E upregulates antioxidant enzymes [31-32]. However, SOD and catalase activity decreased on day 14 in VC + VE reflecting the superoxide and H_2O_2 scavenging activity of vitamin C and vitamin E [5, 33-34]. Therefore, superoxide levels reached a plateau from day 14 onwards in the VC + VE group.

GPX scavenges H_2O_2 at lower levels by using GSH as a co-factor and oxidizes GSH (reduced glutathione) to GSSG (oxidized glutathione) [35]. Supplementation of vitamin C and vitamin E increases cellular glutathione levels, thereby upregulating the GPX activity [36-37]. Previous studies also reported that supplementation of vitamin C and vitamin E increases GPX activity [38-39]. Similarly in this study, glutathione levels and GPX activity elevated towards the end of storage in the VC + VE group with a significant correlation between GSH and GPX activity (r = 0.9389) indicating that VC + VE enhanced antioxidant defenses.

Protein carbonyls declined in the VC + VE group with storage, suggesting the protective influence of Vitamin C and Vitamin E against protein oxidation, evidenced in our earlier in vitro study [29]. Goldfarb et al. and Marino et al. have also reported that vitamin C and E supplementation reduced protein carbonyl formation during exercise-induced and alcohol-induced oxidative stress, respectively [40-41]. Vitamin C and E synergistically quench the free radicals generated in the lipid core of the erythrocyte membrane and protect from protein oxidation, which was also evidenced in our findings [42]. Carbonyl levels increased towards the end of the storage in controls, indicating protein damage resulting from oxidative insult, which was also observed by Jana et al. [43].

Higher sulfhydryl levels in the VC + VE group until 2nd week of storage suggest the protection of sulfhydryl groups against oxidation or the reversible conversion of disulfides to sulfhydryls [44]. Vitamin C and vitamin E supplementation have been associated with elevated cellular GSH and sulfhydryls [36-37]. However, the lower levels of sulfhydryls on day 28 in the VC + VE group imply the conversion of GSH to GSSG, evidenced by an elevation in GPX and nitrites. Sulfhydryls normalized on day 42, due to the reversible conversion of GSSG to GSH due to the action of VC and VE [45].

The MDA levels were similar throughout the storage in the VC + VE group, indicating the lipid peroxyl radical scavenging activity of vitamin C and vitamin E [35, 46-47]. Vitamin C and vitamin E synergistically impede the progression of lipid peroxidation reactions in plasma lipoproteins and membranes [35]. Nonetheless, MDA levels peaked towards the end of storage in controls, indicating that inherent antioxidant defenses were inadequate to mitigate ROS attack on membrane lipids.

Oxidative damage to membrane lipids and proteins contributes to elevations in LDH activity [48]. LDH increased rapidly during the first 4 weeks of storage in controls. Verma et al. and Latham et al. also reported an increase in LDH activity during erythrocyte storage [49-50]. However, the VC + VE protected erythrocytes from LDH leakage until two weeks of storage. This indicates reduced oxidative damage to membrane proteins and lipids, resulting in lower hemolysis. Czubak et al., also demonstrated that VC and VE synergistically protect human erythrocytes from LDH leakage up to 20 days [51].

Total antioxidant capacity (TAC) was relatively higher in the VC + VE group, depicting that vitamin C and vitamin E synergistically enhanced antioxidant capacity. TAC was directly proportional to glutathione and uric acid (endogenous antioxidants). However, TAC decreased towards the end of storage due to oxidative stress. Similarly, Czubak et al. reported a storage-dependent decrease in antioxidant capacity during erythrocyte storage [51].

Glucose levels were higher on day 14 and declined towards the end of storage in the VC + VE group, which can be attributed to the higher glucose consumption by erythrocytes due to an increase in their metabolic activity [52]. Glucose serves as a crucial substrate for both glycolysis and the pentose phosphate pathway to generate NADH and NADPH essential to reduce methemoglobin, which correlated with higher hemoglobin levels towards the end of storage [53]. The effective glucose metabolism plays a role in regulating glutathione levels, thereby protecting the sulfhydryl groups of hemoglobin from oxidation, which was evidenced with higher glutathione levels [35].

Phosphatidyl serine (PS) exposure on the outer leaflet of the erythrocyte membrane indicates storage lesions and the signals for apoptotic senescence [54]. The percentage of PS-exposing cells increases with storage, which was evidenced in our results [48, 55]. However, PS externalization was comparatively lower in VC + VE suggesting that supplementation of vitamin C and vitamin E reduced apoptosis, which also corroborates with the findings of Huang et al. [56].

Hemolysis is a result of protein and lipid oxidation. Vitamin C decreases the tocopheroxyl radicals in the membrane during the lipid–aqueous phase transition [57]. Vitamin C and vitamin E act synergistically to prevent the propagation of oxidation in erythrocyte membranes and hemolysis, which was evident in the hemolysis results [48, 51, 58]. Sakarya et al. and Claro et al., also reported that vitamin C and E attenuates the oxidation of erythrocyte membrane [50, 59].

VC + NAC group

The elevations in Hb levels towards the end of storage in VC + NAC could be due to the reverse conversion of metHb to Hb by the antioxidants. Vitamin C and NAC reduce metHb formation, which was evidenced in the Hb results [60-61].

SOD and catalase activities increased on day 1 in the VC + NAC group, indicating the upregulation of the antioxidant enzymes by vitamin C and NAC supplementation [31, 62]. Catalase activity decreased from day 14 in VC + NAC indicating the H_2O_2 scavenging activity of vitamin C and NAC [32, 63]. Consequently, the lower levels of H_2O_2 towards the end of storage were further mitigated by GPX. There is a positive correlation between GSH and GPX activity towards the end of storage ($r = 0.660$).

Protein carbonyls declined towards the end of storage in VC + NAC, indicating the protective effect of vitamin C and NAC against protein oxidation. Goldfarb et al. and Banaclocha et al. reported that Vitamin C and NAC decrease protein carbonyl formation against exercise and age-related oxidative stress, respectively [40, 64]. MDA levels also decreased towards the end of storage in the VC + NAC group which is consistent with the study by Pallotta et al. [65]. NAC indirectly contributes to lipid peroxyl radical scavenging activity by providing GSH for the reduction of ascorbate radicals to ascorbic acid [66].

Sulfhydryl levels were higher in VC + NAC compared to VC + VE suggesting GSH replenishment due to supplementation of NAC. Pallotta et al. reported that the storage of human erythrocytes with vitamin C and NAC resulted in higher GSH levels till 42 days [65]. Grinberg et al. also demonstrated that NAC protected erythrocytes from oxidative stress by restoring cellular glutathione [67]. VC + NAC protected lipids from oxidation as evidenced by enhanced endogenous antioxidants such as uric acid, glutathione and total antioxidant capacity.

LDH activity increased rapidly during the first 4 weeks of storage in controls whereas, the VC + NAC group showed a lower LDH release reflecting decreased erythrocyte damage as evidenced by reduced hemolysis and PS exposure. Glucose levels were higher in the VC + NAC group compared to controls. Glucose metabolism efficiently maintained GSH and thus protected hemoglobin and membrane from oxidation [35, 53].

Conclusion

Antioxidant combination (VC + VE and VC + NAC) supplements protected hemoglobin, blood proteins, and lipids from oxidation, and enhanced antioxidant defenses. VC + VE elevated glutathione levels and lowered hemolysis. VC + VE was effective against hemolysis compared to VC + NAC due to their synergistic action. VC + NAC was beneficial as it lowered LDH leakage and apoptosis. Both the antioxidant combinations have a positive influence on the efficacy of stored erythrocytes. Our results imply that prior supplementation

augments the antioxidant status and influences the quality of stored blood.

Acknowledgments

The authors acknowledge Dr. Leela Iyengar, Dr. Soumya Ravikumar, Dr. Carl Hsieh, Dr. Manasa Mithun, Ms. Magdaline Christina Rajanand, Anusha Berikai Ananthakrishna, Darmavaram Sravani, and JAIN (Deemed-to-be University) for their support.

Funding

The Authors did not receive any specific grant for this research from funding agencies in the public, commercial or not-for-profit sectors.

Conflict of Interest

There are no conflicts of interest to declare.

References

1. Yoshida T, Prudent M, D'Alessandro A. Red blood cell storage lesion: causes and potential clinical consequences. Blood Transfus. 2019;17(1):27–52. Available from: https://doi.org/10.2450/2019.0217-18
2. Bardyn M, Tissot JD, Prudent M. Oxidative stress and antioxidant defenses during blood processing and storage of erythrocyte concentrates. Transfus Clin Biol. 2018;25(1):96–100. Available from: https://doi.org/10.1016/j.tracli.2017.08.001
3. Dinkla S, Peppelman M, Van Der Raadt J, Atsma F, Novotný VM, Van Kraaij MG, Joosten I, Bosman GJ. Phosphatidylserine exposure on stored red blood cells as a parameter for donor-dependent variation in product quality. Blood Transfus. 2014;12(2):204–9. Available from: https://doi.org/10.2450/2013.0106-13
4. Addis PB, St. Cyr JA. Nutritional Supplementation of Donors May Improve Outcomes Following the Transfusion of Stored Red Blood Cells. J Diet Supplement. 2017;14(4):485–8. Available from: https://doi.org/10.1080/19390211.2016.1272660
5. Knight JA, Blaylock RC, Searles DA. The effect of vitamins C and E on lipid peroxidation in stored erythrocytes. Ann Clin Lab Sci. 1993;23(1):51–6. Available from: http://www.annclinlabsci.org/content/23/1/51.short
6. Racek J, Herynkovà R, Holeček V, Jeřábek Z, Sláma V. Influence of antioxidants on the quality of stored blood. Vox Sang. 1997;72(1):16–9. Available from: https://doi.org/10.1159/000461951
7. D'Alessandro A, Fu X, Kanias T, Reisz JA, Culp-Hill R, Guo Y, Gladwin MT, Page G, Kleinman S, Lanteri M, Stone M. Donor sex, age and ethnicity impact stored red blood cell antioxidant metabolism through mechanisms in part explained by glucose 6-phosphate dehydrogenase levels and activity. Haematologica. 2021;106(5):1290–1302. Available from: https://doi.org/10.3324/haematol.2020.246603
8. Längst E, Tissot JD, Prudent M. Storage of red blood cell concentrates: Clinical impact. Transfus Clin Biol. 2021;28(4):397–402. Available from: https://doi.org/10.1016/j.tracli.2021.08.344
9. Jordan A, Chen D, Yi QL, Kanias T, Gladwin MT, Acker JP. Assessing the influence of component processing and donor characteristics on quality of red cell concentrates using quality control data. Vox Sang. 2016;111(1):8–15. Available from: https://doi.org/10.1111/vox.12378
10. Hsieh C, Prabhu NS, Rajashekaraiah V. Influence of AS-7 on the storage lesion in young and old circulating erythrocytes. Transfus Apher Sci. 2020;59(6):102905. Available from: https://doi.org/10.1016/j.transci.2020.102905
11. Hawk FB. Physiological chemistry. New York: Tata McGraw Hill; 1965.
12. Misra HP, Fridovich I. The role of superoxide dismutase anion in the auto oxidation of epinephrine and a simple assay for superoxide dismutase. J Biol Chem. 1972;247(10):3170–5. Available from: https://doi.org/10.1016/S0021-9258(19)45228-9
13. Aebi H. Catalase in vitro. Methods Enzymol. 1984;105:121–6. Available from: https://doi.org/10.1016/S0076-6879(84)05016-3
14. Flohe L, Gunzler WA. Assays of glutathione peroxidase. Methods Enzymol. 1984;105:114–20. Available from: https://doi.org/10.1016/S0076-6879(84)05015-1
15. Reznick AZ, Packer L. Oxidative damage to protein: spectrophotometric method for carbonyl assay. Methods Enzymol. 1994;233:357–63. Available from: https://doi.org/10.1016/S0076-6879(94)33041-7
16. Habeeb AFSA. Reaction of protein sulfhydryl groups with Ellman's reagent. Methods Enzymol. 1972;25:457–64. Available from: https://doi.org/10.1016/S0076-6879(72)25041-8
17. Ohkawa H, Ohishi N, Yagi K. Assay for lipid peroxidation in animal tissues by thiobarbituric acid reaction. Anal Biochem. 1979;95(2):351–8. Available from: https://doi.org/10.1016/0003-2697(79)90738-3

18. Bar-Or D, Rael LT, Lau EP, Rao NK, Thomas GW, Winkler JV, Yukl RL, Kingston RG, Curtis CG. An analog of the human albumin N-terminus (Asp-Ala-His-Lys) prevents formation of copper-induced reactive oxygen species. Biochem Biophys Res Commun. 2001;284(3):856–62. Available from: https://doi.org/10.1006/bbrc.2001.5042
19. Campos C, Guzmán R, López-Fernández E, Casado A. Evaluation of the copper (II) reduction assay using bathocuproinedisulfonic acid disodium salt for the total antioxidant capacity assessment: the CUPRAC-BCS assay. Anal Biochem. 2009;392(1):37–44. Available from: https://doi.org/10.1016/j.ab.2009.05.024
20. Beutler E, Duran O, Kelley BM. Modified procedure for the estimation of reduced glutathione. J Lab Clin Med. 1963;61:882–8.
21. Thomas L, editor. Clinical laboratory diagnostics: use and assessment of clinical laboratory results. TH-books Verlagsgesellschaft; 1998
22. Basak A. Development of a rapid and inexpensive plasma glucose estimation by two point kinetic method based on glucose oxidase- peroxidase enzymes. Indian J Clin Biochem. 2007;22:156–60. Available from: https://doi.org/10.1007/BF02912902
23. Buhl SN, Jackson KY, Graffunder B. Optimal reaction conditions for assaying human lactate dehydrogenase pyruvate-to-lactate at 25, 30, and 37˚C. Clin Chem. 1978;24(2):261–6. Available from: https://doi.org/10.1093/clinchem/24.2.261
24. Olas B, Wachowicz B. Resveratrol and vitamin C as antioxidants in blood platelets. Thromb Res. 2002;106(2):143–8. Available from: https://doi.org/10.1016/S0049-3848(02)00101-9
25. Yegin SC, Yur F, Çetın S, Güder A. Effect of Lycopene on Serum Nitrite-Nitrate Levels in Diabetic Rats. Indian J Pharm Sci. 2015;77(3);357–60. Available from: https://doi.org/10.4103/0250-474x.159676
26. Senturk UK, Gunduz F, Kuru O, Aktekin MR, Kipmen D, Yalçin O, Bor-Küçükatay M, Yeşilkaya A, Başkurt OK. Exercise-induced oxidative stress affects erythrocyte in sedentary rats but not exercise-trained rats. J Appl Physiol. 2001;91(5):1999–2004. Available from: https://doi.org/10.1152/jappl.2001.91.5.1999
27. Antosik A, Czubak K, Gajek A, Marczak A, Glowacki R, Borowczyk K, Zbikowska HM. Influence of pre-storage irradiation on the oxidative stress markers, membrane integrity, size and shape of the cold stored red blood cells. Transfus Med Hemother. 2015;42(3):140–8. Available from: https://doi.org/10.1159/000371596
28. Lowry OH, Rosenberg NJ, Farr AL, Randall RJ. Protein measurements with Folin-phenol reagent. J Biol Chem. 1951;193: 265–75.
29. Pallavi M, Rajashekaraiah V. Synergistic activity of vitamin-C and vitamin-E to ameliorate the efficacy of stored erythrocytes. Transfus Clin Biol. 2023;30(1):87–95. Available from: https://doi.org/10.1016/j.tracli.2022.09.002
30. Atyabi N, Yasini SP, Jalali SM, Shaygan H. Antioxidant effect of different vitamins on methemoglobin production: An in vitro study. Vet Res Forum. 2012;3(2):97–101. Available from: https://pmc.ncbi.nlm.nih.gov/articles/PMC4312803/
31. Gultekin F, Delibas N, Yasar S, Kilinc I. In vivo changes in antioxidant systems and protective role of melatonin and a combination of vitamin C and vitamin E on oxidative damage in erythrocytes induced by chlorpyrifos-ethyl in rats. Arch Toxicol. 2001;75:88–96. Available from: https://doi.org/10.1007/s002040100219
32. Bhogade RB, Suryakar AN, Joshi NG, Patil RY. Effect of vitamin E supplementation on oxidative stress in hemodialysis patients. Indian J Clin Biochem. 2008;23:233–7. Available from: https://doi.org/10.1007/s12291-008-0052-0
33. Pehlivan FE. Vitamin C: An antioxidant agent. Vitamin C. 2017;2:23–35. Available from: https://www.intechopen.com/chapters/56013?affiliate=30&source=&subid2=&subid=3psdb09qw8cfvztjcq006h&vid=fUOez3Avy5qaX2NZKXRDqXbXKx
34. Lassnigg A, Punz A, Barker R, Keznickl P, Manhart N, Roth E, Hiesmayr M. Influence of intravenous vitamin E supplementation in cardiac surgery on oxidative stress: a double-blinded, randomized, controlled study. Br J Anaesth. 2003;90(2):148–54. Available from: https://doi.org/10.1093/bja/aeg042
35. Çimen MYB. Free radical metabolism in human erythrocytes. Clin Chim Acta. 2008;390(1-2):1–11. Available from: https://doi.org/10.1016/j.cca.2007.12.025
36. Johnston CS, Meyer CG, Srilakshmi JC. Vitamin C elevates red blood cell glutathione in healthy adults. Am J Clin Nutr. 1993;58(1):103-5. Available from: https://doi.org/10.1093/ajcn/58.1.103
37. Jain SK, McVIE RO, Smith TI. Vitamin E supplementation restores glutathione and malondialdehyde to normal concentrations in erythrocytes of type 1 diabetic children. Diabetes Care. 2000;23(9):1389–94. Available from: https://doi.org/10.2337/diacare.23.9.1389
38. Madhikarmi NL, Murthy KR. Antioxidant enzymes and oxidative stress in the erythrocytes of iron deficiency anemic patients supplemented with vitamins. Iran Biomed J. 2014;18(2):82–7. Available from: https://pmc.ncbi.nlm.nih.gov/articles/PMC3933916/
39. Cinar M, Yildirim E, Yigit AA, Yalcinkaya I, Duru O, Kisa U, Atmaca N. Effects of dietary supplementation with vitamin C and vitamin E and their combination on growth performance, some biochemical parameters, and oxidative stress induced by copper toxicity in broilers. Biol Trace Elem Res. 2014;158:186–96. Available from: https://doi.org/10.1007/s12011-014-9926-6

40. Goldfarb AH, Patrick SW, Bryer S, You T. Vitamin C supplementation affects oxidative-stress blood markers in response to a 30-minute run at 75% VO2max. Int J Sport Nutr Exerc Metab. 2005;15(3):279–90. Available from: https://doi.org/10.1123/ijsnem.15.3.279
41. Marino MD, Aksenov MY, Kelly SJ. Vitamin E protects against alcohol-induced cell loss and oxidative stress in the neonatal rat hippocampus. Int J Dev Neurosci. 2004;22(5-6):363–77. Available from: https://doi.org/10.1016/j.ijdevneu.2004.04.005
42. Vani R, Shiva Shankar Reddy CS, Asha Devi S. Oxidative stress in erythrocytes: a study on the effect of antioxidant mixtures during intermittent exposures to high altitude. Int J Biometeorol. 2010;54:553–62. Available from: https://doi.org/10.1007/s00484-010-0304-6
43. Jana S, Kassa T, Wood F, Hicks W, Alayash AI. Changes in hemoglobin oxidation and band 3 during blood storage impact oxygen sensing and mitochondrial bioenergetic pathways in the human pulmonary arterial endothelial cell model. Front Physiol. 2023;14:1278763. Available from: https://doi.org/10.3389/fphys.2023.1278763
44. Cao Y, Qu HJ, Li P, Wang CB, Wang LX, Han ZW. Single dose administration of L-carnitine improves antioxidant activities in healthy subjects. Tohoku J Exp Med. 2011;224:209–13. Available from: https://doi.org/10.1620/tjem.224.209
45. Hsieh C, Rajashekharaiah V. Influence of L-carnitine on stored rat blood: a study on plasma. Turkish J Hematol. 2017;34(4):328. Available from: https://doi.org/10.4274/tjh.2016.0343
46. Halliwell B. Vitamin C: antioxidant or pro-oxidant in vivo?. Free Radic Res. 1996;25(5):439–54. Available from: https://doi.org/10.3109/10715769609149066
47. Traber MG, Atkinson J. Vitamin E, antioxidant and nothing more. Free Radic Biol Med. 2007;43:4–15. Available from: https://doi.org/10.1016/j.freeradbiomed.2007.03.024
48. Antosik A, Czubak K, Cichon N, Nowak P, Zbikowska H. Vitamin E analogue protects red blood cells against storage-induced oxidative damage. Transfus Med Hemother. 2018;45(5):347–54. Available from: https://doi.org/10.1159/000486605
49. Verma M, Dahiya K, Malik D, Sehgal PK, Devi R, Soni A, Ghalaut VG. Effect of blood storage on complete biochemistry. J Blood Disord Transfus. 2015;6(6):1–4. Available from: http://dx.doi.org/10.4172/2155-9864.1000329
50. Latham JT JR, Bove JR, Weirich FL. Chemical and hematologic changes in stored CPDA-1 blood. Transfusion. 1982; 22(2):158–9. Available from: https://doi.org/10.1046/j.1537-2995.1982.22282177126.x
51. Czubak K, Antosik A, Cichon N, Zbikowska HM. Vitamin C and Trolox decrease oxidative stress and hemolysis in cold-stored human red blood cells. Redox Rep. 2017;22(6):445–50. Available from: https://doi.org/10.1080/13510002.2017.1289314
52. Paglia G, D'Alessandro A, Rolfsson Ó, Sigurjónsson OE, Bordbar A, Palsson S, Nemkov T, Hansen KC, Gudmundsson S, Palsson BO. Biomarkers defining the metabolic age of red blood cells during cold storage. Blood. 2016;128(13):e43–50. Available from: https://doi.org/10.1182/blood-2016-06-721688
53. Siems WG, Sommerburg O, Grune T. Erythrocyte free radical and energy metabolism. Clin Nephrol. 2000;53:S9–S17. Available from: https://europepmc.org/article/med/10746800
54. Stewart A, Urbaniak S, Turner M, Bessos H. The application of a new quantitative assay for the monitoring of integrin-associated protein CD47 on red blood cells during storage and comparison with the expression of CD47 and phosphatidylserine with flow cytometry. Transfusion. 2005;45(9):1496–503. Available from: https://doi.org/10.1111/j.1537-2995.2005.00564.x
55. Öhlinger T, Müllner EW, Fritz M, Werning M, Baron-Stefaniak J, Jungbauer C, Baron DM, Salzer U. Storage of packed red blood cells impairs an inherent coagulation property of erythrocytes. Front Physiol. 2022;13:1021553. Available from: https://doi.org/10.3389/fphys.2022.1021553
56. Huang RF, Huang SM, Lin BS, Hung CY, Lu HT. N-Acetylcysteine, vitamin C and vitamin E diminish homocysteine thiolactone--induced apoptosis in human promyeloid HL-60 cells. J Nutr. 2002;132(8):2151–6. Available from: https://doi.org/10.1093/jn/132.8.2151
57. Niki E. Interaction of ascorbate and alpha-tocopherol. Ann N Y Acad Sci. 1987;498:186–99. Available from: https://doi.org/10.1111/j.1749-6632.1987.tb23761.x
58. Claro LM, Leonart MSS, Comar SR, do Nascimento AJ. Effect of vitamins C and E on oxidative processes in human erythrocytes. Cell Biochem Funct. 2006;24(6):531–5. Available from: https://doi.org/10.1002/cbf.1255
59. Sakarya M, Eris FO, Derbent AB, Koca U, TÜZÜN S, Onat T, Veral A, Moral AR. The antioxidant effects of vitamin C and vitamin E on oxidative stress. Clin Intensive Care. 1999;10(6):245–50. Available from: https://doi.org/10.3109/tcic.10.6.245.250
60. Taylor MB, Christian KG, Patel N, Churchwell KB. Methemoglobinemia: Toxicity of inhaled nitric oxide therapy. Pediatr Crit Care Med. 2001;2(1):99–101. Available from: https://journals.lww.com/pccmjournal/fulltext/2001/01000/methemoglobinemia__toxicity_of_inhaled_nitric.19.aspx

61. Wright RO, Woolf AD, Shannon MW, Magnani B. N-acetylcysteine reduces methemoglobin in an in-vitro model of glucose-6-phosphate dehydrogenase deficiency. Acad Emerg Med. 1998;5(3):225–9. Available from: https://doi.org/10.1111/j.1553-2712.1998.tb02617.x
62. Dumaswala UJ, Zhuo L, Mahajan S, Nair PN, Shertzer HG, Dibello P, Jacobsen DW. Glutathione protects chemokine-scavenging and antioxidative defense functions in human RBCs. Am J Physiol. 2001;280(4):C867–73. Available from: https://doi.org/10.1152/ajpcell.2001.280.4.C867
63. Samuni Y, Goldstein S, Dean OM, Berk M. The chemistry and biological activities of N-acetylcysteine. Biochim Biophys Acta. 2013;1830(8):4117–29. Available from: https://doi.org/10.1016/j.bbagen.2013.04.016
64. Banaclocha MM, Hernandez AI, Martınez N, Ferrandiz ML. N-acetylcysteine protects against age-related increase in oxidized proteins in mouse synaptic mitochondria. Brain Res. 1997;762(1-2):256–8. Available from: https://doi.org/10.1016/S0006-8993(97)00493-9
65. Pallotta V, Gevi F, D'Alessandro A, Zolla L. Storing red blood cells with vitamin C and N-acetylcysteine prevents oxidative stress-related lesions: a metabolomics overview. Blood Transfus. 2014;12(3):376–87. Available from: https://doi.org/10.2450/2014.0266-13
66. Rushworth GF, Megson IL. Existing and potential therapeutic uses for N-acetylcysteine: the need for conversion to intracellular glutathione for antioxidant benefits. Pharmacol Ther. 2014;141(2):150–9. Available from: https://doi.org/10.1016/j.pharmthera.2013.09.006
67. Grinberg L, Fibach E, Amer J, Atlas D. N-acetylcysteine amide, a novel cell-permeating thiol, restores cellular glutathione and protects human red blood cells from oxidative stress. Free Radic Biol Med. 2005;38(1):136–45. Available from: https://doi.org/10.1016/j.freeradbiomed.2004.09.025

EUROPEAN JOURNAL OF TRANSLATIONAL
AND CLINICAL MEDICINE 2025;8(1):59-70

RESEARCH ARTICLE

Diet-induced obesity influences atherogenic indices and increases risk of cardiovascular disease in male Wistar rats

Joseph Kofi Kwarteng[1,2], Edwin Laing[1]

[1] Department of Molecular Medicine, School of Medicine and Dentistry, Kwame Nkrumah University of Science & Technology, Kumasi, Ghana
[2] Department of Nursing, Ghana Baptist University College, Kumasi, Ghana

Abstract

Background: Relationship between obesity and cardiovascular diseases is complex. This study aimed to evaluate the correlation between diet-induced obesity and atherogenic indices. **Material and methods:** Two groups of 8-weeks old male Wistar rats (170 ± 15 g) were fed with normal chow and high fat diet (HFD) respectively ad libitum for 10 weeks. Body mass index (BMI), adiposity index, serum lipid profile and atherogenic indices were measured. Associations between lipidemic indices, BMI and atherogenic indices were evaluated. **Results:** The group fed with HFD only had significantly increased BMI (0.7630 ± 0.083, $p = 0.0065$). Serum TG ($p < 0.01$), LDL-c ($p = 0.017$), VLDL-c ($p < 0.01$), and total cholesterol ($p = 0.035$) were significantly elevated among the animals with relatively higher BMI (BMI > 0.0.71 g/cm2). There was a significant positive linear association of BMI with most of the atherogenic indices investigated: coronary risk ratio (CRR) (OR 48; 95% CI 4.993, 461.50; $p < 0.001$), atherogenic index (AI) (OR 1.0; 95% CI = 2.56, 229.57; $p < 0.001$) and atherogenic coefficient (AC) (OR 65.0; 95% CI 6.68, 648.26; $p < 0.001$). **Conclusions:** Consumption of HFD induces hyperlipidemia and increase the risk of coronary artery diseases by increasing the atherogenic indices.

Keywords: obesity · dyslipidemia · high fat diet · atherogenic index · coronary risk ratio

Corresponding author:
Joseph Kofi Kwarteng, Department of Molecular Medicine, School of Medicine and Dentistry, Kwame Nkrumah University of Science & Technology, Kumasi, Ghana
e-mail: joseph.kwarteng@gcuc.edu.gh
Available online: ejtcm.gumed.edu.pl

Citation

Kwarteng JK, Laing E. Diet-induced obesity influences atherogenic indices and increases risk of cardiovascular disease in male Wistar rats. Eur J Transl Clin Med. 2025;8(1):59-70.

DOI: 10.31373/ejtcm/204959

Introduction

Inferring from the World Health Organization report (2016), there are about 2 billion overweight adults globally. Of these, over 650 million adults were obese (body mass index, BMI ≥ 30). In 2016, 39% of adults ≥ 18 years (39% of men and 40% of women) were overweight. Overall, about 13% of the world's adult population (11% of men and 15% of women) was obese in 2016. The worldwide prevalence of obesity nearly tripled over the last five decades [1]. Obesity causes poor health outcomes, reduces quality of life [2], reduces socio-economic productivity and cost nations about 0.7-2.8% of their GDP annually [3]. These staggering statistics presents obesity as a serious global threat that deserves urgent attention.

The principal cause of obesity is due to an organism's inability to physiologically maintain energy balance in the long term. This may result from over-dependence on high calorie diet, low caloric expenditure, and idiopathic inhibition of substrate oxidation [4]. It substantially increases the risk of myocardial infarction, stroke, and chronic illnesses such as type 2 diabetes mellitus, fatty liver disease, hypertension, dementia, osteoarthritis, obstructive sleep apnea and several cancers [5]. Dyslipidemia occurs early in obesity and becomes marked as the patient advances into the morbid stage of obesity either with or without insulin resistance [6]. This is associated with a relative increase in the levels of pro-atherogenic lipids (triglycerides (TGs) and low density lipoprotein (LDL-C)) as opposed to levels of anti-atherogenic lipids (high density lipoprotein – HDL-C). This phenotypic imbalance in plasma lipid distribution is strongly correlated to increased visceral adiposity, increased inflammation (systemic and vascular) increased risk of atherosclerosis (via vascular endothelial dysfunction), plaque formation, and increased plasma circulation of pro-inflammatory and prothrombotic chemokines together with an overtly increased in vulnerability to oxidative stress [7-14]. The decreased plasma nitric oxide levels in obesity further exacerbates the progression of atherosclerotic lesion formation [14].

Cardiovascular diseases are prominent among the various complications of obesity in humans, albeit they usually take many years to develop. Animal models are therefore an indispensable alternative for studying the probable obesity-associated cardiovascular risks associated with the obese condition. Hitherto, rodent models (including spontaneous single-gene loss-of-function mutation, gain-of-function mutation, transgenic model, polygenic models), and others generated from exposure to different environmental conditions have all been employed in the study of obesity [15-18]. However, neither of these models have been found to truly reflect the sequential order of metabolic and morphometric changes that occur in humans with obesity. The need for a more suitable model for the advancement of the study of obese condition cannot be overemphasized.

The aim of this study therefore was to use a high fat diet (HFD) to induce obesity in male Wistar rats as a model to evaluate the zoometric, morphometric and atherogenic risks associated with obesity condition. In this study, we compared the effect of HFD with that of the standard rat chow (SRC) on male Wistar rat population. We measured morphometric indices (e.g. the Lee/Adiposity index) and several biochemical indices (e.g. lipid profile, atherogenic index of plasma (AIP), coronary risk ratio (CRR), atherogenic coefficient (AC), and the atherogenic index (AI)). Finally, we evaluated possible correlations between measured zoometric and atherogenic indices.

Materials and methods

High fat diet formulation

The high fat diet (HFD) was prepared by mixing soya-bean oil and melted pork tallow with commercially-obtained SRC at room temperature to provide 31.25% of the total energy from fat. This mixture was stirred to produce dispersed semi-solid pellets and used for feeding the HFD group. Proximate analysis was undertaken on the feed to determine the proportions of nutrients (proteins, carbohydrate, lipid, and minerals) and energy densities of the HFD and standard chow (Table 1).

Animal care and ethical considerations

In all, 40 male Wistar rats (170 ± 15 g, 8 weeks old) were obtained from the Department of Animal Science, Kwame Nkrumah University of Science & Technology (KNUST) in Kumasi (Ghana) and were randomly distributed into two equal sized groups (n = 20). The test group was fed HFD, while rats in the control group were fed SRC. The rats were housed in metal cages (5 animals per cage) at 28 ± 2 ˚C, under a cycle of 12 hours of light and 12 hours of darkness, with free access to food and water for 10 weeks. The animals were housed and cared for under conditions in accordance with the current National Institute of Health (NIH) Guidelines for the Care of Laboratory Animals [19].

Zoometric measurements

During the 10 weeks period of dietary treatment, the rat's body weight, nose-anal length, body mass index (BMI), and adiposity index were measured weekly. Body weight was measured to the nearest 0.01 g using a digital scale (Shanghai Huachao Industrial Co. Ltd, Shanghai, China). The naso-anal length was measured (to the nearest 0.1 cm) using plastic centimeter ruler (Suzhou Chaosheng Stationery Co. Ltd, Anhui, China). The BMI and adiposity index were determined by calculation from the formula:

$$\text{BMI} = \frac{mass\ of\ rat\ (g)}{(naso-anal\ length)^2} = \ldots\ldots\ldots\ \text{g/cm}^2$$

$$\text{Adiposity Index} = \frac{\sqrt[3]{Body\ mass}}{naso-anal\ length} = \text{cm/g}^3$$

Euthanization

Before the anesthesia, final body weight of animals in each group was recorded. Anesthesia was achieved by intraperitoneal injection of 0.04 mg/g body weight of pentobarbital (Taj Pharmaceutical Ltd, Mumbai, India). About 5 ml of blood was collected by cardiopuncture using disposable syringes (Changzou Standard Medical Devices Co., Xinbei – Changzou, China) into sterile blood sample vacutainers (Becton, Dickinson and Company, Franklin Lakes, New Jersey, USA). Samples were kept still for 1hr to clot, then centrifuged at 3000 g for 5minutes and finally the serum aliquoted into clean eppendorf tubes and stored at –80 °C. After successful cardiopuncture, some of the experimental animals were frail and hence were sacrificed and their cadavers were measured.

Morphometric measurements

Following successful dissection, the wet weights of the vital organs (heart, kidney, liver, pancreas), and the abdominal fat were measured to the nearest 0.01 g using a digital scale (Shanghai Huachao Industrial Co. Ltd, Shanghai, China) and recorded.

Biochemical assays

The serum total cholesterol (TC), HDL, and TG concentrations were measured by semi-automated technique using a commercially available reagent (Fortress Diagnostics©, Antrim, N. Ireland) and the Kenza Max BioChemisTry analyzer (Biolabo Diagnostics, Maizy, France). The serum LDL-C, very low density lipoprotein (VLDL-C), and HDL-C/LDL-C ratio were calculated as below;

$$(1)\ \text{LDL} = \frac{\text{TC}}{\text{HDL}(0.2\ \text{x TG})}$$

$$(2)\ \text{VLDL} = \frac{\text{TG}}{2.2}$$

Nota bene: Equations (1) and (2) are used when TG is measured in mg/dl.

Serum atherogenic indices were calculated as follows [20-24]:

$$\text{Cardiac risk ratio}\ (CRR) = \frac{TC}{HDL - \text{C}}$$

$$\text{Atherogenic index}\ (AI) = \frac{LDL - C}{HDL - C}$$

$$\text{Atherogenic co-efficient}\ (AC) = \left(\frac{TC - HDL}{HDL}\right) or \left(\frac{Non - HDL - C}{HDL}\right)$$

$$\text{Atherogenic index of Plasma}\ (AIP) = log10\left(\frac{TG}{HDL} - C\right)$$

The serum fasting insulin levels were assayed by enzyme-linked immunosorbent assay (ELISA) technique using a commercially available kit according to the manufacturer's instructions (Shanghai Chemical Ltd, Shanghai, China) and 10 µl of serum sample.

Statistical analysis

The data from the study were analyzed using the Prism software version 8.0 (GraphPad software, Boston, USA). All continuous and discrete data were expressed as mean ± standard deviation. For continuous variables, group differences were determined using the student t-test or the one-way ANOVA. The Pearson correlation and logistic regression analysis was used to evaluate the correlation and associations respectively between lipidemic indices, BMI, and atherogenic indices among experimental animal population after the dietary treatment. From the analysis, all p values < 0.05 were considered significant.

Results and discussion

Figure 1 and Figure 2 show marked increases in average weight gain (BMI > 40%) and mean adiposity index (0.35) among the animals fed with HFD for 10 weeks, compared to those fed with SRC. The results are presented as mean ± standard error of the mean and n represents the number of animals in each group (SRC group n = 20, HFD group n = 18), (a) $p < 0.05$ vs SRC group, (aa) $p < 0.01$ vs SRC group, (bb) $p < 0.05$ vs SRC.

Obesity is one of the common findings from reported in various studies involving the treatment of subjects with high fat diets for extended periods [25-30]. Lozano et al., reported significant weight gain among rat population treated with high fat only and high fat and high fructose (HFHF) diets for two months compared to rats rationed on SRC [24]. Despite the strong association established between genes and obesity [31-35] our findings show overtly the influence of an environmental factor (HFD) on weight gain and increased BMI. In other words, long periods of HFD consumption can result in obesity. As expected, our findings from Figure 2M above suggest an average of 40% weight gain probably due to increased abdominal fat accumulation as showed in the elevated adiposity index for the group that received the HFD compared to the controls fed with SRC. Among our study animals, noticeable weight gains were observed from the 3rd week and through to the 10th week of HFD treatment. Diet induced models of obesity (DIO) have been successfully achieved with cafeteria, western, HFHF and cholesterol-rich diets in non-human primates [36-42]. Additionally, findings from our study indicate that HFD consumption over an extended period could be used as a viable alternative for induction of obesity. However, further research will have to be carried out to compare the robustness (or otherwise) of the above alternative models for induction of obesity in non-human primates and their relative suitability for studies relating to the risk factors associated with obesity.

Obesity is implicated as a viable risk factor to a wide spectrum of diseases such as non-alcoholic fatty liver disease (NAFLD), renal insufficiency, obesity-related cardiomyopathy, cancers, immune-suppression, insulin resistance, metabolic syndrome, and diabetes [43-52] From the pathology point of view, increased visceral, subcutaneous, abdominal, and intra-hepatic fat accumulations are a common effect of obesity [53]. Our study findings in Table 2 and Figure 2 above show increased abdominal fat accumulation and elevated body adiposity among the HFD-treated animals compared to those on SRC respectively. This phenotype is associated with marked increase in plasma circulating pro-inflammatory cytokines such as interleukin – 6 and α-tumor necrosis factor (TNF-α) [54-56] The circulating TNF-α provokes induces mitochondrial damage and induces systemic oxidative stress by inducing increased release of reactive oxygen species (ROS), increased expression of TNF-receptor 2 (TNFR-2) and consequent expression of vascular adhesion factors (VCAM-1 and ICAM-1) downstream increasing recruitment, adhesion and infiltration of inflammatory leucocytes hence increasing risk of CAD [57-60] Again, the weight of the various abdominal organs were significantly higher in the obese rats than in controls. This finding further reveals the possible systemic effect of obesity on the vital organs of an organism owing to the significant increase in the gross weights of liver, kidney, heart, and pancreas in the obese rats. While there is sufficient literature correlating obesity with various diseases associated

Table 1. Nutritional composition and proportions of the experimental rats' diet obtained from proximate analysis of SRC and HFD

Composition (p/p)	Standard rat chow (SRC)	High-fat Diet (HFD)
	% weight	% weight
Carbohydrate	41.475	30.500
Protein	18.850	17.475
Fat/lipids	1.975	31.250
Fibre	7.700	8.350
Mineral/vitamins	5.625	5.325
Energy (kCal/kg)	2590.750	4731.500

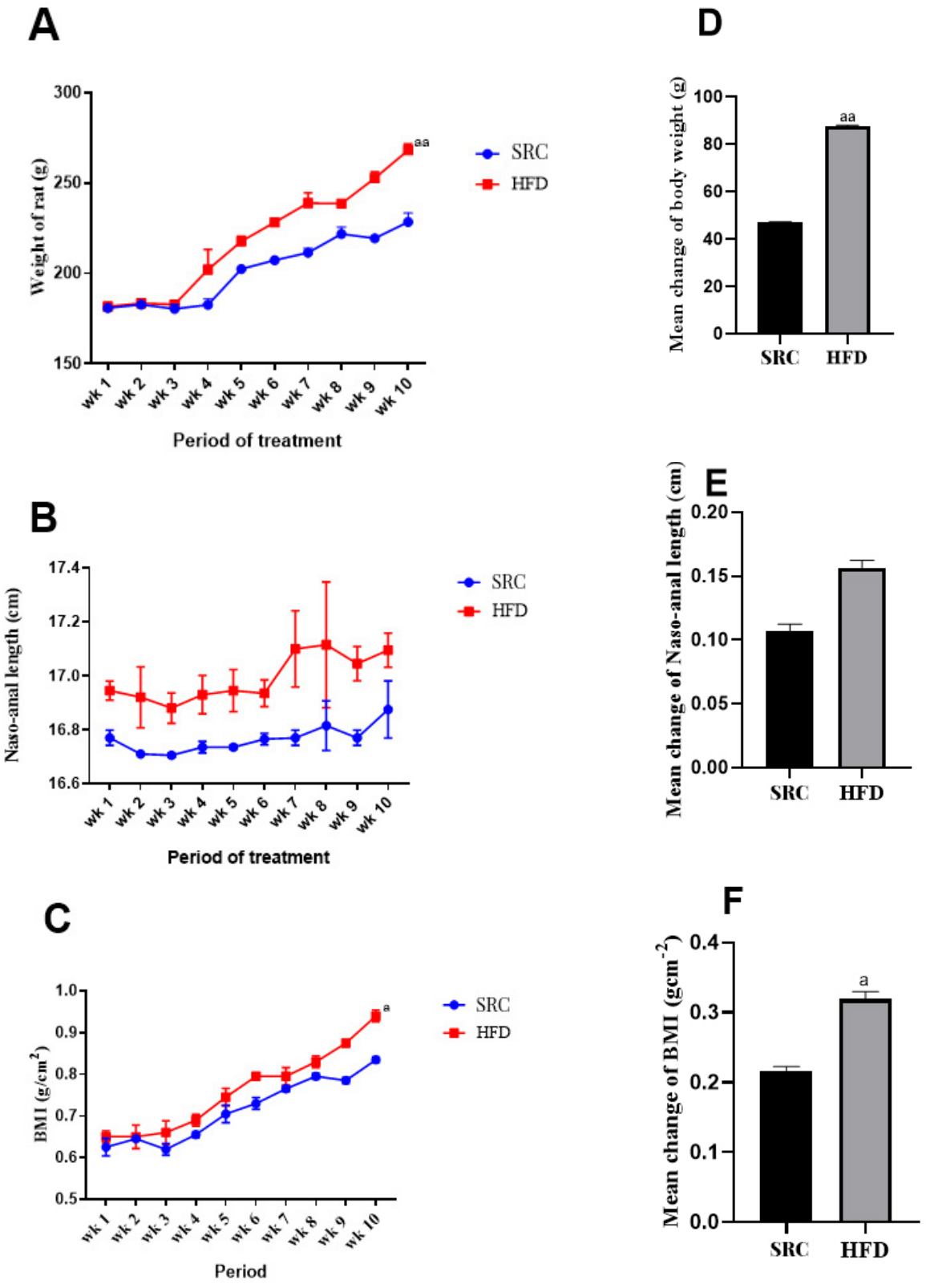

Figure 1. Zoometric measurements of experimental animals
A – body weight evaluation; B – nose-anal length changes; C – body mass index (BMI) evaluation; D – mean change in body weight; E – mean change in nose-anal length; F – mean change in BMI after 10 weeks of dietary treatment; HFD – high fat diet; SRC – standard rat chow

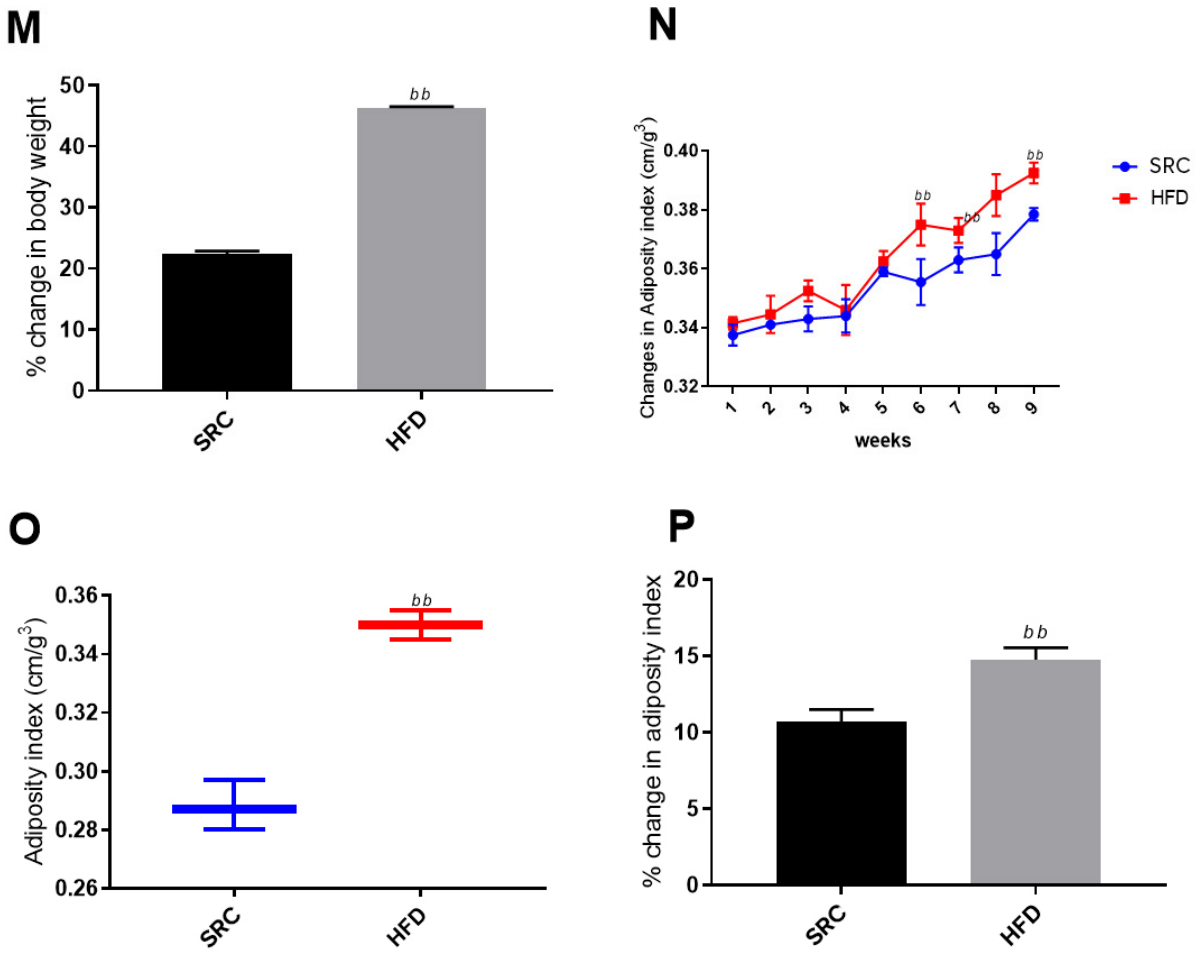

Figure 2. Morphometric measurements of experimental animals
HFD – high fat diet; M – evaluation of percentage body weight; N – change in adiposity index; O – change in adiposity indices; P – percentage change in adiposity index; SRC – standard rat chow

Table 2. Morphometric measurements of Wistar rats after 10 weeks of treatment with SRC and HFD

	SRC (n = 20)	HFD (n = 18)	p-value
Liver weight (g)	5.68 ± 1.41	8.57 ± 3.03[a]	< 0.01
Abdominal fat (g)	0.43 ± 0.27	5.2 ± 1.40[a]	< 0.0001
Kidney weight (g)	0.62 ± 0.25	1.17 ± 0.08[a]	< 0.01
Pancreas weight (g)	0. 69 ± 0.11	1.15 ± 0.45[a]	0.027
Weight gain/pancreas weight	36.2 ± 10.49	63.3 ± 21.57[a]	< 0.001
Adiposity index	0.28 ± 0.08	0.35 ± 0.13[a]	0.042

Results are presented as mean ± standard error of the mean and n represents the number of animals in each group; The p-values were determined using the unpaired t-test, SRC versus HFD. ([a]) $p < 0.05$ was considered significant when compared against the SRC group; HFD – high fat diet; SRC – standard rat chow.

Table 3. Biochemical characteristics of study animals

	BMI (< 0.65 g/cm²) (n = 9)	BMI (0.65-0.70 g/cm²) (n = 16)	BMI (≥ 0.71 g/cm²) (n = 15)	p-value
FBG (mmol/l)	4.3 ± 0.52	4.60 ± 0.28	5.5 ± 0.69[a]	0.028
RBG (mmol/l)	6.20 ± 0.08	6.13 ± 0.45	6.7 ± 0.28	0.076
VLDL-C (mmol/l)	0.16 ± 0.11	0.13 ± 0.08	0.30 ± 0.06[a]	< 0.01
TG (mmol/l)	0.80 ± 0.17	0.65 ± 0.12	1.50 ± 0.83[a]	< 0.01
TC (mmol/l)	2.46 ± 0.13	3.01 ± 0.18	4.68 ± 1.70[a]	0.035
HDL-C (mmol/l)	1.20 ± 0.60	1.50 ± 0.72	1.90 ± 0.59	0.082
LDL-C (mmol/l)	0.44 ± 0.17	1.21 ± 0.05	2.10 ± 0.23[a]	0.017
TG/HDL-C	0.67 ± 0.33	0.43 ± 0.11	0.79 ± 0.29[a]	0.025
CRR	2.05 ± 0.18	2.01 ± 0.58	2.46 ± 0.73	0.069
AIP	−0.176 ± 0.11	−0.366 ± 0.18	−0.102 ± 0.06[a]	0.022
AC	1.05 ± 0.53	1.01 ± 0.17	1.46 ± 0.68[a]	0.0175
AI	0.37 ± 0.04	0.81 ± 0.29	1.11 ± 0.02[a]	0.041

Results are presented as mean ± standard error of the mean and n represents the number of animals used in each group; The p-value was determined by the one-way analysis of variance; $p < 0.05$ was considered significant; (a) p-value < 0.05; AC – atherogenic coefficient; AI – atherogenic index; AIP – atherogenic index of plasma; BMI – body mass index; CRR – cardiac risk ratio; FBG – fasting blood glucose; HDL-c – high density lipoprotein; LDL-c – low density lipoprotein; RBG – random blood glucose; TC – total cholesterol; TG – triglyceride; VLDL-c – very low density lipoprotein cholesterol.

Table 4. Odds ratio (95% confidence interval) of obesity according to the estimated atherogenic indices

Variable	Odds ratio (95% CI)	p-value
AC	65.0 (68 – 648.26)	< 0.001
AIP	6.0 (0.043 – 24.55)	< 0.001
CRR	48 (4.993 – 461.50)	< 0.001
AI	1.0 (2.56 – 229.57)	< 0.001

AC – atherogenic coefficient; AI – atherogenic index (LDL-c/HDL-c ratio); AIP – atherogenic index of plasma; CI – confidence interval; CRR – coronary risk index

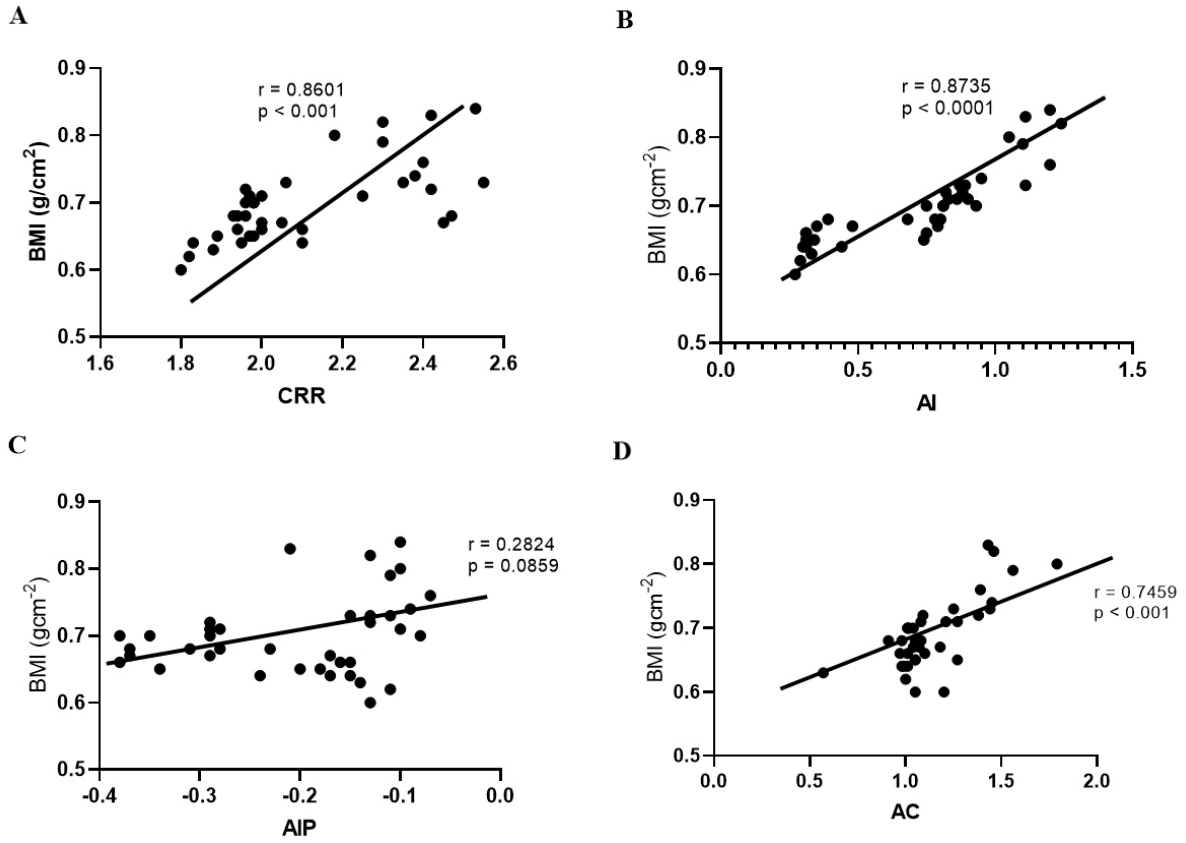

Figure 3. Scatter plot showing significant and positive correlations between different atherogenic indices and increased BMI among experimental animals (r-pearson's coefficient)
From the above figure, the order of increasing strength of correlation among the atherogenic indices with BMI is AIP, AC, CRR, and AI with the strongest positive association (r = 0.28, 0.74, 0.86, and 0.87) respectively. AC – atherogenic coefficient; AI – atherogenic index; AIP – atherogenic index of plasma; CRR – coronary risk ratio

with these organs [61-67] there is rather a paucity of information relating obesity to the function of the kidney, heart, and pancreas. Our findings shown in Tables 1 and 2 provide a justifiable inference for further study into how this change in weight could affect the gross anatomy and function of these organs in obesity.

The atherogenic indices are tools to measure the risk for various forms of coronary artery diseases (CAD)s. Different diseases relate differently to the conventional atherogenic indices. In comprehensive meta-analysis, Wu et al., demonstrated that atherogenic index of plasma (AIP) is independently correlated to CAD among adult population [67]. In another study, AIP, AC, and CRR were implicated in pre-eclampsia among pregnant women [68]. Except for AIP, our findings shown in Table 4 suggest a significant linear relationship between BMI and the principal atherogenic indices namely AC, AI, and CRR. Among them, AI correlated strongly with obesity followed by AC, and CRR with correlation coefficient (r) values of 0.8735 ($p < 0.0001$), 0.7459 ($p < 0.0001$), 0.6811 ($p < 0.0001$) respectively (Figure 3). Notable among our findings is the strong correlation between obesity and the atherogenic indices (Tables 3 and 4). This corroborates the human studies that reported significant increases in atherogenic risks among obese cohorts [69-71]. This further underscores the viability of animal models for studies of human diseases.

Limitations of this study

The animal model we used and the small sample size are a limitation towards extrapolation of our findings to the larger human population. Proximate evaluation of animal diet did not reveal micronutrient distributions which could have played a role in the observed outcomes. Lastly, this experimental study was exploratory and focused primarily on correlational data without exploring the undergirding mechanisms such as oxidative stress, inflammation, insulin resistance among others. Lastly, the 10-week duration of our study was relatively short. Perhaps, a longer duration would have been more appropriate to better explore the effect of diet-induced obesity and coronary artery diseases. These notwithstanding, our findings are consistent with those observed in the human population indicating the usefulness of our model for the further investigations of obesity in humans.

Conclusion

In conclusion, our study corroborates the findings published in various studies that suggest that prolonged consumption of HFD leads to hyperlipidemia and increased cardiovascular risk indicated by increasing several atherogenic indices. This leads to increased vulnerability to heart attack, hypertension, and stroke.

Disclaimer

The findings of this paper are new and solely the responsibility of the authors and do not necessarily represent the official views of any auxiliary agencies.

Conflict of interest

The authors have no conflict of interests regarding the publication of this paper.

Acknowledgements

The authors express their gratitude to the staff of the Animal House, Department of Pharmacology for housing the rats used for this study.

References

1. Obesity and overweight [Internet]. World Health Organization. 2025 [cited 2025 May 27]. Available from: https://www.who.int/en/news-room/fact-sheets/detail/obesity-and-overweight
2. Division of Nutrition, Physical Activity, and Obesity [Internet]. National Center for Chronic Disease Prevention and Health Promotion. 2020 [cited 2020 Sep 17]. Available from: https://www.cdc.gov/obesity/adult/causes.html
3. Withrow D, Alter DA. The economic burden of obesity worldwide: a systematic review of the direct costs of obesity. Obes Rev [Internet]. 2011;12(2):131–41. Available from: https://onlinelibrary.wiley.com/doi/10.1111/j.1467-789X.2009.00712.x
4. Sun M, Schutz Y, Maffeis C. Substrate metabolism, nutrient balance and obesity development in children and adolescents: a target for intervention? Obes Rev [Internet]. 2004;5(4):183–8. Available from: https://onlinelibrary.wiley.com/doi/10.1111/j.1467-789X.2004.00154.x
5. Blüher M. Obesity: global epidemiology and pathogenesis. Nat Rev Endocrinol [Internet]. 2019;15(5):288–98. Available from: https://www.nature.com/articles/s41574-019-0176-8
6. Bamba V, Rader DJ. Obesity and Atherogenic Dyslipidemia. Gastroenterology [Internet]. 2007;132(6):2181–90. Available from: https://linkinghub.elsevier.com/retrieve/pii/S0016508507005823
7. Bhardwaj S, Bhattacharjee J, Bhatnagar MK, Tyagi S, Delhi N. Atherogenic index of plasma, castelli risk index and atherogenic coefficient-new parameters in assessing cardiovascular risk. Int J Pharm Biol Sci [Internet]. 2013;3(3):359–64. Available from: http://ijpbs.com/ijpbsadmin/upload/ijpbs_526938e855804.pdf
8. Bharadwaj R, Mathur K, Sharma D, Sankhla M. The relationship between oxidative stress and atherogenic index (AI) in preeclampsia. Sch J App Med Sci [Internet]. 2014;2(6D):3092–6. Available from: https://saspublishers.com/media/articles/SJAMS_26D3092-3096.pdf
9. Millán J, Xavier P, Anna M, Manuel Z, Joan R-P, Luis Felipe P, et al. Lipoprotein ratios: Physiological significance and clinical usefulness in cardiovascular prevention. Vasc Health Risk Manag [Internet]. 2009;5:757–65. Available from: https://www.tandfonline.com/doi/abs/10.2147/vhrm.s12187457
10. Grundy SM. Metabolic syndrome update. Trends Cardiovasc Med [Internet]. 2016;26(4):364–73. Available from: https://linkinghub.elsevier.com/retrieve/pii/S1050173815002492
11. Rocha VZ, Libby P. Obesity, inflammation, and atherosclerosis. Nat Rev Cardiol [Internet]. 2009;6(6):399–409. Available from: https://www.nature.com/articles/nrcardio.2009.55
12. Couillard C, Ruel G, Archer WR, Pomerleau S, Bergeron J, Couture P, et al. Circulating Levels of Oxidative Stress Markers and Endothelial Adhesion Molecules in Men with Abdominal Obesity. J Clin Endocrinol Metab [Internet]. 2005;90(12):6454–9. Available from: https://academic.oup.com/jcem/article-lookup/doi/10.1210/jc.2004-2438
13. Engin A. Endothelial Dysfunction in Obesity. In 2017. p. 345–79. Available from: http://link.springer.com/10.1007/978-3-319-48382-5_15

14. Powell-Wiley TM, Poirier P, Burke LE, Després J-P, Gordon-Larsen P, Lavie CJ, et al. Obesity and Cardiovascular Disease: A Scientific Statement From the American Heart Association. Circulation [Internet]. 2021;143(21):e984–1010. Available from: https://www.ahajournals.org/doi/10.1161/CIR.0000000000000973
15. Wang C-Y, Liao JK. A Mouse Model of Diet-Induced Obesity and Insulin Resistance. In 2012. p. 421–33. Available from: https://link.springer.com/10.1007/978-1-61779-430-8_27
16. Sampey BP, Vanhoose AM, Winfield HM, Freemerman AJ, Muehlbauer MJ, Fueger PT, et al. Cafeteria Diet Is a Robust Model of Human Metabolic Syndrome With Liver and Adipose Inflammation: Comparison to High-Fat Diet. Obesity [Internet]. 2011;19(6):1109–17. Available from: https://onlinelibrary.wiley.com/doi/10.1038/oby.2011.18
17. Buettner R, Schölmerich J, Bollheimer LC. High-fat Diets: Modeling the Metabolic Disorders of Human Obesity in Rodents. Obesity [Internet]. 2007;15(4):798–808. Available from: https://onlinelibrary.wiley.com/doi/10.1038/oby.2007.608
18. Inui A. Obesity – a chronic health problem in cloned mice? Trends Pharmacol Sci [Internet]. 2003;24(2):77–80. Available from: https://doi.org/10.1016/S0165-6147(02)00051-2
19. Guide for the Care and Use of Laboratory Animals [Internet]. Washington, D.C.: National Academies Press; 2011. Available from: http://www.nap.edu/catalog/12910
20. Brehm A, Pfeiler G, Pacini G, Vierhapper H, Roden M. Relationship between Serum Lipoprotein Ratios and Insulin Resistance in Obesity. Clin Chem [Internet]. 2004;50(12):2316–22. Available from: https://academic.oup.com/clinchem/article/50/12/2316/5639942
21. Frohlich J, Dobiášová M. Fractional Esterification Rate of Cholesterol and Ratio of Triglycerides to HDL-Cholesterol Are Powerful Predictors of Positive Findings on Coronary Angiography. Clin Chem [Internet]. 2003;49(11):1873–80. Available from: https://academic.oup.com/clinchem/article/49/11/1873/5642132
22. Dobiášová M. Atherogenic Index of Plasma [Log(Triglycerides/HDL-Cholesterol)]: Theoretical and Practical Implications. Clin Chem [Internet]. 2004;50(7):1113–5. Available from: https://academic.oup.com/clinchem/article/50/7/1113/5639904
23. Martirosyan DM, Miroshnichenko LA, Kulakova SN, Pogojeva A V, Zoloedov VI. Amaranth oil application for coronary heart disease and hypertension. Lipids Health Dis [Internet]. 2007;6(1):1. Available from: https://doi.org/10.1186/1476-511X-6-1
24. Lozano I, Van der Werf R, Bietiger W, Seyfritz E, Peronet C, Pinget M, et al. High-fructose and high-fat diet-induced disorders in rats: impact on diabetes risk, hepatic and vascular complications. Nutr Metab (Lond) [Internet]. 2016;13(1):15. Available from: http://www.nutritionandmetabolism.com/content/13/1/15
25. RI F. Estimation of the concentration of low-density lipoprotein cholesterol in plasma, without use of the preparative ultracentrifuge. Clin Chem. 1972;18:499–502.
26. Ngala RA, Ampong I, Sakyi SA, Anto EO. Effect of dietary vegetable oil consumption on blood glucose levels, lipid profile and weight in diabetic mice: an experimental case—control study. BMC Nutr [Internet]. 2016;2(1):28. Available from: http://bmcnutr.biomedcentral.com/articles/10.1186/s40795-016-0053-y
27. Woods SC, Seeley RJ, Rushing PA, D'Alessio D, Tso P. A Controlled High-Fat Diet Induces an Obese Syndrome in Rats. J Nutr [Internet]. 2003;133(4):1081–7. Available from: https://doi.org/10.1093/jn/133.4.1081
28. Aslani S, Vieira N, Marques F, Costa PS, Sousa N, Palha JA. The effect of high-fat diet on rat's mood, feeding behavior and response to stress. Transl Psychiatry [Internet]. 2015;5(11):e684–e684. Available from: https://www.nature.com/articles/tp2015178
29. Marques C, Meireles M, Norberto S, Leite J, Freitas J, Pestana D, et al. High-fat diet-induced obesity Rat model: a comparison between Wistar and Sprague-Dawley Rat. Adipocyte [Internet]. 2016;5(1):11–21. Available from: http://www.tandfonline.com/doi/full/10.1080/21623945.2015.1061723
30. Lyon HN, Hirschhorn JN. Genetics of common forms of obesity: a brief overview. Am J Clin Nutr [Internet]. 2005;82(1):215S-217S. Available from: https://linkinghub.elsevier.com/retrieve/pii/S0002916523295349
31. Speakman JR. Obesity: The Integrated Roles of Environment and Genetics. J Nutr [Internet]. 2004;134(8):2090S-2105S. Available from: https://doi.org/10.1093/jn/134.8.2090S
32. Loos RJF. Recent progress in the genetics of common obesity. Br J Clin Pharmacol [Internet]. 2009;68(6):811–29. Available from: https://bpspubs.onlinelibrary.wiley.com/doi/10.1111/j.1365-2125.2009.03523.x
33. Madsen AN, Hansen G, Paulsen SJ, Lykkegaard K, Tang-Christensen M, Hansen HS, et al. Long-term characterization of the diet-induced obese and diet-resistant rat model: a polygenetic rat model mimicking the human obesity syndrome. J Endocrinol [Internet]. 2010;206(3):287–96. Available from: https://joe.bioscientifica.com/view/journals/joe/206/3/287.xml
34. Amri Z, Ghorbel A, Turki M, Akrout FM, Ayadi F, Elfeki A, et al. Effect of pomegranate extracts on brain antioxidant markers and cholinesterase activity in high fat-high fructose diet induced obesity in rat model. BMC Complement Altern Med [Inter-

net]. 2017;17(1):339. Available from: http://bmccomplementalternmed.biomedcentral.com/articles/10.1186/s12906-017-1842-9

35. Lewis AR, Singh S, Youssef FF. Cafeteria-diet induced obesity results in impaired cognitive functioning in a rodent model. Heliyon [Internet]. 2019;5(3). Available from: https://doi.org/10.1016/j.heliyon.2019.e01412
36. Feijó G dos S, de Oliveira S, Thoen R, Schaab EE, de Moura AC, Franco F, et al. Food Selection of Cafeteria Diet Affects Memory Dysfunction Related to Obesity. Neurochem Res [Internet]. 2019;44(8):1869–77. Available from: http://link.springer.com/10.1007/s11064-019-02821-5
37. Shively CA, Appt SE, Vitolins MZ, Uberseder B, Michalson KT, Silverstein-Metzler MG, et al. Mediterranean versus Western Diet Effects on Caloric Intake, Obesity, Metabolism, and Hepatosteatosis in Nonhuman Primates. Obesity [Internet]. 2019;27(5):777–84. Available from: https://onlinelibrary.wiley.com/doi/10.1002/oby.22436
38. Varlamov O. Western-style diet, sex steroids and metabolism. Biochim Biophys Acta - Mol Basis Dis [Internet]. 2017;1863(5):1147–55. Available from: https://www.sciencedirect.com/science/article/pii/S0925443916301430
39. Myles IA. Fast food fever: reviewing the impacts of the Western diet on immunity. Nutr J [Internet]. 2014;13(1):61. Available from: http://nutritionj.biomedcentral.com/articles/10.1186/1475-2891-13-61
40. Dalbøge LS, Pedersen PJ, Hansen G, Fabricius K, Hansen HB, Jelsing J, et al. A Hamster Model of Diet-Induced Obesity for Preclinical Evaluation of Anti-Obesity, Anti-Diabetic and Lipid Modulating Agents. Andrews Z, editor. PLoS One [Internet]. 2015;10(8):e0135634. Available from: https://dx.plos.org/10.1371/journal.pone.0135634
41. Polyzos SA, Kountouras J, Mantzoros CS. Obesity and nonalcoholic fatty liver disease: From pathophysiology to therapeutics. Metabolism [Internet]. 2019;92:82–97. Available from: https://www.sciencedirect.com/science/article/pii/S0026049518302531
42. Koppe SWP. Obesity and the liver: nonalcoholic fatty liver disease. Transl Res [Internet]. 2014;164(4):312–22. Available from: https://www.sciencedirect.com/science/article/pii/S1931524414002151
43. Silva Junior GB da, Bentes ACSN, Daher EDF, Matos SMA de. Obesity and kidney disease. J Bras Nefrol [Internet]. 2017;39(1). Available from: http://www.scielo.br/scielo.php?script=sci_arttext&pid=S0101-28002017000100065
44. Lakkis JI, Weir MR. Obesity and Kidney Disease. Prog Cardiovasc Dis [Internet]. 2018;61(2):157–67. Available from: https://linkinghub.elsevier.com/retrieve/pii/S0033062018301282
45. Ayer J, Charakida M, Deanfield JE, Celermajer DS. Lifetime risk: childhood obesity and cardiovascular risk. Eur Heart J [Internet]. 2015;36(22):1371–6. Available from: https://doi.org/10.1093/eurheartj/ehv089
46. Tiwari S, Fomusi Ndisang J. The role of obesity in cardiomyopathy and nephropathy. Curr Pharm Des [Internet]. 2014;20(9):1409–17. Available from: https://www.benthamdirect.com/content/journals/cpd/10.2174/13816128113199990562
47. Polsky S, Ellis SL. Obesity, insulin resistance, and type 1 diabetes mellitus. Curr Opin Endocrinol Diabetes Obes [Internet]. 2015;22(4):277–82. Available from: https://journals.lww.com/01266029-201508000-00005
48. Leong KS, Wilding JP. Obesity and diabetes. Best Pract Res Clin Endocrinol Metab [Internet]. 1999;13(2):221–37. Available from: https://linkinghub.elsevier.com/retrieve/pii/S1521690X99900179
49. Kolb R, Sutterwala FS, Zhang W. Obesity and cancer: inflammation bridges the two. Curr Opin Pharmacol [Internet]. 2016;29:77–89. Available from: https://linkinghub.elsevier.com/retrieve/pii/S1471489216300650
50. Avgerinos KI, Spyrou N, Mantzoros CS, Dalamaga M. Obesity and cancer risk: Emerging biological mechanisms and perspectives. Metabolism [Internet]. 2019;92:121–35. Available from: https://linkinghub.elsevier.com/retrieve/pii/S0026049518302324
51. Borel A-L, Nazare J-A, Smith J, Aschner P, Barter P, Van Gaal L, et al. Visceral, subcutaneous abdominal adiposity and liver fat content distribution in normal glucose tolerance, impaired fasting glucose and/or impaired glucose tolerance. Int J Obes [Internet]. 2015;39(3):495–501. Available from: https://www.nature.com/articles/ijo2014163
52. Guh DP, Zhang W, Bansback N, Amarsi Z, Birmingham CL, Anis AH. The incidence of co-morbidities related to obesity and overweight: A systematic review and meta-analysis. BMC Public Health [Internet]. 2009;9(1):88. Available from: https://bmcpublichealth.biomedcentral.com/articles/10.1186/1471-2458-9-88
53. Wilson PWF, D'Agostino RB, Sullivan L, Parise H, Kannel WB. Overweight and Obesity as Determinants of Cardiovascular Risk. Arch Intern Med [Internet]. 2002;162(16):1867. Available from: http://archinte.jamanetwork.com/article.aspx?doi=10.1001/archinte.162.16.1867
54. Goyal R, Faizy AF, Siddiqui SS, Singhai M. Evaluation of TNF-α and IL-6 Levels in Obese and Non-obese Diabetics: Pre- and Postinsulin Effects. N Am J Med Sci [Internet]. 2012;4(4):180–4. Available from: http://www.ncbi.nlm.nih.gov/pubmed/22536561

55. Kern L, Mittenbühler M, Vesting A, Ostermann A, Wunderlich C, Wunderlich F. Obesity-Induced TNFα and IL-6 Signaling: The Missing Link between Obesity and Inflammation—Driven Liver and Colorectal Cancers. Cancers (Basel) [Internet]. 2018;11(1):24. Available from: https://www.mdpi.com/2072-6694/11/1/24
56. Shi C, Zhu L, Chen X, Gu N, Chen L, Zhu L, et al. IL-6 and TNF-α Induced Obesity-Related Inflammatory Response Through Transcriptional Regulation of miR-146b. J Interf Cytokine Res [Internet]. 2014;34(5):342–8. Available from: http://www.liebertpub.com/doi/10.1089/jir.2013.0078
57. Liu C, Lei S, Cai T, Cheng Y, Bai J, Fu W, et al. Inducible nitric oxide synthase activity mediates TNF-α-induced endothelial cell dysfunction. Am J Physiol Physiol [Internet]. 2023;325(3):C780–95. Available from: https://journals.physiology.org/doi/10.1152/ajpcell.00153.2023
58. Tran N, Garcia T, Aniqa M, Ali S, Ally A, Nauli SM. Endothelial Nitric Oxide Synthase (eNOS) and the Cardiovascular System: in Physiology and in Disease States. Am J Biomed Sci Res [Internet]. 2022;15(2):153–77. Available from: http://www.ncbi.nlm.nih.gov/pubmed/35072089
59. Król M, Kepinska M. Human Nitric Oxide Synthase—Its Functions, Polymorphisms, and Inhibitors in the Context of Inflammation, Diabetes and Cardiovascular Diseases. Int J Mol Sci [Internet]. 2020;22(1):56. Available from: https://www.mdpi.com/1422-0067/22/1/56
60. Hwang M, Berceli SA, Tran-Son-Tay R. Modeling and Role of Leukocytes in Inflammation BT - Computational Surgery and Dual Training. In: Garbey M, Bass BL, Collet C, Mathelin M, Tran-Son-Tay R, editors. Boston, MA: Springer US; 2010. p. 221–32. Available from: https://doi.org/10.1007/978-1-4419-1123-0_13
61. Landsberg L, Aronne LJ, Beilin LJ, Burke V, Igel LI, Lloyd-Jones D, et al. Obesity-related hypertension: Pathogenesis, cardiovascular risk, and treatment—A position paper of the The Obesity Society and the American Society of Hypertension. Obesity [Internet]. 2013;21(1):8–24. Available from: https://onlinelibrary.wiley.com/doi/10.1002/oby.20181
62. Hampel H, Abraham NS, El-Serag HB. Meta-Analysis: Obesity and the Risk for Gastroesophageal Reflux Disease and Its Complications. Ann Intern Med [Internet]. 2005;143(3):199–211. Available from: https://www.acpjournals.org/doi/10.7326/0003-4819-143-3-200508020-00006
63. Kivipelto M, Ngandu T, Fratiglioni L, Viitanen M, Kåreholt I, Winblad B, et al. Obesity and Vascular Risk Factors at Midlife and the Risk of Dementia and Alzheimer Disease. Arch Neurol [Internet]. 2005;62(10). Available from: http://archneur.jamanetwork.com/article.aspx?doi=10.1001/archneur.62.10.1556
64. Mulnier HE, Seaman HE, Raleigh VS, Soedamah-Muthu SS, Colhoun HM, Lawrenson RA. Mortality in people with Type 2 diabetes in the UK. Diabet Med [Internet]. 2006;23(5):516–21. Available from: https://onlinelibrary.wiley.com/doi/10.1111/j.1464-5491.2006.01838.x
65. Câmara NOS, Iseki K, Kramer H, Liu Z-H, Sharma K. Kidney disease and obesity: epidemiology, mechanisms and treatment. Nat Rev Nephrol [Internet]. 2017;13(3):181–90. Available from: https://www.nature.com/articles/nrneph.2016.191
66. Pérez S, Rius-Pérez S, Finamor I, Martí-Andrés P, Prieto I, García R, et al. Obesity causes PGC-1α deficiency in the pancreas leading to marked IL-6 upregulation via NF-κB in acute pancreatitis. J Pathol [Internet]. 2019;247(1):48–59. Available from: https://pathsocjournals.onlinelibrary.wiley.com/doi/10.1002/path.5166
67. Wu J, Zhou Q, Wei Z, Wei J, Cui M. Atherogenic Index of Plasma and Coronary Artery Disease in the Adult Population: A Meta-Analysis. Front Cardiovasc Med [Internet]. 2021;8. Available from: https://www.frontiersin.org/articles/10.3389/fcvm.2021.817441/full
68. Agu P, Egbugara M, Ogboi J, Ajah L, Nwagha U, Ugwu E, et al. Atherogenic Index, Cardiovascular Risk Ratio, and Atherogenic Coefficient as Risk Factors for Cardiovascular Disease in Pre-eclampsia in Southeast Nigeria: A Cross-Sectional Study. Niger J Clin Pract [Internet]. 2024;27(2):221–7. Available from: https://journals.lww.com/10.4103/njcp.njcp_633_23
69. Mallika DK, Manohar SM, Arslan M. Association of atherogenic indices with obesity and as biomarkers of cardiovascular risk. Int J Res Med Sci [Internet]. 2022;10(5):1126. Available from: https://www.msjonline.org/index.php/ijrms/article/view/10690
70. Wei D, Melgarejo J, Vanassche T, Van Aelst L, Janssens S, Verhamme P, et al. Atherogenic lipoprotein profile associated with anthropometric indices of obesity and their association with cardiometabolic risk markers: a cross-sectional study in community. Eur Heart J [Internet]. 2022;43(Supplement_2). Available from: https://academic.oup.com/eurheartj/article/doi/10.1093/eurheartj/ehac544.2386/6745627
71. M. MM, M. K. J. Impact of obesity on atherogenic index in young adult females in Gadag, Karnataka. Int J Res Med Sci [Internet]. 2024;12(9):3274–8. Available from: https://www.msjonline.org/index.php/ijrms/article/view/13756

EUROPEAN JOURNAL OF TRANSLATIONAL
AND CLINICAL MEDICINE 2025;8(1):71-82

RESEARCH ARTICLE

Sexual satisfaction, quality of life and level of social support of women before, during and after pregnancy

Wiktoria Łaczyńska, Katarzyna A. Milska-Musa

Division of Quality of Life Research, Department of Psychology, Medical University of Gdańsk, Poland

Abstract

Introduction: Quality of life, social support and sexual satisfaction may change across life stages. The aim of this study was to assess these variables in women before, during and after pregnancy. **Material and methods:** The study was cross-sectional, and conducted online among three independent groups of women (N = 160). Standardized tools were used: the WHOQOL-BREF quality of life questionnaire, Female Sexual Function Index (FSFI), and Berlin Social Support Scales (BSSS). Statistical analysis was performed using nonparametric tests (Kruskal-Wallis, Mann-Whitney U, Friedman and chi-square tests). **Results:** The highest level of sexual satisfaction, quality of life, and social support (p 0.05). A statistically significant relationship was demonstrated between the level of support from loved ones and satisfaction with intimate life (χ^2 = 21.974, p = 0.038). **Conclusions:** Women's sexual satisfaction, quality of life and social support vary, taking on different values before, during and after pregnancy. It is important to consider women's needs at each stage to provide them with appropriate support and care.

Keywords: quality of life · social support · sexual satisfaction

Citation

Łaczyńska W, Milska-Musa KA. Sexual satisfaction, quality of life and level of social support of women before, during and after pregnancy. Eur J Transl Clin Med. 2025;8(1):71-82.

DOI: 10.31373/ejtcm/207711

Corresponding author:
Katarzyna A. Milska-Musa, Division of Quality of Life Research, Department of Psychology, Medical University of Gdańsk, Poland
e-mail: katarzyna.milska-musa@gumed.edu.pl
Available online: ejtcm.gumed.edu.pl

Introduction

According to the World Health Organization (WHO), sexual health is "a state of physical, emotional, mental and social well-being in relation to sexuality; it is not merely the absence of disease, dysfunction or infirmity." Looking at this multifaceted definition, it is worth assessing sexual satisfaction in relation to quality of life (QoL) and level of social support, because these are factors that interact [1-2]. Women at different times in their lives may feel different emotions, experience different sensations in both the physical and mental sphere. The greatest number of physiological, hormonal and emotional changes that affect the QoL and sexual life of women can be observed during pregnancy and motherhood [3]. Using the results of the National Sexuality Report 2024, it can be stated that more than half of our society considers sex to be very important to them, while about 1/5 of respondents do not talk about sex at all [4]. The process of transition to motherhood may be associated with a number of challenges. On a sample of 398 respondents Fuchs et al. showed that pregnancy and childbirth significantly reduce women's sexual activity [5]. Similar conclusions were also reached by scientists who analyzed the effect of childbirth on women's sexuality in the first year after childbirth [6]. Studies show that satisfaction with women's sexual life during pregnancy and after childbirth is significantly related to the social support they receive, relationships during pregnancy differ from those before pregnancy, and life satisfaction increases after the birth of a child [7]. Support from a partner, family and medical personnel significantly affects the emotional state and mental health of women during pregnancy and motherhood [8-9]. It has been shown that women after childbirth experience not only a decrease in the level of sexual pleasure and emotional intimacy, but also changes in their body image [10-11].

The quality of a partnership relationship may be determined by many factors. It has been shown that the partner's involvement in household chores and the opportunity to spend personal time significantly affect the quality of the relationship and women's mental health [11]. Moreover, a study conducted on a sample of 1652 married couples demonstrated that greater involvement of husbands in household chores was associated not only with the aforementioned better mental health of wives, overall happiness and also with lower levels of marital dissatisfaction [12]. It was also shown that couples who devote time to common conversations and activities show higher levels of relationship satisfaction and greater emotional intimacy [13].

An equally important factor, often omitted in research, that may affect women's sexuality after childbirth are obstetric interventions, such as episiotomy or episiotomy. Studies indicate that such injuries may lead to pain during intercourse, a decreased sense of attractiveness, and fear of resuming sexual activity [14-15].

The aim of the study was to analyze sexual satisfaction, QoL and level of social support of women at three moments of life: before pregnancy, during pregnancy and after childbirth. We made an effort to study the topic in a cohort of women before pregnancy, during pregnancy and after childbirth in 3 independent groups to analyze differences and similarities between key stages of reproductive life.

Specifically, we aimed to test the following 3 hypotheses:

1. There are statistically significant differences between groups of women before pregnancy, during pregnancy and after childbirth in terms of social support, QoL and sexual functioning.

2. Episiotomy or laceration significantly affects the perception of the respondents' sexuality.

3. Support from loved ones is associated with higher levels of sexual satisfaction.

We also analysed the influence of the period of life on women's sense of attractiveness and sexual experiences as well as obstacles to achieving sexual satisfaction during pregnancy.

Material and methods

We conducted this study was conducted online using the Google Forms software (Google LLC, Mountain View, USA). The desired participant age range was 18-35 years. Participants were recruited on the social networking site Facebook, in Polish-language groups dedicated to women trying to conceive, pregnant women and mothers. Participation in the study was anonymous and voluntary. After giving their consent, respondents were invited to participate in the study and received a survey containing questions in the Polish language about basic socio-demographic data, which consisted of a total of 7 sections. The first part was a section of original general socio-demographic questions, followed by 3 sections of original specific questions dedicated to women before pregnancy, during pregnancy and after childbirth. Then, all respondents completed the next 3 sections containing the following questionnaire tools: WHOQOL-BREF, Female Sexual Function Index (FSFI) and Berlin Social Support Scales (BSSS). Their internal reliability was assessed using Cronbach's alpha coefficient and the obtained results were compared with data from the original validations.

The WHOQOL-BREF is a shortened 26-item questionnaire for assessing the QoL in 4 domains (physical, psychological, social relationships and environmental), reliability of the questionnaire developed by WHOQOL Group (1998), overall reliability in validation studies was $\alpha = 0.89$, with values $\alpha = 0.68$-0.82 for individual domains [16].

The FSFI is a scale developed by Rosen et al. assessing 6 domains of female sexual functioning: desire, arousal, lubrication, orgasm, sexual satisfaction and pain during intercourse in relation to the last 4 weeks. The reliability of the FSFI scale in the original study showed very high internal consistency: Cronbach's α values in individual domains ranged from 0.82 to 0.94, and for the entire scale α = 0.97 [17].

The BSSS was developed by Schwarzer and Schutz to assess social support and we used the Polish version by Łuszczyńska and Kowalska [18]. It contains 17 general statements concerning the following subscales: Perceived Available Emotional Support, Perceived Available Instrumental Support, Need for Support and Seeking Support. The rest of the tool contains 15 statements referring to the person closest to the respondent, referring to Received Emotional Support, Received Instrumental Support and Received Informational Support. The third (optional) part of the Scales (Currently provided support) is dedicated to the person providing support and was not used in this study. The participants respond to each item by choosing 1 of 4 answers (from "completely true" to "completely false").

The respondents' sense of attractiveness after childbirth was assessed based on an original question included in the part of the questionnaire dedicated to women after childbirth: "Do you feel less physically attractive after childbirth than before?" Their responses were provided on a 5-point Likert scale from 1 ("definitely not") to 5 ("definitely yes"), with a higher score indicating a greater decrease in the sense of attractiveness.

Statistical analysis was performed using Microsoft Excel (Microsoft, Redmond, USA) and IBM SPSS (Armonk, NY, United States) software as well as a script written in the Python language (Python Software Fundation, Wilmington, Delaware, USA). The tests of normal distribution we conducted depending on the size of the selected group (Kolmogorov–Smirnov and Shapiro–Wilk) did not show distributions consistent with the normal distribution among the analyzed variables. Therefore, we verified our hypotheses using non-parametric tests: Kruskal-Wallis H, Mann-Whitney U, Friedman and chi-square.

In order to identify factors influencing the level of sexual satisfaction of women, a multiple regression analysis was performed. The dependent variable was the total score on the FSFI scale (FSFI_Total). The model included clinical variables: episiotomy, type of delivery, change in sexual feelings after delivery and sense of attractiveness. Additionally, the level of social support (BSSS) was taken into account. The analysis used the OLS linear model (ordinary least squares), using the Python software. The level of statistical significance was set at $p \leq 0.05$. Consent to conduct this study was obtained from the Independent Bioethics Committee for Scientific Research at the Medical University of Gdańsk (KB/97/2024).

Results

A total of 181 women participated in the study between July 2024 and February 2025. Responses of 21 participants were rejected due to meeting the age criteria of geriatric pregnancy (> 35 years of age) and teenage pregnancy (< 18 years of age) [19-20]. The study group consisted of 160 women: 50 of them were planning pregnancy, 52 were pregnant and 58 were after childbirth. The average age of the respondents was almost 27 years (M = 26.64), almost 57% (n = 91) of women had higher education, the majority of the respondents were married 50.6% (n = 81) and assessed their social and living situation as good – 56.25% (n = 90). 280 of all the participants experienced a miscarriage. In the group of 58 women after childbirth, 51.72% (n = 30) gave birth naturally, 31.04% (n = 18) gave birth by caesarean section, while 17.24% (n = 10) started labor naturally and ended it by caesarean section. The sense of attractiveness after childbirth changed in 65.52% of the respondents (n = 38). Only 13.79% (n = 8) of the respondents sought help from specialists when faced with difficulties related to sexual satisfaction. The detailed characteristics of the study group are presented in Table 1.

The highest average scores were obtained by the respondents in the subscale Actually Received Instrumental Support (3.51 ± 0.79), while the lowest values were recorded in the subscale Buffering and Protective Support (2.15 ± 0.66) (Table 2). The reliability of the subscales was as follows: Perceived Available Support (Cronbach's α = 0.83), Need for Support (Cronbach's α = 0.61), and Seeking Support (Cronbach's α = 0.81) [20]. In our study, the overall reliability of the BSSS scale calculated based on the sum of items was Cronbach's α = 0.89, which indicates high internal consistency in the analyzed sample. Higher values in our own study may result from the homogeneity of the studied sample.

Using the WHOQOL-BREF questionnaire, it was shown that the average Overall Quality of Life of the examined women was (3.92 ± 0.85). The average Self-Rated Health was slightly lower than the Overall Quality of Life and amounted to (3.81 ± 0.83). The participants assessed their QoL in the Physical Domain the lowest (11.61 ± 2.05), and the Social Relationship Domain the highest (14.56 ± 3.44). In the process of analyzing the results, it was assumed that the higher the number of points, the higher the level of QoL of the examined participants (Table 3). In our study, Cronbach's α value was 0.93, which also indicates high internal consistency in the analyzed group.

The results obtained on the FSFI scale are presented in Table 4. Taking into account the scale cut-off points of less than or equal to 26 points, sexual dysfunctions were found in almost 35% of the study participants (n = 55; 34.4%). On the Overall Sexual Function Scale, women obtained an average of 22.29 ± 7.78 points. The highest scores were obtained in the

Sexual Satisfaction Domain (4.52 ± 1.78), while the lowest in the Sexual Pain Domain (2.00 ± 1.38) (Table 4). In our study, we obtained the coefficient α = 0.96, which confirms the high reliability of the tool in our sample of 160 Polish women.

Our 1st hypothesis was that there are statistically significant differences between groups of women before pregnancy, during pregnancy and after childbirth in terms of social support, QoL and sexual functioning. Analysis of the obtained data showed statistically significant differences between the study participants in terms of the level of sexual functioning, including sexual satisfaction (p = 0.009). Pregnant women showed a higher level of sexual satisfaction (M = 5.06) compared to those planning a pregnancy (M = 4.54) and after childbirth (M = 4.02) (Table 5).

Analysis of the obtained data showed statistically significant differences between respondents in terms of the level of social support, including the Perceived Available Support, (p = 0.026), Perception Available Instrumental Support (p = 0.006), Actually Received Support (p = 0.048), Received Emotional Support (p = 0.047) and Instrumental Support (p = 0.027). Pregnant women showed higher levels of the indicated variables compared to women planning a pregnancy and those who had just given birth. It was shown that pregnant women (M = 3.70) had a higher mean in the subscale Perceived Available Support compared to the group of women after childbirth (M = 3.36) and those planning a pregnancy (M = 3.26). The group of women expecting a child also showed the highest mean (M = 3.57) among all the studied groups in the subscale Perceived Available Instrumental Support. Pregnant women (M = 3.62) also had higher scores on the subscale Actually Received Support compared to the other study groups. Pregnant women also achieved the highest mean scores (M = 3.57) on the Emotional Support Received subscale, compared to women planning a pregnancy (M = 3.28) and women after childbirth (M = 3.21), as well as in the subscale Received Instrumental Support (M = 3.72), whereas this result was M = 3.45 in women planning a pregnancy and M = 3.37 in women after childbirth. Detailed results regarding social support in the studied subgroups are presented in Table 6.

Statistically significant differences were found between the 3 study groups in terms of the level of QoL, including all its subscales: Overall Quality of Life (p = 0.004), Self-Rated Health Status (p = 0.001), Physical Domain (p = 0.013), Psychological Domain (p = 0.001), Social Relationships Domain (p = 0.014) and Environmental Domain (p = 0.001). Pregnant women showed higher QoL in all subscales compared to women planning a pregnancy and after childbirth (Table 7).

Our 2nd hypothesis was that episiotomy or laceration significantly affects the perception of the respondents' sexuality. Statistical analysis was performed among postpartum women (n = 58), who were divided into two groups. The first group consisted of women who had experienced an incision or tear of the perineum (n = 25), while the second group did not experience any of the indicated situations (n = 33). There were no statistically significant differences between the studied groups in any of the domains assessing sexual functioning (Table 8).

Our 3rd hypothesis was that support from loved ones is associated with higher levels of sexual satisfaction. The chi-square test result showed a statistically significant relationship between support from close ones and satisfaction with intimate life ($\chi 2 = 21.974$, p = 0.038). Women who rated their intimate life as "good" were more likely to rate support from close ones as definitely good compared to other levels of satisfaction with intimate life (Table 9).

The analysis of differences in the assessment of the body before, during and after childbirth among the respondents showed statistically significant differences (p = 0.001). The surveyed women assessed their bodies better before pregnancy (M = 7.91) than during pregnancy and after childbirth (M = 1.29). The effect of the strength of the relationship between variables is strong (r = 0.73) (Table 10).

In order to identify variables that best predict women's level of sexual satisfaction (FSFI), we conducted multiple regression analysis taking into account clinical factors such as episiotomy, type of delivery, change in sexual feelings after childbirth, sense of attractiveness and the level of social support measured by the BSSS. The regression model was statistically significant (p < 0.001) and its fit was estimated at $R^2 = 0.29$, which means that it explains 29% of the variance in the level of sexual satisfaction. Among the clinical variables, type of delivery (p = 0.090) and change in sexual sensations after delivery (p = 0.090) approached statistical significance, indicating the potential importance of these factors in reducing sexual satisfaction.

Discussion

The reproductive period is a special time for women, during which a number of physical and mental changes occur. Research from 2023 conducted in 32 countries by the Ipsos Group showed that only 63% of all respondents declared satisfaction with their sexual life, with the highest percentage result recorded in China (79%), while in Poland this result amounted to 60% of respondents [21].

The analyzed study indicates the need to deepen knowledge in this area, identify factors influencing this condition and find ways to improve it. There is widely believed in the society that sexual satisfaction after childbirth can be influenced and reduced by an incision or tearing of the perineum. However, we did not find statistically significant results that would confirm this thesis. The conducted multiple regression analysis showed that the type of delivery and the subjective

Table 1. Socio-demographic data of the respondents

Age	18-23 years old	19%
	24-29 years old	56%
	30-35 years old	25%
Education level	Primary	1%
	Secondary	40%
	Vocational	2%
	Higher	57%
Social and living situation	Very good	29%
	All right	56%
	Average	14%
	Very bad	1%
Place of residence	Village	30.6%
	City up to 50 thousand inhabitants	16.3%
	City 50-250 thousand inhabitants	16.9%
	City of 250-500 thousand inhabitants	10.6%
	City with more than 500 thousand inhabitants	25.6%
Marital status	Virgin	17.5%
	In an informal relationship	30.6%
	Married	50.6%
	Divorced	1.3%

Table 2. Basic statistics of the results obtained in the individual subscale Berlin Social Support Scale (BSSS) (n = 160)

BSSS subscale	M (SD)	Me	Min	Max
Perceived Available Support	3.35 ± 0.67	3.50	1.00	4.00
Perceived Available Emotional Support	3.26 ± 0.69	3.37	1.00	4.00
Perceived Available Instrumental Support	3.44 ± 0.73	3.75	1.00	4.00
Need for Support	3.01 ± 0.59	3.00	1.00	4.00
Seeking Support	2.96 ± 0.68	3.00	1.00	4.00
Actually Received Support	3.41 ± 0.69	3.66	1.00	4.00
Received Emotional Support	3.36 ± 0.70	3.65	1.00	4.00
Received Instrumental Support	3.51 ± 0.79	4.00	1.00	4.00
Received Informational Support	3.35 ± 0.79	3.50	1.00	4.00
Buffering and Protective Support	2.15 ± 0.66	2.16	1.00	4.00

M – mean; Max – the highest value of the distribution; Me – median; Min – the lowest value of the distribution; N – number; SD – standard deviation

Table 3. Basic statistics of the results obtained in the individual subscales of the WHOQOL-BREF (n = 160)

WHOQOL-BREF subscale	M (SD)	Me	Min	Max
Overall Quality of Life	3.92 ± 0.85	4.00	1.00	5.00
Self-Rated Health	3.81 ± 0.83	4.00	1.00	5.00
Physical Domain	11.61 ± 2.05	12.00	5.71	16.57
Psychological Domain	13.82 ± 2.06	14.00	7.33	18.67
Social Relationships Domain	14.56 ± 3.44	15.33	4.00	20.00
Environmental Domain	14.50 ± 2.60	14.50	5.00	20.00

M – mean; Max – the highest value of the distribution; Me – median; Min – the lowest value of the distribution; N – number; SD – standard deviation

Table 4. Basic statistics of the results obtained in the individual subscales of the Female Sexual Function Index (FSFI) (n = 160)

FSFI subscale	M (SD)	Me	Min	Max
Desire Domain	3.46 ± 1.04	3.60	1.20	6.00
Arousal Domain	3.99 ± 1.74	4.50	0.00	6.00
Lubrication Domain	4.43 ± 1.96	5.40	0.00	6.00
Orgasm Domain	3.86 ± 1.99	4.40	0.00	6.00
Sexual Satisfaction Domain	4.52 ± 1.78	5.20	0.80	6.00
Sexual Pain Domain	2.00 ± 1.38	1.60	0.00	6.00
Overall Sexual Function	22.29 ± 7.78	25.30	2.00	32.80

M – mean; Max – the highest value of the distribution; Me – median; Min – the lowest value of the distribution; N – number; SD – standard deviation

Table 5. Sexual functioning in the studied groups of women (n = 160)

FSFI subscale	Respondents planning pregnancy (n = 50)	Respondents during pregnancy (n = 52)	Respondents after delivery (n = 58)	H Kruskal-Wallis	P
	M	M	M		
Desire Domain	3.61	3.54	3.26	2.915	0.233
Arousal Domain	4.12	4.44	3.49	5.165	0.076
Lubrication Domain	4.78	4.88	3.74	8.363	**0.015***
Orgasm Domain	4.04	4.15	3.45	1.736	0.420
Sexual Satisfaction Domain	4.54	5.06	4.02	9.318	0.009 **
Sexual Pain Domain	2.25	1.90	1.86	4.192	0.123
Overall Sexual Function	23.36	23.98	19.85	4.631	0.099

* $p < 0.05$, ** $p < 0.01$ **

Table 6. Social support in the studied subgroups (n = 160)

BSSS subscale	Participants planning pregnancy (n = 50)	Tested during pregnancy (n = 52)	Examined after delivery (n = 58)	H Kruskal-Wallis	P
	M	M	M		
Perceived Available Support	3.26	3.70	3.36	7.320	**0.026***
Perceived Available Emotional Support	3.21	3.44	3.13	5.181	0.075
Perceived Available Instrumental Support	3.23	3.57	3.25	10.179	**0.006****
Need for Support	2.97	3.03	3.02	0.235	0.889
Support Seeking	3.01	2.97	2.90	0.493	0.782
Actually Received Support	3.33	3.62	3.27	6.087	**0.048***
Actually Received Emotional Support	3.28	3.57	3.23	6.122	**0.047***
Actually Received Instrumental Support	3.45	3.72	3.37	**7.244**	**0.027***
Actually Received Informational Support	3.28	3.58	3.21	4.959	0.084
Protective Buffering Scale	2.17	1.98	2.28	5.462	0.065

* p < 0.05, ** p < 0.01 **

Table 7. Quality of life level with subscale WHOQOL-BREF in the study group (n = 160)

WHOQOL-BREF subscales	Participants planning pregnancy (n = 50)	Participants during pregnancy (n = 52)	Examined after delivery (n = 58)	H Kruskal-Wallis	P
	M	M	M		
Overall Quality of Life	3.68	4.19	3.91	10.959	**0.004****
Self-Rated Health	3.56	4.17	3.74	14.969	**0.001****
Physical Domain	11.39	12.35	11.14	8.722	**0.013***
Psychological Domain	13.18	14.69	13.58	14.973	**0.001****
Social Relationships Domain	14.32	15.79	13.67	8.516	**0.014***
Environmental Domain	13.69	16.00	13.86	27.779	**0.001****

* p < 0.05, ** p < 0.01 **

Table 8. Perineal incision or laceration and sexual functioning of the studied women (n = 58)

Variable	Participants who had an episiotomy or perineal tear (n = 25)	Participants who did not have episiotomy or perineal tear (n = 33)	P
	M	M	
Desire Domain	2.97	3.49	0.136
Arousal Domain	3.58	3.42	0.969
Lubrication Domain	4.06	3.50	0.450
Orgasm Domain	3.55	3.38	0.936
Sexual Satisfaction Domain	4.22	3.86	0.561
Sexual Pain Domain	2.01	1.75	0.301
Overall Sexual Function	20.42	19.42	0.820

* p < 0.05, ** p < 0.01 **

Table 9. Support from close ones and satisfaction with intimate life in the study group – chi-square test (n = 58)

Variable		Support Rating								Total	
		Rather bad		I have no opinion		Rather good		Definitely good			
		N	%	N	%	N	%	N	%	N	%
Are you satisfied with your intimate life?	Definitely not	1	100%	0	0.0%	3	14.3%	1	3.1%	5	8.6%
	Rather not	0	0.0%	2	50.0%	5	23.8%	2	6.3%	9	15.5%
	Hard to say	0	0.0%	1	25.0%	3	14.3%	7	21.9%	11	19.0%
	Rather yes	0	0.0%	1	25.0%	8	38.1%	14	43.8%	23	39.7%
	Definitely yes	0	0.0%	0	0.0%	2	9.5%	8	25.0%	10	17.2%
Total		1	100.0%	4	100.0%	21	100.0%	32	100.0%	58	100.0%

Table 10. Body assessment before pregnancy, during pregnancy and after delivery in the studied subgroups

Variable	M	χ2	Df	P	W
Pre-pregnancy body assessment	7.91	85.609	2	**0.001****	0.73
Body assessment during pregnancy	6.44				
Post-pregnancy body assessment	1.29				

χ2 – Friedman test; df – degrees of freedom; M –mean, W – Kendal's W; * p < 0.05; ** p < 0.01** **

change in sexual feelings after childbirth may be factors influencing the decrease in sexual function. Despite the lack of significance of individual scale items (BSSS), the inclusion of social support in the regression model increased its explanatory power, suggesting that the overall relational and emotional climate may play an important role in women's sexual well-being.

In a 2018 study conducted by O'Malley et al., 46.3% of postpartum women reported a lack of interest in sexual activity, which was influenced by: dyspareunia (37.5%, understood as pain before, during or after intercourse), lack of lubrication and dissatisfaction with the appearance of their own body [22]. In this study, women asked about changes in their sexual life during pregnancy declared: both decreased and increased libido, less freedom of movement, a limited number of sexual positions and increased body sensitivity. The greatest difficulties in sexual life during pregnancy among the respondents were: general fatigue, nausea, back pain, swollen legs, the size of the belly that makes it difficult to move freely and problems with choosing a sexual position. When asked about changes and the greatest difficulties in sexual life after pregnancy, respondents declared: pain during intercourse, low satisfaction with appearance after childbirth, general fatigue and lack of desire for sex. The available review study from 2024 confirms a decrease in sexual drive after childbirth, an increase in perineal pain and dyspareunia, as well as a lower intensity and shorter duration of orgasm in the first 3 months after childbirth [23]. It is worth emphasizing that numerous studies indicate a strong relationship between social support and the level of sexual satisfaction. The role of the positive influence of support from close people, a good relationship with the partner and a stable emotional state are emphasized, as well as their importance in the context of the perceived sexual satisfaction, which was also confirmed in the conducted study [24-26].

Scientific research also indicates a high need for social support among women during pregnancy and after childbirth. In a cross-sectional study conducted in 2024 Nazzal et al. showed that there is a positive, statistically significant relationship ($p < 0.05$) between social support and the level of QoL, which is consistent with our results. Pregnant women experience greater social support than women before pregnancy and after childbirth [27]. The same results were obtained by Emmanuel et al., showing that social support is a significant and consistent predictor of higher health-related quality of life (HRQoL) in women in the perinatal period [28]. Gebuze et al. showed that social support is a significant factor influencing life satisfaction in pregnant Polish women and after childbirth. Women who received greater social support reported a higher level of life satisfaction [7]. Zhou et al. obtained different results in their study: the surveyed women declared a reduced sense of social support during pregnancy and perinatal period. The COVID-19 pandemic that took place at that time could have had a significant impact on various results, through the restrictions and the resulting reduction in social contacts contributed to a significant deterioration in the mental state of women [29]. In addition, Faleschini et al. demonstrated that support received from a partner and family has a positive effect on a woman, which is a protective factor against postpartum depression and translates into increased physical activity and maintaining healthier eating habits, which in turn prevents obesity [30].

Our results showed that pregnant women assess their QoL higher and their overall health better compared to other groups. This may be influenced by the perception of pregnancy as a special period in a woman's life. Despite the accompanying physical ailments, women experience increased care from their environment during this time and are more motivated to lead a healthy lifestyle. A healthy diet, adequate sleep and avoiding stimulants are factors that can influence a better self-assessment of their condition. The obtained results are consistent with the Iranian study by Mortazavi et al., which showed that women's QoL increases in the third trimester of pregnancy, mainly in the psychological and social sphere, which according to the authors is strongly related to greater support from loved ones and preparations for childbirth. In turn, after childbirth, the QoL often deteriorates, especially in the first months, when women struggle with physical exhaustion, hormonal changes and lack of sleep/time for regeneration [31].

Our results indicate that women evaluate their bodies much better before pregnancy than during pregnancy and after childbirth. These differences are statistically highly significant and confirm the observations from previous studies, which show the impact of physical and psychological changes related to pregnancy and motherhood on the perception of one's own body. A number of hormonal and anatomical changes occur in a woman's body during pregnancy, e.g. body weight increases, body posture changes, swelling and stretch marks appear. Although these changes are physiological and natural, women often find it difficult to come to terms with the loss of their pre-pregnancy image, which is associated with a lower mood and lack of acceptance of their own body [10, 32].

Limitations of this study

Our study group involved 160 women and due to its size it might not reflect trends in the greater population. In addition, the study was made available only online on websites dedicated for women who were either planning to have a child, were pregnant or were postpartum. The women were at different stages of declared pregnancy, which could also have influenced the answers provided and the results obtained.

Another limitation of the study is the lack of measurement of depressive symptoms, which are common in the perinatal period and could affect the level of sexual satisfaction. In the future, it is worth including this variable as a control. Despite the obtained results indicating certain tendencies in the study group, the researchers point to the justification for continuing the conducted research. There is a need to increase the sample size, as well as further explore the discussed issues, taking into account additional variables (e.g. the aforementioned depressive symptoms).

Conclusions

1. Pregnant women experience higher levels of sexual satisfaction compared to women before and after pregnancy.

2. The surveyed pregnant women showed higher levels of perceived available support (instrumental support dimension) and received support (emotional and instrumental support dimension) compared to women planning a pregnancy and after childbirth.

3. Pregnant women assess their health, mental health, social relationships and overall QoL higher than other studied groups.

4. Medical intervention in the form of vaginal incision or laceration during childbirth has no effect on a woman's sexual functioning (the correlations were not statistically significant).

5. Women who rated their intimate life as good were more likely to rate the support of loved ones as definitely good, compared to women with other levels of satisfaction with intimate life.

6. The surveyed women rated their bodies significantly higher before pregnancy than during pregnancy and after childbirth. Changes in appearance can be a challenge on the path to motherhood. It is reasonable to support women in accepting their bodies through social support and education on the physiological changes that occur in a woman during pregnancy and after childbirth.

7. Both physical factors (e.g. mode of delivery) and psychosocial factors (e.g. perception of sexual sensations, social support) should be taken into account in perinatal care and in educational activities (e.g. childbirth classes) aimed at women and their partners.

8. More research is needed in orther to further explore the above-mentioned issues and to include new variables (e.g. symptoms of depression).

Acknowledgments

The authors thank each woman who participated in this study.

Funding

This work was not financed by any scientific research institution, association or other entity and the authors did not receive any grant.

Conflicts of interest

The authors report no conflicts of interest.

References

1. Education and treatment in human sexuality : the training of health professionals, report of a WHO meeting held in Geneva from 6 to 12 February 1974][Internet]. Worth Health Organization. [cited 2025 Jun 30]. Available from: https://iris.who.int/handle/10665/38247
2. Rudolf E. Zdrowie reprodukcyjne kobiet – rozważania terminologiczne [in Polish]. In: Problemy zdrowia reprodukcyjnego kobiet Wstęp do badań [Internet]. 2016. p. 19–36. Available from: https://www.researchgate.net/publication/312220204_Zdrowie_reprodukte_kobiet__rozwazania_terminologiczne
3. Grussu P, Vicini B, Quatraro RM. Sexuality in the perinatal period: A systematic review of reviews and recommendations for practice. Sex Reprod Healthc [Internet]. 2021;30:100668. Available from: https://www.sciencedirect.com/science/article/pii/S1877575621000756
4. Narodowy raport o seksualności 2024 [in Polish] [Internet]. Medycyna Praktyczna. 2024 [cited 2025 Jun 30]. Available from: https://www.mp.pl/kurier/349008,narodowy-raport-o-seksualnosci-2024
5. Fuchs A, Czech I, Dulska A, Drosdzol-Cop A. The impact of motherhood on sexuality. Ginekol Pol [Internet]. 2021;92(1):1–6. Available from: https://journals.viamedica.pl/ginekologia_polska/article/view/68189

6. Zgliczynska M, Zasztowt-Sternicka M, Kosinska-Kaczynska K, Szymusik I, Pazdzior D, Durmaj A, et al. Impact of childbirth on women's sexuality in the first year after the delivery. J Obstet Gynaecol Res [Internet]. 2021;47(3):882–92. Available from: https://obgyn.onlinelibrary.wiley.com/doi/10.1111/jog.14583
7. Gebuza G, Kaźmierczak M, Mieczkowska E, Gierszewska M. Wsparcie społeczne jako determinant zadowolenia z życia u kobiet w okresie ciąży i po cięciu cesarskim [in Polish]. Psychiatr Pol [Internet]. 2018;52(3):598–885. Available from: https://www.psychiatriapolska.pl/Social-support-as-a-determinant-of-life-satisfaction-inpregnant-women-and-women,64194,0,1.html
8. Ilska M, Przybyła-Basista H, Ilski A, Cnota W. Aktywność i satysfakcja seksualna kobiet w ciąży prawidłowej oraz wysokiego ryzyka [in Polish]. Ginekol Poloz [Internet]. 2018;2:34–41. Available from: https://www.researchgate.net/publication/338358100_Aktywnosc_i_spokojcja_seksualna_kobiet_w_ciazy_prawidlowej_oraz_wysokiego_ryzyka
9. Makara-Studzińska M, Wdowiak A, Plewik I. Seksualność kobiet w ciąży [in Polish]. Seksuologia Pol [Internet]. 2011;9(2):85–90. Available from: https://ruj.uj.edu.pl/entities/publication/d46f4ae4-28f5-4291-8437-851ae788da42
10. Duncombe D, Wertheim EH, Skouteris H, Paxton SJ, Kelly L. How Well Do Women Adapt to Changes in Their Body Size and Shape across the Course of Pregnancy? J Health Psychol [Internet]. 2008;13(4):503–15. Available from: https://journals.sagepub.com/doi/10.1177/1359105308088521
11. McDonald E, Woolhouse H, Brown SJ. Sexual pleasure and emotional satisfaction in the first 18 months after childbirth. Midwifery [Internet]. 2017;55:60–6. Available from: https://www.sciencedirect.com/science/article/pii/S0266613817300864
12. Khawaja M, Habib RR. Husbands' Involvement in Housework and Women's Psychosocial Health: Findings From a Population-Based Study in Lebanon. Am J Public Health [Internet]. 2007;97(5):860–6. Available from: https://ajph.aphapublications.org/doi/full/10.2105/AJPH.2005.080374
13. Hogan JN, Crenshaw AO, Baucom KJW, Baucom BRW. Time Spent Together in Intimate Relationships: Implications for Relationship Functioning. Contemp Fam Ther [Internet]. 2021;43(3):226–33. Available from: http://www.ncbi.nlm.nih.gov/pubmed/34334944
14. Fanshawe A-M, De Jonge A, Ginter N, Takács L, Dahlen HG, Swertz MA, et al. The Impact of Mode of Birth, and Episiotomy, on Postpartum Sexual Function in the Medium- and Longer-Term: An Integrative Systematic Review. Int J Environ Res Public Health [Internet]. 2023;20(7):5252. Available from: https://www.mdpi.com/1660-4601/20/7/5252
15. Leal IMP, Lourenço S, Oliveira R, Carvalheira A, Maroco J. Sexual function in women after delivery: Does episiotomy matter? Health (Irvine Calif) [Internet]. 2014;6(05):356–63. Available from: https://www.scirp.org/journal/papercitationdetails?paperid=43131&journalid=65
16. THE WHOQOL GROUP. Development of the World Health Organization WHOQOL-BREF Quality of Life Assessment. Psychol Med [Internet]. 1998;28(3):551–8. Available from: https://www.cambridge.org/core/product/identifier/S0033291798006667/type/journal_article
17. Rosen, C. Brown, J. Heiman, S. Leib R. The Female Sexual Function Index (FSFI): A Multidimensional Self-Report Instrument for the Assessment of Female Sexual Function. J Sex Marital Ther [Internet]. 2000;26(2):191–208. Available from: https://www.tandfonline.com/doi/full/10.1080/009262300278597
18. Łuszczyńska A, Kowalska M, Schulz U, Schwarzer R. Berlin Social Support Scales (BSSS) - Polish Version [Internet]. 2002 [cited 2025 Jun 30]. Available from: https://userpage.fu-berlin.de/~health/soc_pol.htm
19. Frankowicz-Gasiul B, Michalik A, Czerwińska A, Zydorek M, Olszewska J, Olszewski J. Ciąża młodocianych – problem medyczny i społeczny [in Polish]. Stud Med [Internet]. 2008;11:57–63. Available from: https://studiamedyczne.ujk.edu.pl/doc/SM_tom_11/Ciaza mlodocianych.pdf
20. Erasmus E. Pregnancy After 35: Why Science Says It's Safe. [Internet]. Parents. [cited 2025 Jun 30]. Available from: https://www.parents.com/getting-pregnant/age/pregnancyafter-35/psa-its-totally-fine-to-have-babies-after-35-science-backs/
21. Stinson J. Love life satisfaction around the world. A 30-Country Global Advisor Survey [Internet]. 2025. Available from: https://www.ipsos.com/sites/default/files/ct/news/documents/2025-02/ipsos-love-life-satisfaction-index-2025_0.pdf
22. O'Malley D, Higgins A, Begley C, Daly D, Smith V. Prevalence of and risk factors associated with sexual health issues in primiparous women at 6 and 12 months postpartum; a longitudinal prospective cohort study (the MAMMI study). BMC Pregnancy Childbirth [Internet]. 2018;18(1):196. Available from: https://bmcpregnancychildbirth.biomedcentral.com/articles/10.1186/s12884-018-1838-6
23. Rezaei N, Behboodi Moghadam Z, Tahmasebi A, Taheri S, Namazi M. Women`s sexual function during the postpartum period: A systematic review on measurement tools. Medicine (Baltimore) [Internet]. 2024;103(30):e38975. Available from: https://journals.lww.com/10.1097/MD.0000000000038975

24. Leeman LM, Rogers RG. Sex After Childbirth. Obstet Gynecol [Internet]. 2012 Mar;119(3):647–55. Available from: http://journals.lww.com/00006250-201203000-00024
25. Kardasz Z, Szymańska J. Poziom stresu pourazowego, poczucia satysfakcji z życia i satysfakcji seksualnej po porodzie naturalnym, z asystą osoby towarzyszącej i bez niej [in Polish]. Fam Forum [Internet]. 2024 Dec 20;14:267–87. Available from: https://czasopisma.uni.opole.pl/index.php/ff/article/view/5088
26. Stadnicka G, Łepecka-Klusek C, Pilewska-Kozak AB, Pawłowska-Muc AK. Satysfakcja seksualna kobiet po porodzie — część I [in Polish]. Probl Pielęgniarstwa [Internet]. 2015;23(3):357–61. Available from: https://www.termedia.pl/Journal/-134/pdf-35585-1
27. Nazzal S, Ayed A, Zaben KJ, Abu Ejheisheh M, ALBashtawy M, Batran A. The Relationship Between Quality of Life and Social Support Among Pregnant Women: A Cross-Sectional Study. SAGE Open Nurs [Internet]. 2024 Jan 5;10. Available from: https://journals.sagepub.com/doi/10.1177/23779608241301225
28. Emmanuel E, St John W, Sun J. Relationship between Social Support and Quality of Life in Childbearing Women during the Perinatal Period. J Obstet Gynecol Neonatal Nurs [Internet]. 2012 Nov;41(6):E62–70. Available from: https://linkinghub.elsevier.com/retrieve/pii/S0884217515312296
29. Zhou J, Havens KL, Starnes CP, Pickering TA, Brito NH, Hendrix CL, et al. Changes in social support of pregnant and postnatal mothers during the COVID-19 pandemic. Midwifery [Internet]. 2021;103:103162. Available from: https://linkinghub.elsevier.com/retrieve/pii/S0266613821002424
30. Faleschini S, Millar L, Rifas-Shiman SL, Skouteris H, Hivert M-F, Oken E. Women's perceived social support: associations with postpartum weight retention, health behaviors and depressive symptoms. BMC Womens Health [Internet]. 2019;19(1):143. Available from: https://bmcwomenshealth.biomedcentral.com/articles/10.1186/s12905-019-0839-6
31. Mortazavi F, Mousavi SA, Chaman R, Khosravi A. Maternal Quality of Life During the Transition to Motherhood. Iran Red Crescent Med J [Internet]. 2014 May 5;16(5). Available from: https://archive.ircmj.com/article/16/5/15924-pdf.pdf
32. Clark A, Skouteris H, Wertheim EH, Paxton SJ, Milgrom J. The Relationship between Depression and Body Dissatisfaction across Pregnancy and the Postpartum. J Health Psychol [Internet]. 2009;14(1):27–35. Available from: https://journals.sagepub.com/doi/10.1177/1359105308097940

EUROPEAN JOURNAL OF TRANSLATIONAL
AND CLINICAL MEDICINE 2025;8(1):83-96

REVIEW ARTICLE

Revolution in flow cytometry: using artificial intelligence for data processing and interpretation

Szymon Bierzanowski[1,2], Krzysztof Pietruczuk[1]

[1] Division of Biostatistics and Neural Networks, Medical University of Gdańsk, Poland
[2] Faculty of Applied Physics and Mathematics, Gdańsk University of Technology, Poland

Abstract

Flow cytometry (FC) represents a pivotal technique in the domain of biomedical research, facilitating the analysis of the physical and biochemical properties of cells. The advent of artificial intelligence (AI) algorithms has marked a significant turning point in the processing and interpretation of cytometric data, facilitating more precise and efficient analysis. The application of key AI algorithms, including clustering techniques (unsupervised learning), classification (supervised learning) and advanced deep learning methods, is becoming increasingly prevalent. Similarly, multivariate analysis and dimension reduction are also commonly attempted. The integration of advanced AI algorithms with FC methods contributes to a better understanding and interpretation of biological data, opening up new opportunities in research and clinical diagnostics. However, challenges remain in optimising the algorithms for the specificity of the cytometric data and ensuring their interpretability and reliability.

Keywords: flow cytometry · machine learning · data analysis · AI algorithms · automation

Citation

Bierzanowski S, Pietruczuk K. Revolution in flow cytometry: using artificial intelligence for data processing and interpretation. Eur J Transl Clin Med. 2025;8(1):83-96.

DOI: 10.31373/ejtcm/199793

Corresponding author:
Krzysztof Pietruczuk, Division of Biostatistics and Neural Networks, Medical University of Gdańsk, Poland
e-mail: krzysztof.pietruczuk@gumed.edu.pl
Available online: ejtcm.gumed.edu.pl

Introduction

Flow cytometry (FC) is a technique that enables rapid analysis of large numbers of cells in suspension by measuring the light scattered by the cells and fluorescence emitted by fluorochromes conjugated to antibodies [1-2]. The two main detectors are the forward scatter channel (FSC) which detects scattering along the laser beam, determining the size of particle and the side scatter channel (SSC) which measures scattering at 90°, thus assessing the granularity of the cells [3-4]. Other detectors measure the fluorescence produced by excitation of the fluorochrome with laser beam of the appropriate wavelength [3, 5].

FC is used in research and clinical laboratories for the assessment of cell surface antigen and intracellular antigen expression, enzyme activity gene expression and mRNA transcription [6]. This method permits the assessment of the cell cycle, mitochondria and cellular processes (e.g. apoptosis, autophagy, and cell ageing). It allows the quantification of biological substances in various body fluids, including serum and cerebrospinal fluid. FC allows not only the collection and analysis of data about cells, but also the sorting of cells based on the principle of deflecting flowing particles according to their electrical potential [6]. The degree of purity obtained is greater than 99%. This method is also employed to isolate rare cell populations, including cancer cells, fetal erythrocytes, and genetically modified cells [6-7]. The FC technique can be adapted for the detection, characterisation and enumeration of microorganisms in aqueous matrices, as well as somatic and bacterial cells in milk [8]. In medicine, FC is most widely used in haematology and oncology, specifically in cancer diagnosis, classification and monitoring treatment [7].

Despite the technological developments in FC, data analysis remains a key problem, requiring both standardisation and automation [9]. The aim of this article is to present the potential of AI algorithms in the analysis of cytometric data and the problems that still need to be solved to fully automate the process of analyzing this type of data.

Manual analysis of cytometric measurements

Manual gating still is the primary method for analysing the results. This step is essential for obtaining relevant information about the cells under study, whether the goal is to study the phenotype of a population or to identify the internal structures of cells [10]. In the case of the analysis of peripheral blood cells, such as lymphocytes, an FSC vs. SSC plot is initially constructed, which facilitates the distinction of the primary cell populations based on their size and granularity. Once the groups of cells of interest have been selected by setting up further gating, the expression of surface markers in fluorescence plots can be analysed. The manual gating process is complicated, time-consuming, subjectiveand requires advanced knowledge and experience [11-13].

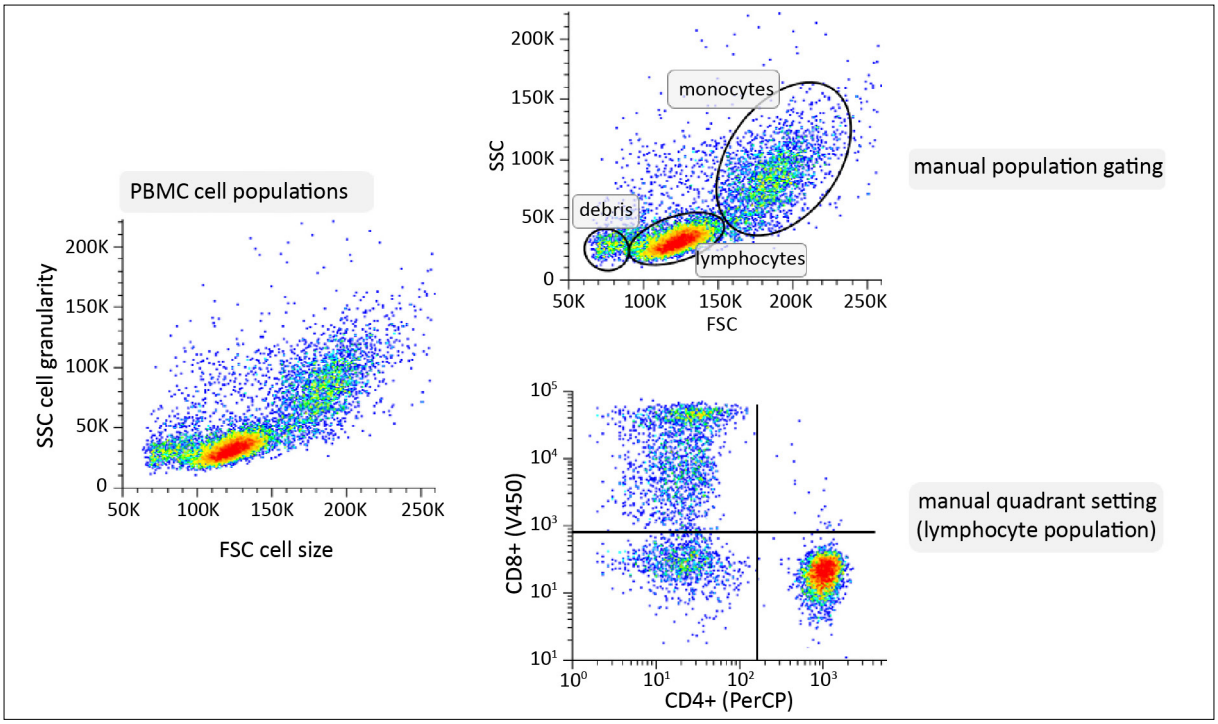

Figure 1. Schematic of manual analysis of cytometric data using peripheral blood mononuclear cells (PBMC) sample as an example

Material and methods

The article is based on a review of the literature available in PubMed (biomedical research publications) and IEEE Xplore (broad access to technical literature in engineering and computer science). The analysis included articles on the application of machine learning algorithms to cytometric data analysis, including methods for mining and interpreting FC data. All included publications were selected for their relevance to the development of ML tools in this field.

Application of AI in cytometric data analysis

The use of artificial intelligence (AI) algorithms to automate the analysis of cytometric measurement data is becoming more common. This approach aims to reduce processing time and improve error resilience compared to manual methods. These algorithms mainly rely on clustering techniques, which involve dividing data based on specific criteria [14]. Clustering includes both classification (data is assigned to predefined classes) and clustering (natural groups in data without prior labels). Dimensionality reduction methods (e.g. principal component analysis, t-distributed stochastic neighbour embedding and uniform manifold approximation and projection) are also increasingly used.

Clustering techniques – unsupervised machine learning

Unsupervised learning, unlike supervised learning, operates on unlabeled data, identifying patterns and structures without pre-assigned categories.

k-means

The first clustering algorithm used for analyzing cytometric data was k-means [15-16]. This iterative algorithm identifies data points with similar features around a central point called the 'centroid'. Points closest to the centroid are grouped together, forming clusters. Distance is crucial in this algorithm and can be defined in various ways, but it is often the smallest sum of distances between the centroids and observations [17]. K-means involves several steps: selecting the number of clusters, initializing centroid positions, assigning each data point to the nearest centroid based on distance, recalcu-

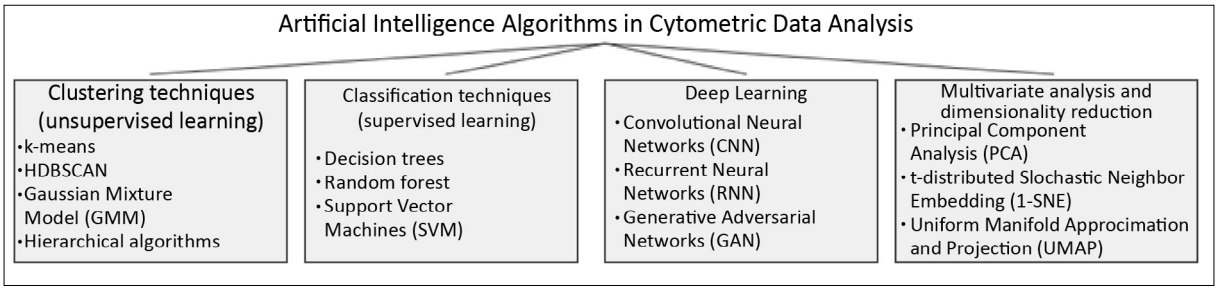

Figure 2. Artifical Intelligence (AI) algorithms currently applicable to the analysis of cytometric measurements in analysis

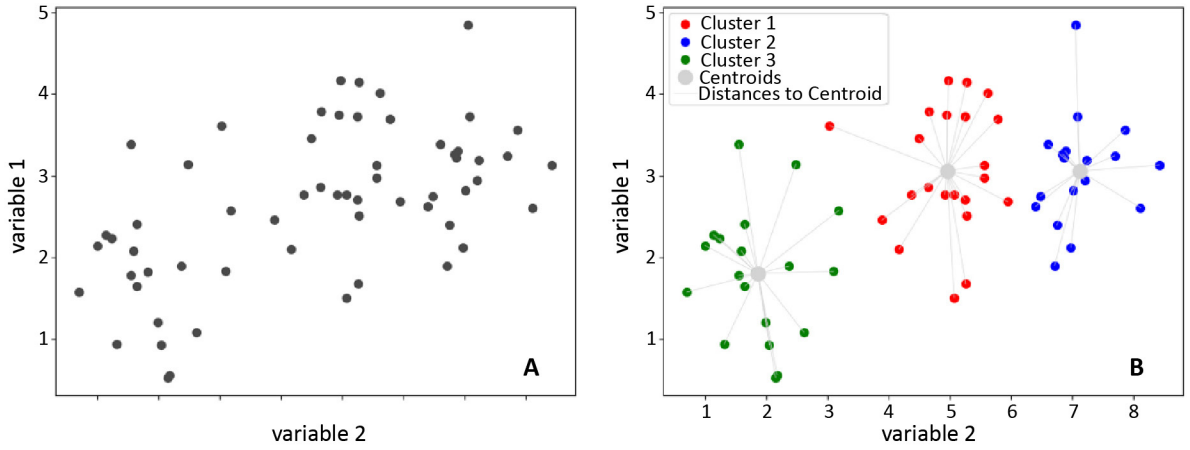

Figure 3. Visualisation of the operation of k-means clustering algorithm
A – before the application of k-means; B – effect of the algorithm

lating centroids, and repeating these steps until the centroids' positions stabilize or a stopping condition is met [15, 17].

K-means is a straightforward and effective clustering method, but it faces challenges like computational scalability, which can limit its use in analyzing cytometric data [18]. This algorithm requires substantial computation, with processing time increasing with the number of data points, clusters, and iterations, making it inefficient for large datasets like those from FC. Scalability can be improved by modifying the method to initialize centroids more efficiently or by using random data samples to update the centroids faster. Additionally, parallel computing is explored to further enhance scalability [19-20].

Another disadvantage of k-means is the need for the user to predefine the number of clusters [18]. Cytometric data are often characterised by a complex structure, which makes it difficult to determine the number of clusters, and choosing the wrong number of clusters can affect the biological interpretation of the results due to both under- and overestimation of their actual number [21]. When using the k-means algorithm, it is important to remember that it assumes the sphericity of the clusters and their separation [18]. These assumptions can be a disadvantage in the case of cytometric data obtained from peripheral blood cell measurements such as peripheral blood mononuclear cells (PBMC). This is because the cluster structure of these data is usually complex. PBMCs include different types of cell populations characterised by irregular distributions in the multidimensional feature space which may be caused, for example, by the fluorescence intensity of different surface markers [22]. At the same time, some cell populations have features that may lead to overlapping clusters causing the assumption of separation to fail.

A number of methods used in attempts to automate cytometric analysis have conceptual similarities to k-means or directly apply this algorithm. These methods include FlowClust, FlowMerge and FlowMeans [23-25]. Methods based on the k-means algorithm are often benchmarked and improved. The FlowMerge and flowClust algorithms were found useful in identifying cell populations in real clinical data from patients with chronic lymphocytic leukemia [23]. It was also pointed out that there were some difficulties in identifying clusters compared to other methods when evaluating their work with synthetic data [24].

Gaussian Mixture Model (GMM)

GMM is a probabilistic model that assumes data are generated from specific probability distributions [36]. It models data as a mixture of Gaussian components, each representing a cluster, estimating parameters like mean, variance and cluster weights to determine the likelihood of data points belonging to each cluster [37]. This makes GMM suitable for biomedical data analysis, including FC [38]. GMM is effective for clustering multimodal data with unknown cluster numbers, performing well with both continuous and discrete data, particularly when multiple peaks are present [39-40]. Cytometric data, such as PBMC phenotypes, often exhibit multimodality, making GMM ideal for identifying distinct cell populations, regardless of subtle differences [41-43]. The algorithm excels with continuous data and the Dirichlet Process Gaussian Mixture Model, an extension of GMM, handles unknown cluster numbers, automatically detecting clusters based on data structure [44-45].

HDBSCAN

Hierarchical Density-Based Spatial Clustering of Applications with Noise (HDBSCAN) is a density-based clustering algorithm [26-27] that groups closely located points and identifies outliers as noise. Unlike k-means, the HDBSCAN does not require a predetermined number of clusters, which makes it useful for analysing cytometric data when the number of subpopulations is unknown [27]. HDBSCAN adapts to different densities, identifies clusters of different shapes, but requires the definition of a minimum number of points to form a cluster and a distance measure [27]. This algorithm uses a hierarchical approach to clustering, assessing data membership based on their position in the cluster tree structure [28]. Points form a cluster if they are sufficiently densely packed, while points that do not meet the density criteria, i.e. without a sufficient number of neighbours within a certain radius, are treated as noise and remain unassigned [29-30].

HDBSCAN starts by calculating the distance of each point to its nearest neighbour, estimating the local density. Based on these distances, it creates a graph in which the points are vertices and the edges have weights corresponding to the distances of each other. This graph is used to create a minimum spanning tree, from which the edges with the lowest weights are iteratively removed, splitting the clusters [31]. Small clusters are labelled as noise and larger clusters are given new labels. Finally, the algorithm identifies the most stable clusters as the final result [30, 32]. Despite its efficiency, the HDBSCAN algorithm has a high computational complexity [28-30], making it slower than k-means [30].

Automated analysis of cytometric data in oncology is crucial for faster and more objective patient monitoring. The combination of uniform manifold approximation and projection (UMAP) and HDBSCAN simultaneously reduces data dimensionality and identifies clusters in AML samples, effectively detecting blasts and improving monitoring of minimal residual disease. This approach is superior to traditional supervised methods, particularly with limited data and high variability of leukemic cells [33]. It was also suggested that the HDBSCAN algorithm is useful for the analysis of mitochondrial features by FC [34]. HDBSCAN is used to identify

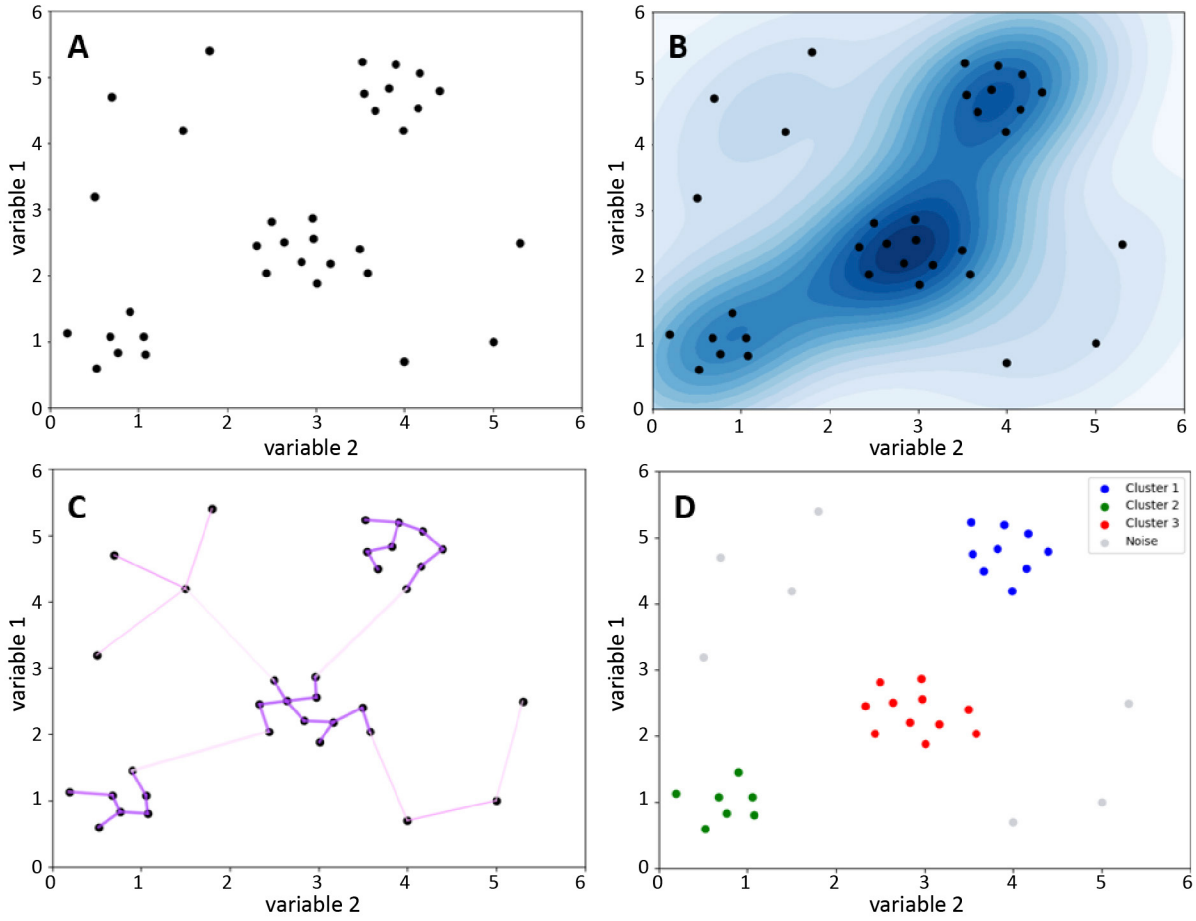

Figure 4. The HDBSCAN clustering algorithm
A – scatter plot showing data points distributed across different feature space regions; B – darker colours indicate higher point concentration, suggesting potential clusters; lighter shades indicate lower density, possibly noise; C – graph where points are connected by edges weighted by their distances; D – HDBSCAN-identified clusters, with dense region points forming clusters and others labelled as noise (grey)

cell populations for cytometric analysis in some commercial programmes, although specific implementations vary depending on the specifics of the tool and analytical requirements [25, 35].

Classification techniques – supervised machine learning

Random forests

Random forest is one of the algorithms of supervised machine learning. The algorithm was developed by Breiman et al. [46]. It may be useful to conceptualise the structure of the proposed algorithm in terms of the organisation of a natural forest. A random forest is composed of individual trees, with each tree functioning as a classifier. These trees operate simultaneously to produce a collective classification output. This outcome is determined by a process of "voting" between the trees, with the result being the classification assigned to the input data.

The random forest algorithm is based on decision trees, which represent sets of decisions to solve problems. Decision trees consist of branches and nodes [47]. Key node types include: root (initial division), internal (specific choices), and leaf (final observations). Branches represent decision paths.

There are several learning algorithms for decision trees, including: Id3, C4.5, CART, CHAID [48]. Decision trees are not complex structures, their implementation is relatively straightforward and does not require the appropriate scaling of features. They demonstrate high precision and accuracy in classification tasks, which is worth considering in analysis of FC data. On the other hand, they are not suitable for working on small datasets which can be a limitation in FC data analysis [49]. Presentation of the structure and functioning of decision trees is important in the context of the random forest algorithm because as mentioned earlier, random forests consist of multiple decision trees. The basic mechanism responsible for

the generation of random forests is bagging (bootstrap aggregation), a method introduced by Breiman et al. [50]. It generates multiple predictor versions and later aggregates them. In random forests, bagging creates independent decision trees, each trained on unique bootstrap samples (random data samples with repetitions) [50]. The classification outcome is determined through a process known as majority voting. The technique of majority voting is a method of combining the predictions of results from multiple classifiers. Each decision tree "votes" for a class, and the class with the most votes becomes the final prediction [51-52]. This algorithm can be used as a classifier in cytometric data analysis.

Random forest, is an easy-to-implement machine learning algorithm, excels at detecting meaningful data patterns [53]. It can reveal subtle features often overlooked by traditional statistical methods. Those features are often crucial in the context of a medical diagnosis [54]. In one study, a random forest model was implemented to identify significant details within the acquired cytometric data, with the objective of increasing the accuracy of diagnosis. Researchers collected blood samples from 230 individuals, including those with myelodysplastic syndromes (MDS) and healthy controls. They then used FC to evaluate the cellular composition of these samples. A random forest model was utilized to analyse the collected cytometric data, facilitating the more accurate detection and classification of significant cellular patterns associated with MDS [54]. The ability of random forests to identify subtle relationships in complex, multi-parameter data has enabled researchers to diagnose the presence of myelodysplastic syndromes with greater accuracy. The model achieved 92% classification accuracy, a high and satisfactory result. The random forest algorithm is relatively resistant to overfitting, a situation in which the machine learning model provides good results based on the data on which it was trained, but is instead ineffective in analysing new, previously unseen data [55]. FC data can include many features (markers) for each cell, and the number of cells analysed is very large [56]. In such complex datasets, it is easy to have random patterns that can be misleading and lead to over-fitting, particularly when using simpler models such as single decision trees. Random forests are easy to interpret [53]. This is a major advantage in the context of cytometric data analysis. It helps to understand which features contribute to the classification of different cell populations. This makes it possible to identify biologically relevant markers [57], which is essential in the context of medical diagnostics and biomedical research. The model, which is simple to interpret, also makes it easier to verify results, which increases the reliability and precision of analyses.

While the random forest algorithm offers a number of advantages, it is not free from limitations that may affect its effective application in FC data analysis. A significant limitation of machine learning models is their high computational cost [58]. Cytometric data is frequently large and complex and multidimensional. As a result, training models based on this type of data can be costly and challenging from an economic perspective. Although random forests are resistant to over-fitting, in some cases they can be prone to this problem, especially when working with data containing a lot of noise.

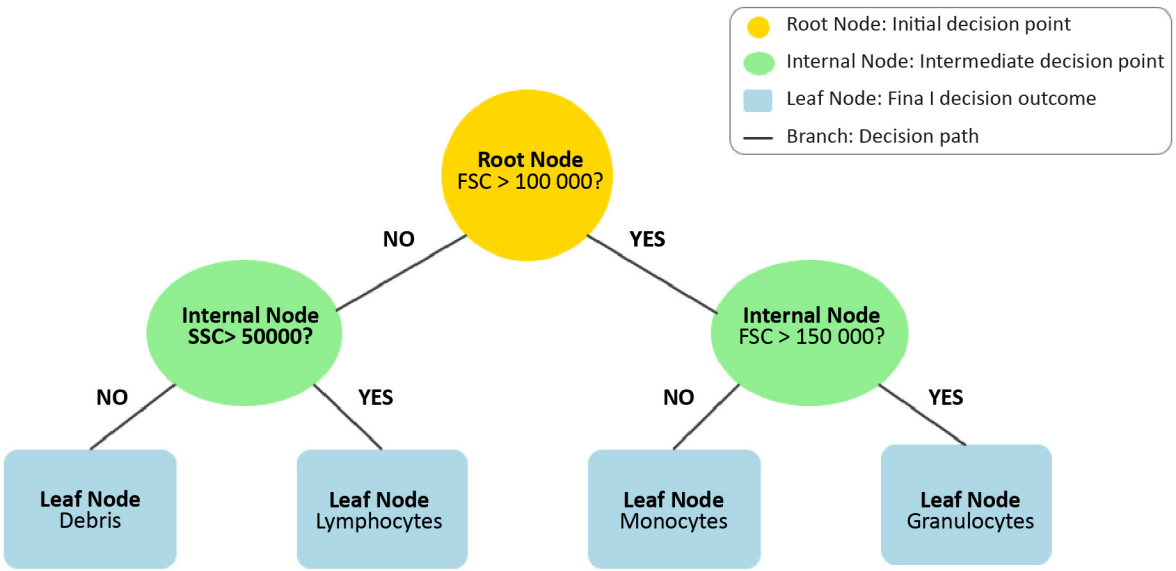

Figure 5. Visualization of a decision tree from Random Forests algorithm
The step-by-step classification process is shown through a series of decision nodes (yellow, green) and final classification outcomes at the leaf nodes (blue). The paths illustrate how data is split based on feature thresholds to reach the final decision.

In the context of FC, we can interpret noisy data as data with measurement errors or issues caused by sample heterogeneity or biological variability [59-60], all of which can affect the generation and propagation of errors in the classification performed by the model.

Support Vector Machines (SVM)

SVM was first introduced by Cortes and Vapnik et al. in 1995 [61]. The model was intended to be an effective alternative to the neural networks, which were still in development and presented certain technical challenges. SVM involves complex mathematical concepts including hyperplanes, margins, support vectors, kernels, and optimization. A hyperplane is a linear decision function that allows separation of data classes from each other. The prefix "hyper" indicates that this plane refers to multiple dimensions. For n dimensions, a hyperplane will take on (n–1) dimensions [61]. The margin is the distance between the hyperplane and the nearest data point [48]. Support vectors are data points that are located on a hyperplane. Optimization is the process of finding a hyperplane with as much margin as possible to best separate data points [62]. A kernel is a mathematical function that enables the transformation of data from a lower-dimensional space into a higher--dimensional space, allowing for the separation of the data [62]. In the context of FC data, an illustrative example would be the separation of cells in a PBMC graph with FSC and SSC parameters. In the two-dimensional space of the graph, it is not possible to linearly separate these cells. However, the kernel can be used to move the data points to a three-dimensional space, where it is possible to linearly separate them. The addition of an extra dimension allows for the creation of a hyperplane that can better represent the dataset.

SVM are particularly effective in classification tasks that require the detailed separation of data. One illustrative example is the use of a SVM as a classification tool for identifying circulating tumour cells (CTCs) in the bloodstream. In one study, blood samples were collected from 41 healthy individuals and 41 patients with colorectal cancer, and CTCs were counted on the basis of the results obtained from FC. An SVM classifier based on the number of CTCs was developed and achieved an 82.3% accuracy [63]. It has been demonstrated that the application of this cytometric data in the context of SVM learning can facilitate the effective differentiation between healthy and cancerous blood samples. The high performance of this model suggests its potential future use as a non-invasive cancer screening tool. SVM models are also suitable for identifying the presence of rare cells in peripheral blood. In one study, an SVM model was developed to identify rare cell types in FC data and it demonstrated an accuracy of 69%, compared to traditional manual classification. This tool could be used in the future for more precise analysis of FC data, particularly in the identification of rare cell types, which may be important in both disease diagnosis and therapy monitoring [64].

Despite their benefits, SVMs have limitations, particularly with data imbalance. FC datasets often contain underrepresented cell types, leading SVMs to create hyperplanes biased towards majority types, which may not be optimal for less abundant cell types [65]. Cytometric data are typically multidimensional and complex, necessitating careful kernel selection and parameter tuning to optimize model performance. This process, though time-consuming, is crucial to prevent over- or under-fitting [66-69]. Additionally, SVMs' computational complexity in high-dimensional spaces can be a drawback, particularly in large cytometric datasets where rapid analysis is required [61, 70].

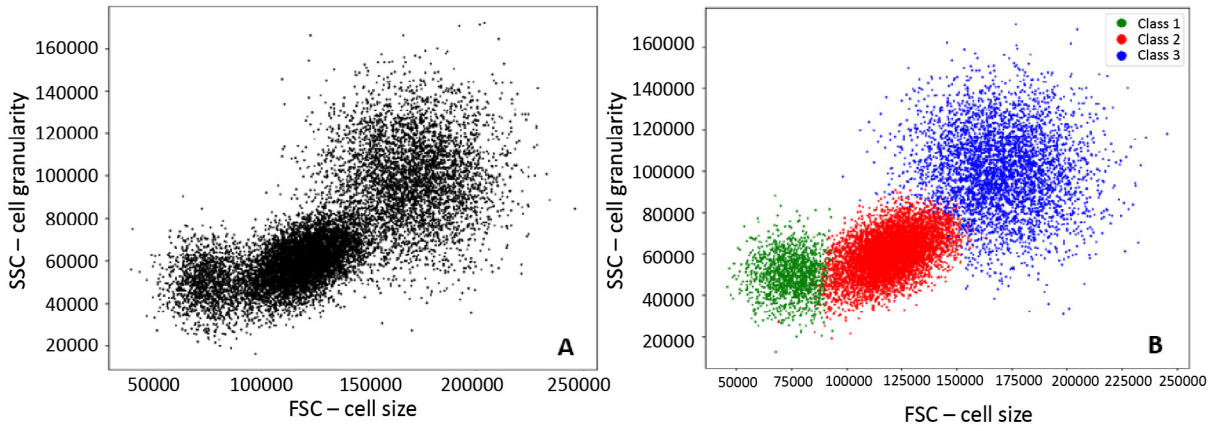

Figure 6. Visualisation of the implementation of Random Forests
A – before the application of Random Forests; B – effect of algorithm, classification into three groups

Deep learning

Although not new, deep learning has rapidly advanced due to increased computing power [71]. It is widely applied in medical fields, including immunology [72]. In simplified terms, neural networks learn through a two-stage process. First, the network receives a substantial amount of data, which it then uses to attempt to predict an outcome. Afterwards, it verifies the difference between the predicted outcome and the assumed outcome. This is an iterative process, in which the accuracy of the predictions is increased through the adjustment of weights. Each iteration results in a greater accuracy in the resulting predictions [73]. The actual learning process of neural networks is inherently complex, relying on several mathematical and statistical principles, which require deep understanding of linear algebra, calculus, probability and mathematical optimization. However it is possible to explain this process in much more simple terms by using one of the simplest models: a single-layer neural network.

To illustrate this, we can take the example of a manually curated FC dataset distinguishing healthy and cancerous cells. A single-layer neural network with an input layer and an output layer connected by randomly initialized weights is used. FC data, representing cell features, are entered, weighted, summed and passed through an activation function to capture patterns. The network predicts the cell's type, and the error between the prediction and the true class is calculated. Using backpropagation, weights are adjusted iteratively to minimize the error [74-76].

In FC, deep learning enhances diagnostic efficiency by reducing analysis time and improving feature extraction [54]. Recent advancements have broadened its applications, even in challenging areas [77]. For example, a deep learning model effectively detected rare tumor cell clusters in breast cancer biopsies, though it showed lower sensitivity, indicating the need for larger datasets [78]. Deep learning models have achieved high efficiency in acute myeloid leukemia (AML) diagnosis, distinguishing AML from acute lymphoblastic leukemia with near-perfect accuracy [79]. Neural networks have proven effective in analysing multi-parameter flow cytometry data, aiding in leukemic classification [80-81]. Automation of pattern detection through neural networks significantly improves the precise classification of leukemic subtypes.

Deep learning in FC relies heavily on large training datasets, which may be challenging to obtain in smaller cytometric studies [78, 82]. Training complex neural networks also demands advanced hardware [71]. An additional drawback is the so-called "black box problem" which refers to the difficulty in explaining how a neural network makes specific decisions and generates the final outcome of its predictions [83]. In the context of cytometric data analysis, it is often unclear which specific cellular characteristics influenced the model to make certain diagnostic decisions. Simpler machine learning algorithms might sometimes offer more efficient solutions in this context.

Dimensionality reduction

Dimensionality reduction is an important group of machine learning methods, particularly in data analysis with many variables. It is the process of simplifying a dataset by reducing the number of variables, while retaining as much relevant information as possible [84]. This is the biggest advantage of the method, as a large number of variables often leads to problems with model over-fitting, often referred to as the 'curse of dimensionality' [85-86]. The second advantage is data compression and faster calculations [86]. The most commonly used methods for dimensionality reduction are principal component analysis (PCA), independent component analysis (ICA), t-Distributed Stochastic Neighbour Embedding (t-SNE) and the previously mentioned UMAP [87-89]. For cytometric data, t-SNE algorithm is often used in commercial software.

t-SNE is a non-linear, unsupervised technique mainly used for the exploration and visualisation of multivariate data [90]. It is a stochastic method, ordering 'neighbours' while preserving local data structures and using the Student's t-distribution to model distances in low-dimensional space [91]. The algorithm allows separation of data that cannot be separated by a straight line, which is important for cytometric data.

It is a valuable tool in cell biology and immunological research, e.g. to profile cells of the immune system to understand their diversity, function and role in the immune response. The t-SNE algorithm has enabled the identification of subpopulations of normal and leukemic lyphocytec and the evaluation of their expression of immunosuppressive markers, clearly separating them from normal haematopoietic cells [92-93]. Combining t-SNE with unsupervised learning algorithms enables analysis of cytometric data to detect residual disease with high sensitivity [94]. The algorithm also supported the analysis of PBMC multicolour FC data, identifying rare subgroups of vaccine-induced T and B-cells [95].

Dimensionality reduction using t-SNE is effective in visualising immune cells and quantifying their frequencies, showing high agreement with conventional manual gating. However, it may not fully separate specific subsets of immune cells, leading to some discrepancies in the identification and quantification of these subpopulations, which is why the need to modify the algorithm in the analysis of cytometric data is highlighted, as standard parameter settings may lead to inaccurate or misleading cell maps [96-97]. The disadvantages of t-SNE are the high computational cost, difficult interpretation and need to set parameters that require tuning and experimentation.

Conclusions

Machine learning algorithms enable automated and precise data analysis, reducing errors due to subjectivity. However, we also face challenges. A key challenge is standardisation to ensure reproducibility and reliability. It is essential in laboratory diagnostics and biomedical sciences, as it enables comparison of results between laboratories and supports the introduction of modern techniques in routine diagnostics and clinical research. Without standardisation, it is difficult for these methods to be accepted in clinical practice. Other challenges include high computational costs, due to the fact that cytometric analyses involve multidimensional data of large size, requiring adequate memory resources and computing power. These costs can be reduced by optimising the performance of algorithms and using cloud-based solutions. As the computational complexity of the algorithms plays a key role here, a more practical selection of algorithms for specific cytometry applications also seems necessary.

Conflict of interest

None.

Funding

None.

References

1. Rieseberg M, Kasper C, Reardon KF, Scheper T. Flow cytometry in biotechnology. Appl Microbiol Biotechnol [Internet]. 2001;56(3):350–60. Available from: https://doi.org/10.1007/s002530100673
2. El-Hajjar L, Ali Ahmad F, Nasr R. A Guide to Flow Cytometry: Components, Basic Principles, Experimental Design, and Cancer Research Applications. Curr Protoc [Internet]. 2023 Mar 1;3(3):e721. Available from: https://doi.org/10.1002/cpz1.721
3. Sędek Ł, Sonsala A, Szczepański T, Mazur B. Techniczne aspekty cytometrii przepływowej [in Polish]. Diagnostyka Lab [Internet]. 2011;46(4):415–20. Available from: https://diagnostykalaboratoryjna.eu/article/59484/pl
4. Skotny A, Pucińska J. Współczesna cystometria przepływowa [in Polish]. Acta Bio-Optica Inform Medica Inżynieria Biomed [Internet]. 2013;19(1):3–11. Available from: https://www.infona.pl/resource/bwmeta1.element.baztech-8a4c262e-3ba3-45d7-aba4-352e2eaa05a8?&locale=pl
5. Sedek L, Mazur B. Przeciwciala monoklonalne i poliklonalne i ich zastosowanie w cytometrii przeplywowej [in Polish}. Postępy Biol Komórki Supl [Internet]. 2008;(24):17–34. Available from: https://agro.icm.edu.pl/agro/element/bwmeta1.element.agro-article-bc87278d-3186-4efe-ac85-f064303a1d3b
6. Adan A, Alizada G, Kiraz Y, Baran Y, Nalbant A. Flow cytometry: basic principles and applications. Crit Rev Biotechnol [Internet]. 2017;37(2):163–76. Available from: https://doi.org/10.3109/07388551.2015.1128876
7. Kaczmarek A, Mackiewicz A, Leporowska E, Osawa T. The role of flow cytometry in clinical diagnosis. Contemp Oncol Onkol [Internet]. 2002;6(6):366–73. Available from: https://www.termedia.pl/The-role-of-flow-cytometry-in-clinical-diagnosis,3,80,1,1.html
8. Gunasekera TS, Attfield PV, Veal DA. A Flow Cytometry Method for Rapid Detection and Enumeration of Total Bacteria in Milk. Appl Environ Microbiol [Internet]. 2000 Mar 1;66(3):1228–32. Available from: https://doi.org/10.1128/AEM.66.3.1228-1232.2000
9. Brestoff JR, Frater JL. Contemporary Challenges in Clinical Flow Cytometry: Small Samples, Big Data, Little Time. J Appl Lab Med [Internet]. 2022 Jul 1;7(4):931–44. Available from: https://doi.org/10.1093/jalm/jfab176
10. Bashashati A, Brinkman RR. A Survey of Flow Cytometry Data Analysis Methods. Adv Bioinformatics [Internet]. 2009 Dec 6;2009:1–19. Available from: https://www.hindawi.com/journals/abi/2009/584603/
11. Montante S, Brinkman RR. Flow cytometry data analysis: Recent tools and algorithms. Int J Lab Hematol [Internet]. 2019 May 8;41(S1):56–62. Available from: https://onlinelibrary.wiley.com/doi/10.1111/ijlh.13016
12. Tung JW, Heydari K, Tirouvanziam R, Sahaf B, Parks DR, Herzenberg LA, et al. Modern Flow Cytometry: A Practical Approach. Clin Lab Med [Internet]. 2007;27(3):453–68. Available from: https://www.sciencedirect.com/science/article/pii/S0272271207000467
13. Caligola S, Giacobazzi L, Canè S, Vella A, Adamo A, Ugel S, et al. GateMeClass: Gate Mining and Classification of cytometry data. Elofsson A, editor. Bioinformatics [Internet]. 2024 May 2;40(5). Available from: https://academic.oup.com/bioinformatics/article/doi/10.1093/bioinformatics/btae322/7679648

14. Jain AK, Murty MN, Flynn PJ. Data clustering. ACM Comput Surv [Internet]. 1999 Sep;31(3):264–323. Available from: https://dl.acm.org/doi/10.1145/331499.331504
15. Aghaeepour N, Nikolic R, Hoos HH, Brinkman RR. Rapid cell population identification in flow cytometry data. Cytom Part A [Internet]. 2011 Jan 22;79A(1):6–13. Available from: https://onlinelibrary.wiley.com/doi/10.1002/cyto.a.21007
16. Jain AK. Data clustering: 50 years beyond K-means. Pattern Recognit Lett [Internet]. 2010;31(8):651–66. Available from: https://www.sciencedirect.com/science/article/pii/S0167865509002323
17. Hearty J. Advanced Machine Learning with Python [Internet]. Packt Publishing; 2016. Available from: https://books.google.pl/books?id=sc2qDQAAQBAJ
18. Pelleg D. Extending K-means with efficient estimation of the number of clusters in ICML. In: Proceedings of the 17th international conference on machine learning. 2000. p. 277–81.
19. Tian X, Xu D, Guo L, Wu D. An Improved Bregman k-means++ Algorithm via Local Search BT - Computing and Combinatorics. In: Kim D, Uma RN, Cai Z, Lee DH, editors. Cham: Springer International Publishing; 2020. p. 532–41.
20. Hicks SC, Liu R, Ni Y, Purdom E, Risso D. mbkmeans: Fast clustering for single cell data using mini-batch k-means. Schneidman-Duhovny D, editor. PLOS Comput Biol [Internet]. 2021 Jan 26;17(1):e1008625. Available from: https://dx.plos.org/10.1371/journal.pcbi.1008625
21. Piao Tan M, A. Floudas C. Determining the Optimal Number of Clusters. In: Encyclopedia of Optimization [Internet]. Boston, MA: Springer US; 2008. p. 687–94. Available from: https://link.springer.com/10.1007/978-0-387-74759-0_123
22. Preglej T, Brinkmann M, Steiner G, Aletaha D, Göschl L, Bonelli M. Advanced immunophenotyping: A powerful tool for immune profiling, drug screening, and a personalized treatment approach. Front Immunol [Internet]. 2023 Mar 24;14. Available from: https://www.frontiersin.org/articles/10.3389/fimmu.2023.1096096/full
23. Finak G, Bashashati A, Brinkman R, Gottardo R. Merging Mixture Components for Cell Population Identification in Flow Cytometry. Adv Bioinformatics [Internet]. 2009 Nov 12;2009:1–12. Available from: https://www.hindawi.com/journals/abi/2009/247646/
24. Cheung M, Campbell JJ, Thomas RJ, Braybrook J, Petzing J. Assessment of Automated Flow Cytometry Data Analysis Tools within Cell and Gene Therapy Manufacturing. Int J Mol Sci [Internet]. 2022 Mar 17;23(6):3224. Available from: https://www.mdpi.com/1422-0067/23/6/3224
25. Cheung M, Campbell JJ, Whitby L, Thomas RJ, Braybrook J, Petzing J. Current trends in flow cytometry automated data analysis software. Cytom Part A [Internet]. 2021 Oct 19;99(10):1007–21. Available from: https://onlinelibrary.wiley.com/doi/10.1002/cyto.a.24320
26. Ram A, Jalal S, Jalal AS, Kumar M. A density based algorithm for discovering density varied clusters in large spatial databases. Int J Comput Appl [Internet]. 2010;3(6):1–4. Available from: https://www.researchgate.net/profile/Anant-Ram/publication/282334683_A_Density_based_Algorithm_for_Discovering_Density_Varied_Clusters_in_Large_Spatial_Databases/links/560d049d08aed543358d5e32/A-Density-based-Algorithm-for-Discovering-Density-Varied-Clust
27. Campello RJGB, Moulavi D, Sander J. Density-Based Clustering Based on Hierarchical Density Estimates. In 2013. p. 160–72. Available from: http://link.springer.com/10.1007/978-3-642-37456-2_14
28. Anibal J, Day AG, Bahadiroglu E, O'Neil L, Phan L, Peltekian A, et al. HAL-X: Scalable hierarchical clustering for rapid and tunable single-cell analysis. Faeder JR, editor. PLOS Comput Biol [Internet]. 2022 Oct 3;18(10):e1010349. Available from: https://dx.plos.org/10.1371/journal.pcbi.1010349
29. Campello RJGB, Moulavi D, Zimek A, Sander J. Hierarchical Density Estimates for Data Clustering, Visualization, and Outlier Detection. ACM Trans Knowl Discov Data [Internet]. 2015 Jul 27;10(1):1–51. Available from: https://dl.acm.org/doi/10.1145/2733381
30. Stewart G, Al-Khassaweneh M. An Implementation of the HDBSCAN* Clustering Algorithm. Appl Sci [Internet]. 2022 Feb 25;12(5):2405. Available from: https://www.mdpi.com/2076-3417/12/5/2405
31. González-Alemán R, Platero-Rochart D, Rodríguez-Serradet A, Hernández-Rodríguez EW, Caballero J, Leclerc F, et al. MD-SCAN: RMSD-based HDBSCAN clustering of long molecular dynamics. Martelli PL, editor. Bioinformatics [Internet]. 2022 Nov 30;38(23):5191–8. Available from: https://academic.oup.com/bioinformatics/article/38/23/5191/6751777
32. Malzer C, Baum M. A Hybrid Approach To Hierarchical Density-based Cluster Selection. In: 2020 IEEE International Conference on Multisensor Fusion and Integration for Intelligent Systems (MFI) [Internet]. IEEE; 2020. p. 223–8. Available from: https://ieeexplore.ieee.org/document/9235263/
33. Weijler L, Kowarsch F, Wödlinger M, Reiter M, Maurer-Granofszky M, Schumich A, et al. UMAP Based Anomaly Detection for Minimal Residual Disease Quantification within Acute Myeloid Leukemia. Cancers (Basel) [Internet]. 2022 Feb 11;14(4):898. Available from: https://www.mdpi.com/2072-6694/14/4/898

34. Dhyani V, Chann AS, Giri L, Russell SM, Charnley M. A Pipeline for Dynamic Analysis of Mitochondrial Content in Developing T Cells: Bridging the Gap Between High-Throughput Flow Cytometry and Single-Cell Microscopy Analysis. In 2024. p. 167–87. Available from: https://link.springer.com/10.1007/978-1-0716-3834-7_12
35. Ye X, Ho JWK. Ultrafast clustering of single-cell flow cytometry data using FlowGrid. BMC Syst Biol [Internet]. 2019 Apr 5;13(S2):35. Available from: https://bmcsystbiol.biomedcentral.com/articles/10.1186/s12918-019-0690-2
36. Blekas K, Likas A, Galatsanos NP, Lagaris IE. A Spatially Constrained Mixture Model for Image Segmentation. IEEE Trans Neural Networks [Internet]. 2005 Mar;16(2):494–8. Available from: http://ieeexplore.ieee.org/document/1402510/
37. Reynolds D. Gaussian Mixture Models. In: Encyclopedia of Biometrics [Internet]. Boston, MA: Springer US; 2009. p. 659–63. Available from: http://link.springer.com/10.1007/978-0-387-73003-5_196
38. Pyne S, Hu X, Wang K, Rossin E, Lin T-I, Maier LM, et al. Automated high-dimensional flow cytometric data analysis. Proc Natl Acad Sci [Internet]. 2009 May 26;106(21):8519–24. Available from: https://pnas.org/doi/full/10.1073/pnas.0903028106
39. McLachlan GJ, Ng SK, Peel D. On Clustering by Mixture Models. In: Schwaiger M, Opitz O, editors. Exploratory Data Analysis in Empirical Research Studies in Classification, Data Analysis, and Knowledge Organization [Internet]. Springer, Berlin, Heidelberg; 2003. p. 141–8. Available from: http://link.springer.com/10.1007/978-3-642-55721-7_16
40. Dang UJ, Gallaugher MPB, Browne RP, McNicholas PD. Model-Based Clustering and Classification Using Mixtures of Multivariate Skewed Power Exponential Distributions. J Classif [Internet]. 2023;40(1):145–67. Available from: https://doi.org/10.1007/s00357-022-09427-7
41. Zioulis N, Alexiadis D, Doumanoglou A, Louizis G, Apostolakis K, Zarpalas D, et al. 3D tele-immersion platform for interactive immersive experiences between remote users. In: 2016 IEEE International Conference on Image Processing (ICIP) [Internet]. IEEE; 2016. p. 365–9. Available from: http://ieeexplore.ieee.org/document/7532380/
42. Sun P, Lyu X, Li X, Wang B, Yi X, Tang Z. Understanding Markush Structures in Chemistry Documents With Deep Learning. In: 2018 IEEE International Conference on Bioinformatics and Biomedicine (BIBM) [Internet]. IEEE; 2018. p. 1126–9. Available from: https://ieeexplore.ieee.org/document/8621264/
43. Rajwa B, Wallace PK, Griffiths EA, Dundar M. Automated Assessment of Disease Progression in Acute Myeloid Leukemia by Probabilistic Analysis of Flow Cytometry Data. IEEE Trans Biomed Eng. 2017;64(5):1089–98.
44. Reiter M, Rota P, Kleber F, Diem M, Groeneveld-Krentz S, Dworzak M. Clustering of cell populations in flow cytometry data using a combination of Gaussian mixtures. Pattern Recognit [Internet]. 2016 Dec;60:1029–40. Available from: https://linkinghub.elsevier.com/retrieve/pii/S0031320316300371
45. Yerebakan HZ, Rajwa B, Dundar M. The infinite mixture of infinite Gaussian mixtures. In: Advances in neural information processing systems. 2014.
46. Breiman L. Random Forests. Mach Learn [Internet]. 2001;45(1):5–32. Available from: https://doi.org/10.1023/A:1010933404324
47. Song Y-Y, Lu Y. Decision tree methods: applications for classification and prediction. Shanghai Arch psychiatry [Internet]. 2015 Apr 25;27(2):130–5. Available from: http://www.ncbi.nlm.nih.gov/pubmed/26120265
48. Burges CJC. A Tutorial on Support Vector Machines for Pattern Recognition. Data Min Knowl Discov [Internet]. 1998;2(2):121–67. Available from: https://doi.org/10.1023/A:1009715923555
49. Khare S, Gourisaria MK, Harshvardhan G, Joardar S, Singh V. Real Estate Cost Estimation Through Data Mining Techniques. IOP Conf Ser Mater Sci Eng [Internet]. 2021 Mar 1;1099(1):012053. Available from: https://iopscience.iop.org/article/10.1088/1757-899X/1099/1/012053
50. Breiman L. Bagging predictors. Mach Learn [Internet]. 1996;24(2):123–40. Available from: https://doi.org/10.1007/BF00058655
51. Zamahsyari, Nurwidyantoro A. Sentiment analysis of economic news in Bahasa Indonesia using majority vote classifier. In: 2016 International Conference on Data and Software Engineering (ICoDSE). 2016. p. 1–6.
52. Daho MEH, Settouti N, Lazouni MEA, Chikh MEA. Weighted vote for trees aggregation in Random Forest. In: 2014 International Conference on Multimedia Computing and Systems (ICMCS). 2014. p. 438–43.
53. Salam MA, Taher A, Samy M, Mohamed K. The Effect of Different Dimensionality Reduction Techniques on Machine Learning Overfitting Problem. Int J Adv Comput Sci Appl [Internet]. 2021;12(4). Available from: http://thesai.org/Publications/ViewPaper?Volume=12&Issue=4&Code=IJACSA&SerialNo=80
54. Palit S, Heuser C, de Almeida GP, Theis FJ, Zielinski CE. Meeting the Challenges of High-Dimensional Single-Cell Data Analysis in Immunology. Front Immunol [Internet]. 2019 Jul 3;10. Available from: https://www.frontiersin.org/article/10.3389/fimmu.2019.01515/full

55. Duetz C, Van Gassen S, Westers TM, van Spronsen MF, Bachas C, Saeys Y, et al. Computational flow cytometry as a diagnostic tool in suspected-myelodysplastic syndromes. Cytom Part A [Internet]. 2021 Aug 12;99(8):814–24. Available from: https://onlinelibrary.wiley.com/doi/10.1002/cyto.a.24360
56. Dietterich T. Overfitting and undercomputing in machine learning. ACM Comput Surv [Internet]. 1995 Sep;27(3):326–7. Available from: https://dl.acm.org/doi/10.1145/212094.212114
57. Boin F, Giardino Torchia ML, Borrello I, Noonan KA, Neil M, Soloski MJ, et al. Flow cytometric discrimination of seven lineage markers by using two fluorochromes. Björkström NK, editor. PLoS One [Internet]. 2017 Nov 30;12(11):e0188916. Available from: https://dx.plos.org/10.1371/journal.pone.0188916
58. Bolón-Canedo V, Morán-Fernández L, Cancela B, Alonso-Betanzos A. A review of green artificial intelligence: Towards a more sustainable future. Neurocomputing [Internet]. 2024;599:128096. Available from: https://www.sciencedirect.com/science/article/pii/S0925231224008671
59. Mazza EMC, Brummelman J, Alvisi G, Roberto A, De Paoli F, Zanon V, et al. Background fluorescence and spreading error are major contributors of variability in high-dimensional flow cytometry data visualization by t-distributed stochastic neighboring embedding. Cytom Part A [Internet]. 2018 Aug 14;93(8):785–92. Available from: https://onlinelibrary.wiley.com/doi/10.1002/cyto.a.23566
60. Browning AP, Ansari N, Drovandi C, Johnston APR, Simpson MJ, Jenner AL. Identifying cell-to-cell variability in internalization using flow cytometry. J R Soc Interface [Internet]. 2022 May 25;19(190). Available from: https://royalsocietypublishing.org/doi/10.1098/rsif.2022.0019
61. Awad M, Khanna R. Support Vector Machines for Classification. In: Efficient Learning Machines [Internet]. Berkeley, CA: Apress; 2015. p. 39–66. Available from: http://link.springer.com/10.1007/978-1-4302-5990-9_3
62. Noble WS. What is a support vector machine? Nat Biotechnol [Internet]. 2006 Dec;24(12):1565–7. Available from: https://www.nature.com/articles/nbt1206-1565
63. Hatzidaki E, Iliopoulos A, Papasotiriou I. A Novel Method for Colorectal Cancer Screening Based on Circulating Tumor Cells and Machine Learning. Entropy (Basel) [Internet]. 2021 Sep 25;23(10). Available from: http://www.ncbi.nlm.nih.gov/pubmed/34681972
64. Special Issue Title Page. Cytom Part A [Internet]. 2015 Jun 28;87(6). Available from: https://onlinelibrary.wiley.com/doi/10.1002/cyto.a.22695
65. Mair F, Hartmann FJ, Mrdjen D, Tosevski V, Krieg C, Becher B. The end of gating? An introduction to automated analysis of high dimensional cytometry data. Eur J Immunol [Internet]. 2016 Jan 30;46(1):34–43. Available from: https://onlinelibrary.wiley.com/doi/10.1002/eji.201545774
66. Núñez H, Gonzalez-Abril L, Angulo C. Improving SVM Classification on Imbalanced Datasets by Introducing a New Bias. J Classif [Internet]. 2017 Oct 14;34(3):427–43. Available from: http://link.springer.com/10.1007/s00357-017-9242-x
67. Huang Y, Zhao H, Shao M, Zhou L, Li X, Wei G, et al. Predictive value of next-generation sequencing-based minimal residual disease after CAR-T cell therapy. Bone Marrow Transplant [Internet]. 2022 Aug 1;57(8):1350–3. Available from: https://www.nature.com/articles/s41409-022-01699-2
68. Chakraborty R, Al Hadidi S, Scheffer Cliff ER, Mohyuddin GR. Is aggressive treatment of smoldering myeloma the path to curing myeloma? Blood Adv [Internet]. 2023 Aug 8;7(15):3932–5. Available from: https://ashpublications.org/bloodadvances/article/7/15/3932/495857/Is-aggressive-treatment-of-smoldering-myeloma-the
69. Biehl M, Bunte K, Schneider P. Analysis of Flow Cytometry Data by Matrix Relevance Learning Vector Quantization. Ma'ayan A, editor. PLoS One [Internet]. 2013 Mar 18;8(3):e59401. Available from: https://dx.plos.org/10.1371/journal.pone.0059401
70. Aghaeepour N, Finak G, Hoos H, Mosmann TR, Brinkman R, Gottardo R, et al. Critical assessment of automated flow cytometry data analysis techniques. Nat Methods [Internet]. 2013 Mar 10;10(3):228–38. Available from: https://www.nature.com/articles/nmeth.2365
71. Thompson NC, Greenewald K, Lee K, Manso GF. The computational limits of deep learning. arXiv Prepr arXiv200705558 [Internet]. 2020;10. Available from: http://arxiv.org/abs/2007.05558
72. Matsuda A, Imada K, Obara N, Iida H, Yamazaki H, Tomiyama Y, et al. Dysmegakaryopoiesis and Transient Mild Increase in Bone Marrow Blasts in Patients With Aplastic Anemia Treated With Eltrombopag May Be Signs of Hematologic Improvement and Not Portend Clonal Evolution. Am J Clin Pathol [Internet]. 2022 Nov 3;158(5):604–15. Available from: https://academic.oup.com/ajcp/article/158/5/604/6677142
73. Grossi E, Buscema M. Introduction to artificial neural networks. Eur J Gastroenterol Hepatol [Internet]. 2007 Dec;19(12):1046–54. Available from: http://journals.lww.com/00042737-200712000-00005

74. Feng Y, Cheng Z, Chai H, He W, Huang L, Wang W. Neural network-enhanced real-time impedance flow cytometry for single--cell intrinsic characterization. Lab Chip [Internet]. 2022;22(2):240–9. Available from: https://xlink.rsc.org/?DOI=D1LC00755F
75. Fisch L, Heming M, Schulte-Mecklenbeck A, Gross CC, Zumdick S, Barkhau C, et al. GateNet: A novel neural network architecture for automated flow cytometry gating. Comput Biol Med [Internet]. 2024 Sep;179:108820. Available from: https://linkinghub.elsevier.com/retrieve/pii/S0010482524009053
76. Bini L, Mojarrad FN, Liarou M, Matthes T, Marchand-Maillet S. FlowCyt: A Comparative Study of Deep Learning Approaches for Multi-Class Classification in Flow Cytometry Benchmarking. arXiv Prepr arXiv240300024 [Internet]. 2024; Available from: https://doi.org/10.48550/arXiv.2403.00024
77. Sun C, Shrivastava A, Singh S, Gupta A. Revisiting unreasonable effectiveness of data in deep learning era. In: Proceedings of the IEEE international conference on computer vision [Internet]. 2017. p. 843–52. Available from: https://openaccess.thecvf.com/content_iccv_2017/html/Sun_Revisiting_Unreasonable_Effectiveness_ICCV_2017_paper.html
78. Vora N, Shekar P, Esmail M, Patra A, Georgakoudi I. Deep Learning-Enabled, Detection of Rare Circulating Tumor Cell Clusters in Whole Blood Using Label-free, Flow Cytometry [Internet]. 2023. Available from: http://biorxiv.org/lookup/doi/10.1101/2023.08.01.551485
79. Lewis JE, Cooper LAD, Jaye DL, Pozdnyakova O. Automated Deep Learning-Based Diagnosis and Molecular Characterization of Acute Myeloid Leukemia Using Flow Cytometry. Mod Pathol [Internet]. 2024;37(1):100373. Available from: https://www.sciencedirect.com/science/article/pii/S0893395223002788
80. Kothari R, Cualing H, Balachander T. Neural network analysis of flow cytometry immunophenotype data. IEEE Trans Biomed Eng [Internet]. 1996;43(8):803–10. Available from: http://ieeexplore.ieee.org/document/508551/
81. Magallon RE, Harmacek LD, Arger NK, Grewal P, Powers L, Werner BR, et al. Standardization of flow cytometry and cell sorting to enable a transcriptomic analysis in a multi-site sarcoidosis study. Chitta S, editor. PLoS One [Internet]. 2023 Mar 9;18(3):e0281210. Available from: https://dx.plos.org/10.1371/journal.pone.0281210
82. Sarker IH. Deep Learning: A Comprehensive Overview on Techniques, Taxonomy, Applications and Research Directions. SN Comput Sci [Internet]. 2021 Nov 18;2(6):420. Available from: https://link.springer.com/10.1007/s42979-021-00815-1
83. Hassija V, Chamola V, Mahapatra A, Singal A, Goel D, Huang K, et al. Interpreting Black-Box Models: A Review on Explainable Artificial Intelligence. Cognit Comput [Internet]. 2024 Jan 24;16(1):45–74. Available from: https://link.springer.com/10.1007/s12559-023-10179-8
84. Goldenberg A. A Survey of Statistical Network Models. Found Trends® Mach Learn [Internet]. 2009;2(2):129–233. Available from: http://www.nowpublishers.com/article/Details/MAL-005
85. Verleysen M, François D. The Curse of Dimensionality in Data Mining and Time Series Prediction. In: Cabestany J, Prieto A, Sandoval F, editors. Computational Intelligence and Bioinspired Systems [Internet]. Berlin, Heidelberg; 2005. p. 758–70. Available from: http://link.springer.com/10.1007/11494669_93
86. Hastie T, Tibshirani R, Friedman J. High-Dimensional Problems: p N. In 2009. p. 649–98. Available from: http://link.springer.com/10.1007/978-0-387-84858-7_18
87. Jolliffe IT. Principal component analysis for special types of data [Internet]. New York: Springer; 2002. Available from: https://link.springer.com/content/pdf/10.1007/0-387-22440-8_13.pdf
88. Hyvärinen A, Hurri J, Hoyer PO. Independent Component Analysis. In Springer; 2009. p. 151–75. Available from: http://link.springer.com/10.1007/978-1-84882-491-1_7
89. McInnes L, Healy J, Saul N, Großberger L. UMAP: Uniform Manifold Approximation and Projection. J Open Source Softw [Internet]. 2018 Sep 2;3(29):861. Available from: http://joss.theoj.org/papers/10.21105/joss.00861
90. Van der Maaten L, Hinton G. Visualizing data using t-SNE. J Mach Learn Res [Internet]. 2008;9(11). Available from: http://www.jmlr.org/papers/volume9/vandermaaten08a/vandermaaten08a.pdf
91. Hinton GE, Salakhutdinov RR. Reducing the Dimensionality of Data with Neural Networks. Science (80-) [Internet]. 2006 Jul 28;313(5786):504–7. Available from: https://www.science.org/doi/10.1126/science.1127647
92. Retraction: Regulation of Tumor Cell Sensitivity to TRAIL-Induced Apoptosis by the Metastatic Suppressor Raf Kinase Inhibitor Protein via Yin Yang 1 Inhibition and Death Receptor 5 Up-Regulation. J Immunol [Internet]. 2016 Dec 15;197(12):4859–4859. Available from: https://journals.aai.org/jimmunol/article/197/12/4859/109147/Retraction-Regulation-of-Tumor-Cell-Sensitivity-to
93. Nollmann C, Moskorz W, Wimmenauer C, Jäger PS, Cadeddu RP, Timm J, et al. Characterization of CD34+ Cells from Patients with Acute Myeloid Leukemia (AML) and Myelodysplastic Syndromes (MDS) Using a t-Distributed Stochastic Neighbor Embedding (t-SNE) Protocol. Cancers (Basel) [Internet]. 2024 Mar 28;16(7):1320. Available from: https://www.mdpi.com/2072-6694/16/7/1320

94. Matthes T. Phenotypic Analysis of Hematopoietic Stem and Progenitor Cell Populations in Acute Myeloid Leukemia Based on Spectral Flow Cytometry, a 20-Color Panel, and Unsupervised Learning Algorithms. Int J Mol Sci [Internet]. 2024 Feb 29;25(5):2847. Available from: https://www.mdpi.com/1422-0067/25/5/2847
95. Cole ME, Guo Y, Cheeseman HM, Pollock KM. Multicolor Flow Cytometry and High-Dimensional Data Analysis to Probe Complex Questions in Vaccinology. In 2022. p. 433–47. Available from: https://link.springer.com/10.1007/978-1-0716-1900-1_23
96. Toghi Eshghi S, Au-Yeung A, Takahashi C, Bolen CR, Nyachienga MN, Lear SP, et al. Quantitative Comparison of Conventional and t-SNE-guided Gating Analyses. Front Immunol [Internet]. 2019 Jun 5;10. Available from: https://www.frontiersin.org/article/10.3389/fimmu.2019.01194/full
97. Belkina AC, Ciccolella CO, Anno R, Halpert R, Spidlen J, Snyder-Cappione JE. Automated optimized parameters for T-distributed stochastic neighbor embedding improve visualization and analysis of large datasets. Nat Commun [Internet]. 2019 Nov 28;10(1):5415. Available from: https://www.nature.com/articles/s41467-019-13055-y

EUROPEAN JOURNAL OF TRANSLATIONAL
AND CLINICAL MEDICINE 2025;8(1):97-102

REVIEW ARTICLE

The role of the Notch signaling pathway in rhabdomyosarcomas

Datis Kalali[1], Emilija Milošević[2], Doxakis Anestakis[1,3]

[1] Medical School, University of Cyprus, Nicosia, Cyprus
[2] Institute of Molecular Genetics and Genetic Engineering, University of Belgrade, Belgrade, Serbia
[3] Laboratory of Autopsy Pathology, Forensic Service of Thessaloniki, Ministry of Justice, Thessaloniki, Greece

Abstract:
Rhabdomyosarcoma (RMS) is a pediatric soft tissue cancer with poor prognosis in cases of metastasis. Different signal transduction pathways have been studied in RMS cells as to shed some light into the tumorigenesis and metastasis mechanisms of this cancer in the search for new diagnostic and therapeutic strategies. The Notch pathway, which regulates cell survival, is widely studied in different cancers, including sarcomas and its activation has been known to induce cell motility. To this end, the present review explores the role of the Notch signaling pathway in the progression of RMS and in potential therapeutic strategies.

Keywords: rhabdomyosarcoma • pediatric sarcomas • Notch signaling • signal transduction pathways

Citation

Kalali D, Milošević E, Anestakis D. The role of the Notch signaling pathway in rhabdomyosarcomas. Eur J Transl Clin Med. 2025;8(1):97-102.

DOI: 10.31373/ejtcm/202612

Introduction

Rhabdomyosarcoma (RMS) is the most frequent type of pediatric soft tissue cancer in the global population, accounting for approximately 7% of malignancies in patients under 15 years of age [1]. Although the survival rates of patients have improved considerably over the past years due to advances in therapeutic strategies, RMS is an aggressive tumor with poor prognosis in case of metastasis [2-3]. RMS is histologically divided into two main subtypes: alveolar and embryonal. Although these subtypes differ anatomically and in terms of the clinical picture, they share many common molecular characteristics [4].

Different signaling pathways have been studied in all types of RMS cells, with the hope of shedding some light on the process of oncogenesis and finding potential novel therapeutic targets [5-6]. The so-called 'pathways of embryonic development' (e.g. the Notch, Hippo, Wnt and Hedgehog pathways) are widely studied in malignant neoplasms and are viewed as potential targets in anticancer therapy [7]. The Notch pathway can result in both cell survival and death, thus it is one of the key pathways in tumorigenesis

Corresponding author:
Datis Kalali, Medical School, University of Cyprus, Nicosia, Cyprus
e-mail: kalali.datis@ucy.ac.cy
Available online: ejtcm.gumed.edu.pl

and tumor progression and is interlinked with various other tumorigenic signal transduction pathways [8-9]. It is triggered by the activation of the Notch transmembrane receptors, namely the Notch1, Notch2, Notch3 and Notch4 proteins encoded by four distinct genes. The binding of Notch proteins with transmembrane Delta and Jagged proteins expressed on adjacent cells, activates the signal transduction pathway [10]. The pathway results in the cleavage and activation of the Notch intracellular domain (NotchIC) with the assistance of gamma-secretase. Subsequently, the NotchIC domain enters the nucleus and induces the expression of different pro-proliferative and anti-apoptotic genes through the RBP-J (recombination signal binding protein for immunoglobulin kappa J region) [10-11].

The evidence on the role of the Notch pathway in RMS cells is scattered in different sources. In this narrative review we aimed to explore in depth the role of this pathway in the tumorigenesis and metastasis of RMS and insights into targeting its proteins as possible therapeutic strategies.

Material and methods

A systematic search was performed in the online databases of PubMed, Scopus, and EMBASE to retrieve all available literature on the role of the Notch pathway in RMS, published from inception till July 2024. A combination of the keywords “Notch”, “Embryonic signaling pathways”, “Rhabdomyosarcoma” and “RMS” were used in combination with the Boolean operators “OR” and “AND.” Due to the narrative nature of the review, there were no specific inclusion and exclusion criteria or screening protocol. Overall, all relevant original research and review articles, written in English were included in our review (total of 11 articles).

Results and discussion

The Notch pathway and oncogenesis of RMS

Recently, various studies have found that the Notch pathway plays a significant role in the tumorigenesis of RMS. Specifically, the Notch pathway has been found to induce overexpression of the transcription factor HES1 (hairy and enhancer of split-1) in RMS cell lines and consequently, promote cell proliferation and inhibit apoptotic pathways [12-13]. Simultaneously, studies have shown that RMS cells tend to express the Notch1 and Notch3 receptors at higher levels compared to healthy muscle cells and that the induction of their respective pathways amplifies the proliferation ability of these cells [14]. Moreover, RMS cells have been found to overexpress RBP-J and therefore activate the p38 MAPKS and MMK3 genes that support malignant proliferation through the Notch pathway [15]. The Notch pathway is also known to activate muscle satellite cells (SMCs) and thus amplify myoblast formation in infants [16]. In this manner, the Notch pathway activation can induce myoblast-like properties in RMS cells. It is also worth mentioning that SMCs are known to trigger the upregulation of MMPs and at the same time, MMPs are necessary for the regulation and proliferation of SMCs [17].

The Notch pathway and metastatic potential of RMS

The activation of the Notch pathway has been found to enhance the metastatic potential of RMS cells. More specifically, Roma et al. showed that the Notch receptor and the transcription factor HEY 1 (hairy/enhancer-of-split related with YRPW motif protein 1) are overexpressed in RMS patients and that the Notch pathway inhibition decreases invasiveness and motility of RMS cells [18]. Furthermore, the induction of the Notch pathway, triggered by the Notch1 receptor has been found to increase the invasiveness of RMS cells through the induction of the N-cadherin and alpha-integrin proteins [19]. It is also worth noting that the Notch pathway is generally known to induce the expression of matrix metalloproteinases in the microenvironment of different tumors including sarcomas. The aforementioned enzymes can assist the process of metastasis by degrading components of the extracellular matrix [20-22]. Overall, by regulating the expression of different proteins and enzymes, the Notch pathway assists RMS cells to overcome barriers of their progression and in turn migrate to other sites. Figure 1 summarizes the pathways through which Notch signaling can contribute to the progression and metastasis of RMS.

The Notch pathway as a potential therapeutic target in RMS

Due to the role of Notch signaling in the proliferation and motility of RMS cells, different studies have been conducted to investigate the effect of inhibiting the aforementioned pathway as a way of controlling

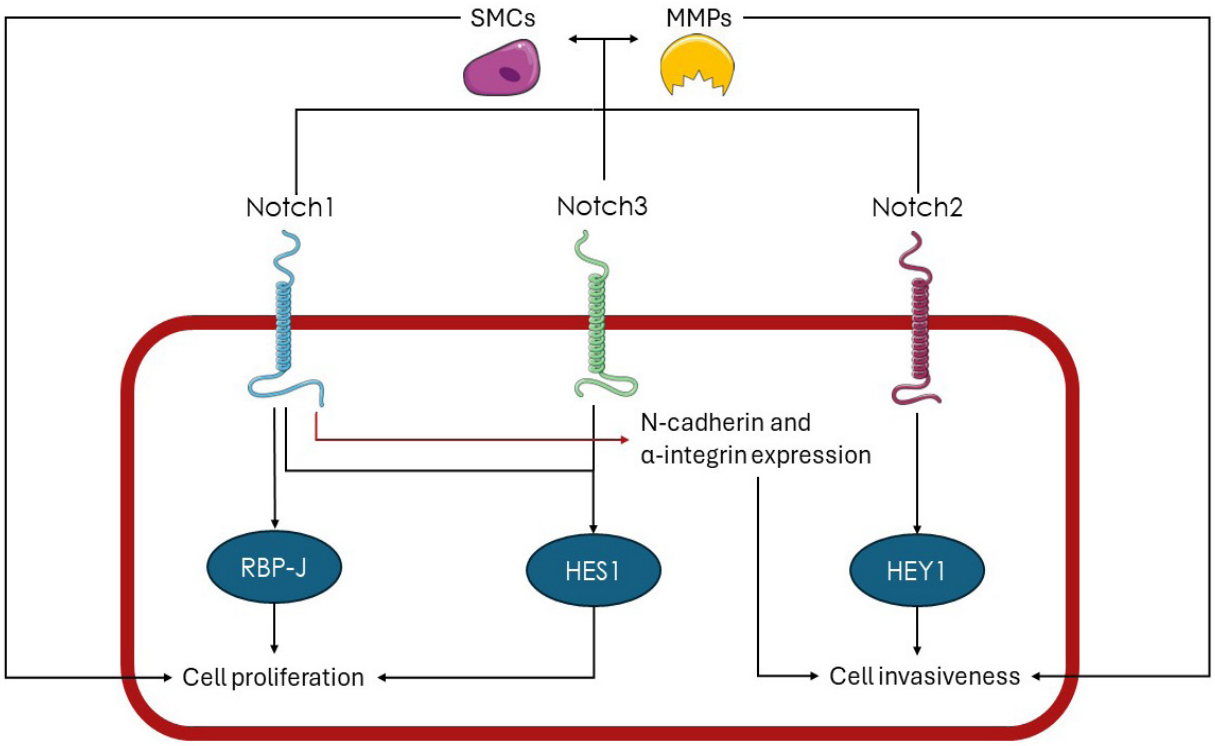

Figure 1. Notch signaling in RMS
HES1 – hairy and enhancer of split-1, HEY1 – hairy/enhancer-of-split related with YRPW motif protein 1, MMPs – matrix metalloproteinases, RBP-J – recombination signal binding protein for immunoglobulin kappa J region, SMCs – satellite muscle cells

the disease. Nagao et al. showed that the knockdown of RBP-J by RNA interference significantly reduced the growth of RMS cells and induced cell cycle arrest, indicating that the inhibition of the Notch pathway through silencing RBP-J can be a potential therapeutic strategy for RMS [15]. Moreover, inhibition of Notch3 signaling using an inhibitor of gamma-secretase has been shown to amplify p21 expression and induce p38 phosphorylation, hence inhibiting cell proliferation and activating apoptotic pathways in RMS cells [12]. Likewise, the use of gamma-secretase inhibitors alongside Notch1 silencing through RNA interference has been shown to exert antiproliferative effects on RMS cells and at the same time, downregulate HEY1 expression, hence decreasing invasiveness in vitro and in vivo [23]. It has been shown that inhibiting the hepatocyte growth factor receptor (HGF receptor), can make RMS cells respond more sensitively to gamma-secretase inhibitors [24].

Furthermore, it is worth mentioning that many clinical trials have been undertaken for potential therapeutic drugs that inhibit the Notch pathway in other types of malignancies [25]. Specifically, phase I clinical trials on anti-Notch1 monoclonal antibody brontictuzumab have shown promising results in patients with lymphomas and refractory solid tumors, with the main toxicity being the induction of diarrhea [26-27]. Moreover, a phase I clinical trial on the monoclonal antibody tarextumab which targets Notch2 and Notch3 simultaneously, presented encouraging results in patients with solid tumors [28]. Gamma-secretase inhibitors were not shown to be effective in the treatment of other advanced solid tumors, although they presented few adverse effects (diarrhea, nausea and vomiting) [29-30]. Table 1 summarizes the potential targets for the Notch pathway inhibition and thus control of RMS cells.

Conclusions

RMS research has been focused on discovering the mechanisms through which the neoplasm progresses, and the ways of inhibiting them [31]. Also, in the last three years, several promising therapeutics have been investigated, but the exact mechanisms through which they act are still unknown [32-33]. As seen in the present review, in vitro and in vivo research has demonstrated a significant role of the Notch signaling pathway in the development of RMS. Hence, it can be

Table 1. Potential therapeutic targets inhibiting Notch in RMS

Therapeutic target	Method of targeting	Biological effect	Studied *in vitro*	Studied *in vivo*	Reference
RBP-J	RNA interference	Cell cycle arrest	✓	✓	[15]
gamma-secretase	Small molecule inhibitor	Notch 3 inhibition, upregulation of p21, phosphorylation of p38, cell cycle arrest	✓	×	[12]
Notch-1 receptor	RNA interference	Enhancement of gamma--secretase inhibition effect, downregulation of HEY1, inhibition of cell motility	✓	✓	[23]
HGF receptor	Small molecule inhibitor	Enhancement of gamma--secretase inhibition effect	✓	×	[24]

viewed as a potential target for developing new targeted therapy drugs for this type of cancer. Combining potential monoclonal antibodies or small molecule inhibitors targeting the Notch pathway with other existing drugs may help reduce the chances of developing drug resistance. Nonetheless, the exact mechanisms through which the Notch pathway promotes proliferation and migration in RMS cells remain unknown. Therefore, more research should be conducted to assess the different biological effects of the Notch pathway activity in RMS.

Conflicts of interest

None.

Funding

None.

References

1. Martin-Giacalone BA, Weinstein PA, Plon SE, Lupo PJ. Pediatric Rhabdomyosarcoma: Epidemiology and Genetic Susceptibility. J Clin Med. 2021;10(9):2028. Available from: https://www.mdpi.com/2077-0383/10/9/2028
2. Haduong JH, Heske CM, Allen-Rhoades W, Xue W, Teot LA, Rodeberg DA, et al. An update on rhabdomyosarcoma risk stratification and the rationale for current and future Children's Oncology Group clinical trials. Pediatr Blood Cancer 2022;69(4). Available from: https://onlinelibrary.wiley.com/doi/10.1002/pbc.29511
3. Kim JR, Yoon HM, Koh K-N, Jung AY, Cho YA, Lee JS. Rhabdomyosarcoma in Children and Adolescents: Patterns and Risk Factors of Distant Metastasis. Am J Roentgenol. 2017;209(2):409–16. Available from: https://www.ajronline.org/doi/10.2214/AJR.16.17466
4. Agaram NP. Evolving classification of rhabdomyosarcoma. Histopathology 2022;80(1):98–108. Available from: https://onlinelibrary.wiley.com/doi/10.1111/his.14449
5. Sun X, Guo W, Shen JK, Mankin HJ, Hornicek FJ, Duan Z. Rhabdomyosarcoma: Advances in Molecular and Cellular Biology. Sarcoma 2015;2015:1–14. Available from: http://www.hindawi.com/journals/sarcoma/2015/232010/
6. Stewart E, McEvoy J, Wang H, Chen X, Honnell V, Ocarz M, et al. Identification of Therapeutic Targets in Rhabdomyosarcoma through Integrated Genomic, Epigenomic, and Proteomic Analyses. Cancer Cell. 2018;34(3):411-426.e19. Available from: https://doi.org/10.1016/j.ccell.2018.07.012

7. Dreesen O, Brivanlou AH. Signaling Pathways in Cancer and Embryonic Stem Cells. Stem Cell Rev. 2007;3(1):7–17. Available from: https://link.springer.com/10.1007/s12015-007-0004-8
8. Anusewicz D, Orzechowska M, Bednarek AK. Notch Signaling Pathway in Cancer—Review with Bioinformatic Analysis. Cancers (Basel) 2021;13(4):768. Available from: https://www.mdpi.com/2072-6694/13/4/768
9. Previs RA, Coleman RL, Harris AL, Sood AK. Molecular Pathways: Translational and Therapeutic Implications of the Notch Signaling Pathway in Cancer. Clin Cancer Res. 2015;21(5):955–61. Available from: https://aacrjournals.org/clincancerres/article/21/5/955/247574/Molecular-Pathways-Translational-and-Therapeutic
10. Zhou B, Lin W, Long Y, Yang Y, Zhang H, Wu K, et al. Notch signaling pathway: architecture, disease, and therapeutics. Signal Transduct Target Ther. 2022;7(1):95. Available from: https://www.nature.com/articles/s41392-022-00934-y
11. Lake RJ, Tsai P-F, Choi I, Won K-J, Fan H-Y. RBPJ, the Major Transcriptional Effector of Notch Signaling, Remains Associated with Chromatin throughout Mitosis, Suggesting a Role in Mitotic Bookmarking. Fortini M, editor. PLoS Genet. 2014;10(3):e1004204. Available from: https://dx.plos.org/10.1371/journal.pgen.1004204
12. Raimondi L, Ciarapica R, De Salvo M, Verginelli F, Gueguen M, Martini C, et al. Inhibition of Notch3 signalling induces rhabdomyosarcoma cell differentiation promoting p38 phosphorylation and p21Cip1 expression and hampers tumour cell growth in vitro and in vivo. Cell Death Differ. 2012;19(5):871–81. Available from: https://www.nature.com/articles/cdd2011171
13. Sang L, Coller HA, Roberts JM. Control of the Reversibility of Cellular Quiescence by the Transcriptional Repressor HES1. Science (80-) 2008;321(5892):1095–100. Available from: https://www.science.org/doi/10.1126/science.1155998
14. De Salvo M, Raimondi L, Vella S, Adesso L, Ciarapica R, Verginelli F, et al. Hyper-Activation of Notch3 Amplifies the Proliferative Potential of Rhabdomyosarcoma Cells. Wang Q, editor. PLoS One 2014;9(5):e96238. Available from: https://dx.plos.org/10.1371/journal.pone.0096238
15. Nagao H, Setoguchi T, Kitamoto S, Ishidou Y, Nagano S, Yokouchi M, et al. RBPJ Is a Novel Target for Rhabdomyosarcoma Therapy. Wang Q, editor. PLoS One. 2012;7(7):e39268. Available from: https://dx.plos.org/10.1371/journal.pone.0039268
16. Conboy IM, Rando TA. The Regulation of Notch Signaling Controls Satellite Cell Activation and Cell Fate Determination in Postnatal Myogenesis. Dev Cell. 2002;3(3):397–409. Available from: https://linkinghub.elsevier.com/retrieve/pii/S153458070200254X
17. Chen X, Li Y. Role of matrix metalloproteinases in skeletal muscle. Cell Adh Migr. 2009;3(4):337–41. Available from: http://www.tandfonline.com/doi/abs/10.4161/cam.3.4.9338
18. Roma J, Masià A, Reventós J, Sánchez de Toledo J, Gallego S. Notch Pathway Inhibition Significantly Reduces Rhabdomyosarcoma Invasiveness and Mobility In Vitro. Clin Cancer Res. 2011;17(3):505–13. Available from: https://aacrjournals.org/clincancerres/article/17/3/505/76773/Notch-Pathway-Inhibition-Significantly-Reduces
19. Masià A, Almazán-Moga A, Velasco P, Reventós J, Torán N, Sánchez de Toledo J, et al. Notch-mediated induction of N-cadherin and α9-integrin confers higher invasive phenotype on rhabdomyosarcoma cells. Br J Cancer 2012;107(8):1374–83. Available from: https://www.nature.com/articles/bjc2012411
20. Hernole J, Narayanappa R. Interactions between Notch and matrix metalloproteinases: the role in cancer. Biul Pol Tow Onkol Nowotw. 2023;8(6):436–43. Available from: https://journals.viamedica.pl/biuletyn_pto/article/view/98685
21. Jawad MU, Garamszegi N, Garamszegi SP, Correa-Medina M, Diez JA, Wen R, et al. Matrix Metalloproteinase 1: Role in Sarcoma Biology. Deb S, editor. PLoS One 2010;5(12):e14250. Available from: https://dx.plos.org/10.1371/journal.pone.0014250
22. Kalali D. The Role of the Matrix Metalloproteinase-9 Gene in Tumor Development and Metastasis: A Narrative Review. Glob Med Genet. 2023 Jun;10(02):048–53. Available from: http://www.thieme-connect.de/DOI/DOI?10.1055/s-0043-1768166
23. Belyea BC, Naini S, Bentley RC, Linardic CM. Inhibition of the Notch-Hey1 Axis Blocks Embryonal Rhabdomyosarcoma Tumorigenesis. Clin Cancer Res. 2011;17(23):7324–36. Available from: https://aacrjournals.org/clincancerres/article/17/23/7324/76712/Inhibition-of-the-Notch-Hey1-Axis-Blocks-Embryonal

24. Perrone C, Pomella S, Cassandri M, Pezzella M, Milano GM, Colletti M, et al. MET Inhibition Sensitizes Rhabdomyosarcoma Cells to NOTCH Signaling Suppression. Front Oncol. 2022;12. Available from: https://www.frontiersin.org/articles/10.3389/fonc.2022.835642/full
25. Li X, Yan X, Wang Y, Kaur B, Han H, Yu J. The Notch signaling pathway: a potential target for cancer immunotherapy. J Hematol Oncol. 2023;16(1):45. Available from: https://jhoonline.biomedcentral.com/articles/10.1186/s13045-023-01439-z
26. Ferrarotto R, Eckhardt G, Patnaik A, LoRusso P, Faoro L, Heymach J V, et al. A phase I dose-escalation and dose-expansion study of brontictuzumab in subjects with selected solid tumors. Ann Oncol. 2018;29(7):1561–8. Available from: https://www.sciencedirect.com/science/article/pii/S092375341932109X
27. Casulo C, Ruan J, Dang NH, Gore L, Diefenbach C, Beaven AW, et al. Safety and Preliminary Efficacy Results of a Phase I First-in-Human Study of the Novel Notch-1 Targeting Antibody Brontictuzumab (OMP-52M51) Administered Intravenously to Patients with Hematologic Malignancies. Blood 2016;128(22):5108. Available from: https://www.sciencedirect.com/science/article/pii/S0006497119351092
28. Smith DC, Chugh R, Patnaik A, Papadopoulos KP, Wang M, Kapoun AM, et al. A phase 1 dose escalation and expansion study of Tarextumab (OMP-59R5) in patients with solid tumors. Invest New Drugs. 2019;37(4):722–30. Available from: https://link.springer.com/10.1007/s10637-018-0714-6
29. Krop I, Demuth T, Guthrie T, Wen PY, Mason WP, Chinnaiyan P, et al. Phase I Pharmacologic and Pharmacodynamic Study of the Gamma Secretase (Notch) Inhibitor MK-0752 in Adult Patients With Advanced Solid Tumors. J Clin Oncol. 2012;30(19):2307–13. Available from: https://ascopubs.org/doi/10.1200/JCO.2011.39.1540
30. Gounder MM, Rosenbaum E, Wu N, Dickson MA, Sheikh TN, D'Angelo SP, et al. A Phase Ib/II Randomized Study of RO4929097, a Gamma-Secretase or Notch Inhibitor with or without Vismodegib, a Hedgehog Inhibitor, in Advanced Sarcoma. Clin Cancer Res. 2022;28(8):1586–94. Available from: https://aacrjournals.org/clincancerres/article/28/8/1586/694158/A-Phase-Ib-II-Randomized-Study-of-RO4929097-a
31. Zarrabi A, Perrin D, Kavoosi M, Sommer M, Sezen S, Mehrbod P, et al. Rhabdomyosarcoma: Current Therapy, Challenges, and Future Approaches to Treatment Strategies. Cancers (Basel) 2023;15(21):5269. Available from: https://www.mdpi.com/2072-6694/15/21/5269
32. Milosevic E, Stanisavljevic N, Boskovic S, Stamenkovic N, Novkovic M, Bavelloni A, et al. Antitumor activity of natural pigment violacein against osteosarcoma and rhabdomyosarcoma cell lines. J Cancer Res Clin Oncol. 2023;149(13):10975–87. Available from: https://link.springer.com/10.1007/s00432-023-04930-9
33. Morel VJ, Rössler J, Bernasconi M. Targeted immunotherapy and nanomedicine for rhabdomyosarcoma: The way of the future. Med Res Rev. 2024;44(6):2730-73. Available from: https://onlinelibrary.wiley.com/doi/10.1002/med.22059

EUROPEAN JOURNAL OF TRANSLATIONAL
AND CLINICAL MEDICINE 2025;8(1):103-112

REVIEW ARTICLE

Multifaced lipoedema: a problematic and complex condition in the population of young women

Jolanta Tomczak[1,2], Julia Dzierla[2], Aleksandra Sarba[2], Aleksandra Fałczyńska[2], Zbigniew Krasiński[1], Marcin Gabriel[1]

[1] Department of Vascular and Endovascular Surgery, Angiology and Phlebology, Poznań University of Medical Sciences, Poland
[2] Student Scientific Society of Poznan University of Medical Sciences, The Student Scientific Group of Ultrasonography at the Clinic of Vascular and Endovascular Surgery, Angiology and Phlebology, Poznan University of Medical Sciences, Poland

Abstract

Lipoedema is a chronic disease with various manifestation of symptoms, related to excessive deposition of subcutaneous adipose tissue in the legs, hips and buttocks. The scale of the problem is enormous and may affect up to one in five women. Lipoedema is often underdiagnosed and misdiagnosed with lymphedema, obesity or lipohypertrophy. In recent years, lipoedema has been diagnosed in an increasing number of younger women, and its first symptoms may manifest already in puberty. Even though it is often perceived as only an aesthetic problem, it has a huge impact on the quality of life, mental health, self-esteem or self-confidence. Moreover, lipoedema causes stigmatization, unfortunately also in healthcare professionals. Nevertheless, recently, diagnostic criteria (also ultrasound) have been created, and lipoedema has been classified in ICD-10 (E88.2). There are also more and more treatment options, with emphasis on the role of psychological care. Awareness and knowledge of lipoedema have also increased despite its underestimation but still is not enough. The multidimensional nature of lipoedema and its impact on many aspects of life highlights the essential role of comprehensive support to patients. Nowadays, in times of caring for mental health, it is crucial to increase public awareness and spread knowledge about lipoedema.

Keywords: young women · women's health · lipedema · mental health · lipoedema

Citation

Tomczak J, Dzierla J, Sarba A, Fałczyńska A, Krasiński Z, Gabriel M. Multifaced lipoedema: a problematic and complex condition in the population of young women. Eur J Transl Clin Med. 2025;8(1):103-112.

DOI: 10.31373/ejtcm/201944

Corresponding author:
Jolanta Tomczak, Department of Vascular and Endovascular Surgery, Angiology and Phlebology, Poznań University of Medical Sciences, Poland
e-mail: jolantatomczak@ump.edu.pl
Available online: ejtcm.gumed.edu.pl

Introduction

Lipoedema (ICD 10 code E88.2, ICD 11 code EF02.2) is a chronic disease marked by excessive deposition of subcutaneous adipose tissue in legs, hips and buttocks, mainly occurring in adult women [1]. Various studies have shown that lipoedema affects 11-19% of females [2]. The first symptoms (e.g. moderate and severe leg heaviness, pain, numbness, cold skin, feeling cold or easy bruising) can appear in puberty, which may explain the hormonal background of this disease [2-4]. Additionally, lipoedema has a significant impact on the patient's mental health and self-esteem [5]. Diagnosis is based on clinical findings and exclusion criteria [6]. The treatment demands a holistic approach, reduction of symptoms severity, preventing impaired function and disease progression. Moreover, the therapeutic approach also includes taking care of factors influencing the course of lipoedema, e.g. obesity [7]. Our aim was to summarize the knowledge about diagnosing and managing patients with lipoedema, a frequently misdiagnosed condition.

Material and methods

We searched for relevant literature published in the years 1950 to 2024 using the PubMed search engine. Due to the spelling differences in British and American literature, we used the keywords "lipedema" and "lipoedema." German-language articles indexed in PubMed contain abstracts translated to English, therefore we also included them in this search.

Results

We found a total of 577 abstracts. After screening the abstracts and reading the full texts, we included 43 articles in this review.

Epidemiology

The available data is insufficient to reveal the specific prevalence of lipoedema in the general population [8]. Lack of accurate diagnostic markers of lipoedema and confusion regarding its definition results in a high rate of misdiagnosis and wrong mistreatment, which may imply rare diagnosis [9-10]. Several studies have already shown greater prevalence of lipoedema than it was previously suggested. Lipoedema affects 11-19% of females [2]. The estimated frequency of lipoedema in the general population varies between 0.06% and 19% depending on the study [2, 11-13]. However, typical symptoms of lipoedema are common among young women. First symptoms appear already in puberty or childhood (57.1-64.2% of cases) [5, 14]. Also, a study of 209 patients with lipoedema showed that symptoms typically appear around age 16 [4]. In another, 70% of women with lipoedema experienced onset before age 30, but unfortunately only 1.6% were diagnosed earlier by a healthcare professional [3]. Furthermore, cases of lipoedema occurring in children have also been recorded [15-16].

Diagnosis is usually made in middle-aged women, although first symptoms can manifest in puberty, which suggest a hormonal basis of lipoedema [4]. In the literature, there are only a few reported cases of male patients with lipoedema and all of them had a medical history of hyperestrogenemia and hypotestosteronemia [6].

Pathogenesis

The pathophysiology of lipoedema remains unexplained, although some factors such as hormones, genetic predisposition, impaired sympathetic system, and vasculature may play an essential role [17]. Estrogens regulate adipogenesis and adipocyte lipid deposition by metabolic signaling. Their excess may form increased adipose depot mass. The fact that lipoedema often appears in phases of hormonal change such as puberty, pregnancy or menopause confirms this theory [10]. According to the literature, family history of lipoedema varies between 16% and 64% [6, 10, 15]. The familial character of lipoedema was confirmed by revealing the mutation of the gene AKR1C1, which is responsible for the progesterone metabolism, although it is present in obese women or with lipoedema [15, 17-18]. Vessel microangiopathy and lymphatic vessel disfunction are suggested to be typical for lipoedema. Pathological changes in the vessels' structure conduct excess accumulation fluid in the subcutaneous adipose tissue, causing remodeling, adipose oedema and hematoma due to increased permeability. All of these processes decrease blood flow in subcutaneous adipose tissue, causing inflammation, hypoxia and formation of fibrotic lesions, which patients may perceive as pain [3].

Symptoms and classification

The typical localization of lipoedema adipose tissue is the gynoid region. In 97% cases it involves the hips, buttocks, thighs, and lower legs; only 3% is located in the upper extremities [8]. Almost all the symptoms reported by patients involve feet. Complaints apply to unpleasant sensations of heaviness and compression due to orthostatic oedema. The oedema increases during the day (also due to warmth and exercise) and there is no specific factor that could reduce its intensity [6, 9]. Concerning microangiopathy, patients bruise easily and their subcutaneous capillaries might be dilated [19]. Another cardinal sign is the daily pain (usually described as moderate to

severe), which is responsible for reduced quality of life (QoL) and impaired mobility [3]. Pain might be associated with lipoedema adipose tissue, but also with joints and osteoarthritis due to increased body mass. Women with lipoedema are at a high risk of eating disorders, depression and other psychological complaints. Misdiagnosis and stigmatization cause mental conditions, it highlights the importance of distinguishing these two conditions. Nowadays, lipoedema is not linked to any metabolic diseases, although obesity may appear and influence the lipoedema subcutaneous adipose tissue [20].

Based on body distribution of adipose tissue, 5 types of lipoedema were determined by Amato et al. In stage I it is located only around the pelvis, hips and buttocks (the 'saddle bag' phenomenon), whereas in stage II it is present in the area from hips to knees, with the formation of folds of fat around the inner side of the knee. Stage III involves the region from hips to ankles, while in the IV stage, adipose edema is concentrated in the arms. The rarest is stage V, which requires involvement of calves [21].

Differential diagnosis

Although there are no specific diagnostic tests or markers that help diagnose lipoedema, some studies highlight the importance of adipose tissue-resident mesenchymal stem cells morphology in lipoedema subcutaneous adipose tissue [22]. Before confirmation of any molecular marker, identification of the condition requires the exclusion of other diseases characterizing oedema and deposition of fat tissue in the lower extremities [9, 15]. Clinicians should always consider localization of symptoms (bilaterally or unilateral). Furthermore, the presence of the Stemmer sign (the examiner pinches the dorsal skin proximal to the metatarsophalangeal joint of the second toe, or metacarpophalangeal joint of the second finger; the sign is positive if the examiner cannot create a fold of pinched skin) enables distinguishing lipoedema from lymphatic edema (lymphedema) and chronic venous insufficiency [8, 23]. Lipoedema typically spares the hands and feet, thus most patients have a negative Stemmer sign. However, a positive Stemmer sign does not rule out lipoedema and suggests the presence of concomitant lymphedema. If both conditions are present, the diagnosis is lipo-lymphedema. Another important symptom is pain (present also in Dercum's disease (*adiposis dolorosa*): multiple painful fatty tumors (lipomas), generalized obesity (usually in menopausal age), weakness, fatigue, mental disturbances (including emotional instability, depression) and central nervous system disfunction (e.g. epilepsy, confusion and dementia) [6, 8, 24]. The absence of pain and oedema, but with the presence of increased symmetrical subcutaneous fat deposits in women is associated with lipohypertrophy [8-9]. The differential diagnosis is presented in Table 1.

Table 1. Differential diagnosis of lipoedema, lymphedema, lipohypertrophy, obesity and Dercum's disease

	Lipoedema	Lymphedema	Lipohypertrophy	Obesity	Dercum's disease
Sex	Female	Female and male	Female	Female and male	Female (mainly in menopausal age) and male
Family history positivity	Common	Common in primary lymphedema	Possible	Common	Possible; very few data about familial occurence
Symmetry	Present	Present in primary lymphedema	Present	Present	In familial cases
Involvement of feet	Absent	Present	Absent	Present	Present
Edema	Absent (present on early stages)	Present	Absent	Absent	Absent
Tenderness	Present	Absent	Absent	Absent	Absent
Response to diet	None	None	None	Excellent	None
Pain	Present	Absent	Absent	Absent	Chronic and severe pain of masses

Diagnostic steps

The diagnosis of lipoedema is based on clinical findings and exclusion criteria. First data was published in 1951 by Wold et al. and in 2017 was extended by Halk and Damstra in the form of guidelines (Table 2) [25-26]. Based on the 2017 guidelines by Wounds UK and others, the key steps in the assessment of a patient with suspected lipoedema are:

- detailed medical history (medical/surgical/family history, impact on daily living, mobility, personal relationships, work, emotional state),
- extent, distribution and severity of adipose tissue enlargement,
- skin assessment,
- vascular assessment,
- pain (measured with the numerical rating scale (NRS), visual analogue scale (VAS) or the Schmeller questionnaire),

Table 2. Diagnosis of lipoedema, table created based on Dutch guidelines [20]

Anamnesis (A) (Criteria by Wold et al.)		
A	1	Disproportionate fat distribution
	2	No/limited influence of weight loss on disproportionate fat distribution
	3	Easily bruised/in pain
	4	Sensitivity to touch/ fatigue in extremities
	5	No reduction of pain when raising extremities
Physical examination (B, C, D, E)		
		Upper leg
B	6	Disproportionate fat distribution
	7	Circularly thickened cutaneous fat layer
		Lower leg
C	8	Proximal thickening of subcutaneous fat layer
	9	Distal thickened of subcutaneous fat, accompanied by slender instep (cuff-sign)
		Upper arm
D	10	Significantly thickened subcutaneous fat layer in comparison with vicinity
	11	Sudden stop at elbow
		Lower arm
E	12	Thickened subcutaneous fat, accompanied by slender back of hand (cuff-sign)
		Extra criteria
F	13	Pain when applying bi-manual palpation
	14	Distal fat tiss ue tendrils of the knee (popliteus)

Diagnosis of lipoedema is certain when present: A1+A2+A3+A4+A5 PLUS ((B6+B7) or (C8+C9) or (D10+D11) or E12). In the case of absence of at most two of these five criteria (A to E), the presence of extra criteria F13 or F14 also assures the diagnosis of lipoedema [20].

- mobility and gait,
- dietary assessment,
- assessment of comorbidities,
- psychosocial assessment (there is a need for a validated survey),
- quality of life (SF-36 questionnaires),
- understanding of disease and expectations of treatment outcomes.

Proper physical examination includes evaluation of typical signs of lipoedema such as subcutaneous tissue enlargement, cuffing (braceleting) at the ankles/wrists, loss of the concave spaces on either side of the Achilles tendon, bruising, altered skin appearance, temperature and texture, abnormal gait and limited mobility, negative Stemmer's sign and pitting oedema. It must be highlighted that there are no specific diagnostic tests for lipoedema. Hence, we must exclude other diagnoses based on routine blood tests (urea, electrolytes, full blood count, thyroid function tests, liver, renal function tests, plasma proteins, brain natriuretic peptide, glucose, lipid profiles and insulin resistance) [10-11]. Imaging investigations such as ultrasound scans, magnetic resonance imaging scans or computed tomography may play a role if the diagnosis is uncertain.

Decisions about further management should be made by an interdisciplinary team. Depending on the needs, such team should consist of a clinician specializing in lipoedema/lymphoedema, physiotherapist, occupational therapist, dietitian, podiatrist, pain specialist, vascular specialist, diabetologist, psychologist, plastic surgeon or bariatric surgeon [27].

Imaging

Marshall and Schwahn-Schreiber first proposed an ultrasound-based classification for lipoedema diagnosis based on specific cut-off values of the dermis thickness and subcutaneous tissue measurements 6 to 8 cm proximal the medial malleolus: average measurement for women without lipoedema (2.1 mm), lipohyperplasia or mild lipoedema (12 to 15 mm), moderate lipoedema (15 to 20 mm), indisputable lipoedema (> 20 mm) and severe lipoedema (> 30 mm) [21, 23, 28-29]. Later, Amato et al. described easy-to-obtain ultrasound measurements with the extension of Marshall's assessment. They suggested evaluating lipoedema at more locations: thigh, pretibial, lateral leg, medial malleolus, and anteromedial region of the proximal leg with typical fat deposition for more precise investigation in the future (Table 3) [21].

Subcutaneous adipose tissue and skin can be likewise examined by computed tomography (CT) and/or magnetic resonance imaging (MRI) [10]. CT can be used to differentiate lipoedema from lymphedema. The presence of subcutaneous fluid accumulation, the honeycomb pattern and muscle enlargement do not occur in lipoedema and therefore confirm the suspicion of lymphedema [8]. MRI is suggested to evaluate lymphatic circulation or to distinguish lipoedema from obesity (examination of subcutaneous fat accumulation) [11, 17]. Non-tracer-based MR lymphangiography evaluates elevated atrial and lymphatic insufficiency in lower extremities [17]. Because of significant changes in body composition presented by patients with lipoedema, bioimpedance and dual-energy X-ray absorptiometry (DXA) are supposed to be diagnostic tools. In some studies, DXA was used to estimate torso and leg fat in comparison to total body mass. In lipoedema fat tissue is mainly localized in lower parts [30]. Alternatively, dysfunction of the lymphatic system might be evaluated by functional tests: lymphoscintigraphy, lymphography or fluorescence microlymphography [10, 17].

Follow-up

Follow-up should include measurement of the body mass index (BMI), waist-hip ratio, waist-height ratio, limb measurements of circumference and volume, and daily activity index.

Table 3. Optimal cut-off values for the clinical diagnosis of lipoedema using ultrasound suggested by Amato (estimated by Youden index) – an extension of Marshall assessment

Location of the lipedema evaluation point	Optimal cut-off values for the clinical diagnosis of lipedema [mm] – right leg	Optimal cut-off values for the clinical diagnosis of lipedema [mm] – left leg
Thigh thickness	19.5	17.9
Lateral leg thickness	8.9	8.4
Pretibial region thickness	11.6	11.8
Supramalleolar thickness	7.1	7.0

Furthermore, the VAS or the Schmeller questionnaire can help track the changes in the patient's pain perception [6, 10]. DXA may be performed [16, 31-32]. Follow-up plays a crucial role in further management and in choice of the proper treatment [6].

Possible treatment options

The main aim of lipoedema treatment is the reduction of symptom severity, prevention of impaired functioning and progression of disease. The therapeutic approach is also focused on factors such as obesity and venous insufficiency and goals such as educating patients about the nature of lipoedema, treatment options and possible impact of a patient on the disease [6, 9-10] The role of weight control and appropriate dietary modifications should be emphasized [6, 10, 19]. An algorithm of potential diagnostic and therapeutic work-up for patients with suspected lipoedema was proposed by Buso et al. [6]. It highlighted the role of conservative treatment based on information, education, a multidisciplinary approach to encourage an active lifestyle, elastic compression stocking, decongestive lymphatic therapy (DLT) and complex decongestive therapy (CDT, more details below). If these methods are not effective after follow-up, surgical methods such as tumescent liposuction or lipectomy should be considered [6, 33-34].

Medicaments

The role of pharmacological treatment in lipoedema has not been explained yet. Favorable results can be obtained with beta-adrenergic agonists, corticosteroids, diuretics, flavonoids and selenium [6, 19, 35].

Complex decongestive therapy

CDT is a part of conservative treatment which reduces pain and discomfort in the extremities. It consists of manual lymph drainage (MLD) associated with multilayered and multicomponent compression bandaging, meticulous skin care and physical exercise [6, 11]. MLD reduces the load of lymph stasis on the limb by directing the lymph into the non-edematous part. It can be combined with intermittent pneumatic compression (IPC) which improves venous flow and reduces edema [11, 17]. However, it is important to apply only mild pressure of IPC in the treatment of lipoedema, considering subsiding superficial lymphatic vessels [10].

Surgery

Surgery is the second line treatment. When symptoms are worsening and affecting the patient's QoL, two options can be considered: liposuction and lipectomy [6, 10, 33, 36-37]. Those two methods result in better outcomes because of less lymphatic tissue damage than in traditional techniques [19, 37-38]. Although liposuction cannot cure lipoedema, it results in decrease in symptoms such as pain and tendency to swell as well as improves the patient's mobility and well-being. Furthermore, it is safe, usually without late complications [9, 37, 39]. Unfortunately, liposuction usually requires multiple sessions related to the extensiveness of adipose tissue that should be removed. Compared to lipectomy, it is performed in the early stages of lipoedema and prevents clinical progression [9, 36]. Advanced stages of lipoedema with accompanying lymphedema usually require surgical debulking due to the presence of multiple fibrotic tissue [10]. Patients with early stages should use a postoperative compression garment for at least 2-3 months to manage postoperative edema, whereas those with advanced stages even for the rest of their life [18, 36].

Quality of life

At this time there are no established guidelines for the psychological care of patients with lipoedema, and there is a lack of data on the most frequently used diagnostic tools or treatments. However, with the growing focus on mental health, this matter should be explored in future research.

Dudek et al. conducted a survey among 130 Polish women aged 22 to 73 with lipoedema and found that 98 of them (75.38%) experienced varying degrees of depression, which depended on the intensity of lipoedema symptoms such as leg pain, heaviness, swelling, bruising, muscle and joint pain [5]. The respondents reported elevated levels of depressive symptoms and reduced QoL across various domains, including physical and psychological health, social relationships and even environment [5]. Another study by Dudek et al. has shown the importance of addressing appearance-related distress in patients with lipoedema [32]. Other studies have also emphasized the impact of this disease on mental health and QoL [4, 40] with a holistic approach. Additionally, confusion between lipoedema and obesity or dietary and lifestyle mistakes can further compound the issue [19].

The final diagnosis of lipoedema brings a relief for some patients, although younger women typically responded to the diagnosis with reduced well-being [7]. Specifically, these women often felt helpless, knowing that treatment might not alleviate their symptoms to the extent they hoped, leading to anxiety and even self-loathing [7, 41]. Regarding the inconvenience associated with the disease, women mentioned difficulties in finding properly fitting clothing [7, 12]. When assessing the level of life satisfaction, more than half of them rated their life satisfaction as low, and 59 individuals (60.1%) reported being dissatisfied or very dissatisfied [5].

In a Dutch study conducted in 2018 by Romejn et al., the QoL of lipoedema patients was analyzed using EQ-5D-3L and

RAND-36 questionnaires, both used to evaluate health-related QoL [8]. Among lipoedema patients, the average EQ-5D--3L index was 66.1/100, while the average score for the Dutch population was 85/100. Additionally, the RAND-36 score for lipoedema patients was 59.3/100, compared to the Dutch population's average score of 74.9/100 [14]. Another challenge is difficulty in forming romantic relationships because patients often feel ashamed of their bodies [7].

Aesthetic issues (complexes) regarding the appearance and disproportion of the body may coexist with lipoedema, e.g. the problem of fat loss from the limb extremities area, a general feeling of discomfort (not accepting one's own body, covering legs), reduced self-confidence, lowered self-esteem, disliking oneself, feeling of heavy lower extremities, problems with choosing the right size of clothes, the shame of showing lower limbs [1, 7, 19, 41-42].

Discussion

It is noteworthy that limited research is focused specifically on lipoedema among young women in their 20s and early 30s [7].

Lipoedema is a complex disease, which despite the increased amount of information about it, still remains an underestimated health problem [19]. Recent studies have increasingly shed light on the psychological aspect of lipoedema [5, 7]. Women often perceive themselves as overweight and try to improve their body's appearance through restrictive diets and exercise which unfortunately cannot reduce the fatty swelling in areas affected by lipoedema [31, 41]. On the contrary, the achieved weight loss further underlines the disproportions of patient's body [42]. The ineffectiveness of these measures reduces self-confidence and sense of self-worth [19, 41].

Most patients had relatives with lipoedema, therefore the hereditary basis of lipoedema is also being discussed more and more frequently [4]. In a genome-wide association study (GWAS) conducted by Yann C. Klimentidis et al., 18 loci across the genome were identified as potential genetic risk factors for lipoedema. Two of these loci (VEGFA and GRB14-COBLLI) were successfully replicated in another study with clinically diagnosed lipoedema cases. These findings could be the background for future studies about prevention strategies or treatment [1].

As revealed by Christoffersen and Tennfjord, awareness of lipoedema is limited not only among patients but also among healthcare professionals in Norway [7]. Moreover, in that study women between 21 and 47 years of age experienced stigmatization by healthcare workers (felt perceived as lazy and believed that their health problem was being dismissed). Stigmatization of lipoedema patients is widespread in all aspects of life, and patients are often blamed for their condition and health status. It is worth noting that lipoedema is often misdiagnosed as lymphedema, leading patients to pursue ineffective treatment [7, 12]. These studies highlight a lack of awareness about lipoedema among medical professionals and there is limited research on its occurrence in young people beyond what has been mentioned. A study by Dudek et al. shows that only 44.9% of participants were diagnosed with lipoedema by medical health professionals [5]. Another study found that a mean time from the first symptoms to the diagnosis was 10-15 years [4]. Thus, it is crucial for medical professionals (e.g. doctors, nurses, physiotherapists, dietitians and students) to gain knowledge and awareness about lipoedema more rapidly.

However, also differential diagnosis is a challenge, as up to 15-17% of women treated for lymphedema at that time had lipoedema [13]. Fortunately, awareness and knowledge of lipoedema have been increasing. Nowadays we can use the ultrasound criteria for diagnosis [21]. Furthermore, in the United States in 2021 Herbst et al. developed and published a standard of care for lipoedema [18]. In 2018 the diagnosis of lipoedema was included in the 11th version of International Classification of Diseases 11 (code EF02.2) [43]. The financial burden of lipoedema has not been estimated yet. Treating patients with lipoedema can be very expensive due to the need for a comprehensive approach that includes not only the causal treatment but also the support of multiple specialists.

Lipoedema often co-occurs with various other diseases, including obesity, as well as heart and vascular complications (for example venous varicose and secondary lymphedema) [14, 18, 44] These comorbidities can further exacerbate symptoms and negative impact on QoL [3, 14]. Moreover, hormonal alterations may play a significant role in the development and progression of lipoedema which frequently coexists with hypothyroidism, diabetes mellitus or sexual hormonal imbalances [1]. Numerous studies have shown that lipoedema can be also influenced by hormonal factors such as the use of contraception, menopause, puberty or pregnancy [2]. Further research in this area is needed to explore lipoedema's association with other chronic diseases.

Conclusions

Lipoedema affects patients' life clinically, psychologically and economically. Lipoedema is probably underdiagnosed and more studies are needed to reveal its prevalence, particularly among young women and teenagers. It is crucial to define the pathophysiology of lipoedema and find accurate, easily-available diagnostic markers. Clinical trials could help establish causal treatment. We need a holistic approach (with psychological support) to patients with lipoedema, standard-

ization of patient care, improved differential diagnosis and awareness, not only among patients, but also in the training of future healthcare professionals. Promoting awareness (e.g. via the internet and social media) can contribute to increased self-acceptance among patients with lipoedema [5, 42].

Conflict of interests

None.

Funding

None.

References

1. Klimentidis YC, Chen Z, Gonzalez-Garay ML, Grigoriadis D, Sackey E, Pittman A, et al. Genome-wide association study of a lipedema phenotype among women in the UK Biobank identifies multiple genetic risk factors. Eur J Hum Genet [Internet]. 2023;31(3):338–44. Available from: https://www.nature.com/articles/s41431-022-01231-6
2. Katzer K, Hill JL, McIver KB, Foster MT. Lipedema and the Potential Role of Estrogen in Excessive Adipose Tissue Accumulation. Int J Mol Sci [Internet]. 2021;22(21):11720. Available from: https://www.mdpi.com/1422-0067/22/21/11720
3. Falck J, Rolander B, Nygårdh A, Jonasson L-L, Mårtensson J. Women with lipoedema: a national survey on their health, health-related quality of life, and sense of coherence. BMC Womens Health [Internet]. 2022;22(1):457. Available from: https://bmcwomenshealth.biomedcentral.com/articles/10.1186/s12905-022-02022-3
4. Bauer A-T, von Lukowicz D, Lossagk K, Aitzetmueller M, Moog P, Cerny M, et al. New Insights on Lipedema: The Enigmatic Disease of the Peripheral Fat. Plast Reconstr Surg [Internet]. 2019;144(6):1475–84. Available from: https://journals.lww.com/10.1097/PRS.0000000000006280
5. Dudek JE, Białaszek W, Gabriel M. Quality of life, its factors, and sociodemographic characteristics of Polish women with lipedema. BMC Womens Health [Internet]. 2021;21(1):27. Available from: https://bmcwomenshealth.biomedcentral.com/articles/10.1186/s12905-021-01174-y
6. Buso G, Depairon M, Tomson D, Raffoul W, Vettor R, Mazzolai L. Lipedema: A Call to Action! Obesity [Internet]. 2019;27(10):1567–76. Available from: https://onlinelibrary.wiley.com/doi/10.1002/oby.22597
7. Christoffersen V, Tennfjord MK. Younger Women with Lipedema, Their Experiences with Healthcare Providers, and the Importance of Social Support and Belonging: A Qualitative Study. Int J Environ Res Public Health [Internet]. 2023;20(3):1925. Available from: https://www.mdpi.com/1660-4601/20/3/1925
8. Forner-Cordero I, Szolnoky G, Forner-Cordero A, Kemény L. Lipedema: an overview of its clinical manifestations, diagnosis and treatment of the disproportional fatty deposition syndrome – systematic review. Clin Obes [Internet]. 2012;2(3–4):86–95. Available from: https://onlinelibrary.wiley.com/doi/10.1111/j.1758-8111.2012.00045.x
9. Langendoen SI, Habbema L, Nijsten TEC, Neumann HAM. Lipoedema: from clinical presentation to therapy. A review of the literature. Br J Dermatol [Internet]. 2009;161(5):980–6. Available from: https://academic.oup.com/bjd/article/161/5/980/6642385
10. Kruppa P, Georgiou I, Biermann N, Prantl L, Klein-Weigel P, Ghods M. Lipedema — Pathogenesis, Diagnosis, and Treatment Options. Dtsch Arztebl Int [Internet]. 2020; Available from: https://www.aerzteblatt.de/10.3238/arztebl.2020.0396
11. Forner-Cordero I, Forner-Cordero A, Szolnoky G. Update in the management of lipedema. Int Angiol [Internet]. 2021;40(4). Available from: https://www.minervamedica.it/index2.php?show=R34Y2021N04A0345
12. Fife CE, Maus EA, Carter MJ. Lipedema. Adv Skin Wound Care [Internet]. 2010;23(2):81–92. Available from: https://journals.lww.com/00129334-201002000-00010
13. Földi M, Földi E, Strössenreuther RHK, Kubik S. Földi's Textbook of Lymphology: For Physicians and Lymphedema Therapists [Internet]. Mosby; 2006. Available from: https://books.google.pl/books?id=b6VwL4eaGyIC
14. Romeijn JRM, de Rooij MJM, Janssen L, Martens H. Exploration of Patient Characteristics and Quality of Life in Patients with Lipoedema Using a Survey. Dermatol Ther (Heidelb) [Internet]. 2018;8(2):303–11. Available from: http://link.springer.com/10.1007/s13555-018-0241-6
15. Child AH, Gordon KD, Sharpe P, Brice G, Ostergaard P, Jeffery S, et al. Lipedema: An inherited condition. Am J Med Genet Part A [Internet]. 2010;152A(4):970–6. Available from: https://onlinelibrary.wiley.com/doi/10.1002/ajmg.a.33313

16. Schook CC, Mulliken JB, Fishman SJ, Alomari AI, Grant FD, Greene AK. Differential Diagnosis of Lower Extremity Enlargement in Pediatric Patients Referred with a Diagnosis of Lymphedema. Plast Reconstr Surg [Internet]. 2011;127(4):1571–81. Available from: http://journals.lww.com/00006534-201104000-00022
17. Poojari A, Dev K, Rabiee A. Lipedema: Insights into Morphology, Pathophysiology, and Challenges. Biomedicines [Internet]. 2022;10(12):3081. Available from: https://www.mdpi.com/2227-9059/10/12/3081
18. Herbst KL, Kahn LA, Iker E, Ehrlich C, Wright T, McHutchison L, et al. Standard of care for lipedema in the United States. Phlebol J Venous Dis [Internet]. 2021;36(10):779–96. Available from: https://journals.sagepub.com/doi/10.1177/02683555211015887
19. Buck DW, Herbst KL. Lipedema: A Relatively Common Disease with Extremely Common Misconceptions. Plast Reconstr Surg - Glob Open [Internet]. 2016;4(9):e1043. Available from: https://journals.lww.com/01720096-201609000-00012
20. Keith L, Seo CA, Rowsemitt C, Pfeffer M, Wahi M, Staggs M, et al. Ketogenic diet as a potential intervention for lipedema. Med Hypotheses [Internet]. 2021;146:110435. Available from: https://linkinghub.elsevier.com/retrieve/pii/S0306987720333260
21. Amato ACM, Saucedo DZ, Santos K da S, Benitti DA. Ultrasound criteria for lipedema diagnosis. Phlebol J Venous Dis [Internet]. 2021;36(8):651–8. Available from: https://journals.sagepub.com/doi/10.1177/02683555211002340
22. Ernst AM, Bauer H, Bauer H-C, Steiner M, Malfertheiner A, Lipp A-T. Lipedema Research — Quo Vadis? J Pers Med [Internet]. 2022;13(1):98. Available from: https://www.mdpi.com/2075-4426/13/1/98
23. Goss JA, Greene AK. Sensitivity and Specificity of the Stemmer Sign for Lymphedema: A Clinical Lymphoscintigraphic Study. Plast Reconstr Surg - Glob Open [Internet]. 2019;7(6):e2295. Available from: https://journals.lww.com/01720096-201906000-00013
24. Kucharz EJ, Kopeć-Mędrek M, Kramza J, Chrzanowska M, Kotyla P. Dercum's disease (adiposis dolorosa): a review of clinical presentation and management. Rheumatology [Internet]. 2019;57(5):281–7. Available from: https://reu.termedia.pl/Dercum-s-disease-adiposis-dolorosa-a-review-of-clinical-presentation-and-management,112434,0,2.html
25. Wold LE, Hines EA, Allen E V. Lipedema of the Legs: a Syndrome Characterized by Fat Legs and Edema. Ann Intern Med [Internet]. 1951;34(5):1243–50. Available from: https://www.acpjournals.org/doi/10.7326/0003-4819-34-5-1243
26. Halk AB, Damstra RJ. First Dutch guidelines on lipedema using the international classification of functioning, disability and health. Phlebol J Venous Dis [Internet]. 2017;32(3):152–9. Available from: https://journals.sagepub.com/doi/10.1177/0268355516639421
27. Hardy D, Williams A. Best practice guidelines for the management of lipoedema. Br J Community Nurs [Internet]. 2017;22(Sup10):S44–8. Available from: http://www.magonlinelibrary.com/doi/10.12968/bjcn.2017.22.Sup10.S44
28. Marshall M, Schwahn-Schreiber C. Prävalenz des Lipödems bei berufstätigen Frauen in Deutschland. Phlebologie [Internet]. 2011;40(03):127–34. Available from: http://www.thieme-connect.de/DOI/DOI?10.1055/s-0037-1621766
29. Seo C. Prävalenz des Lipödems bei berufstätigen Frauen [Internet]. Lipedema Project. 2016 [cited 2024 Apr 13]. Available from: https://lipedemaproject.org/prvalenz-des-lipdems-bei-berufs-ttigen-frauen-in/
30. Czerwińska M, Teodorczyk J, Hansdorfer-Korzon R. A Scoping Review of Available Tools in Measurement of the Effectiveness of Conservative Treatment in Lipoedema. Int J Environ Res Public Health [Internet]. 2022;19(12):7124. Available from: https://www.mdpi.com/1660-4601/19/12/7124
31. Tuğral A, Bakar Y. An approach to lipedema: a literature review of current knowledge of an underestimated health problem. Eur J Plast Surg [Internet]. 2019;42(6):549–58. Available from: http://link.springer.com/10.1007/s00238-019-01519-9
32. Dudek JE, Białaszek W, Ostaszewski P, Smidt T. Depression and appearance-related distress in functioning with lipedema. Psychol Health Med [Internet]. 2018;23(7):846–53. Available from: https://www.tandfonline.com/doi/full/10.1080/13548506.2018.1459750
33. Anne Warren Peled A, Kappos E. Lipedema: diagnostic and management challenges. Int J Womens Health [Internet]. 2016;Volume 8:389–95. Available from: https://www.dovepress.com/lipedema-diagnostic-and-management-challenges-peer-reviewed-article-IJWH
34. Goodliffe JM, Ormerod JOM, Beale A, Ramcharitar S. An under-diagnosed cause of leg swelling. BMJ Case Rep [Internet]. 2013;bcr2013009538. Available from: https://casereports.bmj.com/lookup/doi/10.1136/bcr-2013-009538
35. Herbst KL. Rare adipose disorders (RADs) masquerading as obesity. Acta Pharmacol Sin [Internet]. 2012;33(2):155–72. Available from: https://www.nature.com/articles/aps2011153
36. Warren Peled A, Slavin SA, Brorson H. Long-term Outcome After Surgical Treatment of Lipedema. Ann Plast Surg [Internet]. 2012;68(3):303–7. Available from: https://journals.lww.com/00000637-201203000-00017
37. Rapprich S, Baum S, Kaak I, Kottmann T, Podda M. Treatment of lipoedema using liposuction. Phlebologie [Internet]. 2015;44(03):121–32. Available from: http://www.thieme-connect.de/DOI/DOI?10.12687/phleb2265-3-2015

38. Stiefelhagen P. No lymphedema, no obesity. How can lipedema be treated? MMW Fortschr Med [Internet]. 2001;143 (35–36):15. Available from: http://www.ncbi.nlm.nih.gov/pubmed/11584522
39. Rapprich S, Dingler A, Podda M. Liposuction is an effective treatment for lipedema–results of a study with 25 patients. JDDG J der Dtsch Dermatologischen Gesellschaft [Internet]. 2011;9(1):33–40. Available from: https://onlinelibrary.wiley.com/doi/10.1111/j.1610-0387.2010.07504.x
40. Greene A, Meskell P. The impact of lower limb chronic oedema on patients' quality of life. Int Wound J [Internet]. 2017;14(3):561–8. Available from: https://onlinelibrary.wiley.com/doi/10.1111/iwj.12648
41. Torre YS-D la, Wadeea R, Rosas V, Herbst KL. Lipedema: friend and foe. Horm Mol Biol Clin Investig [Internet]. 2018;33(1). Available from: https://www.degruyter.com/document/doi/10.1515/hmbci-2017-0076/html
42. de Oliveira J. Lipedema, body-related emotional and disordered eating to cope. Surg Obes Relat Dis [Internet]. 2023;19(6): 667–8. Available from: https://linkinghub.elsevier.com/retrieve/pii/S1550728923001302
43. ICD-11 for Mortality and Morbidity Statistics [Internet]. 2024 [cited 2024 Oct 22]. Available from: https://icd.who.int/browse/2024-01/mms/en
44. Czerwińska M, Ostrowska P, Hansdorfer-Korzon R. Lipoedema as a Social Problem. A Scoping Review. Int J Environ Res Public Health [Internet]. 2021;18(19):10223. Available from: https://www.mdpi.com/1660-4601/18/19/10223

EUROPEAN JOURNAL OF TRANSLATIONAL
AND CLINICAL MEDICINE 2025;8(1):113-118

TECHNICAL REPORT

Improving quality of life of completely edentulous patient with oral submucous fibrosis and infantile hemangioma

Shubhaani Singh[1], Pankaj Dhawan[1], Harsimran Kaur[2], Manish Bhargava[3]

[1] Department of Prosthodontics, Manav Rachna Dental College, Manav Rachna International Institute of Research and Studies, Faridabad, India
[2] Department of Dental Surgery, Vardhman Mahavir Medical College and Safdarjung Hospital, New Delhi, India
[3] Department of Oral Pathology, Manav Rachna Dental College, Manav Rachna International Institute of Research and Studies, Faridabad, India

Abstract

Background: Oral submucous fibrosis is a premalignant condition characterized by rigidity of lips, tongue, and buccal mucosa. It makes rehabilitation difficult as it affects the stability and retention of the prosthesis. **Description:** This technical report focuses on the use of intralesional hyaluronidase injections followed by conventional complete denture fabrication for an edentulous patient. These conservative and non-invasive options were chosen due to the presence of infantile hemangioma in the region of interest. **Conclusion:** Hyaluronidase injections in the area of oral submucous fibrosis can bring about a major difference in the process of rehabilitation and potentially eliminate the morbidity associated with the surgical procedures.

Keywords: oral submucous fibrosis · intra-lesional injections · hyaluronidase · mental health · complete denture

Citation

Singh S, Dhawan P, Kaur H, Bhargava M. Improving quality of life of completely edentulous patient with oral submucous fibrosis and infantile hemangioma. Eur J Transl Clin Med. 2025;8(1):113-118.

DOI: 10.31373/ejtcm/202482

Corresponding author:
Harsimran Kaur, Department of Dental Surgery, Vardhman Mahavir Medical College and Safdarjung Hospital, New Delhi, India
e-mail: drsimran97@gmail.com
Available online: ejtcm.gumed.edu.pl

Background

Insidious oral submucous fibrosis (OSMF) is a chronic disorder marked by fibrosis of the submucosa (comprising the lamina propria and deeper connective tissues) and an inflammatory response [1]. It has a prevalence rate of 0.2 percent to 0.5 percent in Southeast Asia and the Indian subcontinent [2]. There are numerous causative factors, although the most common are consumption of areca (betel) nuts, chilli or other spices, genetic susceptibility, and nutritional deficiencies. The most commonly involved areas are buccal mucosa, palate, and sometimes the pharynx and faucial pillars. The signs and symptoms include burning sensation, referred pain in the temporal region, changes in salivation (increased or decreased), difficulty with chewing, phonation, and swallowing, reduced mouth opening, and ulceration of the mucosa [3].

Evidence suggests that OSMF is multifactorial, with certain effects on specific subpopulations of fibroblasts, genetic predisposition and molecular mechanisms (via cytokines and growth factors), which could render the oral mucosa more susceptible to chronic inflammatory changes on exposure to carcinogens. The chemical constituents of the areca nuts can stimulate fibroblast proliferation leading to collagen synthesis. Apart from this, these extracts also have the capability to stabilize the collagen fibrils and make it resistant to enzymatic degradation. It is noteworthy that the areca nuts have a higher copper content than the more commonly eaten nuts. The copper is released in the oral cavity while chewing the nut. Lysyl oxidase, an extracellular copper enzyme is secreted by fibroblasts and initiates post-transitional modification of collagen fibers rendering them resistant to the action of collagenases [1].

In clinical staging, early OSMF presents with stomatitis and vesiculation, moderate OSF has a marble-like appearance and palpable fibrous bands, and severe OSMF is manifested by leukoplakia and erythroplakia. Whereas the histological staging/classification is determined by the number and distribution of fibroblasts, collagen fibers, inflammatory cells and blood vessels. Moreover, biomarkers such as proteins, mRNAs, and non-coding RNAs are also measured in OSF staging and classification [2-3].

Nutritional support, microwave diathermy, immunomodulatory medications, physiotherapy, local drug delivery, combination therapy, and surgical excision of the fibrotic bands are among the various treatment options recommended to manage OSMF. Steroids act as immunosuppressive agents, decrease fibroblast proliferation, and release cellular protease in the connective tissue which stimulates collagenase and zymogen, which consume insoluble collagen [4]. Hyaluronidase breaks down the collagen fibers, dissolves the hyaluronic acid matrix, and lowers the thickness of intracellular cemental materials more quickly in OSMF patients. According to studies, hyaluronidase and intralesional steroid injections reduce the clinical symptoms of OSMF for a longer period of time [5].

Rehabilitation of a completely edentulous patient with OSMF is difficult. One of the options are the commonly chosen sectional complete dentures, although various challenges are related to the impression making, fabrication orientation of denture bases, and risk of losing the attachments. The other option is implant supported prosthesis which can provide predictable functional and esthetic outcomes. In this technical report we present a method of improving the mouth opening of a patient with OSMF by utilizing intralesional injections followed by conventional complete denture prosthesis.

Case description

A 40-year-old female patient reported to the Department of Prosthodontics with a chief complaint of missing teeth and difficulty with chewing. The patient had a past medical history of infantile hemangioma and a 20-year history of chewing areca nuts. She complained of a burning sensation in her oral cavity and difficulty in opening the mouth. On physical examination, a pink to purple discoloration was seen, with undefined margins present on the chin and towards the cheek unilaterally (right side). The dimensions would be 6-7 cm super-inferiorly and 10-12 cm mesiodistally (Figure 1). Using a digital caliper the mouth opening was measured at 27.19 mm (Figure 2).

On intra-oral examination, diffused blanched white bands were seen bilaterally on the buccal mucosa in the molar region (Figure 3). The bands were taut and tough which led to a limited mouth opening. The hemangioma extended up to the buccal mucosa adjacent to the pre-molar region. There were completely edentulous maxillary and mandibular alveolar arches which had red discoloration on the mandibular anterior region due to the hemangioma present intraorally as well (Figure 4). Based on the physical examination and medical history, the patient was diagnosed with grade II OSMF.

Due to the infantile hemangioma, certain invasive procedures for improving the mouth opening (e.g. commisuroplasty) or rehabilitation of edentulous ridges (e.g. implant placement) were not appropriate. The mandibular implant supported overdenture is generally placed in the region between 2 mental foramina. In case of our patient, that area was completely covered with hemangioma, hence every surgical procedure was high risk for her. Furthermore, sectional dentures were also excluded because the thick bands present in the buccal mucosa can compromise retention and stability of the prosthesis.

We decided on pharmacological management of the patient, followed by a conventional complete denture. The mucosa was arbitrarily divided into 3 zones, and approximately

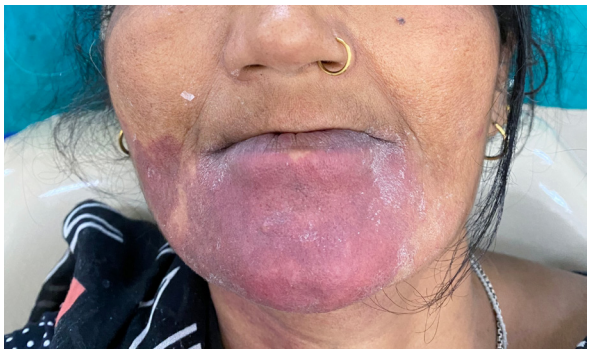

Figure 1. Extraoral congenital haemangioma

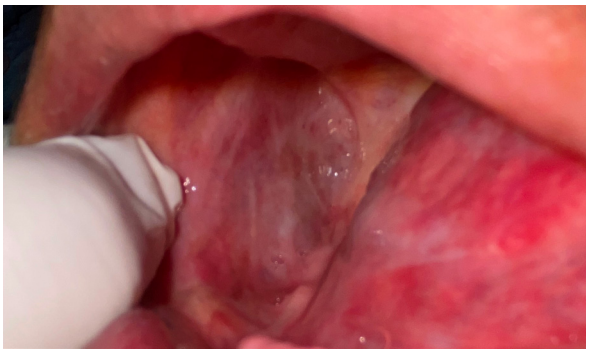

Figure 3. Blanched white bands

Figure 2. Restricted mouth opening upon initial physical examination

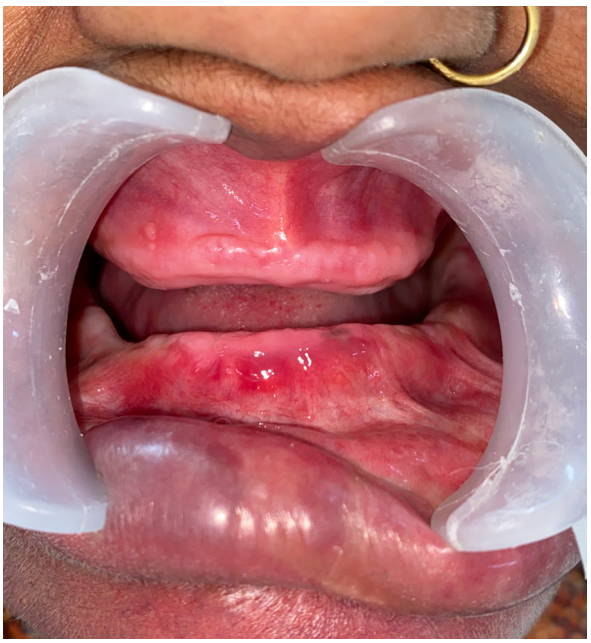

Figure 4. Intraoral pink-red discoloration

equal amounts of hyaluronidase with 1 ml of 2% lidocaine and adrenaline (1:80000), were injected intralesionally (where the most fibrosis was felt on palpation) with a 28 gauge needle, twice weekly for 4 weeks (a total of 8 doses). The patient was instructed to avoid spicy food and the exercises to improve mouth opening were recommended. Transcutaneous electrical nerve stimulation (TENS) was patiensed as an adjunct to mouth opening exercises. The patient had an increase in mouth opening of 33 mm (Figure 5) and the buccal mucosa movement were easily performed. The complete denture prosthesis with balanced occlusion was fabricated conventionally (Figure 6). The patient was kept on regular follow-up after 24 hrs, 72 hrs, 1 month, 3 months, and 6 months.

Discussion

Based on clinical diagnosis, Nagesh and Bailoor [6] categorized OSMF into 3 stages [6] (Table 1). Unfortunately no such classification is available for edentulous patients. Hence, the treatment options to be implied for a particular stage of OSMF are also not specified. Symptomatic relief is provided by conservative methods (vitamins, topical steroids, physiotherapy and antioxidants) that have an anti-inflammatory effect and promote apoptosis. The most common OSMF treatment options are medical, surgical and physiotherapy [7]. Treatment modalities such as implant supported overdentures or sectional dentures are available. Furthermore, to improve the prosthetic outcome, neutral zone technique, intra-oral Gothic arch tracing and 3D printed denture bases can be used. How-

Table 1. Stages of OSMF for the dentulous mouth based on clinical diagnosis (Nagesh and Bailoor) [6]

Stage	Blanching	Mouth opening	Tongue protrusion	Lymphadenopathy
I	Mild	No restriction	No restriction	Absent
II	Moderate to severe	Reduced by 33%	Slight restriction	Present (unilateral or bilateral)
III	Severe	Reduced by 66%	Tongue is fixed	Bilateral

ever we did not consider the above-mentioned options due to our patient's underlying condition of infantile hemangioma. Keeping the stability and retention of a sectional prosthesis is a difficult task for the patient and eventually leads to non-usage of the prosthesis and reduced quality of life.

Steroids act by opposing the action of soluble factors generated by sensitized lymphocytes after activation by specific antigens. This results in anti-inflammatory and immunosuppressive activity and prevents fibrosis by decreasing fibroblastic proliferation and collagen deposition. The initial relief of OSMF symptoms may be due to anti-inflammatory action of steroids (e.g. dexamethasone), which clears the juxtaepithelial inflammation [3, 8]. By breaking down hyaluronic acid (the ground substance in connective tissue), hyaluronidase lowers the viscosity of intercellular cement substance. Better results were observed with respect to trismus and fibrosis.

Our patient achieved considerable improvement in mouth opening after 4 weeks of intra-lesional injections and TENS therapy. Post-treatment follow-up was conducted using

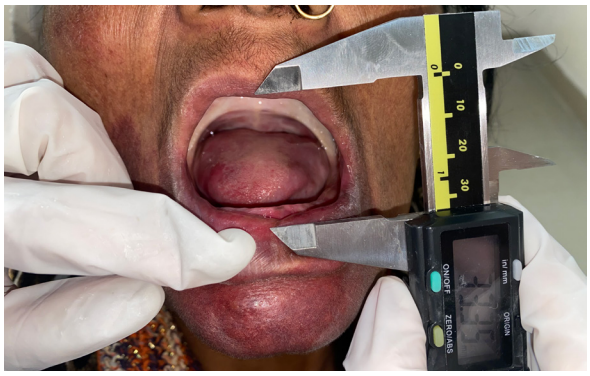

Figure 5. Improved mouth opening

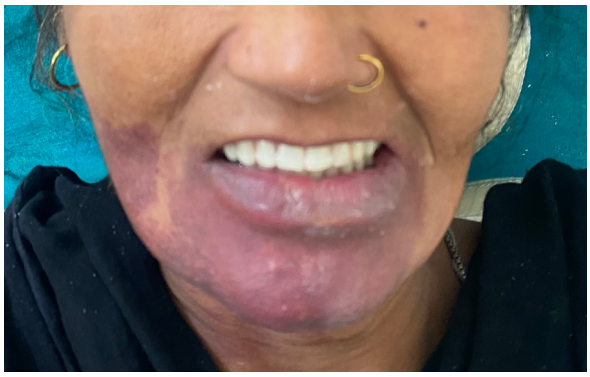

Figure 6. Complete denture in place

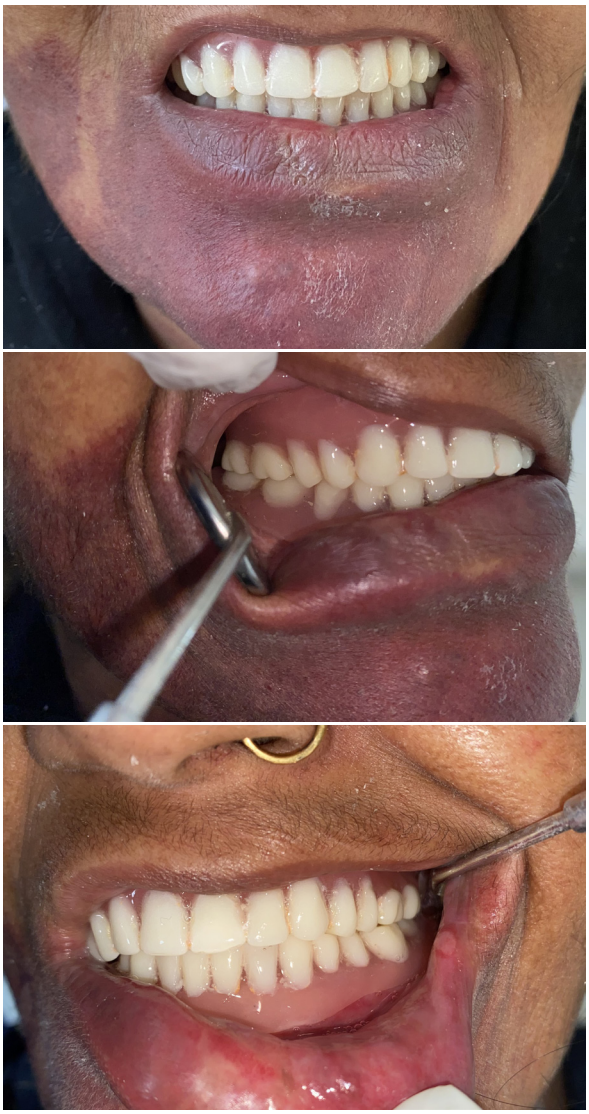

Figure 7-9. Complete denture in occlusion during follow-up appointments

Kapoor's Index, which assesses the retention and stability of dentures. The retention and stability were satisfactory, indicating successful functional performance of the prosthesis (Figures 7-9). In addition to this, a thorough evaluation of the patient's mouth opening was performed. The results showed that the achieved mouth opening after prosthetic rehabilitation was comparable to the outcomes typically observed following intra-lesional injection therapy, suggesting a favourable and functional result (Figure 10).

Kakar et al. reported that patients receiving hyaluronidase alone reported a quicker relief of symptoms, whereas combination with dexamethasone provided better long-term results [3]. Shah et al evaluated the efficacy of hyaluronidase and dexamethasone combination in the treatment of OSMF and reported a reduction of the burning sensation and an improvement in mouth opening [7].

Lanjekar et al. evaluated the efficacy of topical curcumin mucoadhesive semisolid gel, triamcinolone acetonide/hyaluronidase mucoadhesive semisolid gel and a combination of both in the treatment of oral submucous fibrosis (OSMF). They concluded that curcumin has a therapeutic effect on patients diagnosed with OSMF. Maximum utilization and enhanced drug delivery were achieved with the help of a combination other two active drugs, namely triamcinolone and hyaluronidase [3].

Bansal conducted a histopathological study to know the efficacy of local and systemic corticosteroid and hyaluronidase therapy in oral submucous fibrosis. The results of his study revealed that local and systemic corticosteroid and hyaluronidase therapy in patients with OSMF were found effective. However, histopathologically, it was not found statistically significant whether corticosteroids are given locally and/or systemic with or without injection hyaluronidase [10].

Although local corticosteroid injections are considered safe in patients with haemangiomas, we decided not to administer them due to the potential for adverse reactions. During treatment of children with local steroid injections it is suggested to routinely test endocrine/adrenal function and actively consult with an endocrinologist to confirm and then minimize the impact on the adrenal glands, growth and immune status [11].

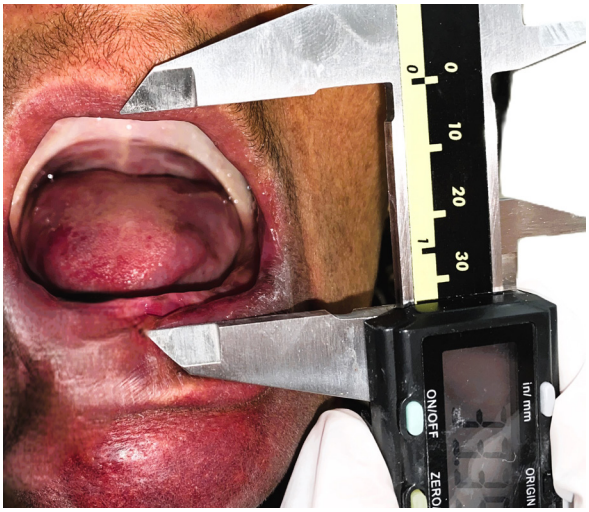

Figure 10. Mouth opening at the 6 months follow-up visit

Conclusion

Injections of hyaluronidase are an effective way to manage and eliminate morbidity in OSMF. The most notable effect of this treatment approach was an increase in mouth opening along with a decrease in a burning sensation. Also, it is a cost-effective method. Careful treatment planning and modification of conventional dentures allowed us to overcome the common clinical challenges of treating OSMF. Periodic recalling and prosthesis maintenance help with keeping the prosthesis stable, functional and easy to use.

Conflict of interests

None.

Funding

None.

References

1. Passi D, Bhanot P, Kacker D, Chahal D, Atri M, Panwar Y. Oral submucous fibrosis: Newer proposed classification with critical updates in pathogenesis and management strategies. Natl J Maxillofac Surg [Internet]. 2017;8(2):89. Available from: https://journals.lww.com/njms/fulltext/2017/08020/oral_submucous_fibrosis__newer_proposed.2.aspx
2. Guna TP, Sathyanarayanan R, Pilavullathil R, Jude NJ, Kumaravel R, Selvakumar C, et al. Management of oral submucous fibrosis with intralesional injection of hyaluronidase and dexamethasone: a case report. J Sci Dent. 2020;10(2).

3. James L, Shetty A, Rishi D, Abraham M. Management of Oral Submucous Fibrosis with Injection of Hyaluronidase and Dexamethasone in Grade III Oral Submucous Fibrosis: A Retrospective Study. J Int Oral Heal JIOH [Internet]. 2015;7(8):82–5. Available from: http://www.ncbi.nlm.nih.gov/pubmed/26464545
4. Yadav A, Nair G, Naidu GS, Makkad RS, Nagi R, Dewangan G. Intralesional Steroid plus Hyaluronidase and Oral Physiotherapy in the management of Oral submucous fibrosis: Clinicians Experience. J Adv Med Dent Sci Res [Internet]. 2020;8(10):122–9. Available from: http://jamdsr.com/uploadfiles/28osmfvol8issue10pp122-129.20201016032628.pdf
5. Kumari A, Roy S. Efficacy of Hyaluronidase in Management of OSMF-A Clinical Study. J Adv Med Dent Scie Res [Internet]. 2016;4(6):299–301. Available from: http://jamdsr.com/uploadfiles/73osmfvol4iss6p299-301.20190214091231.pdf
6. Bhagvan More C, Gupta S, Joshi J, N Verma S. Classification System for Oral Submucous Fibrosis. Kailasam S, editor. J Indian Acad Oral Med Radiol [Internet]. 2012;24:24–9. Available from: http://www.jaypeejournals.com/eJournals/ShowText.aspx?ID=3032&Type=FREE&TYP=TOP&IN=~/eJournals/images/JPLOGO.gif&IID=235&isPDF=YES
7. Shah PH, Venkatesh R, More CB, Vassandacoumara V. Comparison of Therapeutic Efficacy of Placental Extract with Dexamethasone and Hyaluronic Acid with Dexamethasone for Oral Submucous Fibrosis - A Retrospective Analysis. J Clin Diagn Res [Internet]. 2016;10(10):ZC63–6. Available from: http://www.ncbi.nlm.nih.gov/pubmed/27891461
8. Patel TL, Singh S. Comparative evaluation of treatment of Oral submucous fibrosis with intralesional injections of Dexamethasone and hyaluronidase with Triamcinolone Acetonide and hyaluronidase. Group [Internet]. 2015;1(9.81):1–61. Available from: http://www.jcmad.com/admin/pdf/337.pdf
9. Lanjekar AB, Bhowate RR, Bakhle S, Narayane A, Pawar V, Gandagule R. Comparison of efficacy of topical curcumin gel with triamcinolone-hyaluronidase gel individually and in combination in the treatment of oral submucous fibrosis. J Contemp Dent Pr [Internet]. 2020;21(1):83–90. Available from: https://www.thejcdp.com/doi/JCDP/pdf/10.5005/jp-journals-10024-2726
10. Bansal M. Efficacy of local and systemic corticosteroid and hyaluronidase therapy in oral submucous fibrosis: A histopathological study. Int J Otorhinolaryngol Head Neck Surg [Internet]. 2019;5(2):459–64. Available from: https://www.academia.edu/download/67852970/762.pdf
11. Morkane C, Gregory JW, Watts P, Warner JT. Adrenal suppression following intralesional corticosteroids for periocular haemangiomas. Arch Dis Child [Internet]. 2011;96(6):587–9. Available from: https://adc.bmj.com/lookup/doi/10.1136/adc.2010.204859